ANALYSIS OF THE ANTI-TUMOR EFFECTS OF NOVEL COMPOUNDS (83b1, 160a, DpC AND Dp44mT) AGAINST HUMAN ESOPHAGEAL, PROSTATE AND COLORECTAL CARCINOMAS

PUN HO YUEN

PhD

The Hong Kong Polytechnic University

2020

The Hong Kong Polytechnic University

Department of Applied Biology and Chemical Technology

Analysis of the Anti-tumor Effects of Novel Compounds (83b1, 160a, DpC and Dp44mT) Against Human Esophageal, Prostate and Colorectal Carcinomas

PUN Ho Yuen

A Thesis Submitted in Partial Fulfillment of the Requirements for the Degree of Doctor of Philosophy

February 2019

CERTIFICATE OF ORIGINALITY

I hereby declare that this thesis is my own work and that, to the best of my knowledge and belief, it reproduces no material previously published or written, nor material that has been accepted for the award of any other degree or diploma, except where due acknowledgement has been made in the text.

_____ **(Signed)**

PUN Ho Yuen **(Name of student)**

ABSTRACT

Cancer is one of the most common and lethal diseases worldwide including esophageal, prostate and colorectal cancers. Nowadays, although there are different approaches for treating these cancers, the incidence and mortality are still elevating. More effective and efficient therapeutics for treating these cancers are urgently needed. To address such critical issues, the anti-cancer effects of two novel quinoline derivatives 83b1 and 160a, and two novel thiosemicarbazone derivatives DpC and Dp44mT were first studied in attempt to identify novel anti-cancer compounds for future drug development.

For the first part of the present study, the anti-cancer effects of the novel quinoline derivative, 83b1, on mainly esophageal cancer were studied, it showed significant cytotoxic effects on esophageal squamous cell carcinoma (ESCC) cell lines and tumor-xenograft models. Through the *in silico* assessment and isothermal titration calorimetry (ITC), it was demonstrated that Peroxisome Proliferator-activated Receptor Delta (PPARD), which is a cancer-promoting protein over-expressed in cancer cells, was targeted by 83b1 and it resulted in reduction of the number of cancer cells by downregulating cyclooxygenase-2 (COX-2) and COX-2 derived prostaglandin E2 (PGE_2). Moreover, 83b1 also showed the anti-cancer effects on other cancer types including breast, lung, liver and colorectal cancers. Furthermore,

the possible signaling pathways affected by 83b1 in esophageal cancer cell lines were also studied including the signaling proteins AKT-1, JNK-1, ATF-2, MAPK, HSP-27 and MEK.

For the second part, the anti-cancer effects of another quinoline derivative 160a on esophageal cancers were also studied and 160a demonstrated significant cytotoxic effects on ESCC cell lines. By using the *in silico* assessment, it implicated that 160a can target on p-glycoprotein (P-gp) and reverse drug resistance conferred by P-gp via blocking the P-gp binding site to its substrate. 160a also showed the synergistic effects with the use of P-gp substrate doxorubicin.

Furthermore, the anti-cancer effects of two novel thiosemicarbazone derivatives DpC and Dp44mT were also demonstrated on prostate and colorectal cancer cell lines. DpC and Dp44mT also acted as the iron-chelators, and they showed the anti-tumor effects through up-regulation of NDRG1 and down-regulation of LYRIC. By down-regulation of LYRIC, they could also suppress the TNFα-mediated EMT and cell migration; they also showed the ability to reduce the expression of the onco-proteins downstream of LYRIC.

To conclude, the novel anti-tumor compounds used in this study showed the good potentials for treating cancers through the involvement of different molecular

mechanisms. Further studies include the investigation their pharmacokinetics and toxicities in animal models.

PUBLICATIONS INSUPPORT OF THIS THESIS

***First Author in the Publication*:**

Pun, I.H.Y., Chan, D., Chan, S.H., Chung, P.Y, Zhou, Y.Y., Law, S., Lam, A.K.Y., Chui, C.H., Chan, A.S.C., Lam, K.H., Tang, J.C.O., et al., *Anti-cancer Effects of a Novel Quinoline Derivative 83b1 on Human Esophageal Squamous Cell Carcinoma through Down-Regulation of COX-2 mRNA and PGE(2).* Cancer Research and Treatment, 2017.**49**(1): p. 219-229.

Xi, R.X.*, **Pun, I.H.Y.***, Menezes, S.V. Fouani, L., Kalinowski, D.S., Huang, M.L.H., Zhang, X.Z., Richardson, D.R., Kovacevic, Z., et al., *Novel Thiosemicarbazones Inhibit Lysine-Rich Carcinoembryonic Antigen-Related Cell Adhesion Molecule 1 (CEACAM1) Coisolated (LYRIC) and the LYRIC-Induced Epithelial-Mesenchymal Transition via Upregulation of N-Myc Downstream-Regulated Gene 1 (NDRG1).* Molecular Pharmacology, 2017.**91**(5): p. 499-517.

**Authors with equal contribution shown in the publication.*

Co-author in the Publication:

Chung, P.Y.,Bian, Z.X., **Pun, I.H.Y.**, Chan, D., Chan, A.S., Chui, C.H., Tang, J.C.O., Lam, K.H., et al., *Recent advances in research of natural and synthetic bioactive quinolines.* Future Medicinal Chemistry, 2015. **7**(7): p. 947-967.

ACKNOWLEDGEMENTS

I would like to express my greatest gratitude to my supervisor, Dr. Johnny Tang Cheuk-on, who provided me the invaluable opportunity to study with the PhD degree and gave me countless advices, support and guidance, this study could not be finished without his unceasing encouragements and reminders. I deeply appreciate my supervisor gave me unlimited trust and spaces for me to try and plan in my PhD study and also the exchange study in Australia.

Besides, sincere thanks are expressed to all members in Dr. Tang's research group including Dr. Chan Sau Hing and Ms. Chan Po Yee who gave me lots of technical supports in the field of chemistry, Dr. Dessy Chan, Ms. Zhou yuanyuan and Ms. Yami Yeung who worked together with me and shared the experiences.

Moreover, I would like to thank my supervisor, Prof. Des Richardson, my co-supervisor, Dr. Zaklina Kovacevic, and other teammates in my exchange study at the University of Sydney in Australia. They gave me numerous opportunities to learn and they were willing to share and guide me to do the right things in my research report there.

Lastly, special thanks are given to my dear parents, friends and churchmates who support me throughout my study and life.

TABLE OF CONTENT

LIST OF FIGURES

mouse treated by either 83b1 or vehicle control. (***p<0.001). (C) Liver function assessment including albumin (ALB), alanine aminotransferase (ALT), aspartate aminotransferase (AST), Urea and total bilirubin (TBil) of the mice after the treatment of either 10mg/kg or 50mg/kg of 83b1.

Figure 3.14. Image of agarose gel electrophoresis of the PPARD PCR product. Lane 1: 100bp marker, Lane 2: Original purchased PPARD over-expression plasmid, Lane 3: cDNA extracted from KYSE150 as a positive control, Lane 4: 100bp marker, Lane 5: PPARD over-expression plasmid replicate 1 extracted from transformed E.coli, Lane 6: PPARD over-expression plasmid replicate 2 extracted from transformed E.coli, Lane 7: Negative control (water).

Figure 3.15. Agarose gel electrophoresis of the PCR product (Target genes: PPARD, COX-2 and VEGF-A) of the cDNA extracted from parental KYSE150 (KYSE150P) and PPARD-transfected KYSE150 (KYSE150PD) cell lines. (A) Image of the agarose gel electrophoresis. (B) Comparison of the intensity of the target gene expression normalized by reference gene between KYSE150P and KYSE150PD cell lines. (*p<0.05, **p<0.01 and ***p<0.001).

Figure 3.16. Agarose gel electrophoresis of COX-2 gene expression in KYSE150 cell line with the addition of PPARD agonist GW0742. (A) Image of the agarose gel

electrophoresis. (B) Comparison of the intensity of COX-2 expression in KYSE150 with the addition of GW0742. (*p<0.05 and **p<0.01).

Figure 3.17. Real-time PCR of COX-2 mRNA expression in four human ESCC cell lines treated with different concentration of 83b1. (A) Amplification efficiency curve of COX-2 and GAPDH gene. (B) KYSE150, (C) KYSE450, (D) SLMT-1 and (E) HKESC-4. (*p<0.05, **p<0.01 and ***p<0.001).

Figure 3.18. ELISA of PGE_2 production. (A) Standard curve of PGE_2 determination in ELISA. (B) Linearized PGE_2 standard curve for determination of PGE_2 production in ESCC cell lines. (C-E) ELISA of PGE_2 production in KYSE150, KYSE450 and SLMT-1 treated with different concentration of 83b1.

Figure 3.19. Cytotoxic assessment of 83b1 (Maximum concentration: 40μg/ml) in human cancer cell lines: (A) SW1116, (B) HCT15, (C) MCF-7 and (D) AGS.

Figure 3.20. Cytotoxic assessment of 83b1 (Maximum concentration: 50μg/ml) in human cancer cell lines: (A) HCT15, (B) HT29, (C) MCF-7, (D) AGS, (E) HEP3B and (F) A549.

Figure 3.21. Agarose gel electrophoresis of the RT-PCR products (Target genes: PPARD and COX-2) of the cDNA extracted from four cell lines including HEK293 (Non-tumor), HT29 (Colon cancer), AGS (Gastric cancer) and A549 (Lung cancer). (A)

Figure 4.4. Analysis of the structure of 160a. (A) ^{1}H-NMR Spectrum of 160a. (B) ^{13}C-NMR Spectrum of 160a. (C) ESI-MS Spectrum of 160a.

Figure 4.5. Cytotoxic assessment of 160a and Dox in human ESCC cell lines including KYSE70, KYSE150, KYSE450, KYSE520, SLMT-1 and HKESC-4; and non-tumor cell lines including NE-3 and HEK293. (A) 160a (Maximum concentration: 20μg/ml) and (B) Dox (Maximum concentration: 1μg/ml).

Figure 4.6. Molecular docking results of 160a or other P-g p substrate and inhibitors with P-gp obtained in MolecularDockingServer. (A) Doxorubicin, (B) Cyclosporin A, (C) Vinblastin and (D) 160a.

Figure 4.7. Analysis of P-gpexpression. (A) RT-PCR of mRNA expression in human ESCC and non-tumor cell lines (B) IHC images of P-gpprotein expression in human ESCC and non-tumor cell lines.

Figure 4.8. The cell proliferation curve of human ESCC cell lines treated with Dox (0.15μg/ml), 160a (3μg/ml) or both compounds for 4 days. (A) KYSE150 and (B) KYSE450.

Figure 4.9. Determination of Fluorescent Intensity of Calcein AM in different ESCC cell lines treated with either different concentration of 160a or cyclosporin A as the positive control by Confocal Microscopy. (A) KYSE70. (B) KYSE150. (C) KYSE450.

(D) KYSE520. (E) SLMT-1. (F) Summary of Fluorescent Intensity in all cell lines with the treatments compared to DMSO(Key: BF: Bright Field; CAM: Calcein AM; OL: Overlayer). (*p<0.5, **p<0.01 and *** p<0.001)

Figure 4.10. Determination of Green Fluorescent Intensity of Calcein AM in different ESCC cell lines treated with either different concentration of 160a or cyclosporin A as the positive control by Flow cytometry. (A) KYSE70 (Parental). (B) KYSE70 (Doxorubicin-resistant). (C) KYSE150 (Parental). (D) KYSE150 (Doxorubicin-resistant). (E) KYSE450 (Parental). (F) Summary of Fluorescent Intensity in all cell lines with the treatments compared to DMSO. (* p<0.5, **p<0.01 and *** p<0.001).

Figure 4.11. Cytotoxic effects of either Dox or Dox with 2μg/ml 160a on ESCC or non-tumor cell line. (A) KYSE450. (B) NE-3. (C) Comparison of MTS_{50} relative unit of Dox and Dox with 2μg/ml 160a in KYSE450 and NE-3.

Figure 4.12. Analysis of synergistic effect of 160a on Dox in the treatment of KYSE450 or NE-3 by using CompuSyn program.(A) KYSE450 and (B) NE-3.

Figure5.1. Experimental plan for the studies of the effects and mechanisms of the two novel iron chelators, DpC and Dp44mT.

Figure 5.2. Western blot to determine the effects of NDRG1 expression on LYRIC. (A) DU145 and (B) HT29. (**p<0.01 and ***p<0.001).

Figure 5.3. Western blot to determine the effects of NDRG1 expression on LYRIC. (A) DU145 and (B) HT29.(Relative to Vector Ctrl or sh-Ctrl withoutTNFa: **p<0.01 and ***p<0.001; Relative to Vector Ctrl or sh-Ctrl with TNFa: #p<0.05).

Figure 5.4. Western blot to determine the effects of NDRG1 expression on LYRIC, NFκB and Vimentin with addition of TNFα. (A) DU145 and (B) HT29. (Relative to Vector Ctrl or sh-Ctrl withoutTNFa: *p<0.05, **p<0.01 and ***p<0.001; Relative to Vector Ctrl or sh-Ctrl with TNFa: ###p<0.001).

Figure 5.5. Transwell migration assay to determine the effects of NDRG1 expression on cell migration with addition of TNFα. (A) DU145, (B) HT29 and (C) Summary and comparison of each groups in two cell lines. (Relative to Vector Ctrl or sh-Ctrl withoutTNFa:***p<0.001; Relative to Vector Ctrl or sh-Ctrl with TNFa: ##p<0.01 and ###p<0.001).

Figure 5.6. RT-PCR to assess the mRNA of NDRG1 and LYRIC in DU145 and HT29 treated with either Bp2mT (10μM), DFO (250μM), Dp44mT (5μM) or DpC (5μM) for 24 hours at 37°C. (A) DU145 and (B) HT29.(***p<0.001).

Figure 5.7. Real-time PCR to assess the mRNA of NDRG1 and LYRIC in DU145 and HT29 treated with either Bp2mT (5μM), DFO (250μM), Dp44mT (5μM) or DpC (5M) for 24 hours at 37°C. (A) DU145 and (B) HT29. (**p<0.01 and ***p<0.001).

Figure 5.8. Western blot to determine the protein expression of NDRG1 and LYRIC in DU145 and HT29 treated with either Bp2mT (5μM), DFO (250μM), Dp44mT (5μM) or DpC (5μM) for 24 hours at 37°C. (A) DU145 and (B) HT29. (**p<0.01 and ***p<0.001).

Figure 5.9. Western blot to determine the effect of Bp2mT (5μM), DFO (250μM), Dp44mT (5μM) or DpC (5μM) on the rotein expression of LYRIC, NFκB-p65 and Vimentin in addition with TNFα in DU145 and HT29 treated with either (A) DU145 and (B) HT29. (*p<0.05, **p<0.01 and ***p<0.001).

Figure 5.10. Immuno-fluorescent staining to determine the translocation activity of NFκB-p65 and LYRIC in DU145 and HT29 with Bp2mT (5μM), DFO (250μM), Dp44mT (5μM) or DpC (5μM) for 24 day with addition of TNFα. (A) DU145, (B) HT29 and (C) Summary of the co-localization intensity of NFκB-p65 against nucleus and NFκB-p65 against LYRIC.

Figure 5.11. Western blot to determine the effects of DFO, DpC and Dp44mT on the downstream cancer-related proteins of LYRIC. (A) DU145 and (B) HT29.

LIST OF TABLES

Table 4.6. Analysis of synergistic effect of 160a on Dox in the treatment of KYSE450 by calculating the value of FICI.

Table 5.1. Structure of the iron chelators used in this chapter, DFO was the positive control, whereas Bp2mt was the negative control.

LIST of ABBREVIATIONS

ESCC: Esophageal squamous cell carcinoma

EAC: Esophageal adenocarcinoma

CRC: Colorectal cancer

MRP: Multi-drug resistance protein

ABC: ATP-binding cassette

COX: Cyclooxygenase

RXR: Retinoid X receptor

PPAR: Peroxisome proliferator-activated receptor

DFO: Desferrioxamine

MTS: 3-(4,5-Dimethylthiazol-2-yl)-5-(3-carboxymethoxyphenyl)-2-(4-sulfophenyl)-2H-tetrazolium

CDDP: Cisplatin

IC_{50}: Half maximal inhibitory concentration

MTS_{50}: Half maximal MTS signal

siRNA: Small interfering RNA

RT-PCR: Reverse Transcription-Polymerase Chain Reaction

mRNA: Messenger RNA

cDNA: complementary DNA

GAPDH: Glyceraldehyde 3-phosphate dehydrogenase

Ct: Threshold cycle

HRP: Horseradish peroxidase

PPRE: PPAR-response element

PGE_2: Prostaglandin E-2

AA: Arachidonic acid

SEA: Similarity-ensemble assessment

MDR: Multi-drug resistance protein 1

FICI: Fractional inhibitory concentration index

CI: Combination index for the effects on ESCC suppression

Dox: Doxorubicin

DpC: Di-2-pyridylketone 4-cyclohexyl-4-methyl-3-thiosemicarbazone

Dp44mT: Di-2-pyridylketone-4,4-dimethyl-3-thiosemicarbazone

NDRG1: N-myc downstream regulated 1

NFκB: Nuclear factor κB

TNFα: Tumor necrosis factor alpha

EMT: Epithelial-mesenchymaltransition

LYRIC: Lysine-rich CEACAM1 co-isolated protein

Chapter 1 GENERAL INTRODUCTION

In this section, I would like to mention some background information and figure out the essential concepts of the whole study. After the introduction of this project, the objectives would be shown to describe the main foci of the overall study.

1.1. INTRODUCTION TO CANCER

Cancer is one of the leading causes of death with the growing incidence rate around the world. According to the estimation from GLOBOCAN, there are about 14.1 million new cases of cancers worldwide and 8.2 million of the death cases were found in 2012. Nowadays, the occurrence of cancers is still gradually increasing because of numerous factors including growth of population and aging, upward trend of potential risk factors such over-weight, smoking, physical inactivity, unbalanced diet and change of the patterns of reproduction (such as lower parity and first birth at higher age) which is related to urbanization and rapid development of economy.[1-3] Recently, the burden of cancers has been found to shift to the less developed countries which accounted for about 57% of the total cases with about 65% of the mortality rate worldwide.[1] The most important thing is that the incidence rate and the mortality rate are expected to keep on rising.[1]

Cancers can be classified according to the anatomical sites and origins such as prostate cancer, breast cancer, lung cancer, colorectal cancer, bladder cancer, melanoma, renal cancer, ovarian cancer, liver cancer, leukemia and esophageal cancer.[4] Some types of cancer have been reported with higher incidence and mortality rates depending on the gender, age, race and living regions. Patients suffered from breast cancer accounted for 29% (232,670 in 830,320) of all cancer cases in female worldwide and 15% (40,000 in 275,710) of the cases dead in 2014.[1, 5] As for the male patients, prostate cancer has been reported to be the first killer which accounted for 27% (233,000 in 855,220) of total cases in male and 10% (29,480 in 310,010) are the death cases in the same year.[1, 5, 6]

Cancer cells are different to the corresponding normal cells including the gene expression, morphology, proliferation and the ability of invasion. Because of the alteration of gene expression, they always grow uncontrollably and form a tumor population. Furthermore, some of the invasive cancer cells can even metastasize from their origin into the distant tissues or organs through blood system or lymph to cause it more worse and more difficult to treat.[3, 7]

Because of the serious circumstances of cancer development around the world, cancer therapeutics are always considered to be highly demanding.[8-10]Currently, treatments of cancers are manifold depending on the types of cancer, tumor size and

stage; extend of the cancer spread, the age of patients. The main treatments involve endoscopic resection, radiotherapy and chemotherapy, and these treatments are usually combinedto be used for cancer therapy. For example, endoscopic resection followed by chemoradiotherapy, which includes three treatments at the same time, is always used for treating various types of cancers.[4, 7-9]

1.2. OVERVIEW OF HUMAN ESOPHAGEAL, COLORECTAL AND PROSTATE CANCERS

1.2.1. *Epidemiology*

1.2.1.1. Esophageal Cancer

Esophageal cancer is the eighth most prevalent cancer and it is also the sixth leading cause of cancer deathsthroughout the world.[1, 5]In 2012, there were 455,800new cases of esophageal cancer diagnosed and 400,200 deaths occurred in the patients suffering from esophageal cancer worldwide.[1]Although esophageal cancer is not the most common type of cancers, the very low 5-year survival rate makes it become a serious disease.Esophageal cancer is not the most common cancer type but it is also considered as a very serious cancer because of the extremely low 5-year survival rate which is resulted from the poor prognosis and ineffective treatments.[11, 12]

Esophageal cancer is divided into few histopathological subtypes, the two most common subtypes are esophageal squamous cell carcinoma (ESCC) and esophageal adenocarcinoma (EAC).[1, 13, 14] ESCC is the predominant histological subtype throughout the world which accounted for more than 90% of the total cases of esophageal cancer; however, EAC is prevalent in some countries such as United States.[14, 15] Their occurrence is highly dependent on the geographic regions, racial background, and lifestyle.These two types of esophageal cancers are originated from different locations in the esophagus. ESCC is usually found in the middle third part of the esophagus, and it arises from the squamous epithelium of the esophageal wall, the lining cells of esophagus undergoes inflammation, hyperplastic and dysplastic changes (precancerous lesion), and finally develop into cancerous cells. On the other hand, EAC primarily appears in the lower third part of esophagus and it is originated from the glandular cells which are responsible for making mucus. These two histopathological subtypes, except the similar location of origin, always have extremely different biological and epidemiological profiles, and they should be considered as the two separated disease entities.[12, 16, 17]

1.2.1.2. Prostate Cancer

Prostate canceris originated from the glandular cells of the prostate. The progression or prostate cancer is extremely low, patients are always recognized to suffer from prostate cancers after the cancer passes through a long period of latency about 15 to 20 years.[18-20]

Prostate cancer is the fourth most frequent and fifth most mortal cancer type throughout the world.[1] In UK, prostate cancer is the most incident cancer that accounted for 21% (180,890) of the cases of cancers in 2016 and it leaded to the second most deaths in 2016 that accounted for about 8% (26,120) of cancer-related deaths.[1]

1.2.1.3. Colorectal Cancer

Colorectal cancer (CRC) is composed of the cancers originated in colon or rectum, it is the third most common cancer diagnosed and fourth most leading cause of cancer death worldwide. [1, 5, 21]

There were approximately 153,700 new cases of CRC are diagnosed each year, 1,000,000 cases of CRC were diagnosed in 2006 and it leaded to more than 500,000 deaths in both sexes. CRC is much worse in men, according to the findings from Cancer Statistics conducted in US in 2016, CRC accounted for about 8% (70,820) in

total cases in men and 8% (26,020) in total cancer-related death. It has been reported that about 12.5% person develops invasive CRC during their lifetime, and about 36.7% patients suffered from CRC dead in 2016.[1, 22] The prognosis of CRC is still poor although the advanced surgical techniques and early detection, it has also been found that more than 40% of patients suffered from CRC who underwent surgical resection of primary tumor would still die within five years.[23, 24]

1.2.2. *Etiology*

1.2.2.1. Esophageal Cancer

Esophageal canceris divided into different stages depending on the diagnosed location, and it is highly related to the severity of the cancer. Localized tumor means that the tumor is still located at the primary site of origination. Regional tumor is the tumor that has spread to the regional lymphnodes and starts to invade into other tissues or organs. As for the distant tumor, it is the most invasive stage which the tumor cells have already metastasized into other organs.[25]

As mentioned before, the two main subtypes of esophageal cancer show completely different characteristics. The occurrence of ESSC and EAC is distinctiveand some reports have shown that most of the potential risk factors of the

developing ESCC and EAC are also very contrary to each other. However, they are also highly dependent on the regions, race and lifestyles.[15, 26, 27]

The symptoms of gastro-esophageal reflux disease (GERD) and Barrett's esophagus (BE) have been recognized as the most vital factors for EAC development but not ESCC.[28] GRED is defined as the chronic reflux of gastric or bile juice to the esophagus which might result in injury of esophagus. The long-term reflux of juice will trigger the metaplastic change of the normal esophageal squamous cells to the columnar epithelium with metaplasia which is Barrett's esophagus. The cells in BE are identified as the well-established precursors of EAC and reports showed that the risk of EAC development is 40-fold higher in BE than the normal esophageal cells.[29] Some drugs such as beta-blockers, aminophyllines and anti-cholinergic agents that contribute to relaxation of gastro-esophageal sphincter will promote the reflux and it has been reported to increase the risk of EAC about 10%. However, infection of *Helicobacter pylori*, which functions in alleviation of gastro-esophageal reflux diseases, has been postulated to reduce the risk of EAC development.[29] Moreover, few epidemiologic studies showed that people having the problem of overweight and obesity have about 3-fold higher chances to suffer from EAC. Otherwise, smoking is also related to EAC development.[30-32]

The incidence rate of ESCC is more prevalent in developing countries than EAC, whereas EAC is primarily found in the developed countries. In China, nearly 90% of the cases of esophageal cancers are ESCC, and the incidence and mortality rate of esophageal cancer in China are in the top of the world which accounted for more than half of the total cases and deaths. On the other hand, for some developed countries such as United States which ESCC was the prevalent subtype about four decades ago, whereas EAC has become the leading subtype of esophageal cancers now.[27, 33]

ESCC is also closely associated with lower socioeconomic status and lifestyle such as alcoholic consumption, smoking and diets.[27, 32] Alcoholic consumption is highly related to ESCC development, some epidemiologic studies showed that heavy drinker (more than 12 drinks per week) has the relative range from 2.9% to 7.4%. Another case-control study published in Taiwan indicated that recent drinkers have 7.6-fold increases in ESCC compared to people who never drinks, even the former drinkers also have 5.5-fold higher chances to suffer from ESCC than the non-drinkers.[15, 17, 27, 32] However, the mechanisms of how alcoholic consumption affecting ESCC development is still poorly understood. Smoking is another important factor highly increases the risk of developing ESCC. A perspective epidemiologic study showed that the risk of ESCC in smokers is 5-fold higher than the non-smokers, as for the heavy smokers, the risk greatly increases about 10-fold. It

has also been found that people with both alcoholic consumption and smoking might have a synergistic effect on promotion of ESCC development. Besides, Poverty and red meat consumption have also been reported to increase the opportunities to be afflicted with ESCC. [27, 30, 33]

Besides, age and gender have also been reported to greatly contribute to the risk of both ESCC and EAC. A study conducted in China showed that the incidence and mortality rates of esophageal cancers in the age up to 40 years old were extremely low, and the rates were increased rapidly after the age of 40. The incidence and mortality rate in the age up to 40 years old were only 19 in 100,000 and 17 in 100,000, but both of the rates were increased 5-fold in 50 years old. The highest incidence and mortality rate were in the age of 80 years old that accounted for 619 in 100,000 and 640 in 100,000, both rates were increased more than 60-fold in this age-group. As for the gender in the same study, the number of new cases of esophageal cancers in male was accounted for 205,560, that is about 2.4-fold higher than the cases in female which accounted for 85,678. Equally, the number of death cases in male was accounted for 154,587 and it is also 2.4-fold higher than that in female accounted for 64,371.[1, 5, 33]

1.2.2.2. Prostate Cancer

The incidence and mortality of prostate cancers are varied because of different factors. Some reports showed that this situation is highly related to the age, living regions and races.[1, 20]

It has been reported that the probability of developing the invasive prostate cancer was increasing proportional to the ages in the patients' lifetime. In US, only 0.3% (1 in 325) of people lower than 49 years old suffered from prostate cancer, however, it increased dramatically to 2.1% (1 in 48), 5.8% (1 in 17) and 10% (1 in 10) respectively in the range of 50 -59 years old, 60 to 69 years old and larger than 70 years old. Prostate cancer is the second leading cause of cancer death in male in all ages, however, the frequency is not that serious at the age below 60 years old since the mortality of patients suffered from prostate cancer is not that high (out of the fifth highest). Whereas, it is the third highest and second highest mortal disease led to cancer death in the patients with the ages larger than 60 years old.[1]

Besides, the incidence and cases of death due to prostate cancer are highly related to the places of residence, the incidence of prostate cancers varied more than 25foldsthroughout the world.[1, 20] It has been reported the incidence of prostate cancer in developed countries was about 742,000, where its incidence in developing countries was about 353,000 worldwide in 2012. It indicated that there should be

some risk factors related to the increase in incidence of prostate cancers in developed countries such as lifestyle and environmental factors. Conversely, the deaths of patient due to prostate cancers in more developed countries only accounted for about 19.1% (142,000) which was much lower than the deaths in developing countries that accounted for about 46.7% (165,000). It is probably due to the better health care and more advanced techniques in cancer treatments.[1, 19, 34]

Moreover, it has been shown that the incidence and mortality of prostate cancers in white patients were 0.12% and 0.02%, but they were 0.21% and 0.47% in the black patients in US. The probability of black patients suffered from prostate cancer and dead was 2-fold higher than white patients.[1, 34, 35]

1.2.2.3. Colorectal Cancer

As mentioned previously, CRC is one of the common and mortal cancers worldwide, however, the incidence and risk of death of CRC are also varied because of different factors including ages, races, regions and also diets.[1, 36-38]

It has been reported that the mortality of CRC was increased positively related to the ages of the patients.[1, 22] For the patients suffered from CRC, the mortality of CRC in the patients in both sexes below 20 years old was not included in the first five ranks in 2012. However, it jumped to the third mortal cancer type in the patients of 20

to 39 years old in both sexes, and then it became the cancer with the second highest mortality in the patients of 40 to 59 and 60 to 79 years old in both boxes in the same year.[1, 22]

Besides, the findings showed that the incidence and mortality of CRC were related to the races of patients. In male, the cases of white patient suffered from CRC in 2012 were 47.4, where the cases of black patients were 60.3 in the same year, it was increased by about 27.2%. On another hand, in female, the cases of white patient suffered from CRC were 36.2 and there was 44.1 cases of CRC than the black people suffered from, it was also increased by 21.8%. [1, 22, 39]

Moreover, some evidences showed that geographical variation influenced the incident rate of CRC, CRC was more prevalent in the developed countries throughout the world such as Northern, Western Europe, New Zealand, Australia, and North America. However, low incidence has been found in Africa, Asia and South America that are all the developing countries. The incidence is also related to the socioeconomic status, it has been found that the frequency of CRC cases was higher in the upper socioeconomic group of people where the less economically developed countries have lower incidence such as Colombia.[1, 37, 39]

It has also been shown that food intake is related to the CRC incidence. For example, some studies showed that people frequently consumed vegetables would

have lower risk to develop CRC, whereas people with high fat intake usually has higher possibility to suffer from CRC.[1, 22, 40]

1.2.3. *Pathogenesis*

1.2.3.1. General Pathogenesis of Cancer

Genetic alteration is one of the pivotal factors for all types of cancer development. Up to date, many genes that are associated with cancer development have been identified as the biomarkers. These biomarkers are very important for prognosis and diagnosis of the cancers and that might greatly aid in staging the cancers and making the decision of cancer treatments. Moreover, identification of the biomarkers also helps the development of target therapeutics to kill the cancers effectively and selectively. The genes associated with the cancers are divided into many types based on their functions in tumor development including oncogenes, anti-apoptotic genes, metastatic genes and tumor suppressor genes.[21, 39, 41]

1.2.3.2. Oncogenes and oncoproteins

Proto-oncogenes are defined as a group of genes which can result in cellular alteration from normal cells to cancerous cells when these genes got mutated. Mutation in proto-oncogenes has been reported to be typically dominant naturally and

those mutated proto-oncogenes are called oncogenes. Originally, proto-oncogenes are responsible for many important functions in human body such as stimulation of cell division, cell differentiation and prevention of cell death that are crucial for normal human development and maintenance of organs and tissues. However, when these genes are mutated and altered to oncogenes, they will over-exhibit these functions by over-expressing the proteins participating in the processes of the functions. Therefore, they usually lead to uncontrollable cell division and inhibition of cell death, and finally result in the formation of tumor and spreading of the cancer cells throughout the body. Oncogenes are usually divided into few types including growth factors, growth factor receptors, signal transducers, nuclear factors, and transcriptional factors.[39, 41-43]

1.2.3.3. Apoptotic and Anti-Apoptotic Genes and their Proteins

Apoptosis (also called programmed cell death) which is used for eliminating the cells, especially in the cells which are no longer needed, in response to the stimulation of different kinds of factors. The process of apoptosis is described by the morphological characteristics of the cells involving shrinkage of the cells, cell membrane blebbing, condensation of chromatin and nuclear fragmentation.[41, 44] Apoptosis is a genetically programmed mechanism that is regulated by some of the

genes which are called apoptotic genes and anti-apoptotic genes.[44] Apoptosis has been shown to an extremely important system against tumor development since researchers raised the possibility that almost all the cell death in tumor is related to apoptosis. [39, 41, 43]

1.2.3.4. Metastatic Genes and Proteins

Metastasis is defined as the cancer cells which have spread to other tissues or organs throughout the body from the place that they originate, and they start growing and proliferating at those distant sites. Metastasis also makes the cases to be more worse since it would become highly difficult to be treated. In ESCC cases, the cancer cells are usually found to spread to distant lymph nodes or other organs including liver and lungs which are the most common sites to detect the metastatic ESCC.[45, 46] ESCC with lymph node metastasis has been recognized as the stage IV which is the last stage of the tumor staging system. Some genes have been identified to participate in metastasis in ESCC such as *MUC1, NRP2, MMP* and *SPP1* which are found to be over-expressed in metastatic ESCC in the distant lymph node.[13, 25, 46]

1.2.3.5. Tumor Suppressor Genes and Proteins

Tumor suppressor genes, which are also called anti-oncogenes, are responsible for retarding the tumor growth and leading the tumor cells to process apoptosis.[47]Most of the tumor suppressor genes encode the proteins participating in cell cycle regulation to aid in suppressing or retarding the tumor development. They play a crucial role in the balance of cell proliferation and differentiation, and one of the primary controls has been found in the progression of G1/S phases during the cell cycle. During the progression of G1 phase into S phase, subsequent activation of cyclin-dependent kinases (CDKs) and their complementary regulatory subunits, cyclins such as CCND1 which has been mentioned before, will together phosphorylate Rb and result in release of E2F. E2Fs then trans-activate the genes for progression to S phase and proceed to DNA replication.[47] The proteins encoded by tumor suppressor genes including *p15, p16, p27* and *p53* can always inhibit this process.[47]

1.2.3.6. Other Proteins Related to Cancer Development

1.2.3.6.1. P-glycoprotein

P-glycoprotein (P-gp) is the product of human *MDR1* gene which is the first multi-drug resistance proteins (MRPs) to be identified.[48] MRP family has currently been found to have seven members which also confer a broad range of anti-cancer

drug resistance to the tumor cells and hence this usually dramatically reduces the effectiveness of clinical drugs to suppress the growth of cancer cells.[49, 50] Some of the mechanisms of MRPs have been elucidated such as alterations of the checkpoints in cell cycle, suppression of apoptosis and reduction of drug accumulation inside of the cells. All MRPs are also the ATP-binding cassette (ABC) efflux transporters which can export the carcinostatic drugs to the outside of the cells.[48, 49] It has been reported that P-gp (also called ABCB1 or MDR1) can actively bind and pump out the drugs against the concentration gradient by hydrolysis of ATP, therefore the anti-cancer drug cannot accumulate inside of the cells to trigger the cytotoxic effects.[50, 51] There are some commonly used anti-cancer drugs have been shown to be weaken by P-gp including vincristine, etoposide,paclitaxeland doxorubicin.[51-56]

1.2.3.6.2. COX-2

Cyclooxygenase (COX) can be divided in to two isotypes which are cyclooxgenase-1 (COX-1) and cyclooxygenase-2 (COX-2). *COX-1* is ubiquitously expressed in most of the tissues for its functions in maintaining homeostasis and it has been found to be non-inducible, whereas *COX-2* is inducible in response to different kinds of factors such as growth factors, mitogens and cytokines.[57, 58] COX-2 is the rate-limiting enzyme responsible for catalyzing the synthesis of prostanoids,

prostaglandins, prostacyclins and thromboxane. Prostaglandins such as prostaglandin E2 are the well-known molecules participating in carcinogenesis which promotes tumor growth, angiogenesis, metastasis and anti-apoptosis. The over-expression of COX-2 has been found in many types of cancer including ovarian cancer, pancreatic cancer, colon cancer, and esophageal cancer.[59-62]

1.2.3.6.3. Bcl-2 family

Bcl-2 family encoded proteins are widely-known as the most important factors participating in apoptosis, these proteins do not behave like the typical oncogenes as they usually modulate cell survivals through regulating apoptosis.[63, 64] Recently, there are at least 15 *Bcl-2* family member proteins such as Bcl-2, Bcl-X_L, Bax and Bad have been identified in mammalians. The whole family can be divided functionally into two major subgroups which are pro-apoptotic and anti-apoptotic proteins. The pro-apoptotic proteins, including Bax and Bad, promote cell death, whereas anti-apoptotic proteins such as Bcl-2 and Bcl-X_L prevent cell death. They together regulate the apoptosis by the extremely complicated mechanisms, for instance, Bax can promote apoptosis through either activating other pro-apoptotic proteins or inhibiting the anti-apoptotic proteins, and leads to mitochondrial fusion and fission that further induce apoptosis. [64-66]

1.2.3.6.4. p53

p53 is a transcription factor which functions as a tumor suppressor, and plays an important role in monitoring genome integrity and regulation of cellular growth signals.[61, 67] Mutation of *p53* is one of the most common genetic alterations found in human cancers such as ovarian cancer, colorectal cancer, esophageal cancer, breast cancer,and itsmutationsare highly frequent that has been found to be about 50% in all types of tumors.[68-70] When DNA damage or unusual growth signaling is present in the cells, p53 can stop the entry of cells into G1/S phase in cell cycle and hence leads to cell repair system or trigger cell apoptosis (programmed cell death). Mutation of *p53* will cause p53 malfunction, the tumor suppressing pathway of p53 will be disrupted and hence those unusual cells can escape from cell repair system or apoptosis.[67, 71, 72]Eventually, the tumor cells can grow uncontrollably and the tumor will be developed. Therefore, p53 is very important in suppression of tumor growth and metastases.

1.2.3.6.5. Retinoid Receptor

Retinoid receptors are defined as the steroid hormone receptor superfamily that has been divided into two major forms including retinoic acid receptors (RARs) and retinoid X receptors (RXRs), and each of them also consist of three subtypes

which are alpha(α), beta(β) and gamma(γ).[73-75]These receptors can act as the transcription factor in DNA-binding and modulation of transcription of the target genes in the ligand-activated state. Before RXRs function, they will dimerize with other nuclear hormone receptors like peroxisome proliferator-activated receptors (PPARs), farnesoid X receptor (FXR) and liver X receptor (LXR) to influence a series of signal transduction pathways.[74] Besides of the normal functions of retinoid receptors in lipid metabolism, they have been found to be highly associated with carcinogenesis. Some reports showed that some onco-proteins related to tumor development are up-regulated by these receptors.[75]

1.2.4. *Diagnosis and Staging*

Many types of cancers also had high mortalities, poor therapeutic responses and higher recurrent rates, early diagnosis has the great clinical significance on its prognosis. Earlier diagnosis can lead to earlier treatments of the cancers and it is very important for increasing the effectiveness of the therapies, since many types of cancer also rapidly metastasize and spread throughout the body and make the cases became worse.[76-78]

Traditionally, endoscopic biopsy combined with pathological assessments was used to preliminarily diagnose the development of some cancers.[79] As mentioned,

molecular alterations will largely occur when cancer cells are going to develop and that also leads to the significant changes in morphology including the tumor size and shapes, and the growth behaviors, and these macroscopic abnormalities could be identified by endoscopic biopsy and other techniques.[79, 80]

1.2.4.1. Advanced Endoscopic Assessment

Confocal fluorescence microscopy can be applied to diagnose different kinds of cancers through detection of the morphological alterations found in tissues of the dysplasia. As mentioned, many morphology changes are very significant and these can be directly identified under high-level microscopy.[81, 82] However, the cancer development with only slight changes is needed to be determined by other more advanced techniques.[83]

1.2.4.2. Molecular Techniques Used in Diagnosis

However, these morphological changes analyzed by endoscopic imaging are not easy to be observed in the early pathological changes since the early esophageal cancer, particularly at the stage of high-grade dysplasia, always has the normal macroscopic characteristics.[81, 83] Besides, the endoscopic assessment is very time-consuming and relies on consistent diagnostic techniques and interpretation from

the specialists. Although there are some newly developed endoscopic techniques with higher accuracy in diagnosis of esophageal cancers, screening of pathological alteration seems to be the much more ideal method to diagnose early development of cancers.

Molecular techniques used for diagnosing and staging cancers are more ideal than traditional endoscopic examination since they do not require any consistent specialist's interpretation and invasive sampling methods, and these techniques are usually not expensive and time-consuming. The developing techniques for detection of molecular alterations include identification of serum biomarkers, cytological detection, immune-histochemical staining.[84-87]

1.2.4.3. Identification of Serum Biomarkers

Identification of serum biomarkers is always used to screen any changes of molecular expression in order to diagnose the development of different cancers.[88, 89] It is a reliable method because obtaining serum samples is usually simple and quick. Progression of tumor development, even in the earlier stages, always shows different expression level of genes and proteins. After tumor cells die, they will release their proteins or molecules such as growth factors and cytokines into the circulation through their active secretion systems. The level of these proteins or

molecules can be instantly measured in order to detect any abnormal expression in the circulation.[90] Although the most appropriate biomarkers for clinical diagnosis have not been identified yet, more biomarkers are going to be identified and used for cancer diagnosis and staging because of the better understanding of the alteration of gene and protein expression in cancer development and progression, and development of the advanced techniques such as matrix assisted laser desorption ionization-time of flight mass spectrometry (MALDI-TOF MS) now.[90, 91]

1.2.5. *Current Cancer Therapy*

Conventionally there are some primary approaches for cancer therapies including surgical resection, complementary therapy, radiotherapy and chemotherapy.[92, 93]

Surgical resection is the approach to remove the tumor and sometimes the surrounding tissues in order to prevent the progression and spread of the malignancy, it is the most direct approach for cancer therapy. Although it is the oldest type of cancer therapy and it is still the primary treatment for many types of cancer nowadays.[24, 94] However, it usually results in many side-effects including malfunction of the resected tissues, pains, weaker immune system, fatigue, appetite loss and so on. It has been reported that the recurrent rate of cancer after resection was

quite high. For example, some studies showed that the patients who suffered from early-stage non-small cell lung cancer (NSCLC) developed recurrence and eventually dead even they were cured by surgical resection.[95] Moreover, it has been shown that most patients who suffered from metastatic live cancer had the recurrence and the median five-year survival rate of them was about 30%.[92, 93] Thus it shows the insufficiency of surgical resection for cancer therapy; therefore, surgical resection is usually combined with other approaches to treat cancers including radiotherapy and chemotherapy.[92, 96]

Radiotherapy uses high energy radiation such as X-ray or proton beams to directly damage the tumor cells. It is an efficient and effective approach to kill the cancer cells in the tissues, where the normal cells nearby are also affected by the high energy and hence dead or mutated. Therefore, it is possible that radiation therapy will increase the risk of developing a second cancer.[93, 96] As for the chemotherapy, some anti-cancer drugs are used to kill cancer cells and suppress their growth and progression. Current anti-cancer drugs are not selective enough to target and kill the cancer cells without damage of normal cells although they usually show higher cytotoxicity on cancer cells than normal cells. Therefore, treatment with anti-cancer drugs against cancers usually resulted in many side-effects like treating cancers by surgical resection which also leads to some unwanted effects.[92, 93, 96]

Despite there are many existing therapeutic regimes for treating cancers, the survival rates of patients suffered from different cancers are still very low.[11, 12, 92] Thus, it is necessary to develop some more effective and efficient approaches for cancer therapy. Currently, some targeted drugs have been developed for cancer therapies and they showed an excellent potential for treating cancers as they are highly selective and thus they can target and kill the cancers specifically without destructing the normal cells.[97-99] Nowadays, many novel therapeutics are being investigated and developed in order to improve the worse situation of cancer treatment.

1.3. QUINOLINE COMPOUNDS

1.3.1. *Introduction of Quinoline*

Quinoline, also called 1-aza-napthalene or benzo[*b*]pyridine, is a nitrogen-containing heterocyclic aromatic compound, its structure is shown in Figure 1.1. Its molecular formula and molecular weight is C_9H_7N and 129.16 $gmol^{-1}$ respectively.[100, 101] It has been reported that the core structure of quinoline appears in many natural sources or compounds such as cinchona alkaloids. The natural sources or compounds with the quinoline core usually show a wide range of pharmacological activities.[100, 102] The first natural compound containing the

quinoline nucleus is 4-hydroxy-6-methoxy-quinoline-2-carboxylicacid which was extracted from *Ephedra pachyclada ssp. sinaica*, and it has also been widely used as the traditional Chinese herbal medicine for the therapy of different diseases.[103, 104]

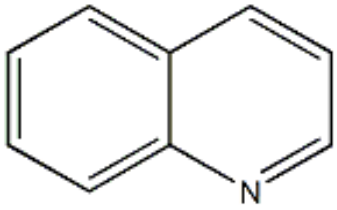

Figure 1.1. Core structure of quinoline.

1.3.2. *Medical Use of Quinoline Derivatives*

As mentioned, quinoline and its derivatives were widely used as the traditional herbal medicines against different diseases such as allergy, inflammation, microbial diseases, and cancers. [105, 106]

Nowadays, different quinoline derivatives are still being developed because of their high therapeutic activities with lower toxicities. For example, it was currently reported that some quinoline-based compounds showed the pharmacological activity in leishmanial and tubercular infections.[107] Besides, some studies also showed that the 8-hydroxyquinoline derivatives had the strong anti-tumor effects on a broad spectrum of cancers including breast cancer, liver cancer, bone cancers and so on. More importantly, the quinoline derivatives usually showed a lower toxicity in cancer

treatments, it showed the potentials of using quinoline derivatives as the anti-cancer therapeutics.[105, 106]

1.4. THIOSEMICABAZONE

1.4.1. *Introduction to Thiosemicarbazone*

Thiosemicarbazone is the compound containing the thiosemicarbazide radical (=N-NH-C(S)-NH_2) and the core structure of thiosemicarbazone is shown in the Figure 1.2.[108] Thiosemicarbazones have been studied for a period of time for their biological functions and they were found to be the chelators of metal ions to sequester the ions from the cellular environment.[109]

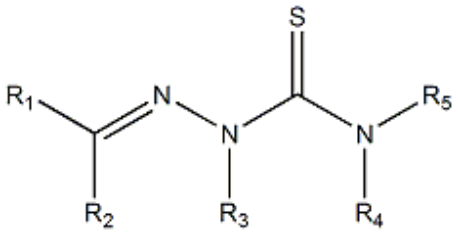

Figure 1.2. Core structure of thiosemicarbazone.

It has been reported that some of the thiosemicarbazones showed the marked iron-chelation effect and this property let these thiosemicarbazone derivatives to be the potential therapeutics since many diseases are risen from overloading of iron molecules.[110-112]

1.4.2. *Medical Use of Thiosemicarbazone*

As mentioned, thiosemicarbazones have been widely used for treating the diseases of iron overload because of their ability to chelate irons in cellular environment.[110, 111, 113] For example, thalassaemias is an iron-overloading disease arisen from mutations of the globin genes, it leads to insufficient supply of effective hemoglobin and results in anaemia.[114] This can be controlled by blood transfusion but it would cause increased uptake of gastrointestinal irons and eventually overload of irons. The thiosemicarbazones such as desferrioxamine (DFO) are the effective treatment for β-thalassemia since they are used to negatively regulate the cellular iron level.[114]

Moreover, it has been found that up-regulation of cellular irons leads to promote cancer development, hence thiosemicarbazones are being tested as an anti-cancer therapeutics for treating cancers. Recently, a derivative of thiosemicarbazones called 3-aminopyridine-2-carboxaldehyde thiosemicarbazone (Triapine) has entered clinical trials, it showed the high *in vitro* and *in vivo* cytotoxicity against neoplasia and other types of cancers by regulation cellular iron level.[114]

Therefore, thiosemicarbazone derivatives also show a great potential as the anti-cancer therapeutics which will be investigated in my study.

1.5. AIMS AND OBJECTIVES OF THIS STUDY

The present study has three primary aims as shown as below:

1. To study the effects of the quinolone derivative, 83b1, in human ESCC and identify the target and downstream regulated genes or proteins influenced by 83b1 that result in suppression of cancer growth.
2. To study the effects of the quinolone derivative, 160a, in human ESCC and identify the target and downstream effects of 160a that lead to suppression of cancer growth.
3. To study the effects of two novel thiosemicarbazones, DpC and Dp44mT, on suppression of cancer growth and invasion through upregulation of N-myc downstream regulated 1 (NDRG1) and downregulation of lysine-rich CEACAM1 co-isolated protein (LYRIC) in colon and prostate cancers.

The objectives related to Aim (1) are listed as follows:

i. To determine the *in vitro* and *in vivo* cytotoxic effects of 83b1 in human ESCC.

ii. To identify the target of 83b1 in human through *in silico* and *in vitro* assessment.

iii. To evaluate the downstream regulated genes and proteins affected by 83b1.

The objectives related to Aim (2) are listed as follows:

i. To determine the *in vitro* cytotoxic effects of 160ain human ESCC.

ii. To identify the target of 160a in human through *in silico* assessment.

iii. To evaluate the synergistic effects of 160a with Doxorubicin in human ESCC.

The objectives related to Aim (3) are listed as follows:

i. To evaluate the correlation between NDRG1 and LYRIC in cancer growth and invasion in human colon and prostate cancers.

ii. To determine the effects of DpC and Dp44mT on the expression of NDRG1 and LYRIC in human colon and prostate cancers.

iii. To evaluate the effects of DpC and Dp44mT on the translocation activities of LYRIC and NFκB in human colon and prostate cancers..

iv. To evaluate the downstream regulated proteins affected by DpC and Dp44mT in human colon and prostate cancers.

It has been shown that the quinoline and thiosemicarbazone derivatives have the great potential in cancer treatments. Therefore, this study aims at determining and evaluating the anti-cancer effects of the novel quinoline and thiosemicarbazone derivatives on different types of human cancers including esophageal, prostate and colorectal carcinomas. Different kinds of experiments were conducted to understand mainly the cytotoxicity and mechanisms of these novel derivatives in cancer treatments.

Chapter 2 MATERIALS AND METHODS

2.1. HUMAN CELL LINES

Four esophageal squamous cell carcinoma (ESCC) cell lines of Hong Kong Chinese origin, SLMT-1, HKESC-2, HKESC-3 and HKESC-4 were kindly provided by Professor Gopesh Srivastava of the Department of Pathology, the University of Hong Kong. The other three ESCC cell lines of Hong Kong Chinese origin, including, and five ESCC cell lines of Japanese origin, including KYSE-70, KYSE-150, KYSE-450, KYSE-510 and KYSE-520, were purchased from DSMZ (Braunschweig, Germany), the PPARD Vector (Cat. #: PV032302) purchased from Applied Biological Material Inc. was used in PPARD overexpression in KYSE150. The other cancer cell lines including two colorectal adenocarcinoma cell lines: HT29 and HCT15, a metastatic breast cancer cell line: MCF-7, a metastatic prostatic cancer cell line: DU145, a gastric adenocarcinoma cell line: AGS, a hepatocellular carcinoma: Hep3B and a lung cancer cell line: A549 were purchased from American Type Culture Collection (ATCC). The HT29 and DU145 used in Chapter 5 were provided by Prof. Des Richardson, the pCMV-tag2-FLAG-NDRG1(GenHunter) was used in NDRG1 overexpression and the empty pCMV-tag2-FLAG vector (Stratagene) was used as a negative control in HT29 and DU145. Two non-tumor esophageal epithelial cell lines including NE-1 and NE-3 were kindly provided by Professor George S. W.

Tsao from the Department of Anatomy, the University of Hong Kong. A human keratinocyte cell line, HEK001, was purchased from the ATCC.

2.2. CELL CULTURES

The cell lines including KYSE-70, KYSE-510, KYSE-520, HCT15, DU145, AGS and A549 were cultured in PRMI-1640 medium (Sigma-Aldrich) supplemented with 10% heat-inactivated fetal bovine serum (FBS, Sigma-Aldrich), while the cell lines including KYSE-150 and KYSE-450 were cultured in RPMI-1640 medium supplemented with 45% F-12 and 10% FBS. The cell lines HKESC-2, HKESC-3, HKESC-4, and SLMT-1 were cultured in MEMα medium (Sigma-Aldrich) supplemented with 10% FBS. Besides, the cell lines MCF-7, Hep3B, HT29 and HEK001 were cultured in DMEM medium (Sigma-Aldrich) with 10% FBS. However, HT29 was also cultured in McCoy's 5Amedium (Sigma-Aldrich) supplemented with 10% FBS for the experiments in chapter 5. The non-tumor esophageal epithelial cell lines, NE-1 and NE-3, were cultured in KSFM medium (Sigma-Aldrich) with suggested amount of complementary supplements including epidermal growth factor (rEGF) and bovine pituitary extract (BPE). All culture media were also supplemented with 100 units/ml penicillin Gand 100 μg/ml streptomycin (Sigma-Aldrich), and all

cell lines mentioned above were cultured at 37°C in a humidified incubator with 5% CO_2.

2.3. MEASUREMENT OF CELL PROLIFERATION

2.3.1. *Cytotoxicity Assay by MTS*

3-(4,5-Dimethylthiazol-2-yl)-5-(3-carboxymethoxyphenyl)-2-(4-sulfophenyl)-2H-tetrazolium (MTS) assay was performed to evaluate the growth inhibitory effects of 83b1 and 160a on the selected cell lines using the CellTiter96 AQueous One Solution (Promega, Madison, WI) for cell proliferation assay. In addition, the commonly used anticancer drugs, including cisplatin (CDDP) and doxorubicin (Dox), were used as the positive control for comparing the cytotoxicity of 83b1 and 160a.

5×10^3 cells were seeded onto each well of the 96-well plate and allowed to grow for 24 hours at 37°C with 5% CO_2. After incubation for 24 hours, the culture medium was then replaced by the fresh medium, and a gradually increased concentration of either 83b1, 160a, CDDP or Dox were added as the treatment. For 83b1 and CDDP, the concentration for treatment was increased from 0 μg/ml to 40 μg/ml. As for 160a, the concentration was from 0 μg/ml to 20 μg/ml, while the concentration of Dox was increased from 0 μg/ml to 1 μg/ml, and the plates were then incubated for either 48 hours or 72 hours at 37°C in dark. After incubation, the

supernatant including the medium and dead cells were removed, and 100 μl of diluted MTS solution was added onto each well. The plates were then incubated at 37°C in dark for 2 hours before reading the results. The absorbance at 495 nm was measured by using a micro-plate reader and normalized with the blanks treated with the same conditions without adding the cells. Finally, the curves of viability against dosage were plotted and the half maximal inhibitory concentration (IC_{50}) of the drugs against each cell lines was determined.

2.3.2. *Proliferation Assay by MTS*

Similar to the cytotoxicity assay, MTS reagent was used. 2×10^3 cells were seeded onto each well of the 96-well plate and allowed to grow for 24 hours at 37°C with 5% CO_2. After incubation for 24 hours, the culture medium was then replaced by the fresh medium with the gradual increase concentration of PPARD agonist, GW0742, from 0 nM to 1 nM, and the plate was then incubated at 37°C in dark for 24, 48 and 72 hours. For each time point, the corresponding plate was taken out for MTS assay as the cytotoxicity assay mentioned above. The proliferation curves were plotted for comparing the proliferative effect of GW0742 on the cancer cell lines of KYSE-450 and SLMT-1.

2.4. MOLECULAR DOCKING ANAYSIS

Evaluation of the possible molecular binding targets of 83b1 was conducted based on the similarity ensemble approach (SEA) using the search engine available from **http://sea.bkslab.org**.[115] The binding of our compounds including 83b1 and 160a to the protein targets was predicted based on molecular structures matched against the ChEMBL medicinal chemistry database version 12 and the updated version in 2017. The program of Chemdraw was used for generating the the structure of 83b1 and 160a in computer in MOL format, and STRUCTURE-TO-SMILE translator was used for translating the structure of 83b1 and 160a to their corresponding SMILE format. The SMILE of 83b1 and 160a was input to the search engine respectively for determining the corresponding targets in human.[115]

After the human targets were predicted by the SEA program, another molecular docking program in the Docking Server: **http://www.dockingserver.com/web** was used to determine the binding affinity of 83b1 to its predicted target relative to the natural ligand, arachidonic acid (AA), and the binding affinity of 160a to its predicted targets relative to the well-known substrates or blockers of the target. The three-dimensional structures, the possible interactions and interaction energy of the compounds and either the natural ligand or antagonists to their targets respectively were then created and predicted by the server.

All the calculation of the interaction energy was conducted also using the algorithms designed in the Docking Server.[116]

2.5. ISOTHERMAL TITRATION CALORIMETRY ASSAY (ITC)

The Malvern MicroCal PEAQ-ITC Automated Ultrasensitive Isothermal Titration Calorimeter (ITC) was used to analyze the binding affinity of 83b1 to PPARD protein.

Recombinant Human PPARD protein (Creative BioMart, US) and Human Serum Albumin (HSA) (Sino Biological, US) were firstly diluted to 15 μM in the filtered Tris-HCl buffer (20 mM Tris-Hcl pH 8.0, 100 mM KCl, 0.2 mM EDTA, 1 mM DTT and 20% glycerol). The substrates including 83b1 and Arachidonic acid (AA)(Cayman, Ann Arbor, MI)were dissolved in DMSO in different concentration according to the below table:

Concentration of PPARD (μM)	Concentration of 83b1 (μM)	Concentration of AA (μM)
15μM	0	0
	75	0
	300	0
	600	0
	0	150
Concentration of PPARD (mM)	Concentration of 83b1 (mM)	Concentration of AA (mM)

15	150	0
	0	150

Table 2.1. Combination of 83b1 or AA with PPARD or HSA for the ITC Assessment.

The diluted proteins and substrates were added into the 96-well rack which was then put into the ITC machine for measurement according to the manufacturer's instructions. The results were then obtained by using the software correlated with the machine.

2.6. IMMUNOHISTOCHEMICAL STAINING

At first, cell pellets were prepared by harvesting the living cells cultured in nutrient-rich medium and washes by PBS before fixing. After the pellets were prepared, 1 ml of formalin solution (Sigma-Aldrich, USA) was used to fix the pellets followed by paraffin-embedding. The cells embedding in paraffin were cutting into a thin section of 16 μm and mounted on the glass slides. The sections containing the cells were then de-paraffinized and rehydrated by soaking in xylene, ethanol, and deionized water. Microwave was used to heat the side to retrieve the antigen of the cells for 10 to 15 minutes and let the slides cool down for about 30 minutes, the slides were then washed in distilled water for 10 minutes. Afterward, the slides were incubated with the specific primary antibodies diluted in 1% BSA/PBS-T (according

to the manufacturer's instruction) at 4^{o}C overnight, the slides were then washed by PBS-T and incubated with enzyme-conjugated secondary antibody for 1 hour at room temperature. Finally, diaminobenzidine tetrachloride (DAB)was added, the images were detected by microscopy. Primary antibody: PPARD (1:500) (Origene, USA), P-gp (1:500) (Abnova, Taiwan).

2.7. TRANSFORMATION OF PLASMID INTO BACTERIA

2.7.1. *Transformation*

ArcticExpress (DE3) RP competent cells (Agilent Technology, USA) was used for transformation. Competent cells were firstly thawed on ice and then mixed with 2 µl of diluted XL10-Gold β-mercaptoethanol (provided with the kit), the cells were swirled gently on ice for 10 minutes. Afterwards, 25 ng of expression plasmid DNA containing the gene of interest was added to the tube of competent cells, the tube was then incubated for 30 minutes on ice. After incubation, the tube was incubated at 42^{o}C water bath for 25 seconds and immediately put on ice for 2 minutes, 600 µl of pre-warmed super optimal broth with catabolite repression (SOC) medium was added to the cells and incubated at 37^{o}C for 1 hour on a shaker at 225 rpm. LB agar plates were prepared by mixing 100 ml of LB molten agar with kanamycin in a final concentration of 50 µg/ml. 50 µl or 100 µl of the cells were added and spread on

the agar plates, therefore, the plasmid DNA containing the kanamycin-resistant gene can be selected and grows on the plates at 37^{o}C overnight.

On the second day, single colony was picked out and incubated in 10 ml LB broth with kanamycin in a final concentration of 50 μg/ml for 18 hours. The bacterial cells were then used for plasmid extraction or stored at -80^{o}C in 50% glycerol/LB.

2.7.2. *Plasmid Extraction*

Hybrid-QTM Plasmid Rapid prep kit (GeneAll, USA) was used for plasmid extraction. 3 ml of bacterial cells were pelleted by centrifugation at 10,000 rpm for 1 minute in 1.5 ml eppendorf tube (by collecting repeatedly). Supernatant was discarded and 170 μl of re-suspension buffer (buffer S1) was added to thoroughly re-suspend the cell pellet. 170 μl of lysis buffer (buffer S2) was added to the bacterial cells and mixed by inverting for 5 times. The bacterial cells were then incubated at room temperature for 4 minutes for cell lysis. Afterwards, 250 μl of precipitation buffer (buffer G3) was added to the cell lysate for DNA precipitation, the tube was gently inverted for 10 times for complete precipitation of DNA. The lysate was then transferred to EzClear^{TM} filter column and centrifuged at 10,000 rpm for 1 minute, the upper EzClear^{TM} filter column unit and the flow-through were discarded. 700 μl of washing buffer (buffer PW) was added to wash the filter membrane and centrifuged at

10,000 rpm for 1 minute, this washing step was repeated once again. The column was put into a new 1.5 ml Eppendorf tube, 50 µl of nuclease-free water was carefully added exactly on the filter membrane of the column and incubated at room temperature for 1 minute. Finally, the plasmid DNA was obtained by centrifugation at 10,000 rpm for 1 minute. The plasmid of interest was examined by PCR and gel electrophoresis.

2.8. PLASMID TRANSFECTION

Approximately30%confluent cells grown on 6-well plates were transfected with 2 ng of interested plasmid DNA. 2 ng of plasmid was added to 100 µl of pure medium without adding FBS in a final volume with 3µl of FuGENE HD transfection reagent (Promega) in a PCR tube, the tube was vortexed and then incubated at room temperature for 15 minutes.

The medium on the 6-well plate was replaced by the fresh medium, the transfection mixture was then added to the respective well drop by drop. Afterwards, the cells were incubated in a humidified incubator at 37^{o}C for 3 days to let the cells grow and process the transfection. After 3 days, the cells were transferred to a bigger flask and relative amount of antibiotic, such as geneticin (G418; Thermo Scientific, USA) and hygromycin (Thermo Scientific, USA), was used for selecting the

transfected cells. The expression of the gene of interest was examined by PCR and gel electrophoresis.

2.9. GENE SILENCING BY SMAILL INTERFERING RNA (siRNA)

Approximately 60% confluent cells (parental cell lines or transfected cell lines) grown on 6-well plates were transfected with either 1nM of LYRIC Silencer® Select siRNA duplexes (si-LYRIC; Thermo Scientific, USA) or10nMof Silencer® Negative Control siRNA (si-Ctrl) by mixing with10nM of Lipofectamine 2000® (Invitrogen, Carlsbad, CA, USA). 150 µl of si-RNA was firstly mixed with 150 µl of lipofectamine followed by incubation at room temperature for 5 minutes. The medium was removed and the cells were rinsed by Opti-medium (Thermo Scientific, USA) followed by adding 2 ml Opti-medium on each well. 150 µl of siRNA mixture was added to the cells and incubated at 37^{o}C with 5% CO_2 for 1 day, fresh medium was then added for a further 48 hours incubation at 37^{o}C with 5% CO_2. Afterward, the cells were harvested for analysis.

2.10. REVERSE TRANSCRIPTION POLYMERASE CHAIN REACTION (RT-PCR)

2.10.1. *RNA Extraction from Cell Lines*

For Chapters 3 and 4, total RNA was extracted by using the RNeasy Mini Kit (Qiagen, CA, USA) and it was performed according to the manual suggested. Approximately 80% confluent cells grown on the bottom of 25 cm^3 flask were used for RNA extraction after corresponding treatments (83b1, GSK3787 which is a PPARD agonist or DMSO as the negative control) or without any treatment. The cells were firstly suspended by using a scrapper. Suspended cells in medium were centrifuged at 1,500 rpm, the medium was then removed. 4 ml of phosphate buffer saline (PBS) was added to re-suspend the pellet, and suspended cells in PBS were centrifuged at 1,500 rpm to acquire the cell pellets. The cell pellets were firstly re-suspended by adding 300 μl lysis buffer RLT, 600 μl of 70% ethanol was then added to the lysate. Each of the lysate was transferred into each RNeasy spin column and was centrifuged at 12,000 rpm at room temperature for 1 minute, the flow-through was then discarded. 700μl of washing buffer RW1 was added to the column for washing purpose and was centrifuged at 12,000 rpm at room temperature for 1 minute, the flow-through was then discarded. After that, 500 μl of another washing buffer PRE buffer was added to the column and was centrifuged at 12,000 rpm at room temperature for 1 minute, the flow-through was then discarded, this step was repeated once again. After that, the column was put onto a new 1.5 ml Eppendorf tube, 50 μl of RNase-free water was added into the column and incubated for 1

minute on ice. Finally, the RNA was collected by centrifugation at 12,000 for 1 minute. The concentration of RNA was measured by CLARIOstar microplate reader (BMG LABTECH, Germany) and the quality of RNA was analyzed by 1.5% agarose gel electrophoresis.

As for Chapter 5, the total RNA was extracted by using TRI-reagent (Applied Biosystems, CA, USA). Approximately 80% confluent cells grown on the petri dish were used for RNA extraction after corresponding treatments (DFO, DpC, Dp44mT or DMSO as the negative control) or without any treatment. The medium was firstly removed, 2 ml of PBS was then added to wash the dish and was removed. 2 ml of TRI-reagent was added to homogenized the cells for 5 minutes and transferred into a 1.5 ml eppendorf tube. 200 µl of chloroform was then added to the lysate, the tube was inverted 10 times and incubated at room temperature for 15 minutes. After that, the tube was centrifuged at 12,000 rpm at 4^{o}C for 15 minutes to separate the two phases which are the aqueous and phenol-chloroform phase, the upper aqueous phase containing the RNA was then transferred into a new tube. 500 µl of isopropanol was added to the aqueous solution, the tube was inverted 10 times and then incubated at room temperature for 10 minutes for RNA precipitation. The tube was then centrifuged at 12,000 rpm at 4^{o}C for 8 minutes to obtain the visible RNA pellet, the

supernatant was removed. The RNA pellet was then washed by 75% ethanol for two times and placed at room temperature to make sure the pellet was dried. Finally, 50µl of diethyl pyrocarbonate (DEPC)-treated water was added to dissolve the RNA pellet at room temperature. The concentration of RNA was measured by Nanodrop 1000 spectrophotometer (Thermo Scientific, Erembodegem, Belgium).

2.10.2. *Reverse Transcription-Polymerase Chain Reaction (RT-PCR)*

For Chapter 3 and 4, reverse-transcriptase (Promega) was used to convert the messenger RNA (mRNA) into complementary DNA (cDNA). 0.2 µg of total RNA was mixed in a PCR tube with 4 µl of 5X reaction buffer, 2 µl of 25 mM $MgCl_2$, 0.5 µg of random primers and oligo$(dT)_{15}$ primers, 1 µl of 10 mM PCR nucleotide mix, 20 u of ribonuclease inhibitor, and 0.5 µl of reverse transcriptase in a total volume of 20 µl for cDNA synthesis, all steps were performed on ice. The tubes with the samples were put in a thermo-cycler with the thermal cycling profile as follow: 25^{o}C for 5 minutes, 40^{o}C for 1 hour and 70^{o}C for 15 minutes. After the whole process, the cDNA was instantly used or stored at -20^{o}C for later use. While for Chapter 5, RT-PCR was performed together with PCR amplification in one-step reaction and it was mentioned in further section.

2.11. DETECTION OF mRNA EXPRESSION

2.11.1. *Amplification of cDNA by PCR*

For chapter 3 and 4, PCR reaction was performed by using AmpliTaq Gold DNA polymerase (Applied Biosystems). For one reaction, 4 μl of cDNA template was mixed in a PCR tube with 2 μl of 10X PCR buffer, 1μl of 25 mM $MgCl_2$, 0.4 μl of 10 mM dNTP mix, 1.25 u of AmpliTaq Gold DNA polymerase, 0.4 μM of β-actin forward and reverse primer, and 1.6 μM of forward and reverse primers of the target genes in the total volume of 20 μl. The tubes with the samples were put in the thermo-cycler (MWG-BIOTECH, Germany) with the thermal cycling profile as follow: denaturation of cDNA at 95^{o}C for 4 minutes followed by 30 cycles of denaturation at 95^{o}C for 1 minute, annealing at 60^{o}C for 1 minute and primer extension at 72^{o}C for 1 minute. Finally, there is a further extension step at 72^{o}C for 4 minutes. After the whole process, the samples were instantly analyzed by gel electrophoresis or stored at -20^{o}C for later use.

As for Chapter 5, as mentioned, RT-PCR was performed together with PCR amplification by SuperScript™ III One-Step RT-PCR System with Platinum™ Taq DNA polymerase (Life Technologies, CA, USA). 0.12 μg of total RNA was mixed with 10 μl of 2X reaction mix, 0.2μM of forward and reverse primers of the target gene and β-actin and 0.8μl of SuperScript™ III RT/Platinum™ Taqmix in a total

volume of 20 µl. The tubes with the samples were put in the thermo-cycler with the thermal cycling profile as follow: cDNA synthesis at 56°C for 30 minutes followed by 94°C for 2 minutes, PCR amplification with 30 cycles of denaturation at 94°C for 15 seconds, annealing at 56°C for 30 seconds and primer extension at 68°C for 1 minute. Finally, there is a further extension step at 68°C for 5 minutes. After the whole process, the samples were instantly analyzed by gel electrophoresis or stored at -20°C for later use.

The specific primers for COX-2, PPARD, PTEN, β-actin were shown below:

GENE	PRIMER	SEQUENCE
COX-2	Forward	5'-CCAGCACTTCACGCATCAGT-3'
	Reverse	5'-ACGCTGTCTAGCCAGAGTTTCAC-3'
PPARD	Forward	5'-CACATCTACAATGCCTACCT-3'
	Reverse	5'-CTTCTCTGCCTGCCACAATGTCT-3'
VEGF-A	Forward	5'-CGGTATAAGTCCTGGAGCGT-3'
	Reverse	5'-TTTAACTCAAGCTGCCTCGC-3'
β-actin	Forward	5'-GTGGGGCGCCCCAGGCACCA-3'
	Reverse	5'-CTCCTTAATGTCACGCACGATTTC-3'

Table 2.1. The nucleotide sequences of the primers used in RT-PCR.

2.11.2. *Gel Electrophoresis*

1.5% agarose gel was prepared by dissolving 0.75 g agarose powder (Invitrogen, USA) in 50 ml 1X TBE buffer, and heated by microwave. GelRed (Biotium, CA, USA) was then added for staining the DNA in the gel. Gel

electrophoresis was performed in 1X TBS buffer at 100V for 1 hour. The DNA bands in the gel were then detected and analyzed by ChemiDoc XRS (Bio-Rad, USA).

2.11.3. *Real-time quantitative PCR of cDNA*

For Chapter 3 and 4, GoTaq qPCR system (Promega) was performed to analyze the mRNA expression of target genes in real-time PCR. After 2 μg of total RNA was extracted and reverse-transcribed into cDNA as mentioned above, 2 μl of the cDNA was mixed in a PCR tube with 10μl of 2X qPCR master mix with SYBR green dye, 2 μl of 2 μM forward and reverse primers of either target genes or reference gene (Glyceraldehyde 3-phosphate dehydrogenase, GAPDH) in a total volume of 20 μl. All 20 μl of sample mixtures were added into the wells of PikoReal 96-well strips, and the qPCR reactions were carried out through PikoReal Real-Time PCR System (Thermo Scientific, Erembodegem, Belgium). The thermo-cycling profile was as follow: polymerase activation at 95^{o}C for 2 minutes followed by 40 cycles of denaturation at 95^{o}C for 15 seconds, annealing and primer extension at 60^{o}C for 1 minute. Threshold cycle (Ct) for each sample was then determined and recorded by the program PikoReal Software 2.0 (Thermo Scientific, Erembodegem, Belgium).[117]

As for Chapter 5, SensiFASTSYBR No-ROX qPCR kit (Bioline, NSW, Australia) was performed to analyze the mRNA expression of target genes in real-time PCR. After 0.12 μg of total RNA was extracted and reverse-transcribed into cDNA as mentioned above, 50 ng of the cDNA was mixed in a PCR tube with 10 μl of 2X SensiFASTSYBR No-ROX Mix, 0.8 μl of 10 μM forward and reverse primers of either target genes or reference gene (β-actin) in a total volume of 20 μl.The thermo-cycling profile was as follow: polymerase activation at 95°C for 2 minutes followed by 40 cycles of denaturation at 95°C for 10 seconds, annealing at 60°C for 20 seconds and primer extension at 72°C for 45 seconds. Ct for each sample was then determined and recorded by the program LightCycler 480 Software (Roche, NSW, Australia).[118]

For all the qPCR reactions in Chapters 3, 4 and 5, the relative expression of target genes in different samples were compared by using $2^{-\Delta\Delta Ct}$ method and the expression level of the target genes was normalized by the reference gene, β-actin, as mentioned. Besides, melting curves were also recorded by gradual increase of temperature until the fluorescent signal was dropped to zero after 40 cycles of amplification were finished.

The calculation of $2^{-\Delta\Delta Ct}$ method was as follow: [119, 120]

$$\Delta Ct \text{ of target gene} = Ct \text{ of target gene} - Ct \text{ of reference gene}$$

$\Delta\Delta$Ct of target gene = ΔCt of target gene in treated group - ΔCt of target gene in control group

Therefore, the fold change of gene expression level = $2^{-(\Delta\Delta Ct \text{ of target gene})}$

The specific primers for COX-2 and GAPDG were shown below:

GENE	PRIMER	SEQUENCE
COX-2	Forward	5'-CCAGCACTTCACGCATCAGT-3'
	Reverse	5'-ACGCTGTCTAGCCAGAGTTTCAC-3'
GAPDH	Forward	5'-AAATCAAGTGGGGCGATGCTG-3'
	Reverse	5'-GCAGAGATGATGACCCTTTTG-3'
NDRG-1	Forward	5'-TCACCCAGCACTTTGCCGTCT-3'
	Reverse	5'-GCCACAGTCCGCCATCTT-3'
LYRIC	Forward	5-GTTGAAGTGGCTGAGGGT-3'
	Reverse	5'-GGAAATGATGCGGTTGTA-3'
β-actin	Forward	5'-CCCGCCGCCAGCTCACCATGG-3'

Table 2.2. The nucleotide sequences of the primers used in real-time PCR.

2.12. ENZYME-LINKED IMMUNOSORBENT ASSAY (ELISA)

The effects of 83b1 on the production of PGE2 in the cell lines (KYSE-150, KYSE-450, and SLMT-1) were examined using an enzyme-linked immuno-sorbent assay (ELISA) kit (Cayman, Ann Arbor, MI).

Approximately 1×10^6 cells from each cell line were evenly separated into eight replicates and then seeded for 24 hours. Three different concentrations of 83b1 (5, 10, and 20 μg/ml) and a negative control (0.05% DMSO) were used to incubate the cells for 48 hours. The culture medium was then removed for quantitative

determination of PGE_2 at 405 nm by a microplate reader with reference to the standard curve according to the manufacturer's instructions.

2.13. FLOW CYTOMETRIC ANALYSIS

8×10^5 cells were seeded onto each well of the 6-well plate and allowed to grow for 24 hours at 37°C with 5% CO_2. After incubation for 24 hours, PBS was used to rinse the cells once and1ml of the culture medium was then added with the gradually increased concentration (2, 5 and 10 μg/ml) of 160a, Cyclosporin A (1:1000 diluted in appropriate medium) as a positive control and 0.05% DMSO as a negative control, the cells were then incubated at 37°C for 30 minutes. Afterwards, 1ml of diluted Calcein AM (0.2 μl in 7 ml medium) was added to the cells and the cells were incubated for further 25 minutes, one of the wells was double-negative (without treatment and Calcien AM). After incubation, the cells were harvested and put into a 1.5 ml eppendorf tube. The tubes were then centrifuged at 8,000 rpm for 2 minutes to obtain the cell pellets, the cells were re-suspended by appropriate medium and analyzed by the BD Accuri C6 flow cytometry (BD Biosciences, CA, USA).

0.05% DMSO ×Calcein AM	0.05% DMSO ✓Calcein AM	2 μg/ml 160a ✓Calcein AM
5 μg/ml 160a ✓Calcein AM	10 μg/ml 160a ✓Calcein AM	Cyclosporin A ✓Calcein AM

Table 2.3. Treatment of cell lines with 160a and Calcein AM in 6-well plate.

2.14. CONFOCAL MICROSCOPIC DETERMINATION

8×10^5 cells were seeded onto each well of the 6-well plate and allowed to grow for 24 hours at 37°C with 5% CO_2. After incubation for 24 hours, PBS was used to rinse the cells once and1ml of the culture medium was then added with the gradually increased concentration (2, 5 and 10 μg/ml) of 160a, Cyclosporin A (1:1000 diluted in appropriate medium) as a positive control and 0.05% DMSO as a negative control, the cells were then incubated at 37°C for 30 minutes. Afterwards, 1ml of diluted Calcein AM (0.2 μl in 7 ml medium) was added to the cells and the cells were incubated for further 25 minutes, one of the wells was double-negative (without treatment and Calcien AM). After incubation, the medium was replaced by PBS and the cells were then analyzed by Leica TCS SPE Confocal microscopy (Leica, USA)

2.15. IN VIVO NUDE-MICE XENOGRAFTS MODEL

Athymic nude mice 4 weeks of age were purchased from the State Key Laboratory of Chinese Medicine and Molecular Pharmacology (Shenzhen, China), the Hong Kong Polytechnic University. All procedures were approved by the ethics committee of the State Key Laboratory of Chinese Medicine and Molecular

Pharmacology (Shenzhen, China), the Hong Kong Polytechnic University. For preparation of the nude mice xenograft model, approximately 80% confluent KYSE450 cells were harvested by trypsinization and injected subcutaneously into the mid-dorsal region of athymic nude mice. Tumor was allowed to grow without any treatment until the tumor size reached about 150 mm^3, the tumor was then harvested from the nude mice and divided into ten even pieces of approximately 1 mm^3 each under PBS. Each of the pieces of the tumor was transplanted into the flanks of ten nude mice and the tumors were then allowed to grow until the tumor size was about 150 mm^3. The fifteen nude mice were randomly divided into two groups which were the 83b1 treatment group and the control group. 83b1 was dissolved in 6% PEG and then injected into five nude mice intraperitoneally at a final dosage of 10 mg/kg/day. The rest of the nude mice was used as the vehicle control with 6% PEG.

The tumor dimension was measured everyday calipers, the tumor volume was then estimated by using the two-dimensional measurements of length and width followed by the calculation with the formula [l x w^2] x 0.52, while l is the length and w is the width. After the treatment for 4 weeks, the nude mice were sacrificed by CO_2 inhalation. The xenografts in the nude mice were harvested, the xenograft tumor was fixed in 10% formalin for later study. Besides, the blood of each nude mice treated with either 10 mg/ml or 50 mg/ml 83b1 were also extracted for evaluation of liver

functions through determination of the amount of albumin (ALB), alanine aminotransferase (ALT), aspartate aminotransferase (AST), urea and total bilirubin (TBil) in blood by using Hitachi 7600-210 automatic biochemical analyzer

2.16. DETECTION OF PROTEIN EXPRESSION BY BIOPLEX PRO CELL SIGNALING ASSAY

2.16.1. *Protein Extraction*

Bio-Plex Pro™ Cell Signaling MAPK Panel (9-plex) assay kit (#LQOOOOOS6KL8lS) (Bio-Rad, USA) was used to quantitatively measure the protein expression in designated pathway. Approximately 50% confluent of KYSE-450 and HKESC-4 cells grown on the bottom of 6-well plates were treated with 83b1 in the gradually ascending concentration (0, 10, 30 μg/ml or DMSO as the negative control) for 48 hours at 37^{o}C with 5% CO_2. After 48 hours, the medium was removed and cold signaling cell washing buffer was then added to the wells to stop the treatment. Cell lysis buffer was added to the cell, the cells were lysed by the buffer with gently scraping. The mixture was transported to eppendorf tubes and stored at 4^{o}C for 20 minutes, afterwards, the cell lysates were obtained by centrifugation at 14,000 rpm for 10 minutes at 4^{o}C.

2.16.2. *BCA Assay*

Pierce BCA Protein Assay Kit (Thermo Scientific, USA) was used to quantify the amount of the whole cell protein lysates. BCA buffer A was mixed with BCA buffer B in a ratio of 50:1, the color of mixture was changed to green from blue. The calibration curve was constructed by making the serial dilution of bovine serum albumin (BSA) standard from 0μg/ml to 2000 μg/ml followed by mixed with 1ml BCA mixture and incubated at 37ºC for 30 minutes. The protein lysate was then diluted 20-fold by milli-Q H_2O and mixed with 1ml BCA mixture also followed by incubation at 37ºC for 30 minutes. After incubation, the absorbance of the serial dilutions of BCA standard was measured by a spectrophotometer at 562 nm and the calibration curve was plotted. Afterwards, the absorbance of the protein samples were also measured at 562 nm and the amount of protein was calculation according to the calibration curve and dilution factors.

2.16.3. *Quantitative Determination of Protein Expression*

The concentration of the protein lysates was diluted to 200 ug/ml by the cell resuspension buffer provided in the assay kit and the protein lysates were analyzed according to the to the manufacturer's instructions. By using the assay kits, the phosphorylated cancer-related proteins, including p-ATF2 (Activated transcription

factor-2), p-HSP27 (Heat shock protein-27), p-JNK1 (c Jun N-terminal kinase-1/MAPK8), p-p38-MAPK (p38 mitogen-activated protein kinase/MAPK11), p-MEK1 (Mitogen-activated protein kinase kinase/MAP2K1),and p-AKT1 (RAC-alpha serine/threonine-protein kinase-1) in KYSE-450 and HKESC-4 treated with 83b1 were analyzed.

2.17. DETECTION OF PROTEIN EXPRESSION IN CHAPTER 4

2.17.1. *Protein Extraction*

Approximately 80% confluent cells grown on the bottom of 6-well plates were used for protein extraction after corresponding treatments (DFO, DpC, Dp44mT or DMSO as the negative control) or without any treatment. At first, the medium was removed and the wells were rinsed with PBS for two times. 200 μl of self-prepared cell lysis buffer containing 10 mM Tris buffer, 150 mM NaCl, 0.5% SDS, 1% Triton X-100, 1 m EDTA, 0.04 mM NaF and 8 μl of protease inhibitor cocktail solution (Sigma-Aldrich), was added to each of the wells, the cells were then suspended by using a scrapper on ice. Suspended cells in lysis buffer were transferred into a 1.5 ml eppendorf tube and sonicated to further break down the cells. The tubes were then centrifuged at 14,000 rpm for 40 minutes at 4^{o}C, the supernatant containing the

proteins was transferred into a new 1.5 ml eppendorf tube for further analyses or storing at -80^{o}C.

2.17.2. *BCA Assay*

The procedures were the same as that shown in 2.16.2.

2.17.3. *Western Blotting*

Western blotting was performed to compare the expression of different proteins in the cell lines with different treatments. 5 μl of 5X SDS loading buffer, which contains 0.05% bromophenol blue, 5% β-mercaptoethanol, 20% glycerol, 0.2 M Tris-HCl pH 6.8 and 10% SDS, was mixed with 20 μl of diluted protein sample (40 to 100 μg) and boiled at 95^{o}C for 5 minutes. The protein samples were separated by the 4% stacking gel followed by 8 to 12% SDS-polyacrylamide separating gel depending on the molecular size of the interested proteins. The samples and the protein standard marker (Bio-Rad, USA) were then loaded into the wells of the gel, the gel electrophoresis was carried out at 80V for 30 minutes followed by 100V for 2 hours.

Afterwards, the stacking gel was removed from the separating gel, and the separating gel with the interested proteins was used for protein transfer. The gel was

firstly soaked and washed by the transfer buffer and then placed on the PVDF membrane followed by putting into the mini-transblot cell (Bio-Rad, USA) for protein transfer at 100V for 1 hours. After the protein transfer, the membrane containing the protein of interested was firstly fixed by methanol and then cut according to the protein size depending on which proteins were going to be determined after it was dried. The membranes were then incubated with the specific primary antibody diluted by 5% milk or BSA according the manufacturers' recommendation at 4^{o}C on a shaker overnight. On next day, the membranes were washed with Tris Buffered Saline with Tween (TBS-T) for three times with 10 minutes each. After that, the membranes were incubated with the diluted corresponding horseradish peroxidase (HRP)-conjugated secondary antibody by 5% milk according to manufacturers' recommendation at room temperature on a shaker for 1 hour.

Finally, the membranes were washed with TBS-T for three times with 10 minutes each again followed by adding the Luminata HRP western substrate, either Forte, Crescendo or Classico (Merck Millipore, NSW, Australia). ChemiDoc XRS (Bio-Rad, USA) was used to visualize the expression of proteins, and the software Imagelab (Bio-Rad) was used to record and analyze the results.

For the western blotting, the primary antibodies used were NDRG1 (1:2000) and LYRIC (1:1000) (Abcam, Cambridge, UK); vimentin (1:1000), NFκB p65

(1:1000), E-cadherin (1:1000), PTEN (1:000), PI3K-p85 (1:1000), PI3K-p110α/β/γ (1:1000), AKT (1:1000), p-AKT (1:1000) and c-Myc(1:1000) (Cell Signaling Technology, MA, USA); and β-actin (1:10000) (Sigma-Aldrich).While the secondary antibodies used were anti-goat (1:10000), anti-rabbit (1:10000) and anti-mouse (1:10000) antibodies (Sigma-Aldrich).

2.18. IMMUNOFLUORESCENT STAINING

Approximately 30% confluent of cells was firstly grown on a 70% ethanol-sterilized cover slip in 24-well plate at 37ºC with 5% CO_2 for 1 day, different treatments (DFO, DpC, Dp44mT or DMSO as the negative control) were then applied to the cells on the second day for a certain period of time also at 37ºC with 5% CO_2. Afterwards, the medium was removed and the wells were rinsed with PBS for two times, 180 μl of 4% cold paraformaldehyde (PFA) was then added to each well for cell fixation for 10 minutes at room temperature. PFA was removed and the wells were rinsed with PBS for three times with 5 minutes each, 180 μl of Triton was then added to each well for permeabilization of the cell membrane for 5 minutes at room temperature. Triton was removed and the wells were rinsed with PBS for three times with 10 minutes each, 180 μl of 5% BSA in PBS was then added to the cells for blocking the non-specific binding of antibody to the proteins for one hour at room

temperature. BSA was removed and the wells were rinsed again with PBS for three times with 5 minutes each, 180 µl of primary antibody (in 1%BSA diluted by PBS) was added to the cells and the cells were incubated at 4^{o}C for 24 hours.

After incubation, the primary antibody was removed and the wells were rinsed with PBS for three times with 5 minutes each. Secondary antibody complementary to the primary antibody was added to the cells and the cells were incubated at room temperature for one hour in dark. Afterward, secondary antibody was removed and the wells were rinsed with 0.2% BSA in PBS for three time with 10 minutes each followed by PBS for two times with 5 minutes each.

Finally, the glass cover slips were taken out from the wells by using the forceps carefully and mounted on the glass slides with a single drop of Pro-Long Gold anti-fade mounting solution containing 4',6-diamidino-2-phenylindole (DAPI; Invitrogen, USA). The fluorescent signal was then determined by using a Zeiss fluorescent microscope equipped with an AxioCam camera, all images were taken and analyzed using AxioVisionsoftware (Carl Zeiss AG, Germany). Mander's overlap coefficient was determined using ImageJ (National Institutes of Health, Maryland, USA) and the co-localization intensity of the proteins of interest was examined by using the intensity value determined also through ImageJ software. Mander's coefficient was determined or comparing the co-localization intensities of LYRIC and

NFκB or NFκB and DAPI by using ImageJ software (National Institutes of Health, USA).

The two primary antibodies used were anti-LYRIC antibody (Abcam) and anti-NFκB p65 antibody (Cell Signaling Technology) and the two secondary antibodies used were anti-rabbit IgG 594 and anti-mouse IgG 488 (Cell Signaling Technology).

2.19. STATISTICAL ANALYSIS

All statistical analyses were conducted using the statistic program Prism ver. 5. The p-value of<0.05 was considered statistically significant, $p<0.05$, $p<0.01$ and $p<0.001$ were denoted by *, ** and ***. When there two sets of data needed to be compared in the same graph, # was used.

Chapter 3 CHARTERIZATION OF A NOVEL QUINOLINE DERIVATIVE 83b1 IN HUMAN ESOPHAGEAL CANCER CARCINOMAS

3.1. INTRODUCTION

Human esophageal cancer, as mentioned previously, is a very severe and mortal disease worldwide with the high incidence and the extremely low 5-year survival rate. Although there are numerous therapeutic approaches for treating esophageal cancers, the worse situation seems not to be improved. This is the reason why it is an urgent need for finding a new therapeutic or technique to deal with that formidable disease. [15, 17, 121]

A list of novel quinoline derivatives have been synthesized by our research team and preliminarily tested. Preliminary cytotoxicity assessment of the quinolone derivatives against different cancer cell lines was conducted by Dr. Penny Sau Hing CHAN and it has been found that 83b1 showed the significant anti-cancer effect on human esophageal squamous cell carcinoma (ESCC) cell lines. Moreover, the results of preliminary molecular docking analysis of 83b1 also implicated the potential of 83b1 to be used against cancers. In this chapter, synthesis of 83b1, anti-cancer activities of 83b1 in ESCCs and its potential for other cancers were reported.

3.2. SYNTHESIS OF 83b1

8-(4-(trifluoromethyl)benzyloxy)-1,2,3,4-tetrahydro-2-methylquinoline (83b1) was kindly provided by a member in our research group, Dr. Penny Sau Hing CHAN, and was prepared by asymmetric hydrogenation of 8-(4-(trifluoromethyl)benzyloxy)-2-methylquinoline (83b) under the conditions: 0.15 mmol of 83b, $[Ir(COD)Cl]_2$ (0.0015 mmol), P-Phosligand (0.0032 mmol), I_2 (0.015 mmol), 1.5 ml tetrahydrofuran (THF) as solvent at room temperature and 700psi H_2 for 20 hours. 83b1 was obtained through nucleophilic substitution of commercially available 2-methyl-8-quinolinol with 4-trifluoromethylbenzyl bromide in DMF at room temperature. The structure and purity of 83b1 was examined through 1H-NMR and liquid chromatography mass spectrometry (LC-MS).[122]

3.3. MECHANISMS OF PPARD RELATED TO CANCER DEVELOPMENT

According to our preliminary docking results, one of the most possible targets of 83b1 in human was predicted as the peroxisome proliferator-activated receptor delta (PPARD) and PPARD has been widely identified as a cancer biomarker in different human cancers including colorectal cancer, lung cancer and so on. In this part, we would discuss about the normal functions of PPARD in our body followed by discussing the functions of PPARD in cancer development.

3.3.1. *Introduction to PPARs*

Peroxisome proliferator-activated receptors (PPARs) are widely known as the ligand-activated transcription factors which regulates the expression of different gens in cell differentiation and various metabolic pathways.[123] There are three known isotypes of PPARs including PPARα (NR1C1), PPARβ (also called PPARδ/D; NR1C2) and PPARγ (NR1C3), they exhibit distinct distribution patterns in different tissues to function.[123] PPARα is highly expressed in liver as a regulator of lipid catabolism and transportation. As for the PPARγ, it is mainly expressed in white and brown adipose tissue to regulate the differentiation of adipocytes and its functions such as lipid storage and glucose homeostasis. However, PPARD is ubiquitously expressed throughout all of the tissues inside of the body and it plays a crucial role in many biological processes including cholesterol transportation, lipid metabolism and wound healing. Besides, all three PPAR isotypes have been found to share some common functional features which are anti-inflammatory reactions, and implications in cell differentiation and carcinogenesis.[123, 124]

The size of the three PPAR isotypes is also about 49 to 56kDa that includes multiple structural and functional domains. PPARs consist of four primary domains (Fig. 3.1) encoded by six exons.[125] The N-terminal (A/B domain) is the least conserved part in the three PPARs, it has a ligand-independent trans-activation

domain called activation function 1 (AF-1) which is responsible for co-factor binding and Map-kinase phosphorylation. Another important part is the DNA binding domain (DBD) which is located at the C domain and it is highly conserved in all PPARs.[125, 126]

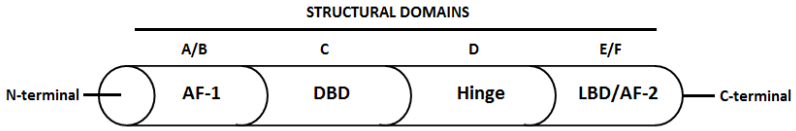

Figure 3.1.Structural and functional domains of PPARs.

The DBD is important for recognizing the core hexa-nucleotide motif (AGGTCA) on the functional PPAR-response element (PPRE), as PPARs need to recognize and bind to the PPRE for their functions after they form a hetero-dimer with 9-*cis* retinoic acid receptor (RXR) in the ligand binding state. The D domain is also called hinge domain which is highly conserved and it connects the DBD to the ligand binding domain (LBD), it plays an important role in nuclear localization of the activated PPAR dimers. The C-terminal is LDB which is involved in the E/F domain. The LBD of PPARs contains a big hydrophobic pocket which is called ligand-dependent trans-activation function (AF-2), it allows PPARs to bind with different types of hydrophobic ligands. The LBD also participates in hetero-dimerization with RXR and facilitates the functions.[125, 127]

3.3.2. *Mechanisms of Action of PPARD for Biological Functions in Human*

Without the presence of the specific ligands for PPARs or RXR, the PPAR/RXR hetero-dimer is inactivated and non-functional because they are associated with the co-repressors including nuclear receptor co-repressor (NCoR) or some other silencing mediators for retinoid receptor (SMRT) which influences the activity of histone deacetylase. At this state, the histone proteins are deacetylated and the structure of the chromatin is hence condensed, gene transcription is thus suppressed. However, in presence of the ligands, the PPAR/RXR is activated. The ligand-binding induces the conformational alteration of AF-2 closed to the C-terminal, this results in dissociation of co-repressors from the PPAR/RXR, the specific co-activators such as PPAR-binding protein (PBP), thyroid hormone receptor-associated protein 220 (TRAP-220) and mediator complex subunit 1 (MED-1) can then interact with PPAR/RXR. The activated PPAR/RXR, in association with cofactors such as CREB-binding protein, would bind to the PPRE which is located in the promoter region of the target gene and activate the acetylation of histone proteins. Therefore, the structure of chromatin is changed and gene transcription is then activated.[123, 125, 127, 128]

It has been reported that PPARD regulates a broad spectrum of physiological functions in human, especially in lipid absorption and intestinal functions. PPARD

can be activated by the long-chain saturated or unsaturated fatty acids and prostacyclins, there are some identified natural fatty acids such as arachidonic acid, eicosapentaenoic acid, linoleic acid and so on. After they are activated by the ligands, they will promote the absorption of lipid by promoting the transcription of the genes which are involved in lipid uptake including fatty acid binding protein (FABP) and fatty acid translocase (FAT). On another hand, it has been found that PPARD is significantly overexpressed in skeletal muscle and heart. After PPARD is activated by the ligands, it can induce the expression of the genes for fatty acid catabolism and fatty acid oxidation, and the muscular lipid is hence reduced.[123, 124, 127, 128]

PPARD seems to play a crucial role in many biological functions in human body, however, some studies have reported that PPARD also highly contributes to many disease development such as type-II diabetes, cancers, inflammation and liver diseases.[123, 125, 127, 128]

3.3.3. *Mechanisms of PPARD in Tumor Development*

Besides of the normal physiological functions, as mentioned, some studies have shown that PPARD is highly implicated in tumor development. One known mechanism is related to cyclooxygenase-2 (COX-2) which is a well-known oncogenic protein and prostaglandin E-2 (PGE_2) which is also widely known to participate in

different oncogenic pathways. This mechanism is driven by the free arachidonic acid (AA) which is one of the ligands that can bind to PPARD and activated the receptor to promote the gene transcription. [129]

Natural Ligands	Synthetic Agonists	Synthetic Antagonists
Arachidonic acid	GW0742	GSK3787
Eicosapentaenoic	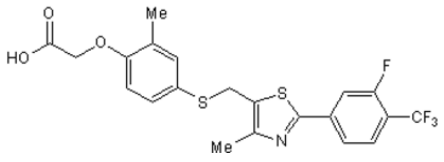	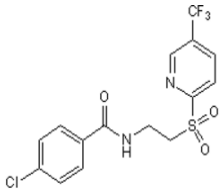
Linolenic acid		
Linoleic acid		
Palmitic acid	GW501516	GSK0660
Strearic acid		
Prostacyclin	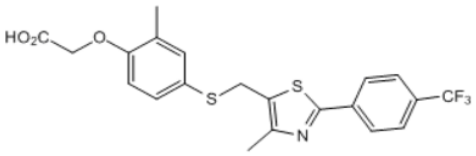	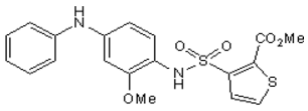
		83b1
	L-165,041	
	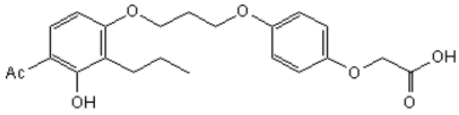	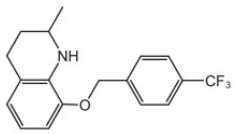

Table 3.1. Several identified natural PPARD ligands, synthetic PPARD agonists and antagonists, and 83b1.

AA can either be released from the cell membrane phospholipid bi-layers catalyzed the enzyme called cytosolic phospholipase A2 (cPLA2) or dietary fatty acids. A portion of AA is then converted into prostaglandin G2 (PGG_2) through cyclization and oxygenation by the catalysis of COX-2 and addition of the 15-hydroperoxy group. The hydroperoxy group of the $PGG_2$is then immediately reduced to a hydroxy group of PGH_2which is an intermediate of the prostaglandin and it acts as the substrate which is further converted into different kinds of prostaglandins by the enzyme called terminal prostanoid synthase. There are different types of prostanoid synthases depending on the prostaglandin they synthesize, for instance, prostaglandin-F- synthase catalyzes the synthesis of $PGF_{2,}$ whereas prostaglandin-E-synthase catalyzes the PGE_2 synthesis and so on. PGE_2can trigger a series of effects on the target cells through either autocrine or paracrine ways by interacting with the four types of PGE_2G-protein coupled receptors (GPCRs) which are divided into EP1, EP2, EP3 and EP4 receptors based on their pharmacological functions. For example, activation of EP1 receptor by PGE_2 increases the transportation of calcium ions, it results in accumulation of intracellular calcium. Interaction of PGE_2 with either EP2 or EP4 increases intracellular cyclic adenosine mono-phosphate (cAMP) accumulation. EP3 receptor is different from other EP receptors since there are some different splice variant of EP3 receptors. Activation of

EP3 receptors can also increase the intracellular inositol triphosphate (IP_3), however, the intracellular cAMP may whether be increased or decreased depending on the variance of EP3 receptors. [124, 127, 129]

It has been reported that PGE_2 play an important role in many oncogenic pathways. As mentioned, PGE_2 can interact with the EP receptors on the cell membranes through autocrine or paracrine pathway. After activation of EP receptors by the PGE_2, some oncogenic pathways are also triggered. For example, some studies reported that activation of EP receptors can activate the anti-apoptotic and proliferative pathways including the PI3K/AKT pathways, Ras-MAPK/Erk signaling pathway, cAMP/protein kinase A signaling pathway, epidermal growth factor receptor (EGFR) signaling pathway and adenomatous polyposiscoli (APC)/β-catenin pathway (also known as Wnt signaling pathway) in different kinds of cancers such as colorectal cancers, lung cancers, gastric cancers and breast cancers and so on. [125, 127, 130, 131]

3.3.4. *Formation of a Positive Feedback Loop Between PPARD and COX-2/PGE_2 in Tumor Development*

Among the COX-2/PGE_2 pathway, PPARD participates as a promoter to facilitate this pathway through a positive feedback loop. As mentioned, AA, which is

one of the natural ligands for PPARD activation, can be released after the catalysis of $cPLA_2$enzymes. The activated PPARD/RXR dimer will bind to the target genes and promote the gene transcription. It has been widely reported that COX-2 is one of the target genes that will be up-regulated by the activation of PPARD, overexpression of COX-2 can then lead to the tumor development through over-production of different kinds of prostaglandins such as PGE_2 to activate the EP receptors. More importantly, over-production of the COX-2 derived PGE_2would further promote the release of AA through activation of $cPLA_2$enzymes by phosphorylation. Therefore, more the AA is released from the plasma membrane and available, more PPARD/RXR dimer will be activated by the free AA. Hence, the interaction between COX-2/PGE_2 signaling pathway and PPARD performs as a positive feedback loop for promoting the tumor development.[126, 127, 129, 132, 133]

Besides of the COX-2/PGE_2 signaling pathway, PPARD has also been found to participate in cancer development through other oncogenic pathways. In breast cancers, EGFR is the widely known receptors which play an important role in many oncogenic signaling pathways. Some studies showed that activation of PPARD by the synthetic agonist would promote the phosphorylation of EGFR in cancer cell lines, activation of EGFR results in protection of the cancer cells against apoptosis,

promotion of cell invasion and angiogenesis. Moreover, activation of PPARD with the higher expression of COX-2 would promote the phosphorylation of AKT, the activated AKT takes part in the tumor development signaling pathways in many cancers including breast cancers, esophageal cancers, colorectal cancers, lung cancers, liver cancers, gastric cancers and so on.[126, 131, 133-135]

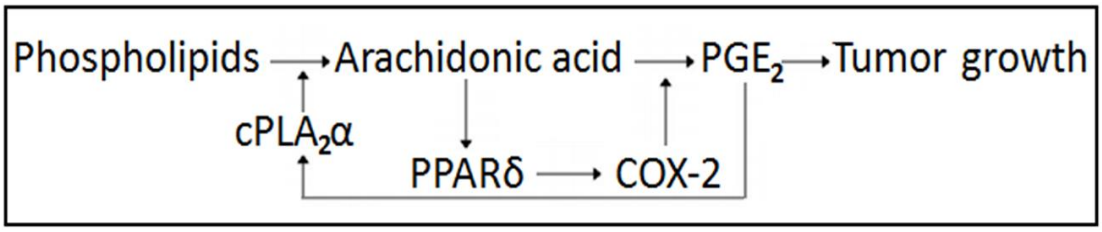

Figure 3.2. Proposed mechanisms of PPARD correlated with COX-2 and COX-2 derived PGE_2 in tumor development.[129]

Therefore, it is possible that PPARD would act as a therapeutic target in cancers. Blocking the ligand-binding domains of PPARD by using the potent and selective antagonists can lead to inactivation of PPARD because of the association between PPARD and the co-repressors, the downstream oncogenic pathways, as mentioned, would hence be suppressed. In this chapter, the efficacy and mechanisms of a novel quinoline derivative 83b1, which has been shown to block PPARD, were characterized through the *in vitro* and *in vivo* experiments.

3.4. EXPERIMENTAL DESIGNS

As first, the structure and the purity of 83b1 were examined by using the ^{1}H-NMR, HPLC and ESI-MS/MS, this is important to confirm we were using the

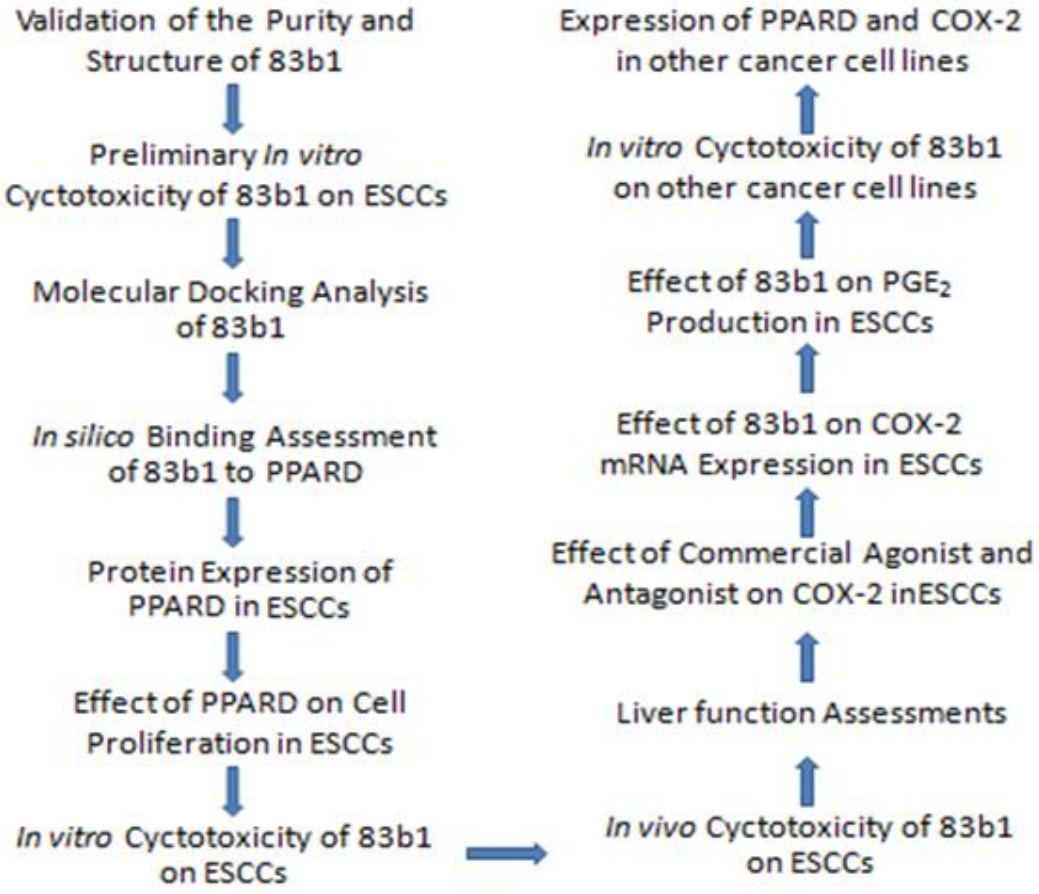

Figure 3.3. Experimental plan for the studies of the effects and mechanisms of 83b1.

correct target compound. Afterwards, a preliminary *in vitro* cytotoxicity assessment of 83b1 on few ESCC cell lines was conducted by using MTS reagent according to the instructions, CDDP was used as a positive control to analyze whether 83b1 is effective to ESCC cell lines or not. After the cytotoxic effect of 83b1 was determined,

it is important to predict the possible targets and then validate it in order to further analyze the mechanisms of the compound for suppressing tumor growth.

A similarity-ensemble assessment (SEA) molecular docking analysis[115]was conducted to predict the possible target of 83b1 in human and one of the possible target found was PPARD, the *in silico* and *in vitro* binding assessing were conducted to validate it. For the *in silico* assessment, the binding interaction and binding energy between PPARD and either 83b1 or one of the natural ligand, AA, were determined by using a program in Molecular Docking Server. By comparing their binding energy, the ability of 83b1 to compete the binding site of PPARD with the abundant natural ligand would be predicted.

Afterwards, the mRNA and protein expression of PPARD in a series of ESCC cell lines compared to the non-tumor cell lines were determined by using PCR and HIC respectively. Furthermore, the ability of PPARD to promote proliferation in ESCC cell lines was determined by monitoring the cell growth everyday with the addition of the PPARD agonist, GW0742, compared to the negative control. After understanding the effect of PPARD on cell proliferation in ESCC, the comprehensive *in vitro* cytotoxicity test of 83b1 on a spectrum of ESCC cell lines compared to few non-tumor cell lines was determined by using MTS again followed by *in vivo* cytotoxic assessment in nude mice xenografts. It is very important to know the

effectiveness of 83b1 for killing the cancer cells as well as the toxicity for the non-tumor effects. Actually, the existing cancer drugs usually show a very strong anti-cancer effect on different cancers, but the side-effects of the drugs on the patients are also serious and severe at the same time. Therefore, the toxicity of 83b1 and CDDP on the non-tumor cell lines was also determined to compare the therapeutic index between 83b1 and the anticancer drug.

Moreover, the effect of 83b1 on the expression of COX-2 and production of COX-2 derived PGE_2in ESCC cell lines were analyzed by real-time PCR and ELISA respectively to understand the mechanism of 83b1 to suppress the growth of ESCCs.

Finally, the cytotoxic tests of 83b1 in other cancer cell lines were conducted to analyze the suppressive effect of 83b1 on other cancers. Besides, the effect of 83b1 on expression of few other proteins related to PPARD such as p-ATF-2, p-HSP-27, p-JNK-1, p-MAPK and p-MEK-1in ESCC cell lines was also determined in order to further understand the downstream mechanisms for suppression of cancer growth after the PPARD was targeted by 83b1.

3.5. RESULTS

3.5.1. *Determination of the structure of 83b1 through ^{1}H-NMR*

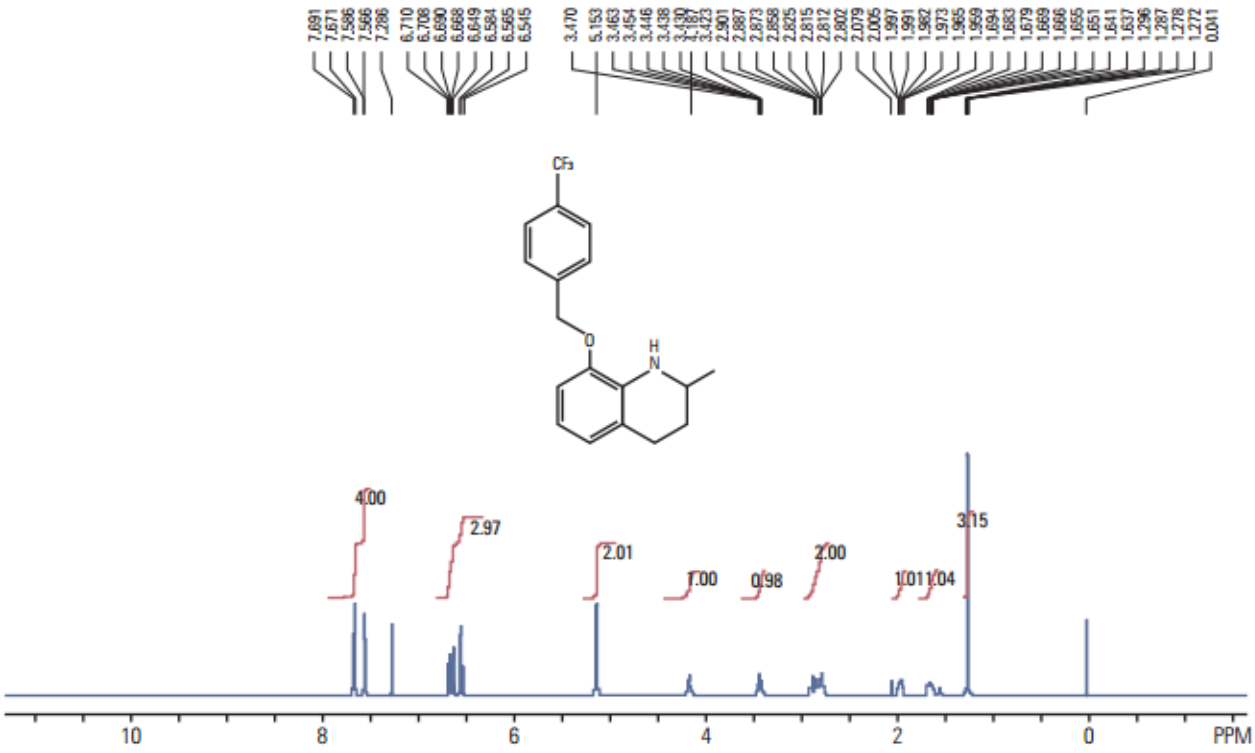

Figure 3.4. ^{1}H-NMR Spectrum of 83b1.

According to works conducted by Dr. Chan Sau Hing as mentioned above, 83b1 was completely dissolved in $CDCl_3$ and examined by the ^{1}H-NMR, the spectrum was reported as followed: ^{1}H-NMR (500 MHz, $CDCl_3$): 1.30 (d, 3H, J=6.0 Hz), 1.63-1.72 (m, 1H), 1.95-1.98 (m, 1H), 2.75-2.79 (m, 1H), 2.85-2.90 (m, 1H), 3.39-3.43 (m, 1H), 4.17 (bs, 1H), 5.13 (q, 2H, J=12.5 Hz), 6.54 (t, 1H, J=8.0 Hz), 6.68 (d, 1H, J=8.0 Hz), 6.72 (d, 1H, J=7.5 Hz), 7.55 (d, 2H, J=8.0 Hz), 7.66 (d, 2H, J=8.5

Hz). According to the spectrum and the data obtained, it is consistent to the expected structure of 83b1.

3.5.2. *Examination of the Molecular Weight and Purity of 83b1 through HPLC followed by ESI-MS*

A

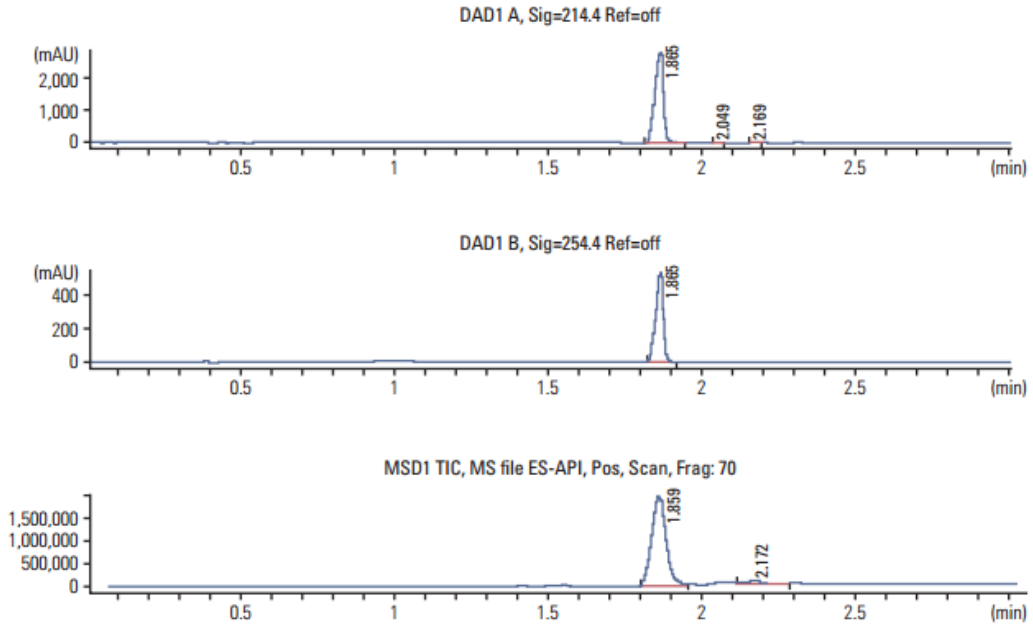

B

Integration results for ELS1 A, Voltage

RetTim	Width	Area	Height	Area

Integration results for DAD1 A, Sig=214.4 Ref=off

RetTim	Width	Area	Height	Area
1.87	0.03	5,477.53	2,844.69	99.70
2.05	0.01	9.68	10.85	0.18
2.17	0.01	6.74	6.92	0.12

C

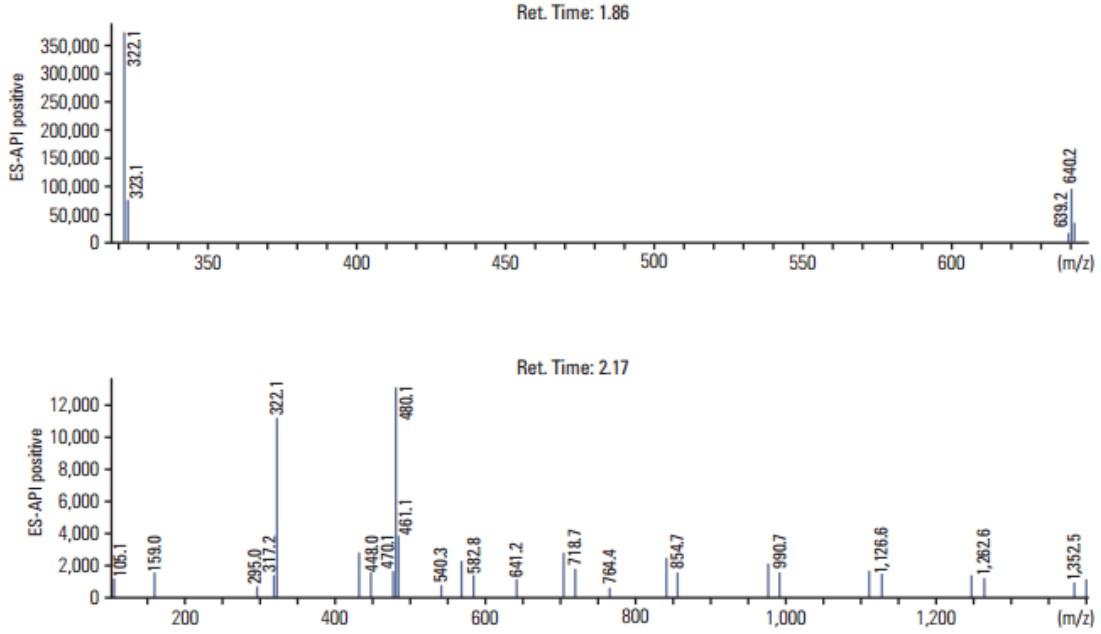

Figure 3.5. Analysis of 83b1 by using HPLC followed by ESI-MS. (A) HPLC Chromatogram of 83b1. (B) Determination and analysis of the peaks obtained in the HPLC of 83b1. (C) Analysis of the two peaks obtained in HPLC of 83b1 (Retention time = 1.865 min. and Retention time = 2.169 min.) by using ESI-MS.

The 83b1 was diluted in methanol and analyzed in high-pressure liquid chromatography (HPLC) and electrospray ionization mass spectrometry (ESI-MS) by Ms. Zhou yuanyuan in our research group. According to the HPLC chromatogram of 83b1, there are three peaks separated in the retention time of 1.865, 2.049 and 2.169 minutes respectively. The peak at the retention time of 1.865 minutes is the largest peak which occupied 99.7%, whereas the two other peaks only occupied 0.3% totally. The peaks at the retention time of 1.865 and 2.169 minutes were then analyzed by

ESI-MS. According to the results, the peak comprising 99.7% of the total area showed a m/z ratio about 322.1^{+} which is consistent to the molecular weight of 83b1 (M.W.: 321 g/mol), whereas another peak was found to be the impurities with very low intensity. Therefore, it showed that the purity of 83b1was very high as 99.7%.

3.5.3. *Molecular Docking Analysis by SEA Program*

Rank	Reference Name	Species	Expected Value	Maximum Target Complementary Value
1	Sodium- and chloride-dependent glycine transporter 2	Human	$1.76e^{-20}$	0.38
2	Peroxisome proliferator-activated receptor delta		$2.80e^{-17}$	0.39
3	Tyrosine-protein phosphatase non-receptor type 6		$1.87e^{-10}$	0.37
4	Presenilin-1		$5.36e^{-10}$	0.34
5	Peroxisome proliferator-activated receptor alpha		$1.88e^{-09}$	0.35
6	Prostaglandin E2 receptor EP1 subtype		$3.74e^{-07}$	0.33
7	Peroxisome proliferator-activated receptor gamma		$1.27e^{-06}$	0.34

Table 3.2. The first seventh predicted targets for 83b1.

Table 3.2 showed the first seven possible targets for 83b1 which were predicted by using SEA program. According to the instruction of the program, the binding probability of the compound to the protein target is significant when the

expected value is lower than 1×10^{-10}, the protein targets with the lower expected value are more preferential to be bound by the compound. Moreover, the binding preference is also affected by the maximum target complementary value which indicates the level of the ligand-target complementarity, higher the complementarity means the ligand is more suitable for binding to the target.

As shown in the Figure, PPARD was the predicted target with the second lowest expected value which is $2.80e^{-17}$and highest maximum target complementary value which is 0.39. Therefore, PPARD should be one of the possible target for 83b1 and it is necessary and deserved to investigate the function of PPARD involved in cancer development and the effects of 83b1 on PPARD.

3.5.4. *In silico Binding Assessment of PPARD with 83b1 or AA*

A

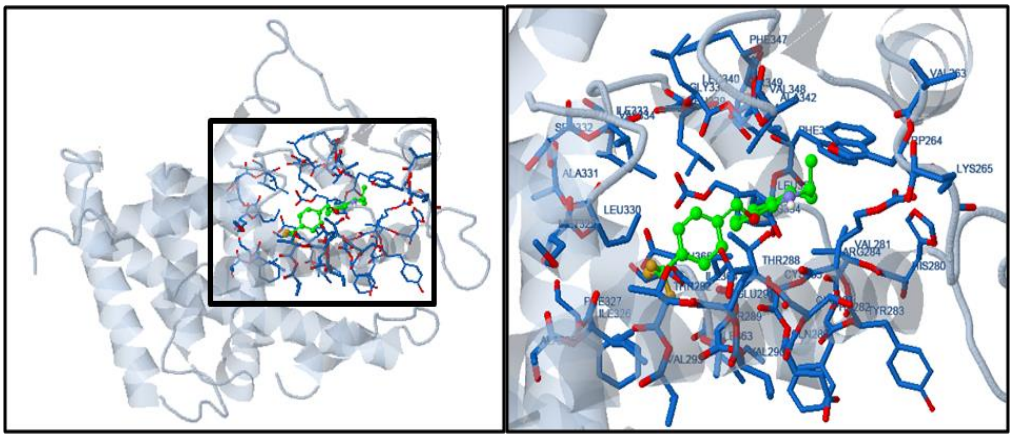

B

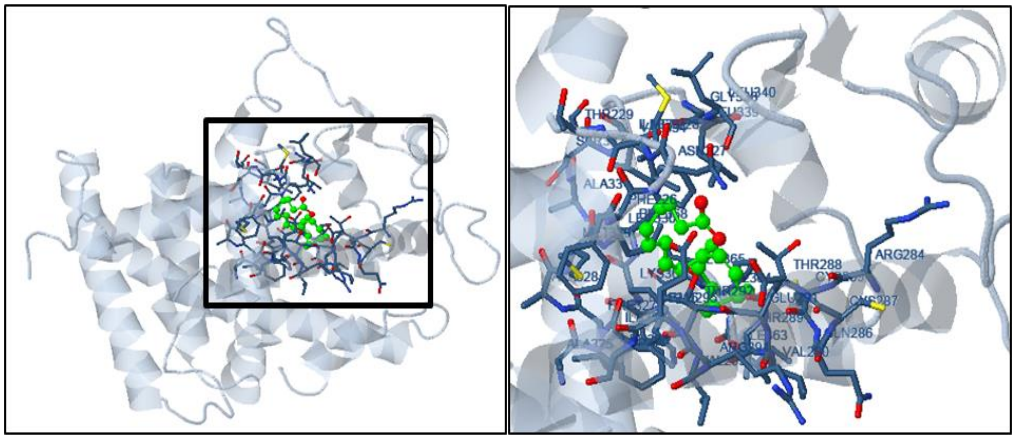

Figure 3.6. Three-dimensional model of 83b1 or AA interacting with PPARD constructed in Molecular- Docking Server. (A) 83b1 interacting with PPARD and (B) AA interacting with PPARD.

Compound	Estimated Free Energy of Binding	Estimated Inhibition Constant, Ki
83b1	-7.41 kcal/mol	3.68μM
Arachidonic acid (AA)	-5.66 kcal/mol	70.63μM

Table 3.3. The estimated free binding energy and inhibition constant of 83b1 or AA to PPARD.

The Figure 3.6 showed the results obtained in Molecular Docking Server. The interaction of either 83b1 or AA with PPARD was determined through analyzing the structural formation and amino acid group of PPARD, and the structure of 83b1 or AA by the algorithm of the program. Based on the algorithm of the program, the free energy of their binding and the inhibition constant were also predicted. The free binding energy refers to the free energy change determined under the conditions (1 atm pressure, the temperature of 298K, and 1M of the protein and ligand), the more

negative the free binding energy indicates the binding of the protein and ligand is more feasible and stable. Besides, the inhibition constant (Ki) refers to the concentration of the compound required for reducing half of the reaction rate of the protein, the lower the value indicates the higher suppressive activity of the compound.

This approach was used to examine the feasibility and affinity of 83b1 to PPARD, therefore an abundant natural ligand for PPARD, AA, was as a positive control to determine the competitiveness of 83b1 for PPARD. According to the table 3.3, the free binding energy of 83b1 to PPARD was -7.41 kcal/mol which indicates the interaction between 83b1 and PPARD is stronger and more stable than the interaction between AA and PPARD that the free binding energy of AA to PPARD was only -5.66 kcal/mol. On another hand, the estimated inhibition constant of 83b1 on PPARD was 3.68 μM that is much lower than AA, it shows that the complementarity of 83b1 with PPARD is much higher than AA. This *in silico* estimation was further validated by using *in vitro* binding assessment.

3.5.5. *In Vitro Binding Assessment of PPARD with 83b1 or AA by Isothermal Titration Calorimetry (ITC)*

A

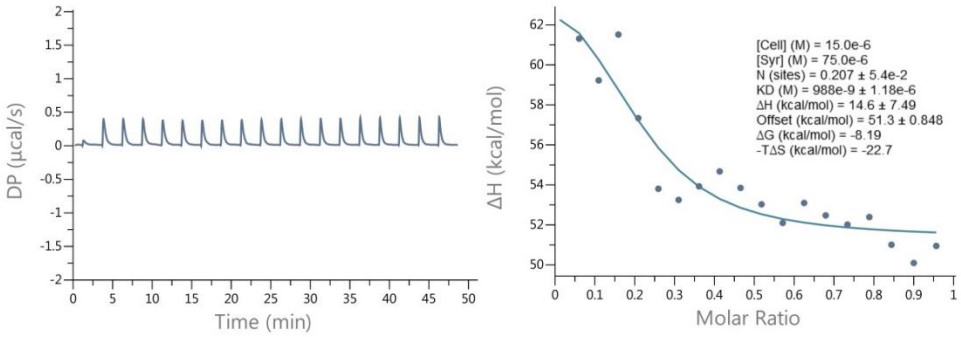

B

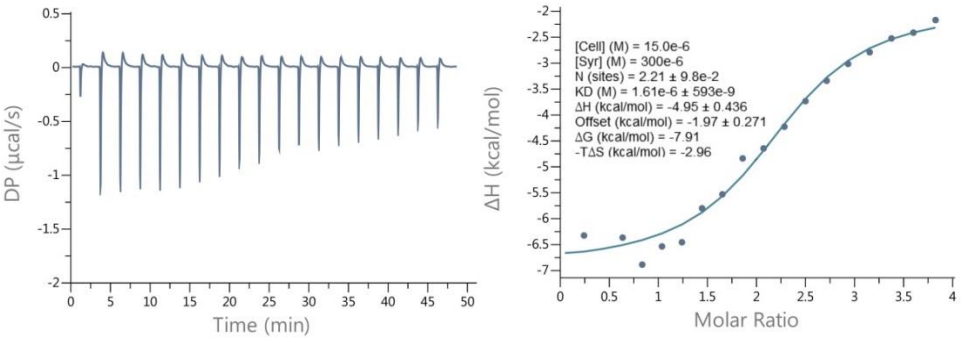

C

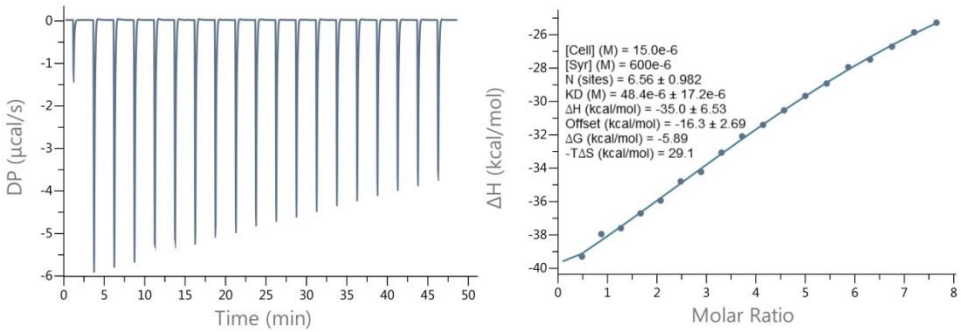

D

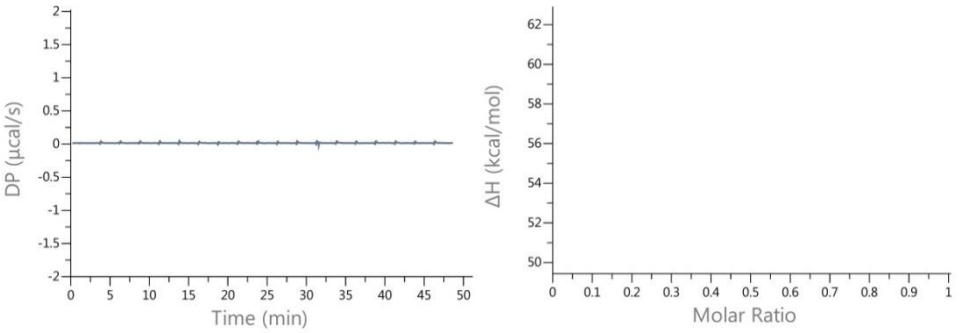

E

F

G

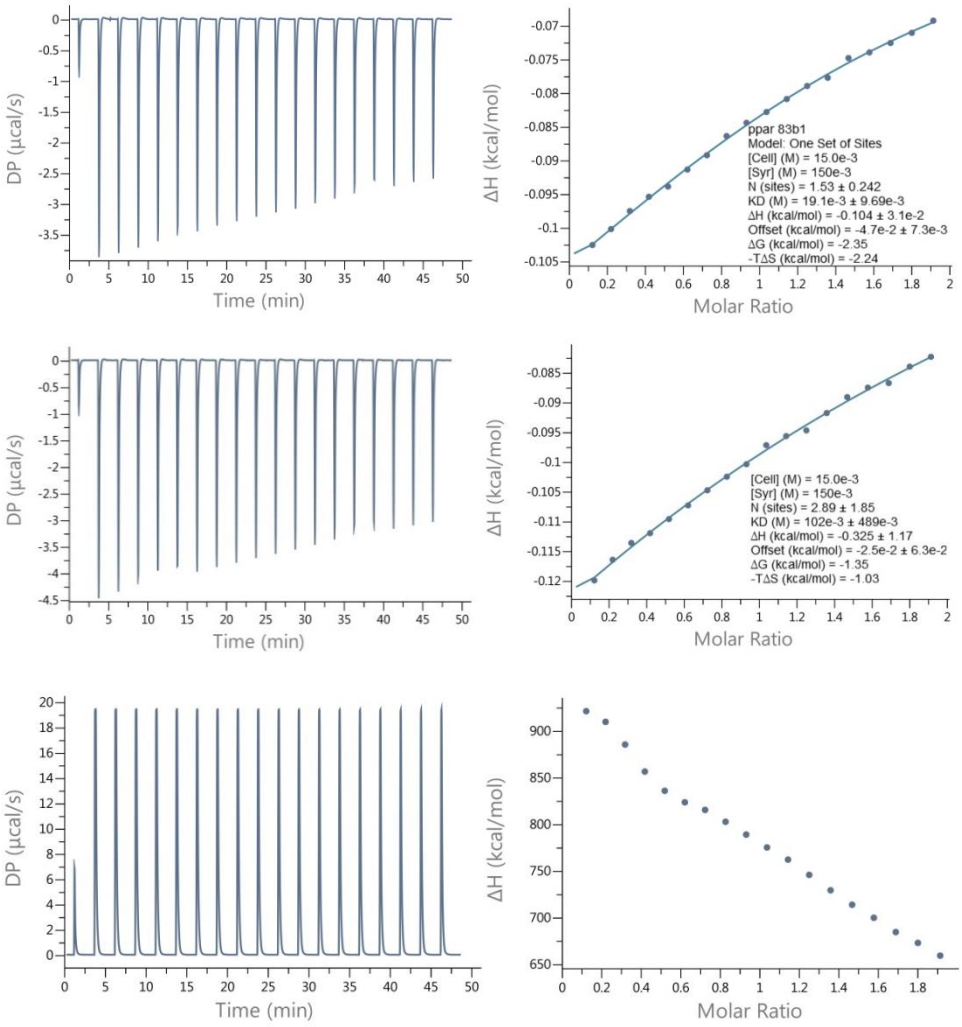

Figure 3.7. *In Vitro* Binding Assessment of PPARD with 83b1 or AA by Isothermal Titration Calorimetry (ITC). (A) 75 µM of 83b1 with 15 µM PARD, (B) 300 µM of 83b1 with 15 µM PPARD, (C) 600 µM of 83b1 with 15 µM PPARD, (D) Buffer with 15 µM PPARD, (E) 15 mM of 83b1 with 150 mM of PPARD, (F) 15 mM of AA with 150 mM of PPARD and (G)15 mM of HAS with 150 mM 83b1.

Concentration of PPARD (μM)	Concentration of 83b1 (μM)	Concentration of AA (μM)	Enthalpy, ΔH (kcal/mol)
15	0	0	Not Detected
	75	0	+14.6
	300	0	-4.95
	600	0	-35.0
Concentration of PPARD (mM)	Concentration of 83b1 (mM)	Concentration of AA (mM)	Enthalpy, ΔH (kcal/mol)
15	150	0	-0.104
	0	150	-0.325
Concentration of HSA (mM)	Concentration of 83b1 (mM)	Concentration of AA (mM)	Enthalpy, ΔH (kcal/mol)
15	150	0	N/A

Table 3.4. Change of enthalpy during interaction between PPARD and 83b1 or AA.

Figure 3.7 showed the results of enthalpy change during the interaction between PPARD and either different concentration of 83b1 or AA. As shown in Figure 3.7A - C, 15 μM of PPARD was interacted with 83b1 (75 μM, 300 μM and 600 μM) in the ITC assay. A positive enthalpy change was detected when PPARD was interacted with 75 μM of 83b1, while much negative enthalpy changes were detected when PPARD was interacted with 300 μM of 83b1 and 600 μM of 83b1. It showed lower concentration of 83b1 cannot efficiently interact with PPARD and it

resulted in an endothermal reaction. However, 83b1 can efficiently bind to PPARD in higher concentration and it resulted in an exothermal reaction. It showed that the interaction between 83b1 and PPARD was very stable and feasible when the concentration of 83b1 was sufficient. As shown in Figure 3.7D, it was a negative control conducted by interacting 15 μM PPARD with buffer, enthalpy change was not detected. As for the Figure 3.7F, 150 mM of AA interacting with 15 mM PPARD was used as a positive control to show that negative enthalpy change was detected when PPARD was bound by its complementary ligand. As for the Figure 3.7G, 150 mM of HSA interacting with 15 mM 83b1 was used as a false negative control, a much positive enthalpy change was detected.

Therefore, it is further confirmed that the affinity of 83b1 to PPARD and the interaction between 83b1 and PPARD was feasible and very stable.

3.5.6. *Expression of PPARD in ESCC and Non-Tumor Cell Lines*

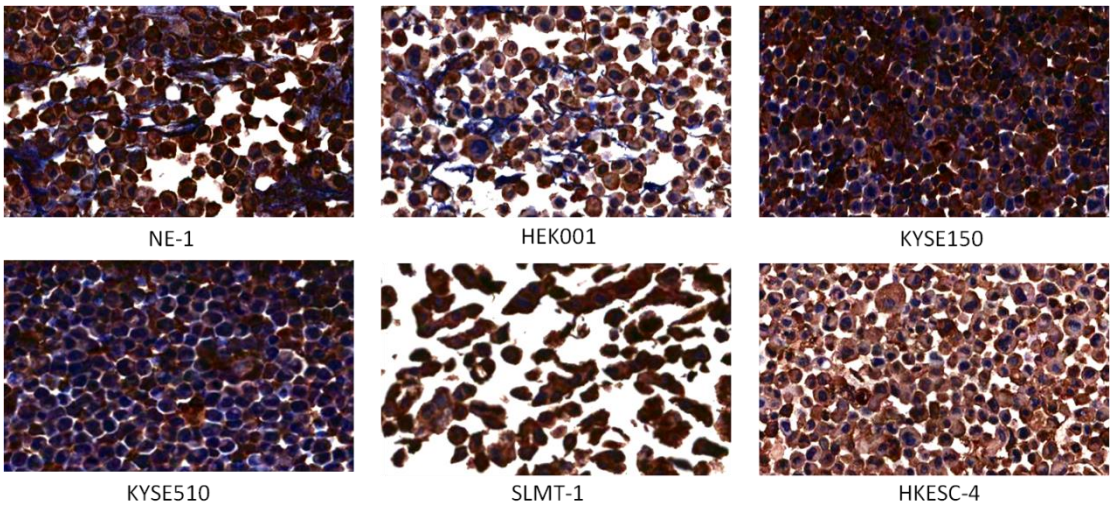

Figure 3.8. Analysis of PPARD expression through IHC in human ESCC and non-tumor cell lines.

The PPARD protein expression of the human ESCC and non-tumor cell lines was determined by using IHC staining which was shown in Figure 3.8. According to the result, the expression of PPARD protein in human esophageal ESCC cell lines including KYSE150, KYSE510 and SLMT-1 were found obviously higher than the non-tumor cell lines such as NE-1 and HEK001.

3.5.7. *Effect of PPARD Activation on ESCC ProliferationUsing GW0742 (a PPARD Agonist)*

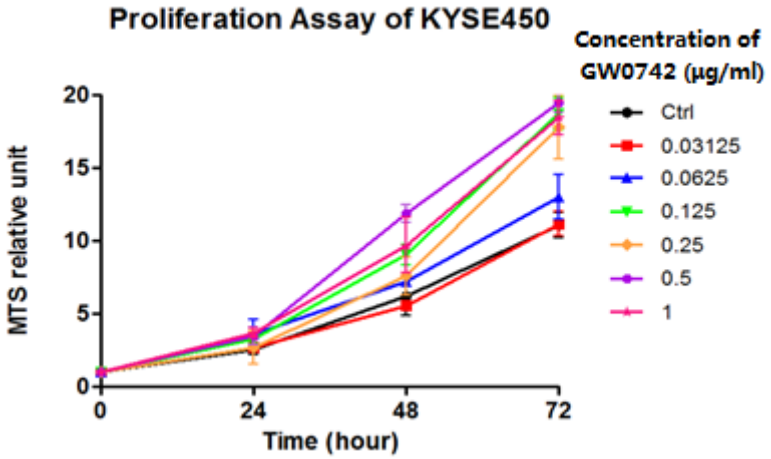

Figure 3.9. Proliferation curve of KYSE450 in different concentration of GW0742 in 24, 48 and 72 hours.

KYSE450			
Concentration of GW0742(µg/ml)	Increase of Proliferation Compared to Negative Control (%)		
	24 Hours	48 Hours	72 Hours
0.00	0.00	0.00	0.00
0.03	6.59	2.82	1.00
0.06	43.96	33.33	17.60
0.13	30.77	68.21	69.29
0.25	6.04	40.77	61.05
0.50	37.91	120.77	75.91
1.00	46.15	80.00	66.92

Table 3.5. Summary of the percentage increase in proliferation of KYSE450 by addition of GW0742 in 24, 48 and 72 hours.

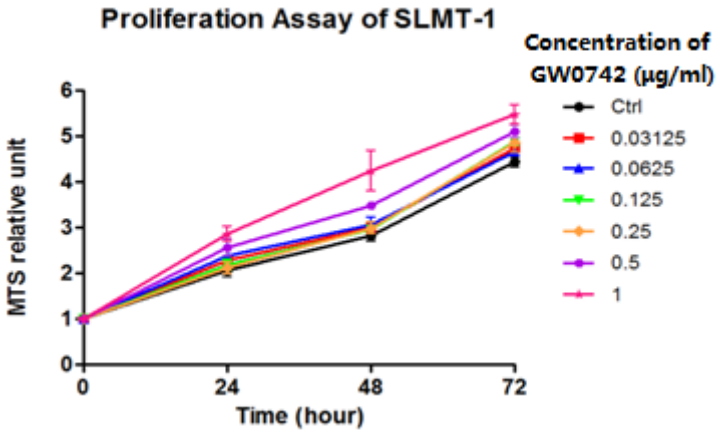

Figure 3.10. Proliferation curve of SLMT-1 in different concentration of GW0742 in 24, 48 and 72 hours.

SLMT-1			
Concentration of GW0742(µg/ml)	Increase of Proliferation Compared to Negative Control (%)		
	24 Hours	48 Hours	72 Hours
0.00	0.00	0.00	0.00
0.03	10.89	6.72	6.82
0.06	15.70	9.10	5.05
0.13	6.36	5.27	9.83
0.25	3.11	6.31	9.37
0.50	24.61	23.89	14.94
1.00	39.18	50.78	23.46

Table 3.6. Summary of the percentage increase in proliferation of SLMT-1 increased by addition of GW0742 in 24, 48 and 72 hours.

The proliferation rate of the ESCC cell lines including KYSE450 and SLMT-1 with the addition of a potent PPARD agonist, GW0742, was measure through MTS assay in 24, 48 and 72 hours. For the KYSE450, it showed that the proliferation rate

of the cell line with the addition of GW0742 was completely higher than the proliferation rate of the cell line without any GW0742 at all time points. Generally, from the results, the concentration of GW0742 was positively proportional to the increase of the growth rate of KYSE450 cell line on day 2. On day 1, the growth rate was not increased after the concentration is higher than 0.06 μg/ml. Besides, the growth rate was not changed after the concentration is greater than 0.13 μg/ml on day 3.

As for the SLMT-1, the proliferation rate of the cell lines was not obviously increased at the lower concentration of GW0742 (0.03 - 0.25 μg/ml) at all time points. However, the proliferation rate of the cell lines was dramatically increased when the concentration of GW0742 is higher than 0.5 μg/ml.

Based on the results of the two ESCC cell lines, it obviously showed that activation of PPARD by addition of the PPARD agonist would significantly increase the cell proliferation of ESCC cell lines.

3.5.8. *In vitro Cytotoxicity Assessment of 83b1 in ESCC and Non-tumor Cells*

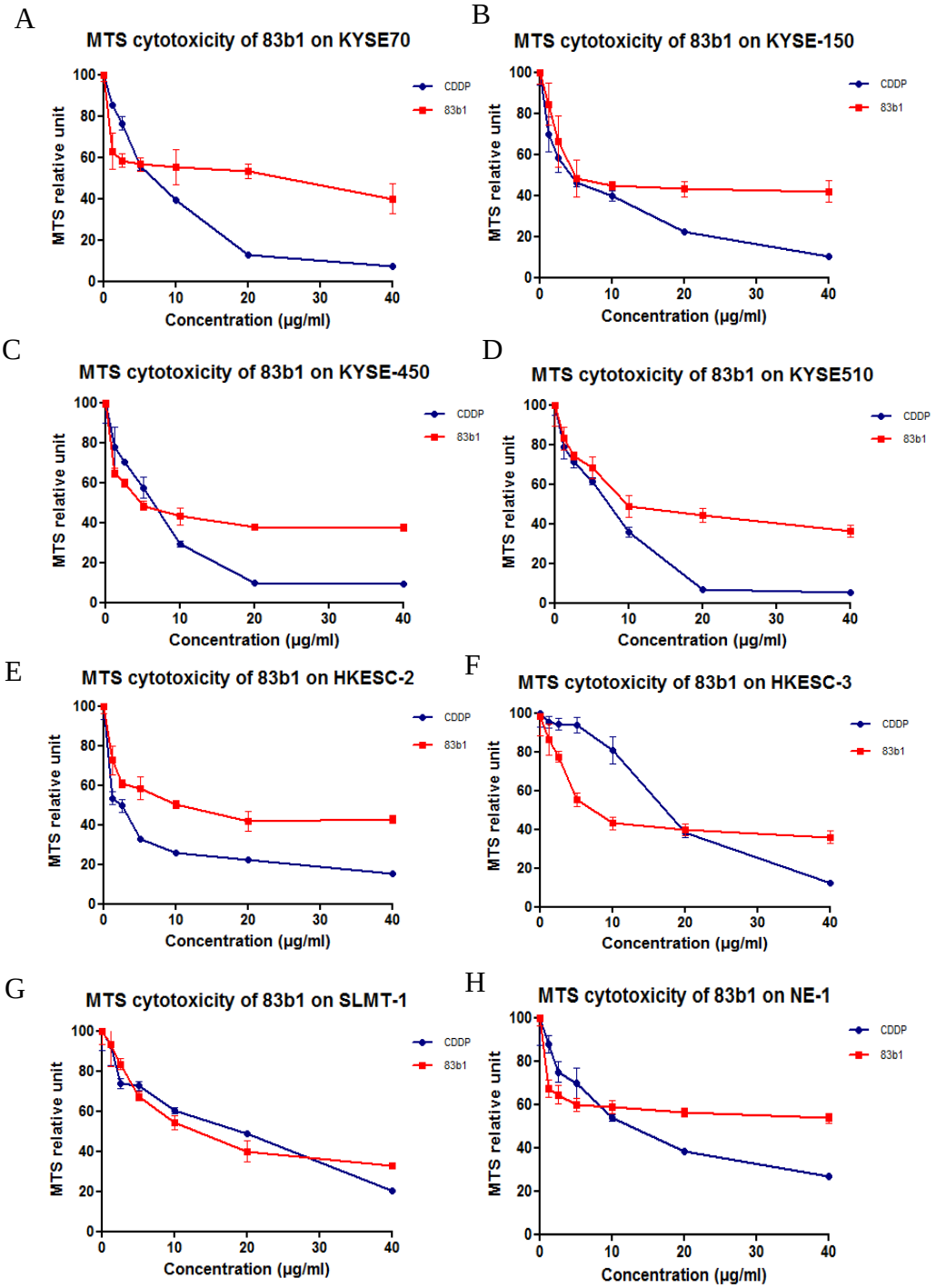

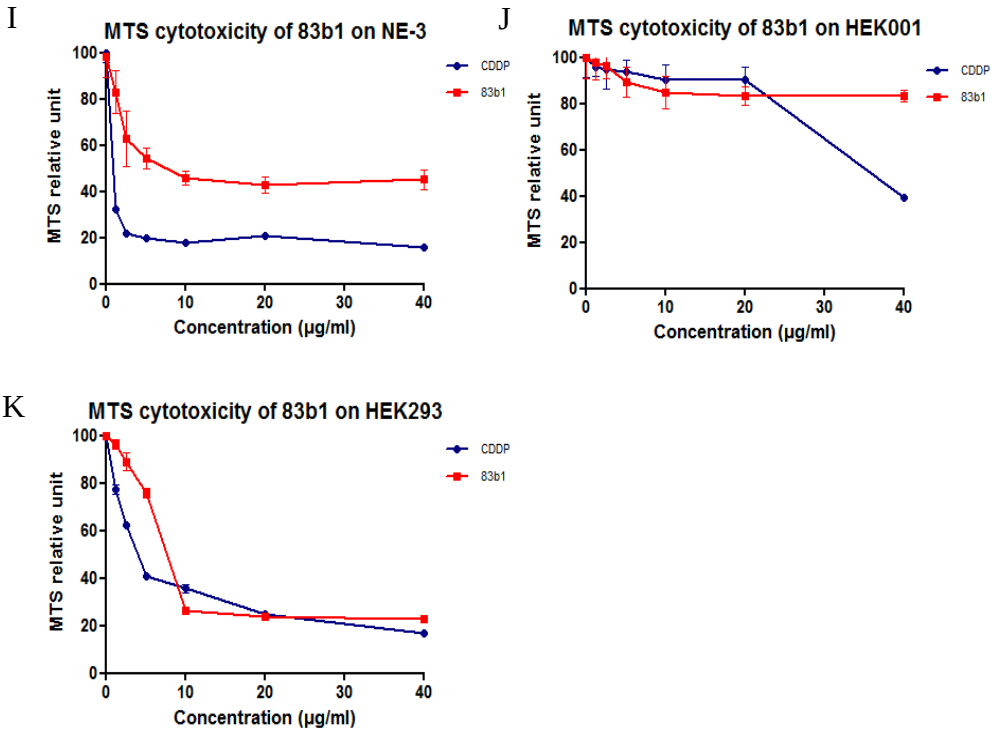

Figure 3.11. Cytotoxic assessment of 83b1 (Maximum concentration: 40μg/ml) in human ESCC and non-tumor cell lines: (A) KYSE70, (B) KYSE150, (C) KYSE450, (D) KYSE510, (E) HKESC-2, (F) HKESC-3, (G) SLMT-1, (H) HEK001, (I) NE-1, (J) NE-3 and (K) HEK293.

Cell Lines	MTS_{50} of 83b1 (μg/ml)	MTS_{50} of CDDP (μg/ml)	MTS_{50} of 83b1/ MTS_{50} of CDDP
KYSE70	10.56	5.977	1.77
KYSE150	10.51	4.145	2.54
KYSE450	5.93	5.067	1.17
KYSE510	13.64	5.566	2.45
HKESC-2	11.81	1.77	6.67
HKESC-3	10.48	16.96	0.62
SLMT-1	13.67	13.99	0.98
HEK001	>40	35.61	N/A
NE-1	>40	11.86	N/A
NE-3	12.31	0.08	146.55
HEK293	8.14	4.50	1.81

Table 3.7. Summary of the MTS_{50} of 83b1 and CDDP, and the ratio of MTS_{50} of 83b1 (Max. conc.: 40 μg/ml) to CDDP.

A

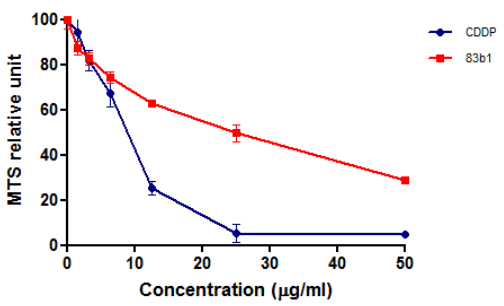
MTS cytotoxicity of 83b1 on KYSE-70
MTS relative unit
Concentration (μg/ml)
CDDP
83b1

B

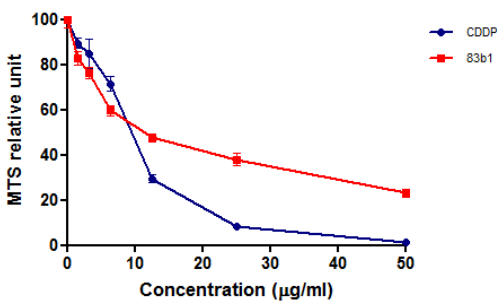
MTS cytotoxicity of 83b1 on KYSE-150
MTS relative unit
Concentration (μg/ml)
CDDP
83b1

C

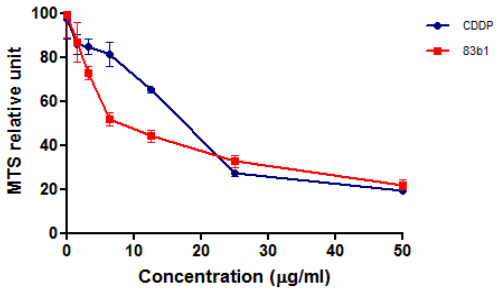
MTS cytotoxicity of 83b1 on KYSE-450
MTS relative unit
Concentration (μg/ml)
CDDP
83b1

D

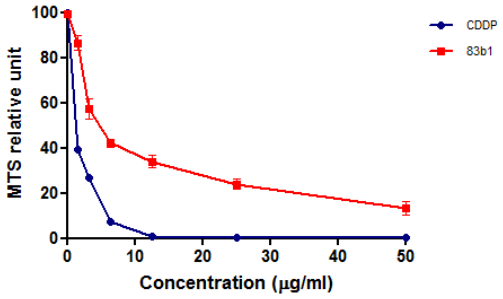
MTS cytotoxicity of 83b1 on KYSE-510
MTS relative unit
Concentration (μg/ml)
CDDP
83b1

E

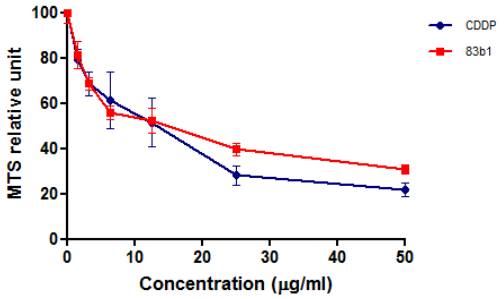
MTS cytotoxicity of 83b1 on KYSE-520
MTS relative unit
Concentration (μg/ml)
CDDP
83b1

F

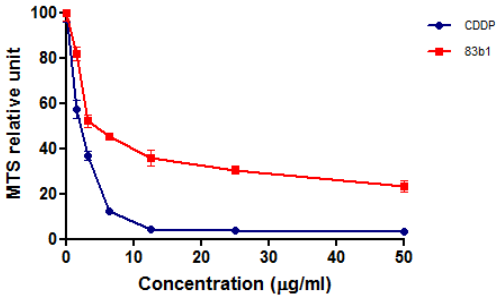
MTS cytotoxicity of 83b1 on HKESC-2
MTS relative unit
Concentration (μg/ml)
CDDP
83b1

G

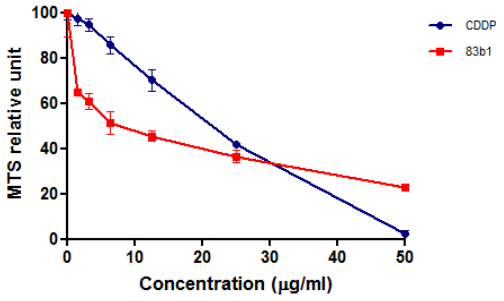
MTS cytotoxicity of 83b1 on HKESC-4
MTS relative unit
Concentration (μg/ml)
CDDP
83b1

H

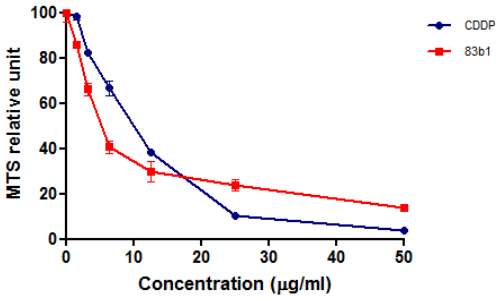
MTS cytotoxicity of 83b1 on SLMT-1
MTS relative unit
Concentration (μg/ml)
CDDP
83b1

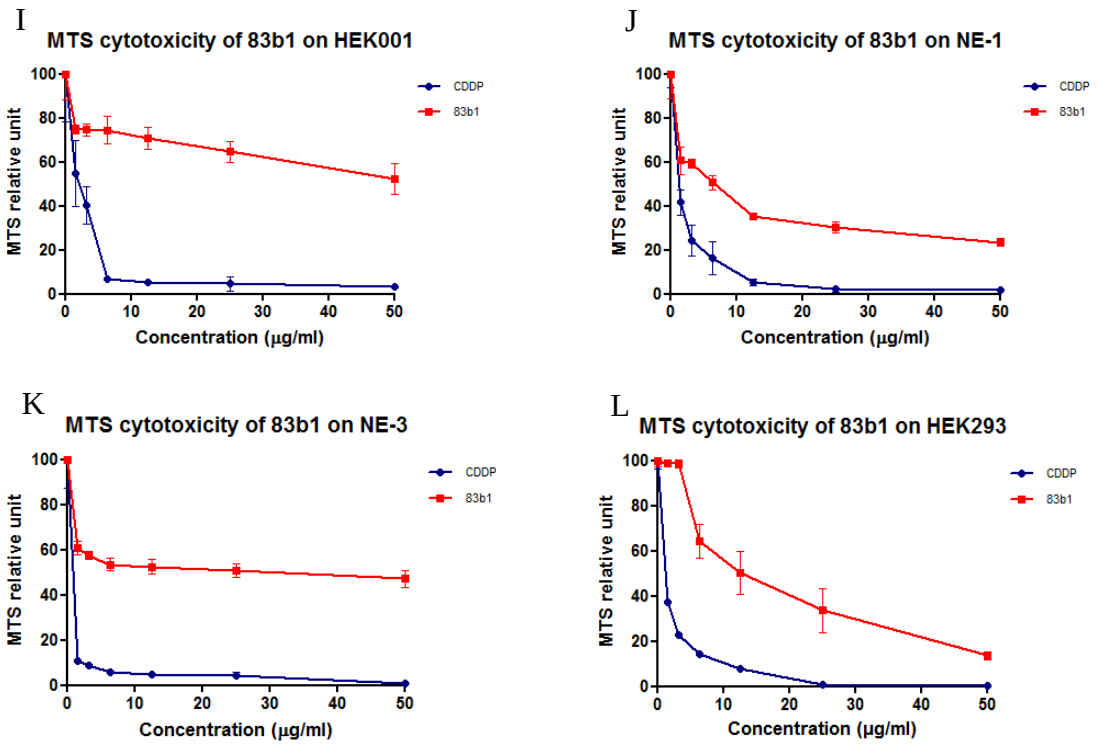

Figure 3.12. Cytotoxic assessment of 83b1 (Maximum concentration: 50 μg/ml) in human ESCC and non-tumor cell lines: (A) KYSE70, (B) KYSE150, (C) KYSE450, (D) KYSE510, (E) KYSE520, (F) HKESC-2, (G)HKESC-4, (H) SLMT-1, (I) HEK001, (J) NE-1, (K) NE-3 and (L) HEK293.

The cytotoxicity of 83b1 on human ESCC and non-tumor cell lines was determined through MTS assay and measured by a microplate reader in a dose-dependent manner, a widely used anti-cancer drug, CDDP, was used as a positive control to compare the effect of 83b1 on the human ESCC and non-tumor cell lines. The dose-response curves of 83b1 and CDDP on the human ESCC and non-tumor cell lines were shown in Figure 3.11 and Figure 3.12, all these results were summarized as MTS_{50} in table 3.7 and 3.8.

Cell Lines	MTS_{50} of 83b1 (μg/ml)	MTS_{50} of CDDP (μg/ml)	MTS_{50} of 83b1/ MTS_{50} of CDDP
KYSE70	21.29	7.87	2.71
KYSE150	11.72	8.58	1.37
KYSE450	9.71	15.85	0.61
KYSE510	5.68	1.21	4.69
KYSE520	12.47	10.08	1.24
HKESC-2	5.94	1.98	3
HKESC-4	6.87	18.81	0.37
SLMT-1	5.89	8.99	0.66
HEK001	>50	1.94	N/A
NE-1	5.03	1.15	4.37
NE-3	>50	0.02	N/A
HEK293	13.19	0.95	13.88

Table 3.8. Summary of the MTS_{50} of 83b1 and CDDP, and the ratio of MTS_{50} of 83b1 (Max. conc.: 50 μg/ml) to CDDP.

From the Figure 3.11, the highest dosage of 83b1 used for treating all of the cell lines was 40 μg/ml, whereas the highest dosage of 83b1 used in Figure 3.12 was 50 μg/ml. According to the results, 83b1 showed a significant cytotoxic effect on all human ESCC cell lines, the cytotoxicity of 83b1 on the ESCC cell lines was increased in the dose-dependent manner. To summarize all of the results from Figure 3.11 and 3.12, the MTS_{50} of 83b1 for the ESCC cell lines was 6 – 21 μg/ml, whereas the $MTS_{50}$of CDDP for the ESCC cell lines was 2 - 19μg/ml. On another hand, the MTS_{50} of 83b1 for the non-tumor cell lines was 5 - >50μg/ml, whereas the MTS_{50} of CDDP for the non-tumor cell lines was 0.02 – 36 μg/ml. The cytotoxicity of 83b1 on the

human ESCC cell lines was found to be slightly weaker than CDDP, whereas the toxicity of 83b1 on the non-tumor cells was extremely lower than CDDP. For some non-tumor cell lines, the MTS_{50} of 83b1 was even undetectable as the highest concentration of 83b1 used still could not reduce the viability of the cells by half.

The therapeutic index of 83b1 and CDDP on either human ESCC or non-tumor cell lines was also estimated by comparing the MTS_{50} of 83b1 and CDDP directly, the ratio > 1 indicates the cytotoxicity of CDDP is higher than 83b1, whereas the ratio < 1 indicates the cytotoxicity of 83b1 is higher than CDDP. Generally, the ratio is smaller than 1 in ESCC cell lines; it means that the cytotoxicity of CDDP on ESCC cell lines was higher than 83b1. Conversely, the ratio is much larger than 1 in non-tumor cell lines; it means that the toxicity of CDDP on human non-tumor cell lines was much higher than 83b1.

However, it was found that the cytotoxicity of 83b1 against ESCC cell lines were not directly proportional to the expression of PPARD in ESCC cell lines according to the result of IHC showing the expression of PPARD protein in ESCC cell lines in Figure 3.8.

3.5.9. *In vivo assessment of 83b1-induced anti-tumor effecton KYSE450 nude mice xenograft model*

A

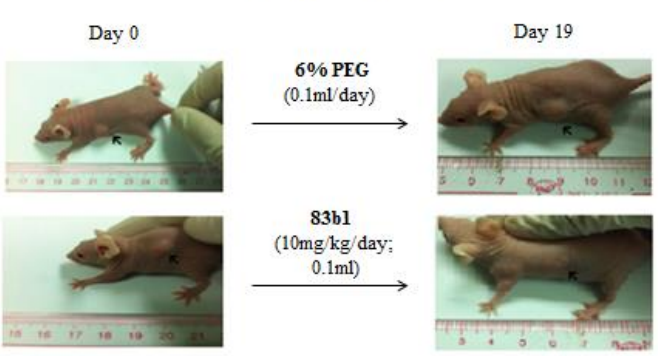

B

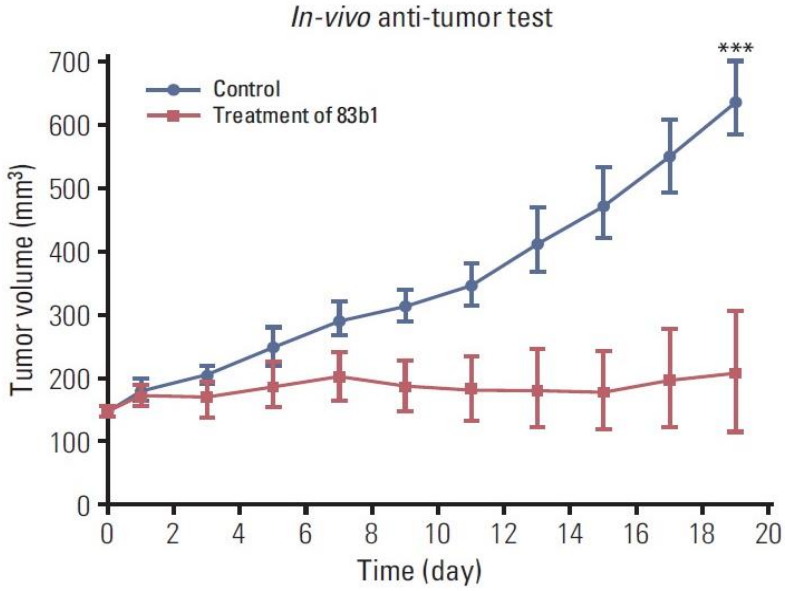

C

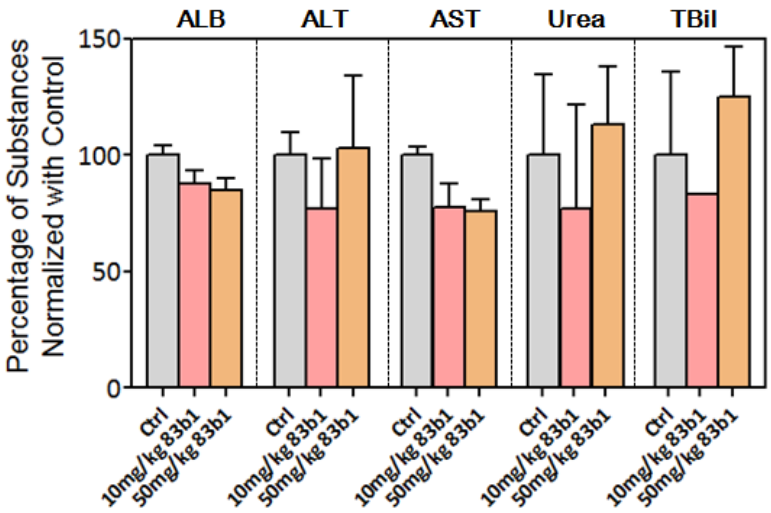

Figure 3.13. *In vivo* cytotoxic assessment of 83b1 in KYSE450 athymic nude mice xenografted model. (A) Images of nude mouse treated with 10mg/kg/day of 83b1 or vehicle control on the 19thday. (B) Plotting of the tumor volume versus day of nude mouse treated by either 83b1 or vehicle control. (***$p<0.001$). (C) Liver function assessment including albumin (ALB), alanine aminotransferase (ALT), aspartate aminotransferase (AST), Urea and total bilirubin (TBil) of the mice after the treatment of either 10 mg/kg or 50 mg/kg of 83b1.

The cytotoxic effect of 83b1 on ESCC tumor in animal was examined by recording the size reduction of the tumor with administration of either 10 mg per kg of nude mice of 83b1 or 0.1 ml of 6% PEG as the vehicle control to nude mice xenograft every day, the results were shown in Figure 3.13.

Initially, the tumor of the nude mice was allowed to grow until about 150 mm^3 and either 83b1 or PEG was administered. The tumor volume of the nude mice without the treatment of 83b1 was increased gradually every day until about 600 mm^3, whereas the tumor volume of the nude mice with the administration of 83b1 everyday was controlled at about 150 mm^3 on the 19th day. Until the 19th day, the volume of the tumor in the nude mice with the treatment of 83b1 compared to the vehicle control was significantly reduced ($p<0.001$). Therefore, 83b1 showed a significant *in vivo* anti-tumor effect on the ESCC cell line developed in animal.

Moreover, the liver function analysis was conducted through determination of the parameters including the amount of albumin (ALB), alanine aminotransferase (ALT), aspartate aminotransferase (AST), urea and total bilirubin (TBil) in blood of the mice. From the results shown in Figure 3.12C, all parameters of the mice treated with 10 mg/kg/day of 83b1 were decreased compared to the vehicle control. The value of ALB, ALT and AST of the mice treated with 50 mg/kg/day of 83b1 were not significantly higher than the value of control, however, the urea and Tbil values were increased by about 10% and 20% respectively.

3.5.10. *Effect of Over-expression and Activation of PPARD on COX-2 Expression*

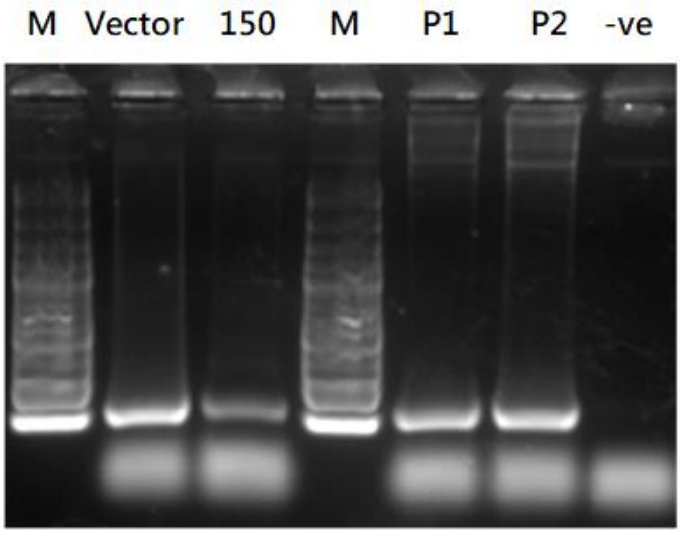

Figure 3.14. Image of agarose gel electrophoresis of the PPARD PCR product. Lane 1: 100bp marker, Lane 2: Original purchased PPARD over-expression plasmid, Lane 3: cDNA extracted from KYSE150

a positive control, Lane 4: 100bp marker, Lane 5: PPARD over-expression plasmid replicate 1 extracted from transformed E.coli, Lane 6: PPARD over-expression plasmid replicate 2 extracted from transformed E.coli, Lane 7: Negative control (water).

The effect of PPARD over-expression on COX-2 expression was determined by developing a PPARD over-expression ESCC cell line and analyzing the gene expression. In order to develop the PPARD-overexpressed KYSE150 cell line, PPARD over-expression plasmid was firstly transformed into E.coli and selected by the kanamycin in LB agar plate. The PPARD over-expression plasmid was extracted from the E.coli, and analyzed through PCR and agarose gel electrophoresis, the result was shown in the Figure 3.14. From the results, the PPARD over-expression plasmid, which was shown in lane 5 and 6, was successfully transformed and extracted from the E.coli. Therefore, the plasmid was then used for transfection into the ESCC cell lines.

After transfection of PPARD over-expression plasmid into an ESCC cell lines (KYSE150), the total RNA was extracted out from the cells and reverse-transcribed into cDNA. The cDNA was then analyzed through PCR and agarose gel electrophoresis. There are three target genes which were analyzed at the same time including PPARD, COX-2 and VEGF-A, the result was shown in Figure 3.15.

From the result, PPARD was overexpressed in the KYSE150PD (PPARD-transfected KYSE150) cell line compared to the parental KYSE150 (KYSE150P) cell line. Besides, it showed that the expression of COX-2 and VEGF-A in KYSE150PD were also higher than KYSE150P. All of the bands were analyzed by using a software called Image Lab from Bio-Rad and the intensity of each band was normalized by the reference gene β-actin, the summarized result was shown in Figure 3.15B. From the chart, the expression of PPARD, COX-2 and VEGF-A in KYSE150PD cell line were also significantly higher than that in KYSEP cell line ($p<0.01$, $p<0.05$ and $p<0.001$ respectively).

Moreover, the effect of PPARD activation on COX-2 expression was determined by analyzing the COX-2 expression in a ESCC cell line with the addition of GW0742 which is a PPARD agonist, the results were shown in Figure 3.16.

From the result, the expression of COX-2 was significantly increased in KYSE150 with the addition of GW0742 (0.1 and 1 μM: $p<0.05$ and 10 μM: $p<0.001$), it showed that promoting activation of PPARD by providing the potent PPARD agonist could increase the COX-2 expression.

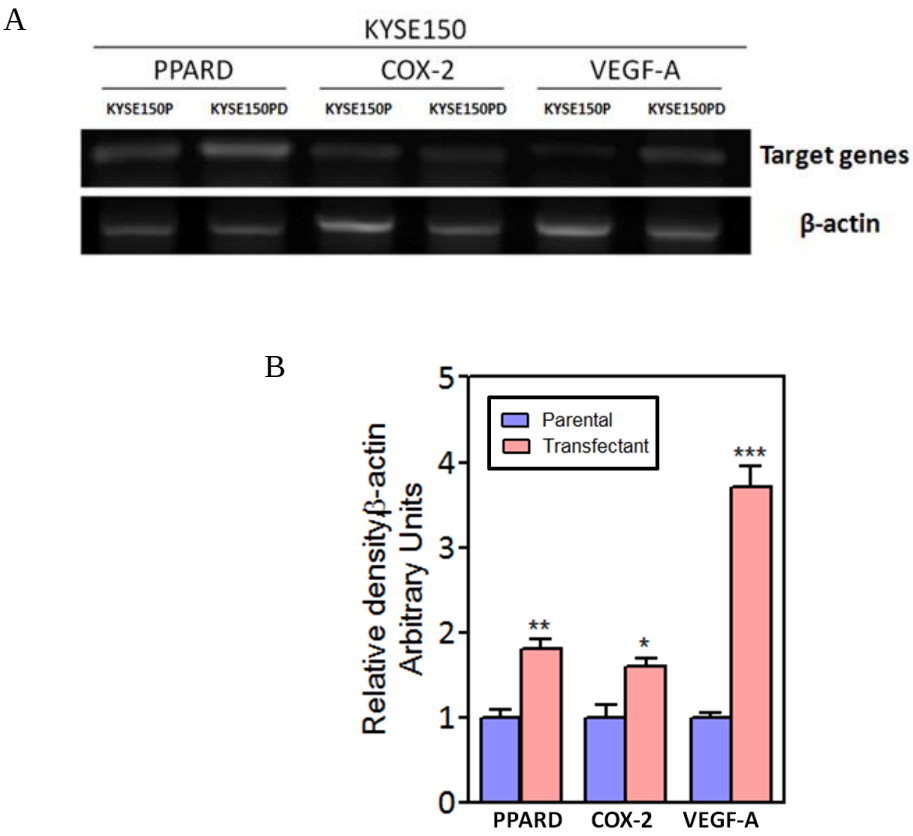

Figure 3.15. Agarose gel electrophoresis of the PCR product (Target genes: PPARD, COX-2 and VEGF-A) of the cDNA extracted from parental KYSE150 (KYSE150P) and PPARD-transfected KYSE150 (KYSE150PD) cell lines. (A) Image of the agarose gel electrophoresis. (B) Comparison of the intensity of the target gene expression normalized by reference gene between KYSE150P and KYSE150PD cell lines. (*p<0.05, **p<0.01 and ***p<0.001).

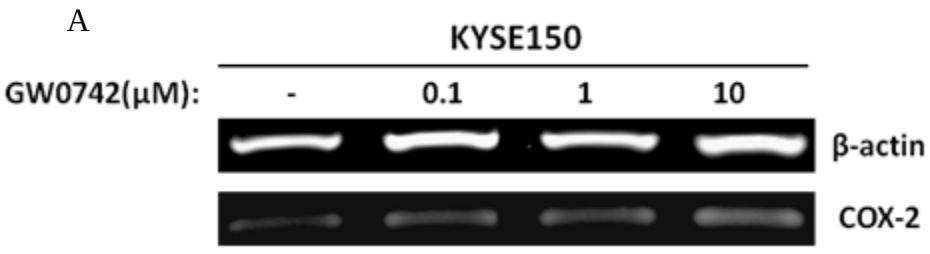

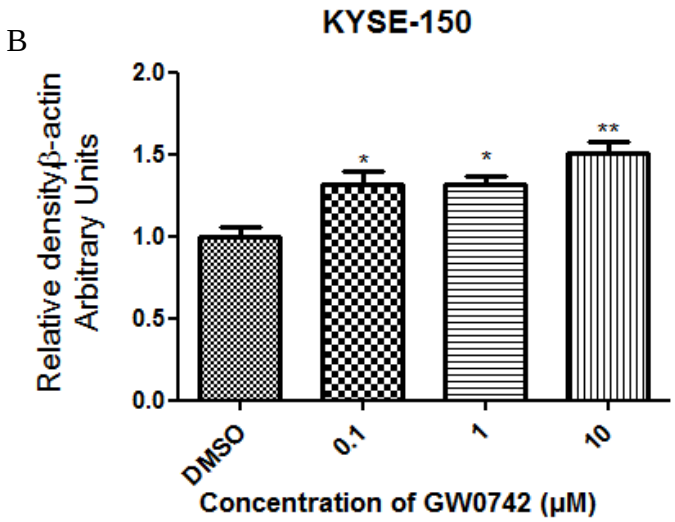

Figure 3.16. Agarose gel electrophoresis of COX-2 gene expression in KYSE150 cell line with the addition of PPARD agonist GW0742. (A) Image of the agarose gel electrophoresis. (B) Comparison of the intensity of COX-2 expression in KYSE150 with the addition of GW0742. (*p<0.05 and **p<0.01)

3.5.11. *Effect of 83b1 on COX-2 mRNA Expression*

The effect of 83b1 on COX-2 mRNA expression was determined by analyzing the expression of COX-2 in the ESCC cell lines with the treatment of 83b1 in dose-dependent manner through real-time PCR. Two ESCC cell lines from Japanese origin, including KYSE150 and KYSE450, and two ESCC cell lines from Chinese origin, including SLMT-1 and HKESC-4, were used for the analysis. The expression of COX-2 was normalized by the reference geneGAPDH and the results were shown in Figure 3.17.

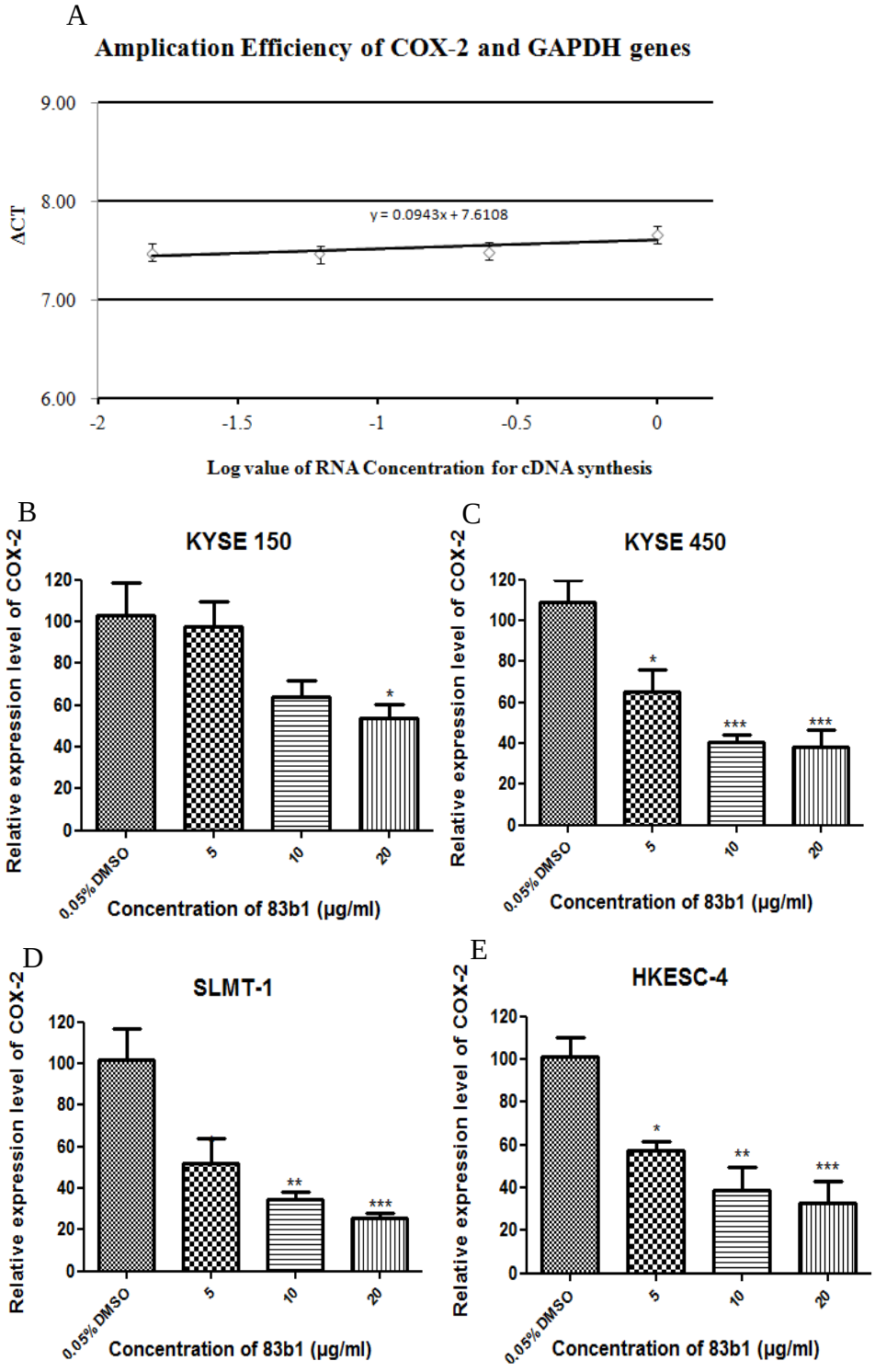

Figure 3.17. Real-time PCR of COX-2 mRNA expression in four human ESCC cell lines treated with different concentration of 83b1. (A) Amplification efficiency curve of COX-2 and GAPDH gene. (B) KYSE150, (C) KYSE450, (D) SLMT-1 and (E) HKESC-4. (*p<0.05, **p<0.01 and ***p<0.001).

From the results shown in Figure 3.17, the COX-2 expression in the four ESCC cell lines were also significantly reduced by the treatment of 83b1 in the dose-dependent relationship. Therefore, it showed that 83b1 could suppress the mRNA production in human esophageal cancers.

3.5.12. *Effect of 83b1 on COX-2 derived PGE_2 Production*

Conc. of BSA Standard (ρg/ml)	Log (Conc. of BSA Standard)	Std./Bo	Std./Bo/(1-Std./Bo)	ln [Std./Bo/(1-Std./Bo)]
1000	3	0.0343	0.0356	-3.336
500	2.699	0.0507	0.0534	-2.93
250	2.398	0.1188	0.1348	-2
125	2.097	0.2446	0.3238	-1.128
62.5	1.796	0.4391	0.7830	-0.245
31.3	1.496	0.6494	1.8522	0.616
15.6	1.193	0.7548	3.0784	1.124
7.8	0.892	0.8672	6.5307	1.877

Table 3.9. Data for PGE_2 standard curve obtained from ELISA.

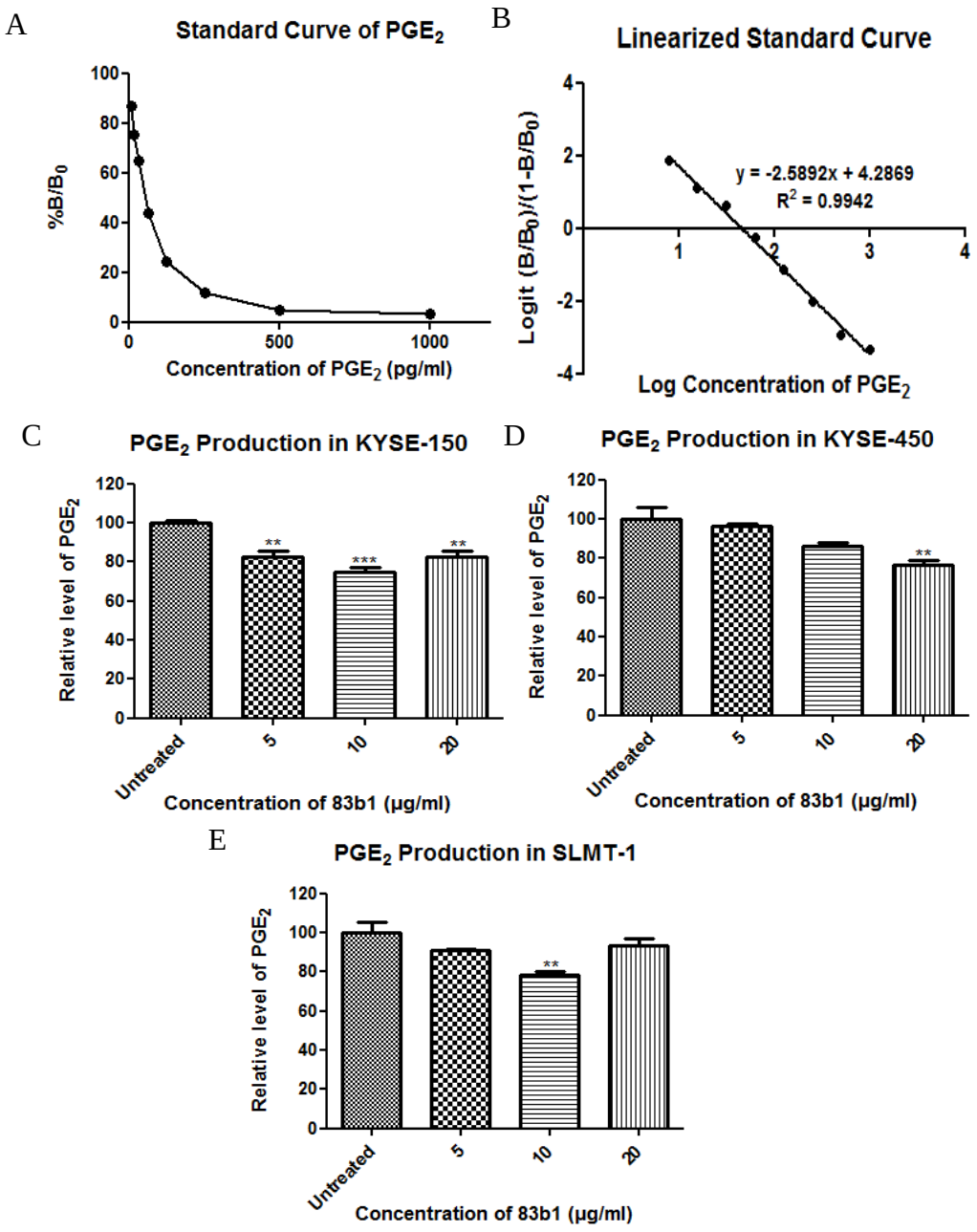

Figure 3.18. ELISA of PGE_2 production. (A) Standard curve of PGE_2 determination in ELISA. (B) Linearized PGE_2 standard curve for determination of PGE_2 production in ESCC cell lines. (C-E) ELISA of PGE_2 production in KYSE150, KYSE450 and SLMT-1 treated with different concentration of 83b1.(**p<0.01*** and p<0.001).

The effect of 83b1 on COX-2 derived PGE_2 production in ESCC cell lines was examined by using the ELISA kit from Cayman. The table 3.9 showed the raw data obtained from the ELISA of standard PGE_2 reagent, the data was summarized for plotting the standard curve and the linearized standard curve shown in the Figure 3.18 A and B. The linearized standard curve was used for calculating the amount of PGE_2 production to the culture medium for each ESCC cell lines with the treatment of different concentration of 83b1.

According to the results shown in Figure 3.18C to E, the production of $PGE_2$of all ESCC cell lines was significantly reduced by 83b1. For KYSE450, it showed a negatively dose-dependent relationship between the PGE_2 production in medium and concentration of 83b1, the most effective dosage of 83b1 is 20μg/ml ($p<0.001$). As for the other two ESCC cell lines which were KYSE150 and SLMT-1, the most effective dosage of 83b1 for reducing the PGE_2 production was 10μg/ml ($p<0.001$ and $p<0.01$ respectively), the production of PGE_2 was then slightly increased in these two cell lines with the treatment of the higher concentration of 83b1.

3.5.13. *Cytotoxicity Assessment of 83b1 in other Cancer Cell Lines*

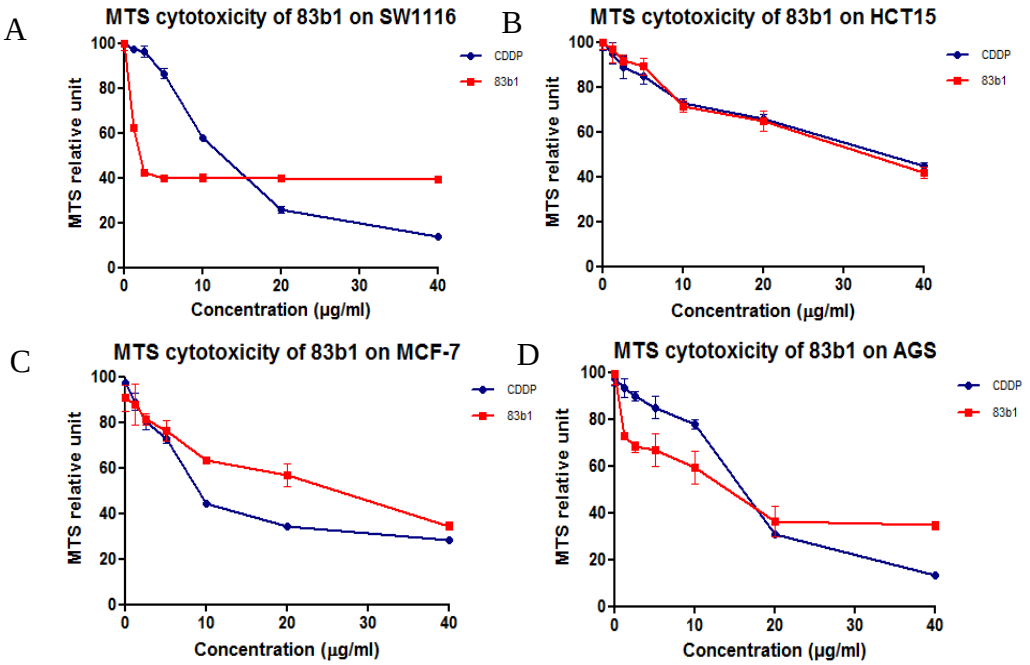

Figure 3.19. Cytotoxic assessment of 83b1 (Maximum concentration: 40μg/ml) in human cancer cell lines: (A) SW1116, (B) HCT15, (C) MCF-7 and (D) AGS.

Cell Lines	MTS_{50} of 83b1 (μg/ml)	MTS_{50} of CDDP (μg/ml)	MTS_{50} of 83b1/ MTS_{50} of CDDP
SW1116	2.30	12.12	0.189769
HCT15	30.73	34.76	0.884062
MCF-7	21.78	10.83	2.01108
AGS	12.52	15.04	0.832447

Table 3.10. Summary of the MTS_{50} of 83b1 and CDDP, and the ratio of MTS_{50} of 83b1 to CDDP according to the results from Figure 3.19.

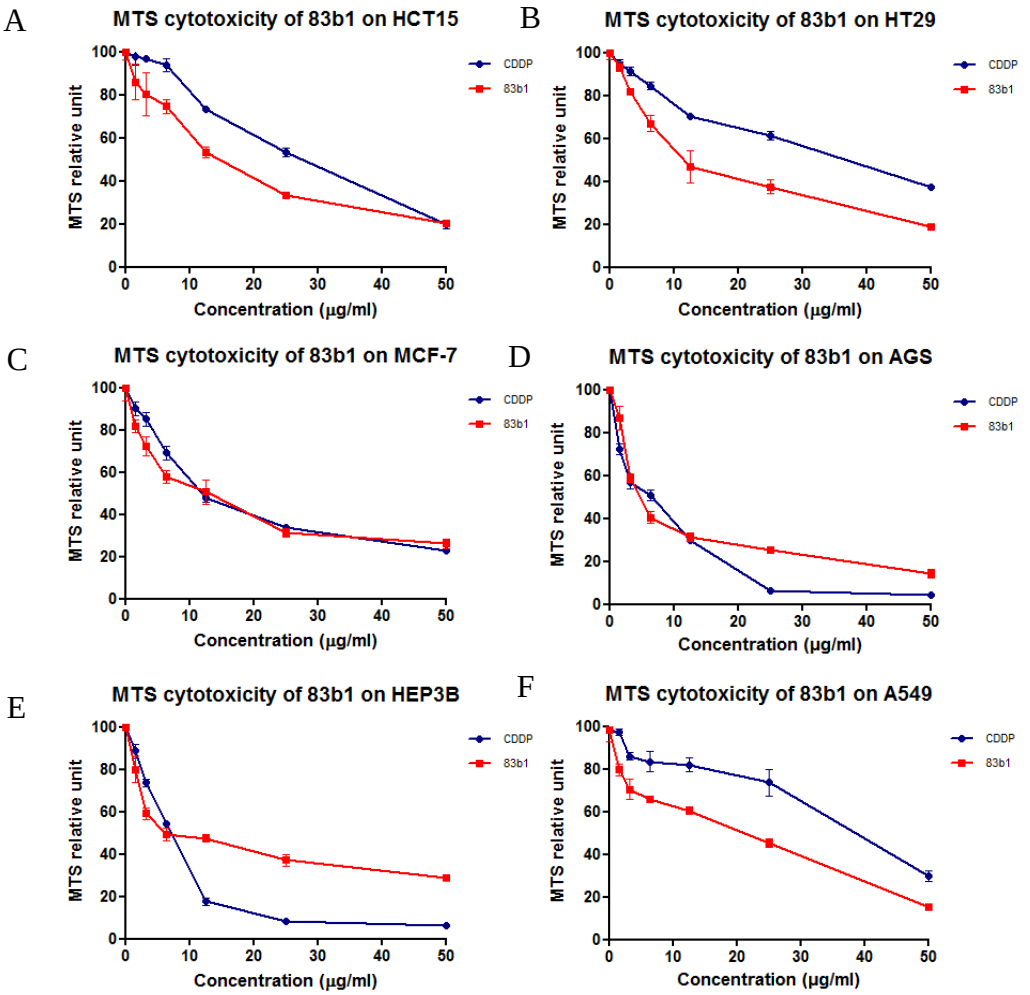

Figure 3.20. Cytotoxic assessment of 83b1 (Maximum concentration: 50μg/ml) in human cancer cell lines: (A) HCT15, (B) HT29, (C) MCF-7, (D) AGS, (E) HEP3B and (F) A549.

Cell Lines	MTS_{50} of 83b1 (μg/ml)	MTS_{50} of CDDP (μg/ml)	MTS_{50} of 83b1/ MTS_{50} of CDDP
HCT15	13.86	24.75	0.56
HT29	12.87	33.11	0.388704
MCF-7	10.90	13.25	0.822642
AGS	5.60	4.65	1.204301
HEP3B	8.88	6.08	1.460526
A549	13.82	35.59	0.388311

Table 3.11. Summary of the MTS_{50} of 83b1 and CDDP, and the ratio of MTS_{50} of 83b1 to CDDP according to the results from Figure 3.19.

The *in vitro* cytotoxic assessment of 83b1 for other cancer cell lines including SW1116, HCT 15 and HT29 (Colon cancer), MCF-7 (Breast cancer), AGS (Gastric cancer), HEP3B (Liver cancer) and A549 (Lung cancer) was conducted also by MTS assay, the results were shown in Figure 3.19 and 3.20.

For the Figure 3.19, the highest concentration of 83b1 used for treating the cancer cells was 40μg/ml, as for the Figure 3.20, the highest concentration of 83b1 used was 50μg/ml. The results were summarized as MTS_{50} and shown in table 3.10 and 3.11.

The concentration of 83b1 required for reducing the MTS_{50} value by half was about 2.30 - 13.86μg/ml, whereas the concentration of CDDP required for reducing the MTS_{50} value by half was about 4.65 - 35.59 μg/ml. It showed that the anti-cancer effect of 83b1 was generally stronger than the widely used anti-cancer drug CDDP. As shown in table 3.10 and 3.11, the toxicity of 83b1 on the human non-tumor cell lines was extremely lower than CDDP, it means that, beside of ESCC cell lines, 83b1 is also more effective and safer than CDDP for treating the cancer cell lines.

3.5.14. *Expression of PPARD and COX-2 in other Cancers*

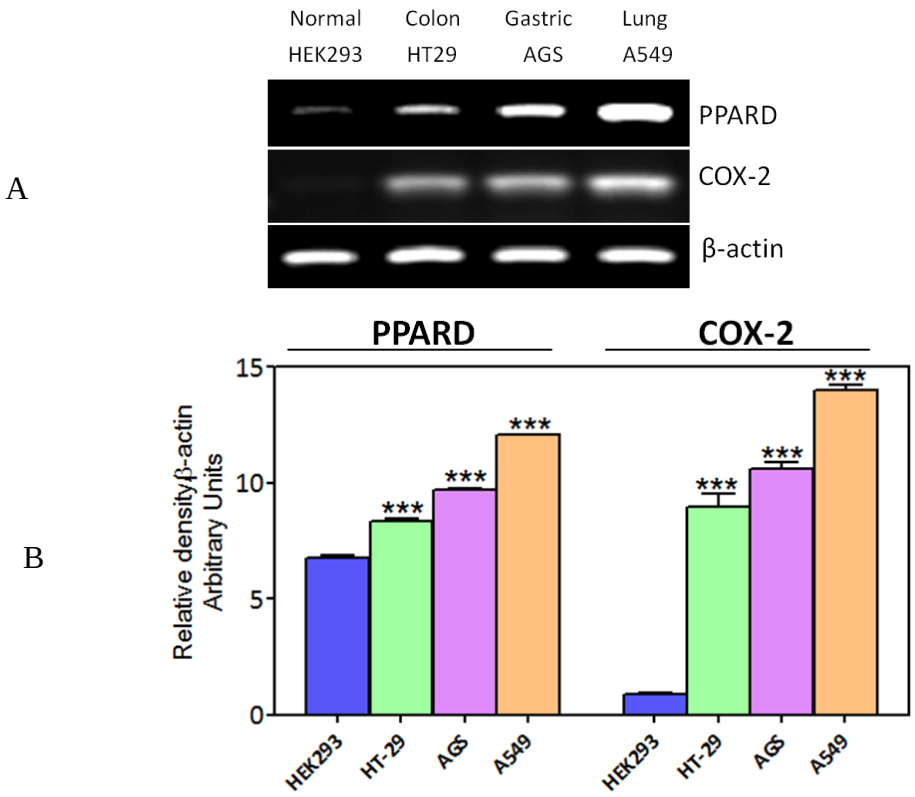

Figure 3.21. Agarose gel electrophoresis of the RT-PCR products (Target genes: PPARD and COX-2) of the cDNA extracted from four cell lines including HEK293 (Non-tumor), HT29 (Colon cancer), AGS (Gastric cancer) and A549 (Lung cancer). (A) Image of the agarose gel electrophoresis. (B) Comparison of the intensity of the target gene expression normalized by reference gene between the three cancer cell lines and the non-tumor cell line. (***p<0.001).

The expression of PPARD and COX-2 in other cancer cell lines including colon cancer (HT29), gastric cancer (AGS) and lung cancer (A549) compared to a human non-tumor embryonic kidney cell line was determined by RT-PCR and

agarose gel electrophoresis, the result was shown in Figure 3.21 and the expression intensity was analyzed and summarized in Figure 3.21 B.

From the results, the expression of PPARD and COX-2 in HT-29, AGS and A549 were also significantly lower than HEK293 ($p<0.001$). Therefore, it showed that PPARD and COX-2 are also overexpressed in other cancers, at least including colon cancer, gastric cancer, and lung cancer.

3.5.15. *Effects of 83b1 on Cancer-related proteins in ESCC*

The expression of cancer-promoting proteins including ATF-2, HSP-27, JNK-1, MAPK, MEK-1 and AKT in ESCC cell lines (KYSE-450 and HKESC-4) with treatment of different concentration of 83b1 was assessed by using Bio-plex assay kit from Bio-Rad.

According to the results shown in Figure 3.22, the proteins including ATF-2, HSP-27, JNK-1, MAPK, MEK-1 and AKT in the phosphorylated form were significantly (**$p<0.01$*** and $p<0.001$) down-regulated by 30μg/ml of 83b1 for 48 hours in the two ESCC cell lines including KYSE-450 (Figure 3.22 A) and HKESC-4 (Figure 3.22 B).

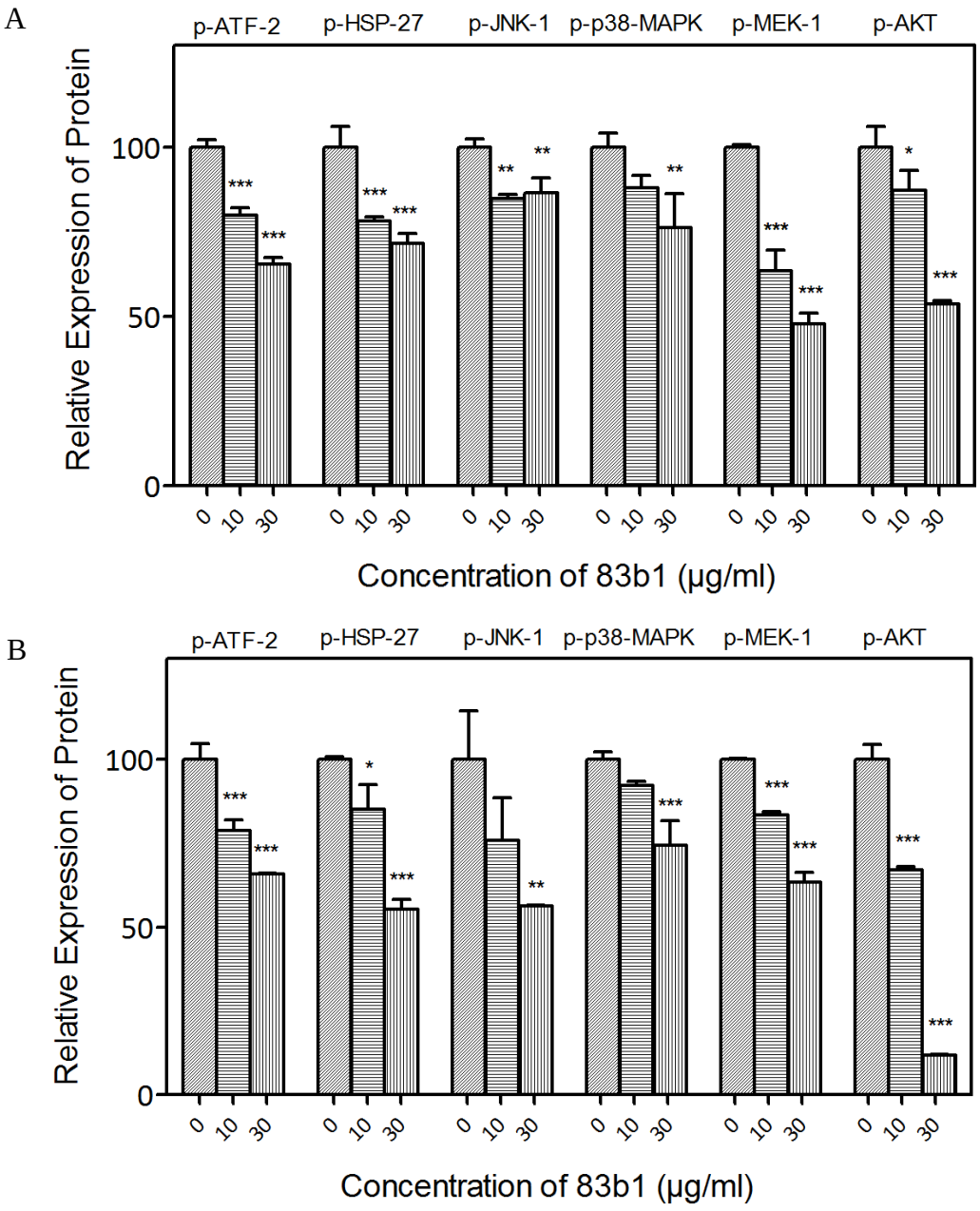

Figure 3.22. Relative expression of target proteins with treatment of 83b1 in different concentrations assessed by Bio-plex, (A) KYSE-450 and (B) HKESC-4 (*p<0.05, **p<0.01*** and p<0.001).

3.6. DISCUSSION

In this chapter, the anti-cancer effects of 83b1 on human cancer, especially in ESCC, were characterized. Before starting the examination of the anti-cancer effects

of 83b1 on cancers, the structure and purity of 83b1 were firstly determined through ^{1}H-NMR and HPLC followed by ESI-MS. It is important to confirm that the structure of the compound used for all experiments was really what we would like to use, the results showed that the structure of 83b1 was under our expectation. As for the result from HPLC and ESI-MS, it showed that the purity of 83b1 was very high (about 99.7%). It is necessary to obtain the compound which is pure enough in order to confirm the anti-cancer effects were from the compound but not from other impurities, and it is also important to avoid any unwanted side-effects from the impurities.

After validation of the structure and purity of 83b1, the SEA program was performed to predict the possible targets of 83b1 in human. From the results of the program, there were many targets with different expected value and maximum target complementary value in different species, however, only the possible targets ranking the first seven highest expected value in human were taken out from the whole list for further consideration. Among these seven targets shown in the table 3.2, the second possible target, which was PPARD, was firstly chosen for the investigation since this target also had the highest maximum target complementary value and it is much well-understanding in tumor development than the possible target found in the first rank which is sodium- and chloride-dependent glycine transporter 2. However, there are some other possible targets of 83b1 which might also be important in tumor

development; they will be investigated in future because of the time limitation. Besides of the SEA program, *in silico* binding assessment of 83b1 to PPARD was conducted by using the molecular docking analysis to further confirm the binding affinity of 83b1 to PPARD. At the same time, an abundant PPARD ligand, AA, was also used as a positive control to compare the affinity to PPARD. It very important to estimate the binding competitiveness for PPARD as there are many natural ligands surrounding this receptor, 83b1 may not be able to compete for PPARD with the natural ligands even 83b1 can really bind to PPARD. As mentioned from the results, the free binding energy of 83b1-PPARD complex was more negative than AA-PPARD complex, it showed that 83b1 has certain competitiveness for PPARD. Furthermore, the binding of 83b1 to PPARD was further confirmed by using the *in vitro* binding assessment, ITC assay. Therefore, the comprehensive assessment of the anti-cancer effects of 83b1 was then carried out.

Although previous studies from other researchers have shown that the role of PPARD in carcinogenesis is still controversial, there were some reports revealed that PPARD promotes cancer development in lung cancer, melanoma, ovarian cancer, liposarcoma and colorectal cancer in human.[136-140] However, there is insufficient information to show the carcinogenesis of PPARD in esophageal cancer which is one of the most lethal cancers since lack of studies about PPARD in esophageal cancers

have been conducted; and there is no any U.S FDA (Food and Drug Administration)-approved anti-cancer drug for targeting PPARD due to its controversy.[141] Therefore, the first main part in this chapter is to determine the expression of PPARD in ESCCs compared with non-tumor cells and whether activation of PPARD promotes ESCC growth. The expression of PPARD in the ESCC cell lines and the function of PPARD in ESCC cell proliferation were determined before examination of the anti-cancer effects of 83b1 on human ESCC. From the results of RT-PCR and IHC staining shown in the Figure 3.8, the gene and protein expression of PPARD were also found to be highly expressed in ESCC cell lines. Moreover, according to the results shown in Figure 3.9 and 3.10, activation of PPARD by its potent agonist GW0742 in ESCC cell lines was shown to promote their proliferation by more than 50% compared to the negative control when the dosage of GW0742 was higher than 0.13 μg/ml in KYSE450 and more than 20% when the dosage of GW0742 was higher than 0.5 μg/ml in SLMT-1.

It showed that the gene and protein of PPARD was over-expressed in ESCCs and activation of PPARD in ESCCs promotes cell proliferation. Hence, 83b1 is possible to suppress the development of ESCC or even kill the ESCC through targeting and antagonizing PPARD.A series of experiments were then conducted to demonstrate the effects of 83b1 on cancer suppression in ESCCs.

In vitro MTS assay was performed to determine the cytotoxic effect and toxicity of 83b1 on a series of ESCC cell lines and non-tumor cell line respectively compared to a widely used anti-cancer drug, CDDP, which was used as the positive control. From the results shown in Figure 3.11 and 3.12 and summarized in table 3.7 and 3.8, 83b1 showed the comparable cytotoxicity on ESCC cell lines with CDDP. The ratio of MTS_{50} of 83b1 to CDDP was about 0.37 to 6.67, it showed that the tumor suppression effect of 83b1 was stronger than CDDP in some ESCC cell lines but also weaker in some cell lines. However, the ratio of MTS_{50} of 83b1 to CDDP in the human non-tumor cell lines was always higher than 1, and sometimes, the ratio was higher than hundred folds in some non-tumor cell lines. It showed that the toxicity of 83b1 was extremely lower than CDDP which is usually used for the current cancer treatment. It is the important potential of 83b1 for being an anti-cancer therapeutic as it showed the strong cytotoxic effects on ESCC cell lines but the weaker toxicity in non-tumor cells, it is believed that 83b1 can lead to fewer unexpected side-effects on our body. It was also found that the cytotoxicity of 83b1 against ESCC cell lines were not directly proportional to the expression of PPARD in ESCC cell lines according to the result of IHC showing the expression of PPARD protein in ESCC cell lines in Figure 3.8. Since the cytotoxicity of anti-cancer compounds on cancer cells was affected by multiple factors rather than only the expression of targets, the cytotoxicity

is also influenced by the anti-cancer resistance, drug permeability of the cell membrane, healthy status of the cancer cells and so on.

Furthermore, *in vivo* assessment of 83b1 was conducted to determine the cytotoxic effects of 83b1 on a real malignant tumor in the mice. The KYSE450 tumor was developed in athymic nude mice to about 150mm^3 large followed by administration of either 10 mg/kg/day of 83b1 or vehicle control (6% PEG) to examine the effect of 83b1 on the tumor. After 19 days, the tumor in the mice treated with the vehicle control was increased to about 600 mm^3, whereas the tumor in the mice treated with the 10 mg/kg/day of 83b1 was controlled at about 150mm^3. It showed that 83b1 significantly suppress the growth of the tumor in animal.

After the *in vivo* cytotoxic assessment of the nude mice, the blood of the mice treated with 83b1 was obtained for liver function assessments. The value of ALB, ALT, AST, urea and TBil in blood were measured in order to know the liver damages by 83b1. From the results shown in Figure 3.13C, it showed that all of the parameters in the mice treated with 10 mg/kg/day of 83b1 were lower than the control. For the value of ALB, it directly refers to the functions of liver as albumin is one of the main proteins made by liver, and there are two reasons why the amount of albumin was decreased. The first one is that the liver got damage and another reason is that the liver was focusing on other functions such as detoxification of the metabolites,

therefore the synthesis of albumin was being slow down. Both ALT and AST values were used to monitor the hepatocellular injuries, elevation of the level of these two enzymes indicates the liver got damages and they are used for repairing the liver. As for the value of TBil, it refers to ability of liver for breaking down the wastes as bilirubin is originally a waste processed by liver. All parameters, except ALB, in the mice treated with 10 mg/kg/day of 83b1 were also decreased, it indicated that the liver functions were still fine and they were not affected by 83b1. Therefore, it showed that 83b1 was safe for cancer treatment in animals.[142-144]

After both *in vitro* and *in vivo* cytotoxic assessment of 83b1 had been conducted, the mechanisms how 83b1 suppresses tumor growth were then investigated. At first, the influence of over-expression and activation of PPARD on COX-2 expression was carried out by RT-PCR and agarose gel electrophoresis. It has been found that over-expression of PPARD in the KYSE150PD cell line showed the significant up-regulation of COX-2 and also VEGF-A expression, at the same time, activation of PPARD by the potent PPARD agonist GW0742 also significantly increased the expression of COX-2 in KYSE150 cell line. It demonstrated that both over-expression and activation of PPARD also up-regulated the expression of COX-2 in human esophageal cancer. Therefore, it was important to know the effect of 83b1

on the expression of COX-2 and the downstream product which is COX-2 derived PGE_2 in human ESCC cell lines.

The gene expression of COX-2 in ESCC cell lines was determined through real-time PCR, the results were analyzed by using $2^{-\Delta\Delta Ct}$ and shown in Figure 3.17. Since one of the most important criteria of using the $2^{-\Delta\Delta Ct}$ method is that the amplification efficiency of the target gene and reference gene should be close enough, then the reference gene can be used for normalizing the Ct value of target gene in the cell lines treated with different concentration of 83b1. Hence, before using the $2^{-\Delta\Delta Ct}$ for analyzing the results from real-time PCR, A plot of ΔCt value against the log dilution of total RNA used for making cDNA was needed. It is necessary that the slope of the curve should be close to 0, then the efficiencies of the target gene and reference gene were similar enough to use the $2^{-\Delta\Delta Ct}$ method to calculate the semi-quantitative expression of the target genes in different treated cell lines. From the result, the slope of the curve was 0.094; therefore, it showed that the GAPDH gene can be used as the reference gene for normalizing the COX-2 gene and the $2^{-\Delta\Delta Ct}$ method was allowed to use.

By using the $2^{-\Delta\Delta Ct}$ method, as mentioned, 83b1 showed the significant down-regulation effect on COX-2 expression in the dose-dependent manner in all four ESCC cell lines including KYSE150, KYSE450, SLMT-1 and HKESC-4. After the

suppressive effect of 83b1 on COX-2 expression was found, it was also important to know the effect of 83b1 on the production of the final product, the COX-2 derived PGE_2, which directly participates in cancer development.

ELISA kit was used to determine the production of COX-2 derived PGE_2 in culture medium. Since the PGE_2 is freely secreted out to the medium from the cells, the medium can be directly obtained and the amount of PGE_2 in medium can be measured by the ELISA with reference to the standard curve plotted by using the standard PGE_2 reagents. It showed that 83b1 can also significantly reduce the production of PGE_2 in all ESCC cell lines. Therefore, it is possible that 83b1 can target PPARD and antagonize it, the expression of COX-2 and COX-2 derived PGE_2 were hence reduced. Consequently, the cancer cells were suppressed and killed through apoptosis.

Besides of the comprehensive analysis of 83b1 on ESCC cell lines, the *in vitro* cytotoxic assessment of 83b1 in other cancer cell lines was conducted, and the expressions of both PPARD and COX-2 were also determined in order to know the potential of 83b1 for treating other cancers through targeting PPARD apart from esophageal cancers.

From the results shown in Figure 3.19 and 3.20, it demonstrated the strong anti-cancer effects of 83b1 on other cancer cell lines including colon cancer, gastric

cancer, breast cancer, liver cancer and lung cancer, even stronger than CDDP on some cell lines. Moreover, the expressions of PPARD and COX-2 in colon cancer, gastric cancer and lung cancer were significantly higher in non-tumor cell line as shown in Figure 3.21. Therefore, 83b1 has the potential to be used for treating other types of cancers through targeting PPARD and suppressing COX-2 and PGE_2 expression.

Furthermore, it showed 83b1 can also significantly down-regulate some important cancer-promoting proteins including ATF-2, HSP-27, JNK-1, MAPK, MEK-1 and AKT which participates in many cancer induction pathways such as Fibroblast growth factors (FGF) signaling pathway and Erk/MAPK signaling pathway as shown in the Figure 3.23 and 3.24 which were analyzed and generated by using the cell signaling program, Ingenuity Pathway Analysis (IPA).

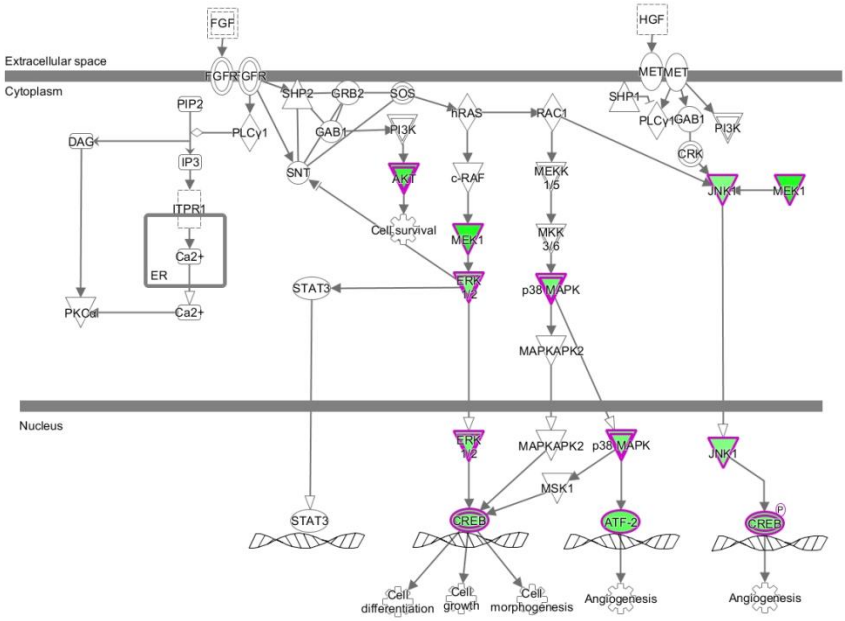

Figure 3.23. Fibroblast growth factors (FGF) signaling pathway.

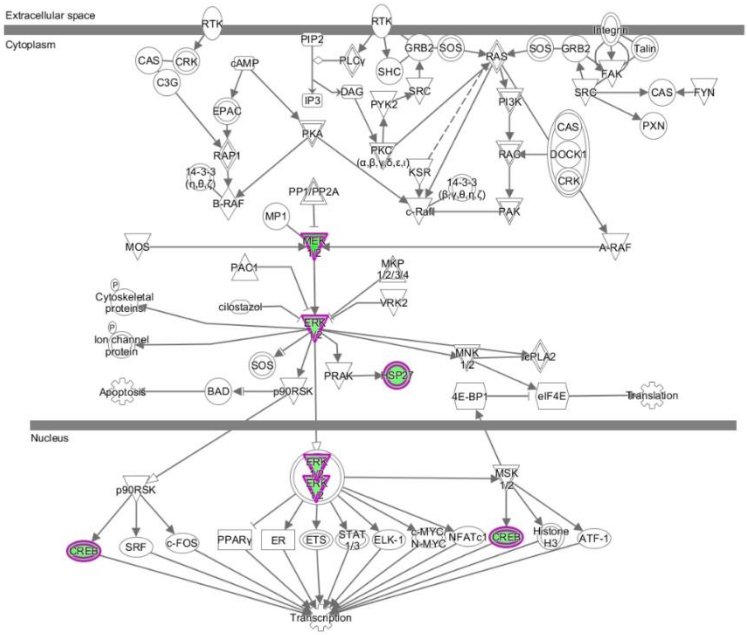

Figure 3.24. Erk/MAPK Signaling pathway.

Although the complete carcinogenesis of PPARD in different cancers is still not clearly understood and controversial in different cases, these studies demonstrated the functions and parts of the mechanisms of PPARD in tumor development in ESCCs. It also showed the anti-cancer effects of the novel quinoline derivative, 83b1, on tumor suppression with down-regulation of a series of cancer-related proteins in ESCCs. This study offers the prospect of suppressing cancers, especially in esophageal cancer, through targeting PPARD if the investigation of PPARD in cancer can be further studied deeply or extended to the human studies in future. This also showed the potential of 83b1 to be used against ESCC after it is more comprehensively studied in different aspects.

3.7. OTHER INFORMATION ABOUT 83b1

A simple, fast and sensitive UHPLC-MS/MS method for quantifying the amount of 83b1 in plasma and how it can be applied in bioavailability assessment of 83b1 in rats have been studied and reported by Mr. Wen and Prof. Zhong.[145] They found that the plasma concentration of 83b1 increased very fast after oral administration of 10 mg/kg of 83b1 by oral gavages and it reached the maximal concentration in about one hour, the concentration of 83b1 in plasma was then decreased gradually with half life time ($t_{1/2}$) of 4.13 h and total clearance of 25.2 l/kgh shown in Figure 3.25 and table 3.12. The oral bioavailability of 83b1 was determined as about 20.9% which showed the potential of 83b1 to be developed into an oral drug, and it is also important for the further studies of the bioavailability of 83b1 to be used for treating cancers.

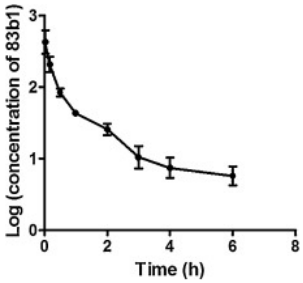

Figure 3.25. The log concentration of plasma 83b1 after administration of 10mg/kg of 83b1 in rat through oral gavages.

Parameter	Oral administration of 83b1 (10 mg/kg)
Maximal concentration, Cmax (μg/l)	246.5 ± 137.9
Time to reach Cmax, Tmax (h)	1.08 ± 0.49
$t_{1/2}$ (h)	4.13 ± 2.79
Clearance (l/kgh)	25.4 ± 11.7
Bioavailability (%)	20.9 ± 8.8

Table 3.12. The pharmacokinetics parameters of 83b1 after oral administration of 10mg/kg of 83b1 in rat.

3.8. CONCLUSION

In summary, the anti-cancer activities of 83b1 in human esophageal cancers and the possible mechanisms on how 83b1 inhibit the growth of esophageal cancer were demonstrated. 83b1 is a potential anti-cancer compound for suppressing tumor development of esophageal cancers through targeting PPARD and down-regulating the expression of COX-2 and production of COX-2 derived PGE_2. Furthermore, 83b1 also showed its potentials for treating other types of cancers with higher expression of PPARD and COX-2.

Chapter 4 CHARTERIZATION OF A NOVEL QUINOLINE DERIVATIVE 160a IN HUMAN ESOPHAGEAL CANCER CARCINOMAS

4.1. INTRODUCTION

As mentioned in the chapter 3, it is necessary to develop more potential therapeutics for treating esophageal cancers because of the incidence, severity and mortality of the disease. It has also been shown that the ingredients extracted and purified from natural sources would show the very strong anti-disease activities after chemical modification of the original structure of the ingredients.

Besides of the 83b1 discussed in chapter 3, there is another novel quinoline derivative named 160a which showed the potential to be used in cancer treatments. In this chapter, the synthesis of 160a, anti-cancer activities of 160a in human ESCC cell lines and its potential for other cancers were reported.

4.2. SYNTHESIS OF 160a

(8-(3-methoxybenzyloxy)quinoline-2-carbaldehyde (160a) was also kindly provided by a member in our research group, Dr. Penny Sau-hing CHAN, and was prepared by oxidation of 8-(3-methoxybenzyloxy)-2-methylquinoline with addition of selenium dioxide, pre-dried 1,4-dioxane and water in reflux for 24 hours. Whereas,

8-(3-methoxybenzyloxy)-2-methylquinoline was synthesized by nucleophilic substitution of commercially available 2-methyl-8-quinolinol with 3-methoxybenzyl bromide in DMF at room temperature and monitored by thin-layer chromatography (TLC). The structure of 160a was further determined and validated in this study.

4.3. MECHANISMS OF P-GLYCOPROTEIN RELATED TO CANCER DEVELOPMENT

According to our preliminary docking results, the most possible target of 160a in human was predicted as P-glycoprotein-1 (P-gp). P-gp has been identified as a cancer biomarker in different human cancers, hence 160a has the great potential for treating cancers through targeting P-gp and antagonizing it.

In this part, we would have a brief introduction of P-gp and then discuss the functions of P-gp in tumor development.

4.3.1. *Introduction to P-gp*

P-glycoprotein (P-gp) is also known as multi-drug resistance protein 1 (MDR1), multi-drug resistance protein (MRP) plays an important role in physiological and protective activities in different species such as mammals, bacteria, yeasts and plants. They are capable of transporting a broad range of molecules across

the cellular membrane to the outside of the cells, this is one of the primary protective mechanisms in many species through removing the toxic substances or foreign substance including pathogens and drug molecules from the cells.[48, 146]

P-gp is also a polytopic membrane transporter which belongs to the ATP-binding cassette (ABC) superfamily.[48, 147] ABC transporters are classified into 7 subfamilies from A to G based on their relative sequence homology and there are several members grouped in each super-family, P-gp is classified into ABCB group (ABCB1) and it is encoded by the *MDR1* gene on the chromosome 7q21.[148] P-gp has been identified as an onco-protein, as mentioned, it is a MDR which is one of the biggest clinical challenges for cancer treatments since they confer the anti-therapeutic abilities to the cancer cells for protecting them from anti-cancer therapeutics, it usually results in limited therapeutic options and poor patient outcome in many types of cancers including prostate cancer, breast cancer, lung cancer, esophageal cancer, colon cancer and so on.[48, 54, 149]

The secondary structure of P-gp was shown in Figure 4.1, the size of P-gp is about 170 kDa which consists of two pseudo-symmetrical halves and each of the halves contains a transmembrane domain (TMD) and nucleotide binding domain (NBD). There are 6 transmembrane putative α-helix in each of the halves and total of 12 transmembrane units in one P-gp. As for the NBD, it plays a crucial role in ATP

binding. It has been reported that binding and hydrolysis of ATP at the NBD would trigger a large conformational change of P-gp, the alteration will switch conformation of TMD from "facing to cytoplasm" to "facing to cytosol". This conformational change allows the molecules to be transported across the biological membrane from cytoplasm to the extracellular space. It has been shown that P-gp is able to bind and export a wide spectrum of cationic amphipathic molecules ranging in the size from 100 to 4000 Da.[48, 148, 150]

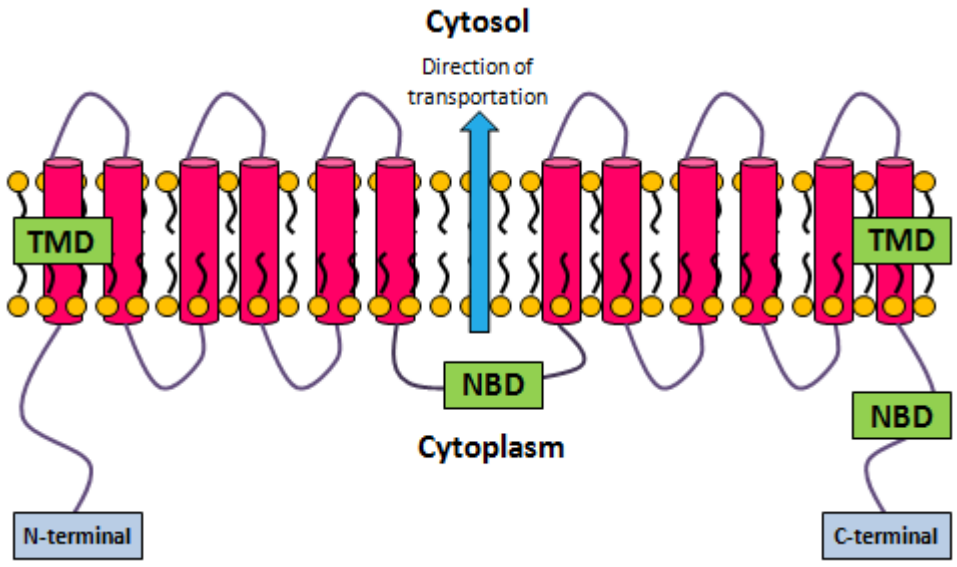

Figure 4.1. Secondary structure of P-gpwith two halves and each contains one TMD and NBD.

4.3.2. *Mechanisms of P-gp in tumor development*

In spite of the ubiquitous expression of P-gp in normal tissues throughout the body, many studies have shown that the expression of P-gp is up-regulated in many cancer cells such as breast cancer, lung cancer, prostate cancer and esophageal

cancers. P-gp, as mentioned, can confer the ability to the cancer cells for resisting the anti-cancer reagents through exporting them from the cytoplasm to the outside of the cells, the anti-cancer reagents hence cannot be accumulated inside of cells to a functional dosage and ultimately the cancer cells survive even they are treated by the chemotherapeutics. Therefore, higher expression of P-gp implies the poor response of the cancer cells to the anti-cancer drugs and poor survival rates of the patients.[54, 149, 151]

The mechanisms of P-gp conferring drug resistance to tumor cells require binding of ATP to the NBD of P-gp, hydrolysis of ATP and conformational alteration, and the flow chart of the mechanisms of P-gp is shown in the Figure 4.2. The first step of the mechanisms is the binding of substrate such as doxorubicin (Dox), paclitaxel and vinblastine which are the widely-used anti-cancer chemotherapeutics to P-gp, the structures of these anti-cancer drugs are shown in the table 4.1.[48, 146-148] When the anti-cancer drugs is accumulated inside of the cells at a certain concentration, some of them will bind to the "on" site of P-gp which is the higher affinity binding site of the substrates to P-gp, and this triggers the free ATP to bind to either one or both of the two NBDs of P-gp. The ATP is then hydrolyzed into ADP

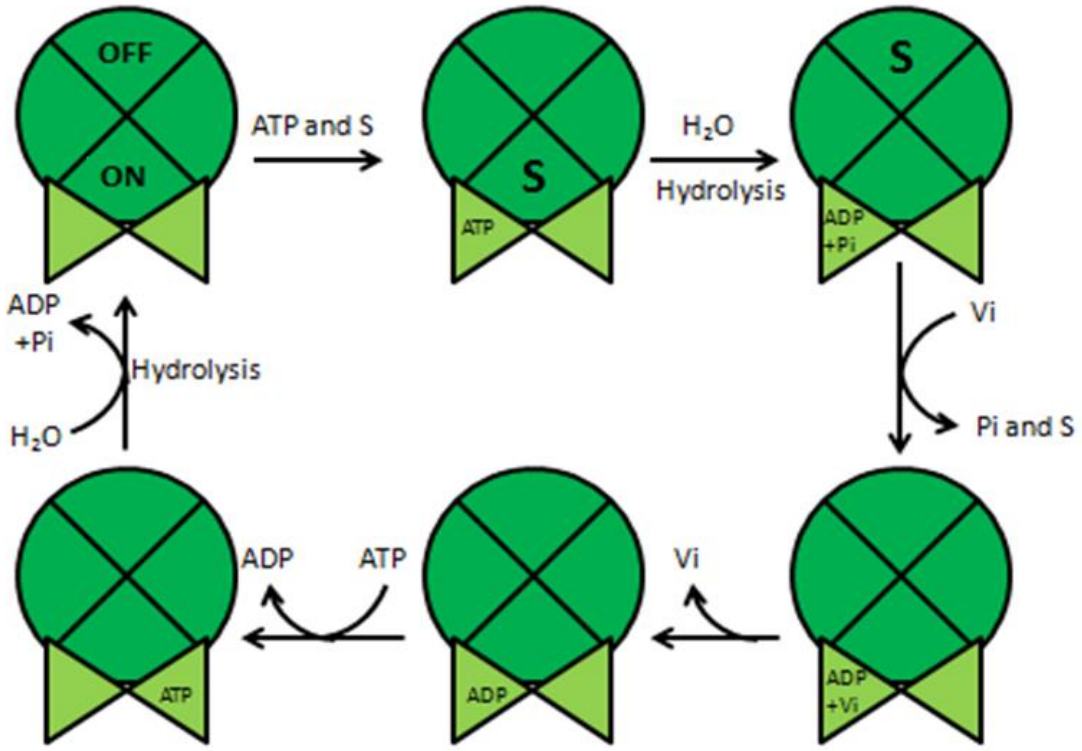

Figure 4.2. The flow chart of the mechanisms of P-gp to extrude substrates by hydrolysis of ATP and conformational change. S: Substrate.

and Pi, and catalyzes the conformational alteration of the P-gp. The drug is hence migrated to the "off" site of P-gp which is the lower affinity binding site of substrate to P-gp, afterwards, the Pi molecule is released and the drug is also extruded from the P-gp because of the lower affinity to the drug and the conformational movement of P-gp. After removal of the drug, the Pi will be replaced by vanadate molecule (Vi) to form the P-gp-ADP-Vi complex which has a lower affinity to the drug, it is important to avoid the reverse-transportation of the drug back into the cells again. The ADP and Vi are disassociated from the complex, a new ATP molecule is then instantly

interacted with the complex and immediately hydrolyzed to provide energy for restoration of the conformation of P-gp into the original state which has the higher affinity to the substrate for binding again.[48, 56, 146, 148, 149]

This is a non-stopped process when the supply of free ATP is abundant; therefore, the anti-cancer drugs cannot be accumulated inside of the cancer cells and exhibits their anti-cancer activities since most of them are exported by P-gp from the cells to the extra-cellular spaces. This is the primary mechanism of P-gp that contribute to the tumor cells for the chemotherapeutic resistance and this is the reason why the higher expression of P-gp in tumor cells usually results in poor therapeutic outcomes.[50, 54, 147]

4.3.3. *Current approach for treating the cancers with high expression of P-gp*

As mentioned, P-gp confers the chemotherapeutic resistance to the cancer cells by extruding the anti-cancer drugs out of the cells, it hinders the accumulation of the drugs for their activities and it hence extremely reduces the effects of the drugs on the tumors.

The current approach for treating the cancers with high expression of P-gp is to use the P-gp blockers or inhibitors for suppressing the functions of P-gp.[52] The P-gp blockers or inhibiters can either block or antagonize the substrate-binding sites

Anticancer Drug Substrates	**Inhibitors**
Doxorubicin 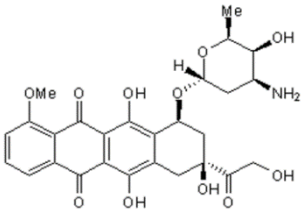	Cyclosporin A 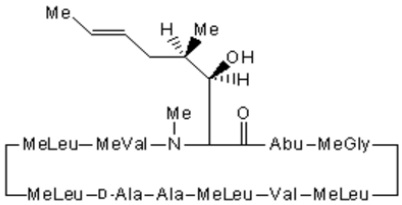
Paclitaxel 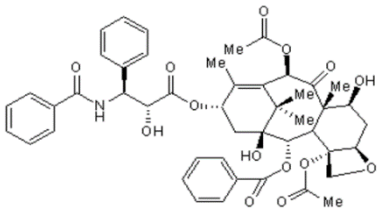	Verapamil 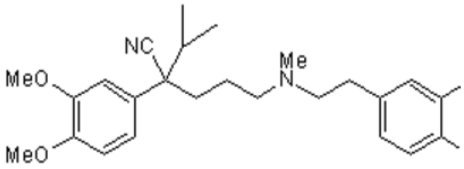
Vinblastine 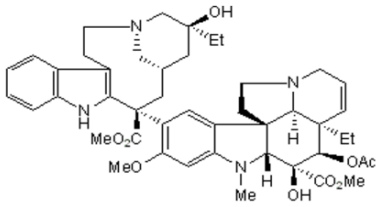	160a 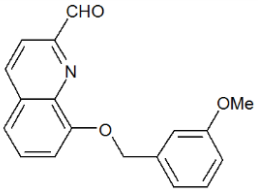

Table 4.1. Several common anti-cancer substrates and inhibitors for P-gp.

P-gp inhibitors can interrupt the interaction between P-gp and substrate or the NBDs of P-gp to prevent the free ATP to bind with P-gp for catalyzing the conformational change of P-gp, some inhibitors for P-gp were shown in the table 4.1. At the same time, some chemotherapeutic drugs such as doxorubicin, cisplatin and

paclitaxel will be used together with the P-gp inhibitor, the therapeutic effects of the drugs on the cancer cells are usually increased dramatically because of reduction of the drug-resistance.[48, 51, 56, 152]

According to the results of the preliminary molecular docking analysis, it showed that P-gp was one of the possible targets of 160a in human. It implicated that 160a was a potential cancer therapeutics as P-gp inhibitor could be used to reverse the multi-drug resistance conferred by P-gp in cancer cells. In this chapter, the cytotoxicity and drug-resistance reversal ability of the novel quinolone derivative, 160a, in human ESCC cell lines will be demonstrated.

4.4. EXPERIEMENTAL DESIGNS

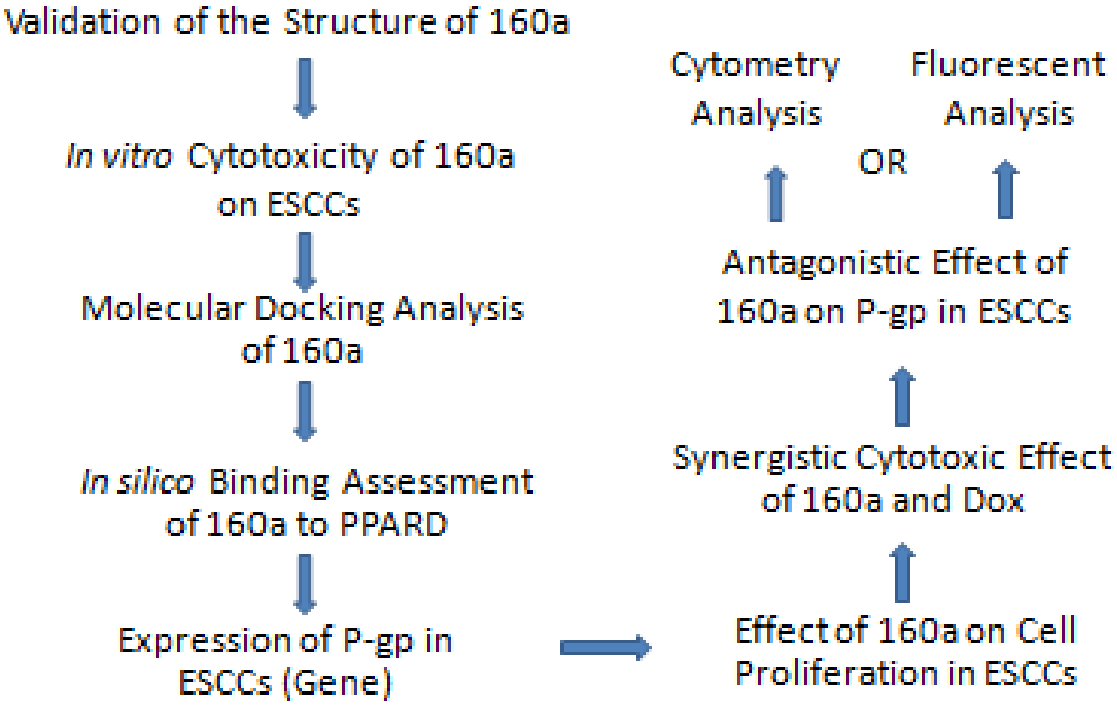

Figure 4.3. Experimental plan for the studies of the effects and mechanisms of 160a in ESCC treatments.

At first, the structure of 160a was examined by using the ^{1}H-NMR, ^{13}C-NMR and ESI-MS to validate the structure of the compound used for investigation was correct. Afterwards, the *in vitro* cytotoxic assessment of 160a was conducted in human ESCC cell lines compared to human non-tumor cell lines in order to determine the anti-cancer effects and toxicity of 160a.

The SEA molecular docking analysis was also conducted to predict the possible target of 160a in human and one of the possible target predicted was P-gp, the *in silico* binding assessing was conducted to validate it. For the *in silico*

assessment, the binding interaction and binding energy between P-gp and 160a was determined by using a program in Molecular Docking Server, some other P-gp blockers were used as the positive control. By comparing the binding energy of 160a to other well- known P-gp blockers, the ability of 160a to target P-pg would be predicted.

Besides, the protein and gene expression of P-gp in ESCC cell lines compared to the non-tumor cell lines was determined by using IHC and RT-PCR respectively. The effect of 160a with doxorubicin in the P-gp over-expressing ESCC cell lines was then determined in order to see how 160a can suppress the cancer growth cooperated with doxorubicin. The synergistic effect of 160a and doxorubicin was also determined in ESCC cell lines.

Furthermore, the inhibitory effects of 160a on P-gp in ESCC cell lines were determined by cytometric analysis and confocal microscopy, for these two approaches, a P-gp substrate called Calcein AM was used. Calcein AM is a cell-permeable non-fluorescent dye, after it enters into the living cells, its acetomethocy group will be cleaved by intracellular esterases. It will be trapped inside of the cells and exhibit a strong green fluorescence. As a substrate of P-gp, Calcein AM can be extruded out from the cells by P-gp like other anticancer drugs and lower the fluorescent Calcein AM will be determined in the cell. After treatment of 160a and other P-gp blockers,

the fluorescent signal from Calcien AM was measured in order to analyze the blocking effect of 160a on P-gp compared to the negative control. Finally, the confocal microscopy could also allow the fluorescent signals to be visualized as the images.[153]

Finally, the synergistic effects of 160a on doxorubicin in ESCC treatments were investigated by two methods including determination of their fractional inhibitory concentration index (FICI)[154, 155] and their combination index for the effects on ESCC suppression (CI).[156]

4.5. RESULTS

4.5.1. *Determination of the structure of 160a through ^{1}H-NMR, ^{13}C-NMR and ESI-MS*

A

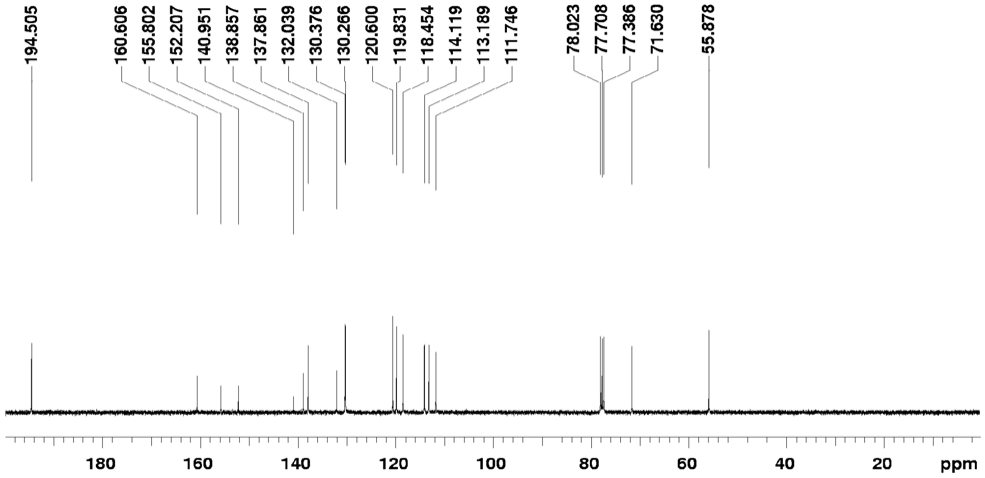

B

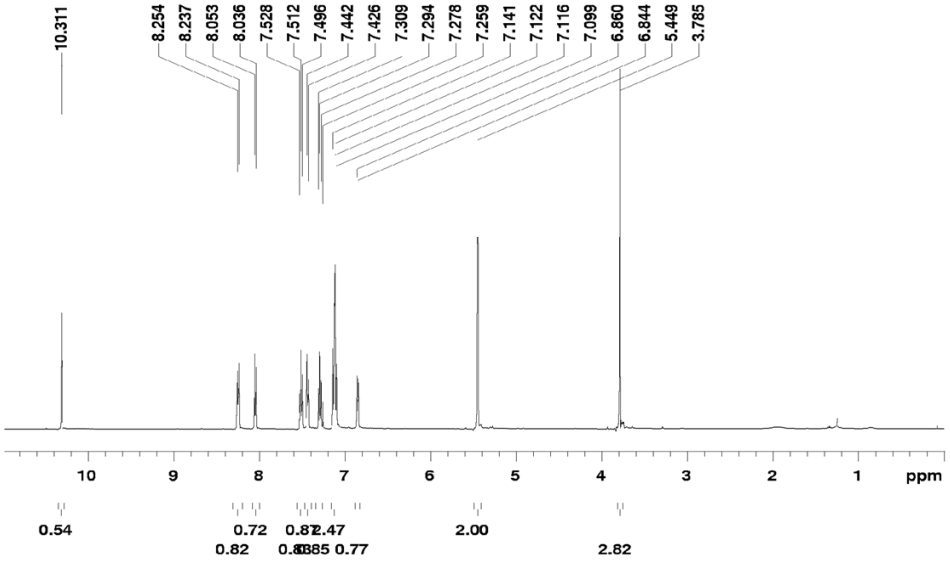

C

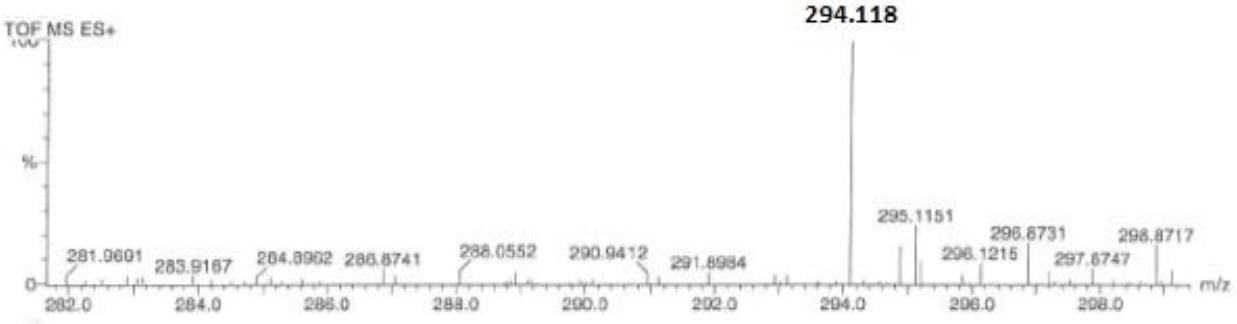

Figure 4.4. Analysis of the structure of 160a. (A)^{1}H-NMR Spectrum of 160a. (B)^{13}C-NMR Spectrum of 160a. (C) ESI-MS Spectrum of 160a.

For the ^{1}H-NMR analysis of 160a, the compound was completely dissolved in $CDCl_3$ and examined by the ^{1}H-NMR. The spectrum was reported as followed: ^{1}H-NMR (500 MHz, $CDCl_3$): δ3.79 (s, 3H), 5.45 (s, 2H), 6.85 (d, 1H, J = 8.0 Hz), 7.12 (t, 3H, J = 8.5 Hz), 7.29 (t, 1H, J = 7.5 Hz), 7.43 (d, 1H, J = 8.0 Hz), 7.51 (t, 1H, J = 8.0 Hz), 8.04 (d, 1H, J = 8.5 Hz), 8.25 (d, 1H, J = 8.5 Hz), 10.31 (s, 1H). Besides, as for the ^{13}C-NMR analysis of 160a, the compound was dissolved again in $CDCl_3$ and analyzed by the ^{13}C-NMR. The spectrum was reported as followed: δ55.88, 71.63, 111.75, 113.19, 114.12, 118.45, 119.83, 120.60, 130.27, 130.38, 132.04, 137.86, 138.86, 140.95, 152.21, 155.80, 160.61, 194.51. The molecular weight detected was about 294.11. The data obtained by the two NMR analyses and ESI-MS were consistent to the expected structure of 160a.

4.5.2. *In vitro Cytotoxicity Assessment of 160a in ESCC and Non-tumor Cell Lines*

The cytotoxicity and toxicity of 160a on human ESCC and non-tumor cell lines respectively were determined through MTS assay and recorded by the

microplate reader in a dose-dependent manner, a widely used anti-cancer drug, doxorubicin (Dox), was used as a positive control to compare the effect of 160a on the human ESCC and non-tumor cell lines. The dose-response curves of 160a and Dox on the human ESCC and non-tumor cell lines were shown in Figure 4.5 A and 4.5 B respectively, and these results were summarized as MTS_{50} in table 4.2.

According to the results, 160a showed a significant cytotoxic effect on all human ESCC cell lines and the cytotoxicity of 160a on the ESCC cell lines was increased in the dose-dependent manner. After summarization of the results, it showed that the MTS_{50}referring to $IC_{50}$of 160a for ESCC cell lines was 2.47 - 7.10μg/ml, whereas the $MTS_{50}$of Dox for the ESCC cell lines was 0.28 - 0.52μg/ml. On another hand, the MTS_{50} of 160a for the non-tumor cell lines was 2.47 - 4.19μg/ml, whereas the MTS_{50} of 160a for the non-tumor cell lines was 0.041 - 0.048μg/ml. From the results of the therapeutic index (ratio of MTS_{50} of 160a to MTS_{50} of Dox), it showed that the cytotoxicity of 160a was weaker than Dox about 10 folds, however, the toxicity of Dox was found to be higher than 160a about 50 to 100 folds.

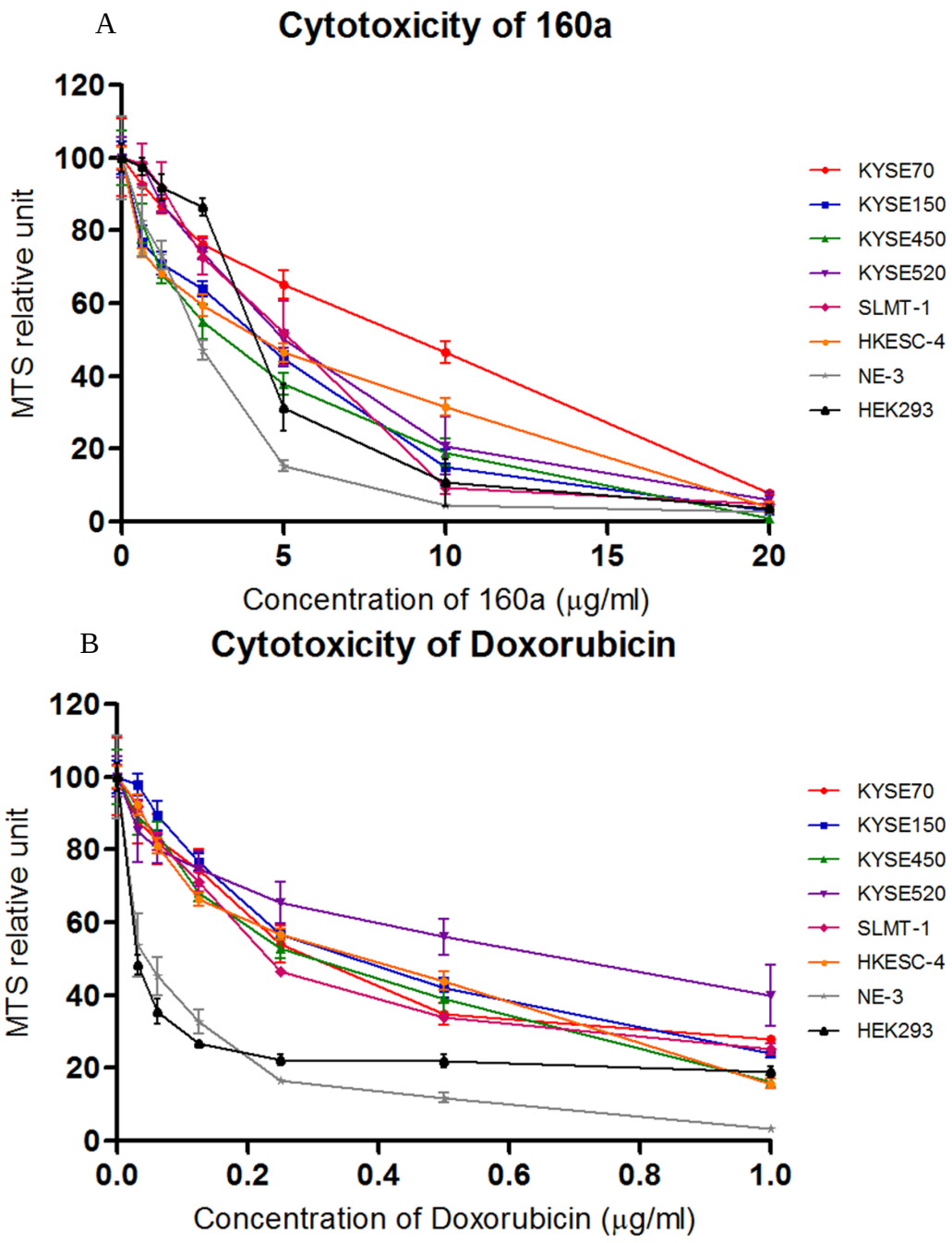

Figure 4.5. Cytotoxic assessment of 160a and Dox in human ESCC cell lines including KYSE70, KYSE150, KYSE450, KYSE520, SLMT-1 and HKESC-4; and non-tumor cell lines including NE-3 and HEK293. (A) 160a (Maximum concentration: 20μg/ml) and (B) Dox (Maximum concentration: 1μg/ml).

Cell Lines	MTS_{50} of 160a (μg/ml)	MTS_{50} of Dox (μg/ml)	MTS_{50} of 160a/ MTS_{50} of Dox
KYSE70	7.10	0.31	22.90323
KYSE150	3.09	0.37	8.351351
KYSE450	2.69	0.28	9.607143
KYSE520	4.75	0.52	9.134615
HKESC-4	3.31	0.30	11.03333
SLMT-1	4.47	0.28	15.96429
NE-3	2.47	0.048	51.45833
HEK293	4.19	0.041	102.1951

Table 4.2. Summary of the MTS_{50} of 160a and Dox, and the ratio of MTS_{50} of 160a to Dox.

4.5.3. *Molecular Docking Analysis by SEA Program*

According to the table 4.3, it showed the first seven possible targets for 160a in human which were predicted by using SEA program, the meanings of expected value and the maximum target complementary value have been mentioned in chapter 3. As shown in the Figure, multi-drug resistance protein-1 (MDR-1, also known as P-gp) was the predicted target with the second lowest expected value which is

$3.24e^{-18}$and highest maximum target complementary value which is 0.46. Therefore, P-gp should be one of the possible targets for 160a.

Rank	Reference Name	Species	Expected Value	Maximum Target Complementary Value
1	Melatonin receptor type 1A	Human	$2.272e^{-19}$	0.40
2	Multidrug resistance protein 1		$3.235e^{-18}$	0.46
3	Rho-associated protein kinase 2		$3.902e^{-18}$	0.32
4	Rho-associated protein kinase 1		$6.595e^{-14}$	0.32
5	cAMP-specific 3',5'-cyclic phosphodiesterase 4C		$2.541e^{-13}$	0.41
6	Melatonin receptor type 1B		$9.097e^{-11}$	0.40
7	Protein tyrosine phosphatase type IVA 3		$1.389e^{-10}$	0.34

Table 4.3. The first seventh predicted targets for 160a.

4.5.4. *In silico Binding Assessment of P-gp with 160a or other inhibitors*

A

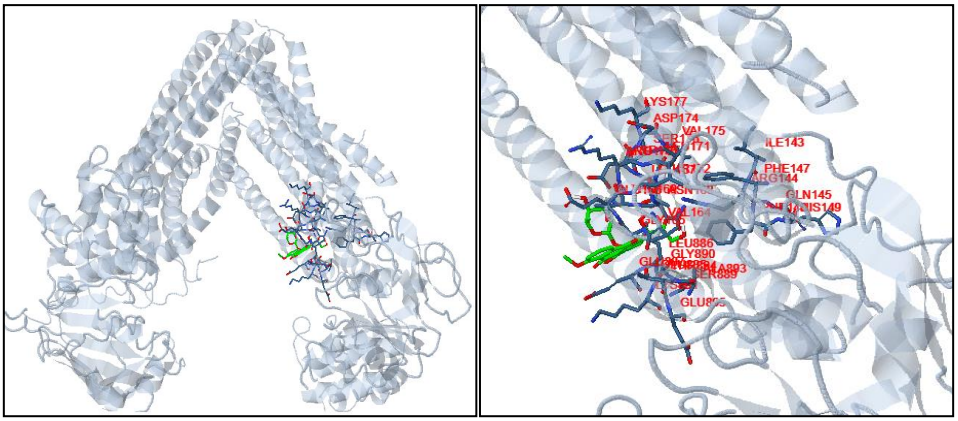

B

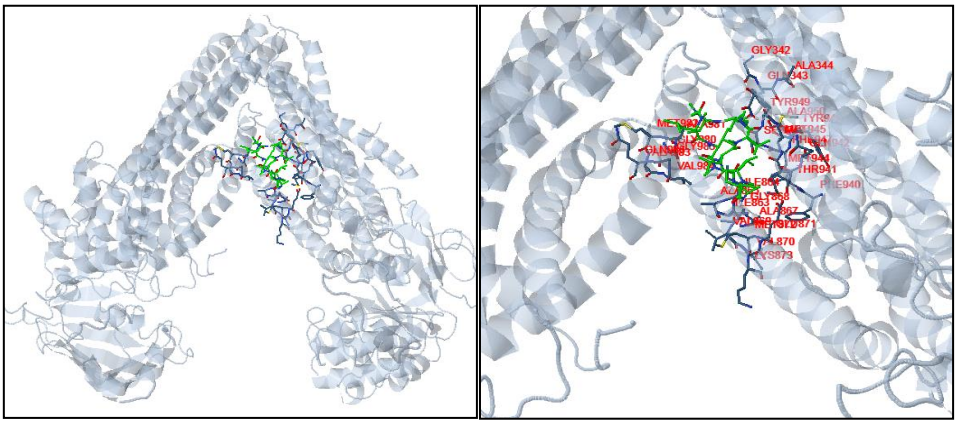

C

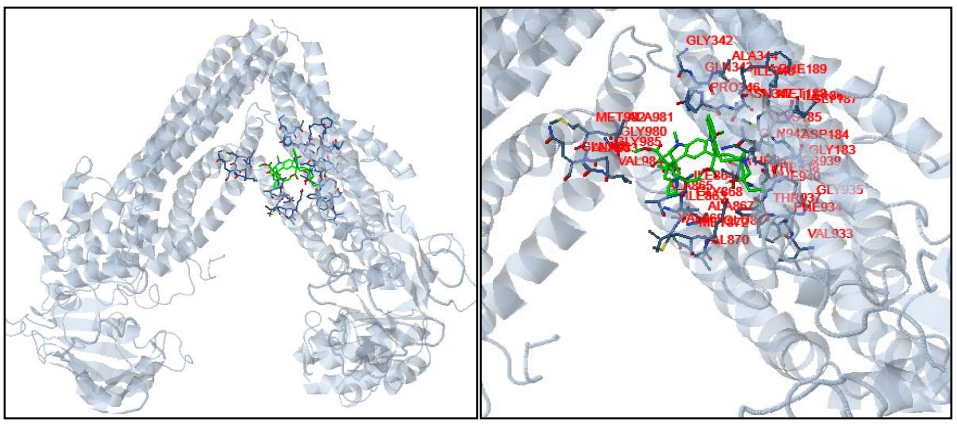

D

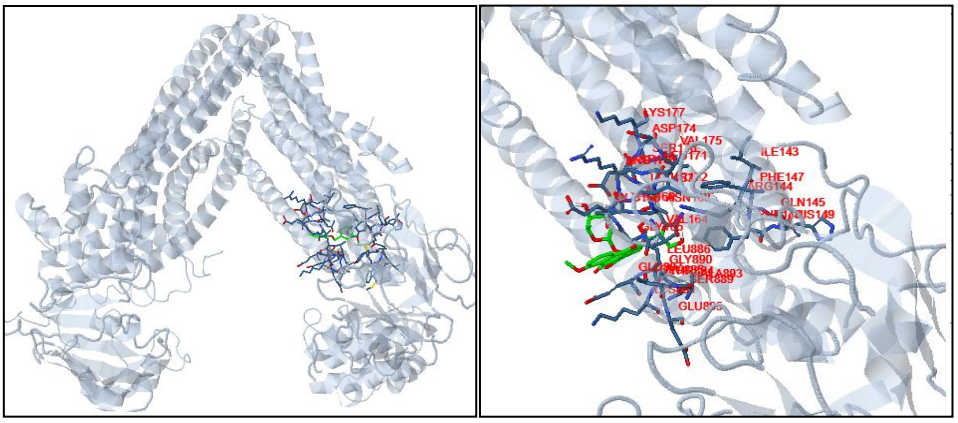

Figure 4.6. Molecular docking results of 160aor other P-gp substrate and inhibitors with P-gpobtained in Molecular Docking Server. (A) Doxorubicin, (B) Cyclosporin A, (C) Vinblastin and (D) 160a.

Compound	Estimated Free Energy of Binding	Estimated Inhibition Constant, Ki
Doxorubicin	-8.47 kcal/mol	0.62μM
Cyclosporin A	-2.68 kcal/mol	10.8μM
Vinblastin	-7.16 kcal/mol	5.62μM
160a	-7.92 kcal/mol	1.56μM

Table 4.4. The estimated free binding energy and inhibition constant of 83b1 or AA to PPARD.

The Figure 4.6 showed the results obtained in Molecular Docking Server. The interactions of either 160a or other P-gp substrates and inhibitors with P-gp were determined through the algorithm of the program. Based on the algorithm of the program, the free energy of their binding and the inhibition constant were also predicted as mentioned.

As shown in Figure 4.6, the target site on P-gp that the common P-gp blockers including Cyclosporin A and Vinblastin were different to where Dox binds. However, 160a was found to bind to the P-gp at the same target site as where Dox binds, it implied that 160a had certain degree of affinity to compete the binding site of Dox to P-gp. Moreover, as shown in table 4.4, the free binding energy and the inhibition constant of Dox to P-gp was -8.47 kcal/mol and 0.62 μM, it indicates the interaction

between Dox and P-gp is very strong and table. On another hand, the free binding energy of Cyclosporin A and Vinblastin were -2.68 and -7.16 kcal/mol where their inhibition constants were 10.8 and 5.62 μM, it showed the interactions between theses blockers and P-gp were much weaker than the substrate Dox. However, it showed that 160a had a stronger binding affinity to P-gp than these P-gp blockers since the free binding energy and inhibition constant of 160a to P-gp were only -7.92 kcal/mol and 1.56 μM, although its affinity to P-gp was still slightly weaker than the P-gp substrate Dox.

4.5.5. *Expression of P-gp in ESCC and Non-tumor Cell Lines*

A

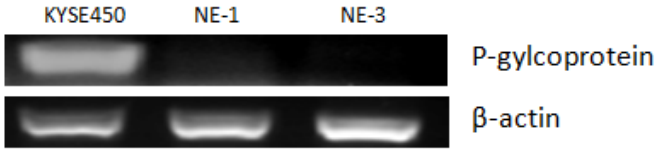

B

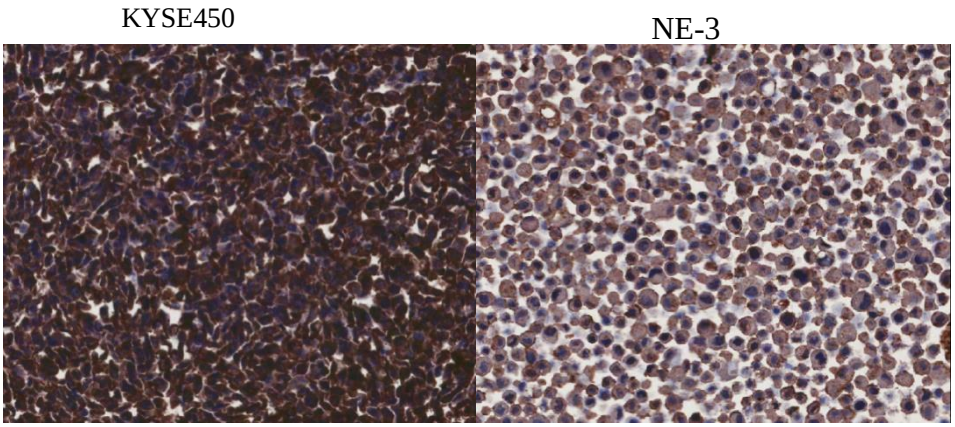

Figure 4.7. Analysis of P-gp expression. (A) RT-PCR of mRNA expression in human ESCC and non-tumor cell lines (B) IHC images of P-gp protein expression in human ESCC and non-tumor cell lines.

The mRNA and protein expression of P-gp in esophageal cancer and non-tumor cell lines were determined respectively by RT-PCR and IHC staining, the results were shown in Figure 4.7.

From the results, the mRNA expression of P-gp in KYSE450 was higher than the non-tumor cell lines NE-1 and NE-3, besides, KYSE450 also showed the higher protein expression of P-gp than NE-3 as well as mRNA expression. It implied that P-gp was over-expressed in ESCC cell lines compared to normal cells.

4.5.6. *Effect of 160a on ESCC Proliferation*

The effect of 160a on ESCC proliferation was assessed by MTS assay in two human ESCC cell lines including KYSE150 and KYSE450, the results were shown in Figure4.8.

The two ESCC cell lines were seeded on the 96-well plates followed by the treatment of 0.15 μg/ml Dox, 3 μg/ml of 160a or both of them for 4 days. From the results shown in both ESCC cell lines, the cancer cells grew -rapidly without

treatment of either 160a or Dox, the amount of viable cells was increased by about 4 to 5 folds after 4 days. However, it showed that the growth of the cancer cells with the treatment of either Dox and 160a was suppressed, whereas treatment of both Dox and 160a together showed the stronger suppressive effects on the cancer growth. For the KYSE150 treated with both Dox and 160a, the amount of viable cells was even lower than the first day before treatment. It showed that 160a would enhance the cytotoxic effects of Dox on cancer cells but not antagonistic.

A

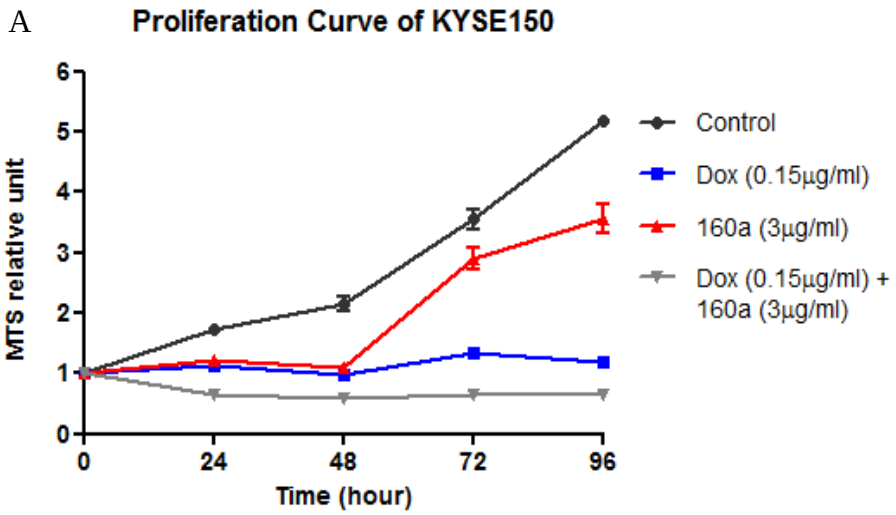

B

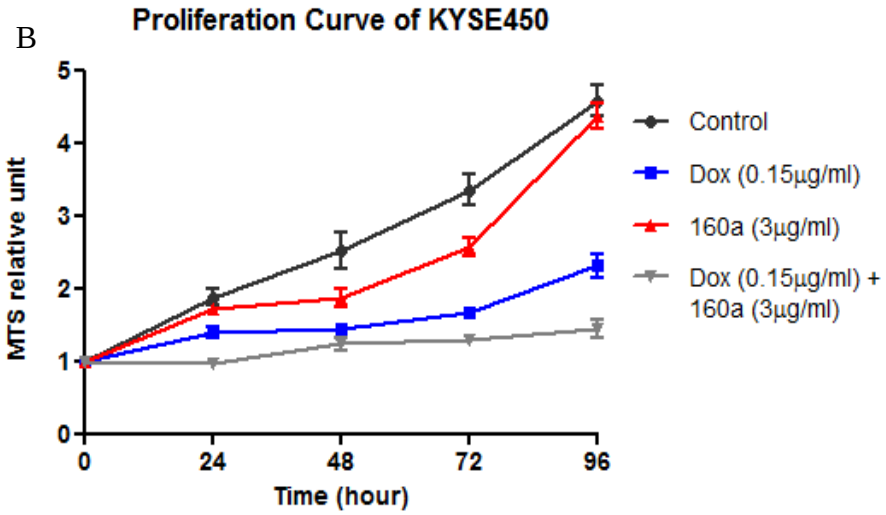

Figure 4.8. The cell proliferation curve of human ESCC cell lines treated with Dox (0.15μg/ml), 160a (3μg/ml)or both compounds for 4 days. (A) KYSE150 and (B) KYSE450.

4.5.7. *Effect of 160a on Calcein AM Accumulation Visualized by Confocal Microscopy*

The effect of 160a on the accumulation of Calcein AM in different ESCC cell lines was firstly visualized by using confocal microscopy, the results were shown in Figure 4.9.

As mentioned, the Calcein AM molecules can pass through the cell membrane and emit green fluorescent signals after enzymatic reaction, the green fluorescent light was then detected and captured by using the confocal microscope. The bright field images were used for clearly visualizing the location of green fluorescence. According to the results shown in Figure 4.9, the green fluorescent signals in all ESCC cell lines without the treatment with 160a were very weak, it implicated that high amount of Calcein AM was removed by the P-gp and it resulted in lower green fluorescent signals that can be detected inside of the cells. After treatment of either 160a or cyclosporin A, the signal of green fluorescence was increased and the cells treated with higher concentration of 160a showed higher intensity of green fluorescence in the images except the KYSE150 cell line. The effects of 160aon the

cellular green fluorescent signal in the ESCC cell lines were analyzed and compared by using ImageJ program, the results were showed in Figure 4.9 F. It showed that 160a significantly increased the cellular green fluorescent signals in all ESCC cell lines in a dose-dependent manner except KYSE150.

A

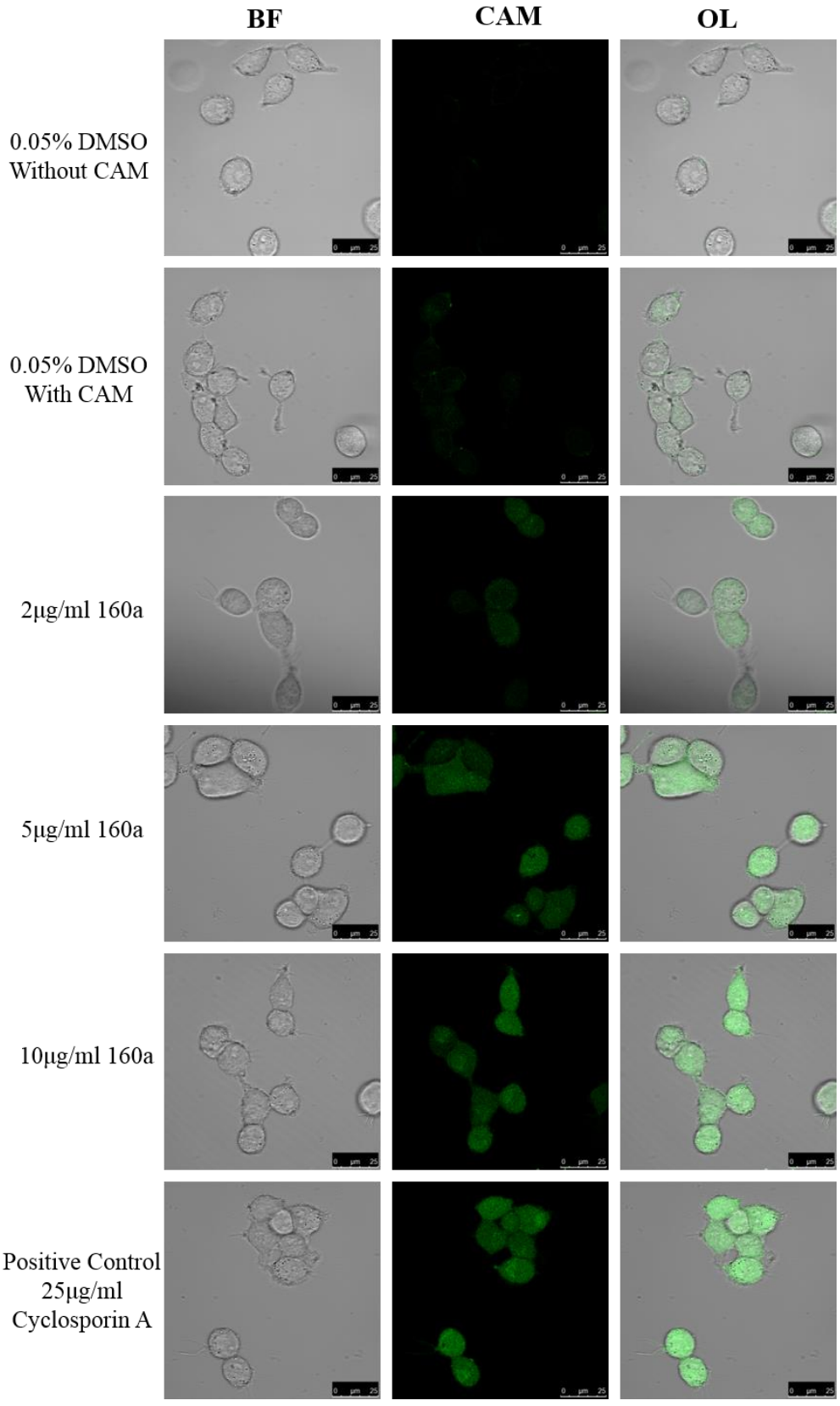
BF
CAM
OL
0.05% DMSO
Without CAM
0.05% DMSO
With CAM
2µg/ml 160a
5µg/ml 160a
10µg/ml 160a
Positive Control
25µg/ml
Cyclosporin A

B

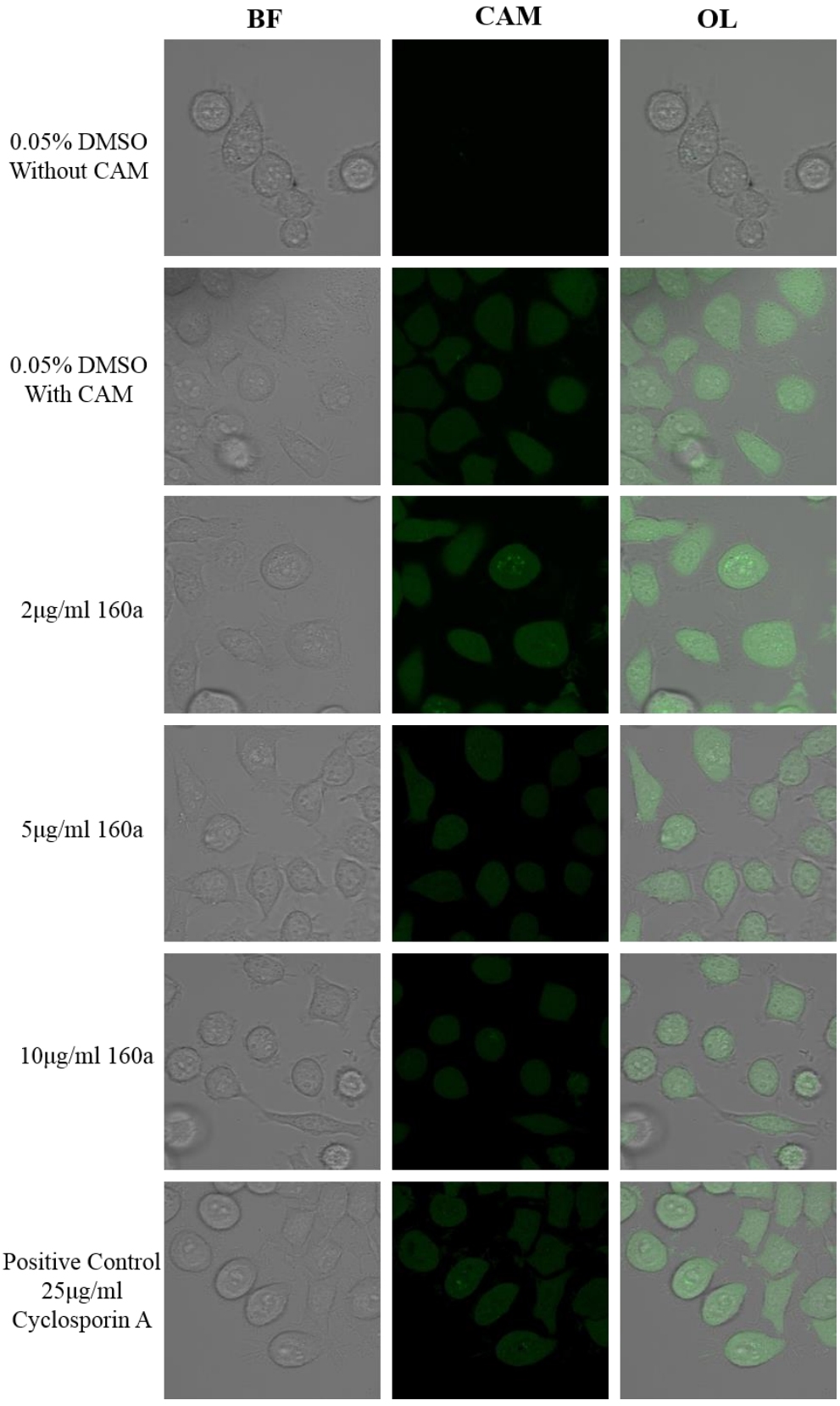
BF
CAM
OL
0.05% DMSO
Without CAM
0.05% DMSO
With CAM
2µg/ml 160a
5µg/ml 160a
10µg/ml 160a
Positive Control
25µg/ml
Cyclosporin A

C

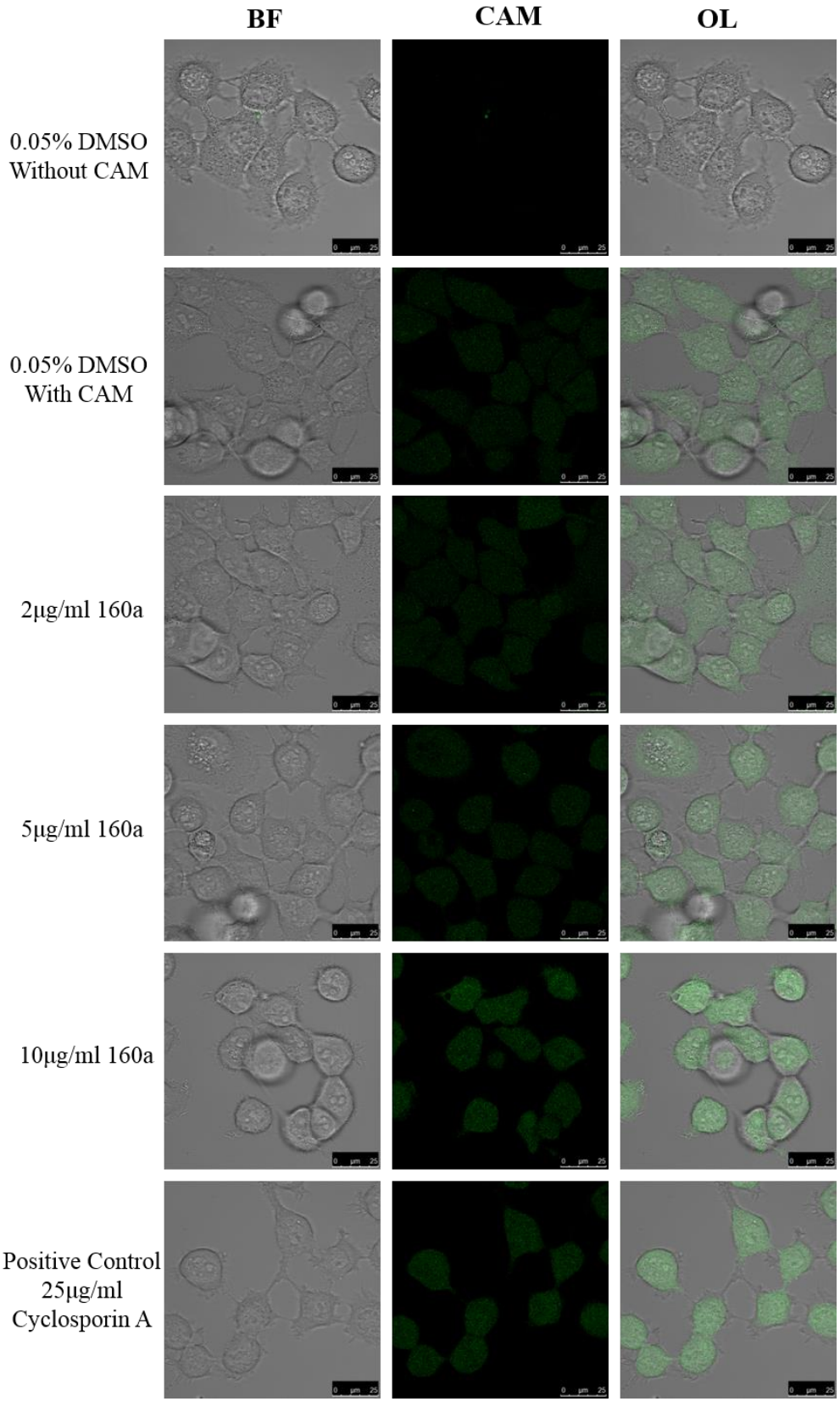
BF
CAM
OL
0.05% DMSO Without CAM
0.05% DMSO With CAM
2µg/ml 160a
5µg/ml 160a
10µg/ml 160a
Positive Control 25µg/ml Cyclosporin A

D

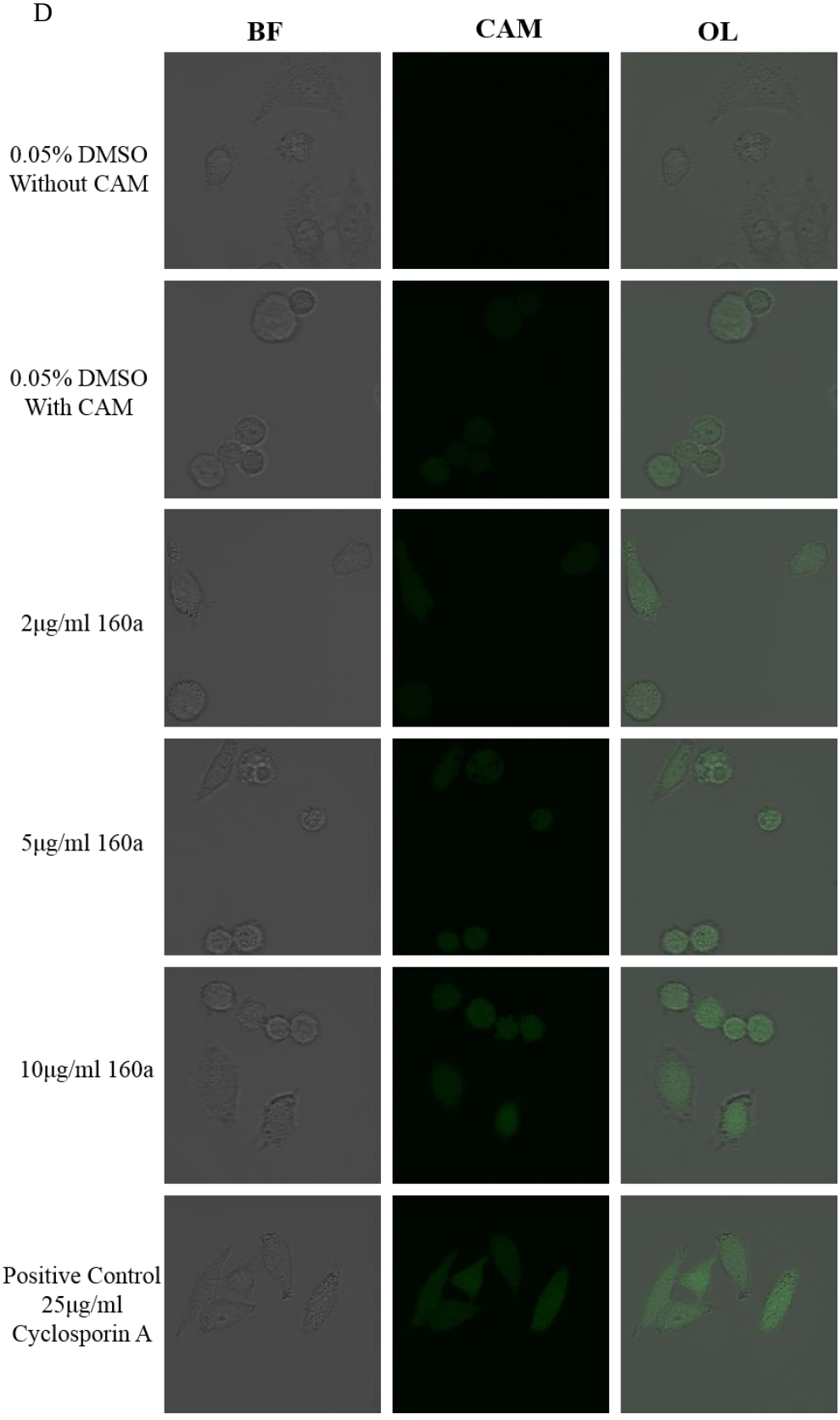
BF
CAM
OL
0.05% DMSO
Without CAM
0.05% DMSO
With CAM
2µg/ml 160a
5µg/ml 160a
10µg/ml 160a
Positive Control
25µg/ml
Cyclosporin A

E

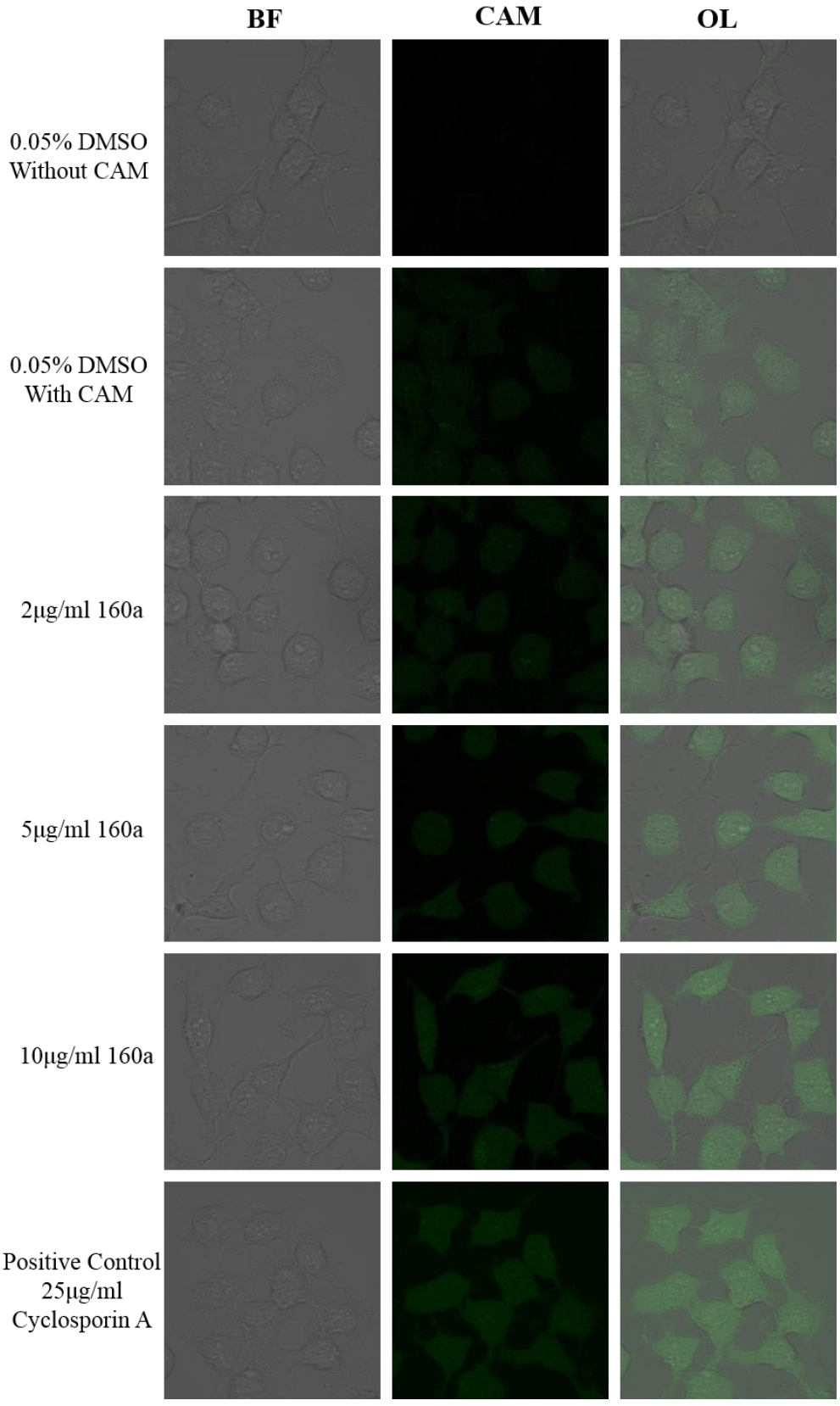
BF
CAM
OL
0.05% DMSO
Without CAM
0.05% DMSO
With CAM
2μg/ml 160a
5μg/ml 160a
10μg/ml 160a
Positive Control
25μg/ml
Cyclosporin A

F

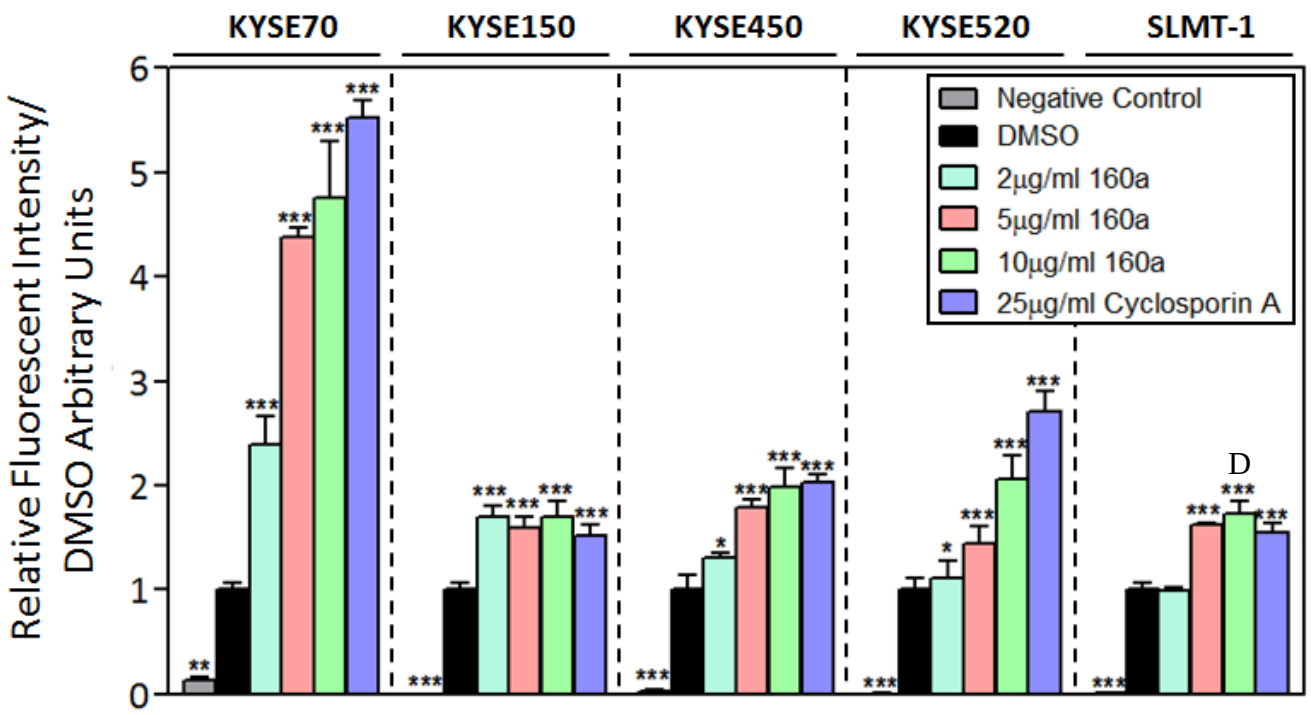

Figure 4.9. Determination of Fluorescent Intensity of Calcein AM in different ESCC cell lines treated with either different concentration of 160a or cyclosporin A as the positive control by Confocal Microscopy. (A) KYSE70. (B) KYSE150. (C) KYSE450. (D) KYSE520. (E) SLMT-1. (F) Summary of Fluorescent Intensity in all cell lines with the treatments compared to DMSO (Key: BF: Bright Field; CAM: Calcein AM; OL: Overlayer). (*p<0.5, **p<0.01 and *** p<0.001)

4.5.8. *Effect of 160*a *on Calcein AM Accumulation Examined by Flow Cytometry*

The effect of 160a on Calcein AM accumulation was further examined by flow cytometry and the results were shown in Figure 4.10, the retention percentage of Calcein AM refers to the percentage increase of the intensity of green fluorescence

recorded by the filter channel (FL-1). Dox-resistant ESCC cell lines were used to further confirm treatment with 160a can further increase the susceptibility of the cancer cells to Dox compared with the parental cell.

From the results, the retention of Calcein AM was increased after the treatment of either different concentration of 160a or cyclosporin A, which is the positive control, in all of the ESCC cell lines. Sometimes, the relationship between the retention of Calcein AM and the concentration of treatment was not proportional to each other. However, it showed that both 160a and cyclosporin A significantly increased the green fluorescent intensity.

A

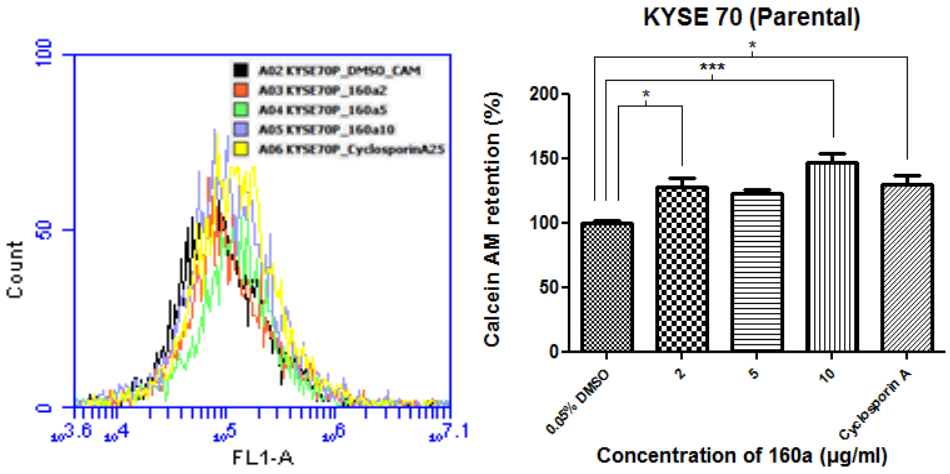

B

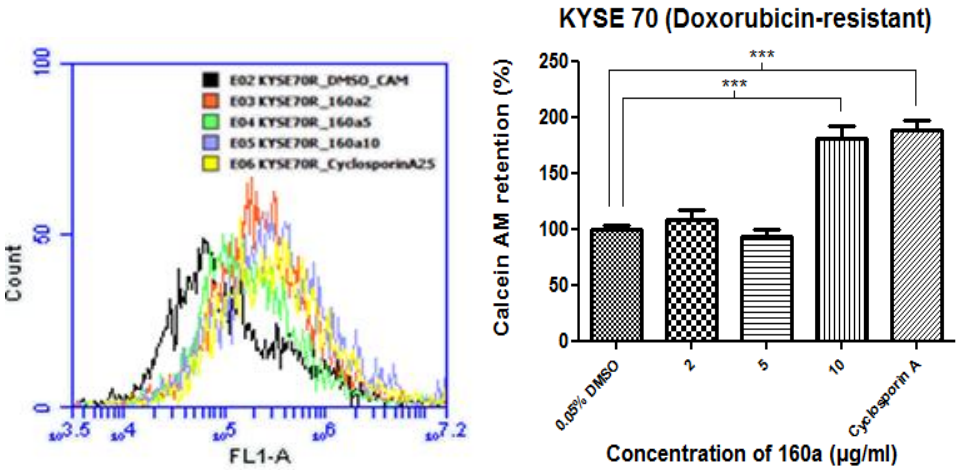
E02 KYSE70R_DMSO_CAM
E03 KYSE70R_160a2
E04 KYSE70R_160a5
E05 KYSE70R_160a10
E06 KYSE70R_CyclosporinA25
Count
FL1-A
KYSE 70 (Doxorubicin-resistant)
Calcein AM retention (%)
0.05% DMSO
2
5
10
Cyclosporin A
Concentration of 160a (μg/ml)

C

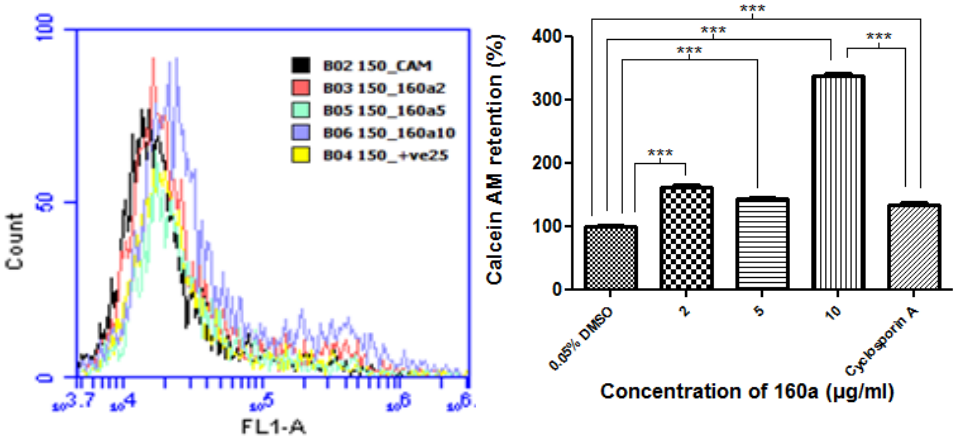
B02 150_CAM
B03 150_160a2
B05 150_160a5
B06 150_160a10
B04 150_+ve25
Count
FL1-A
KYSE 150 (Parental)
Calcein AM retention (%)
0.05% DMSO
2
5
10
Cyclosporin A
Concentration of 160a (μg/ml)

D

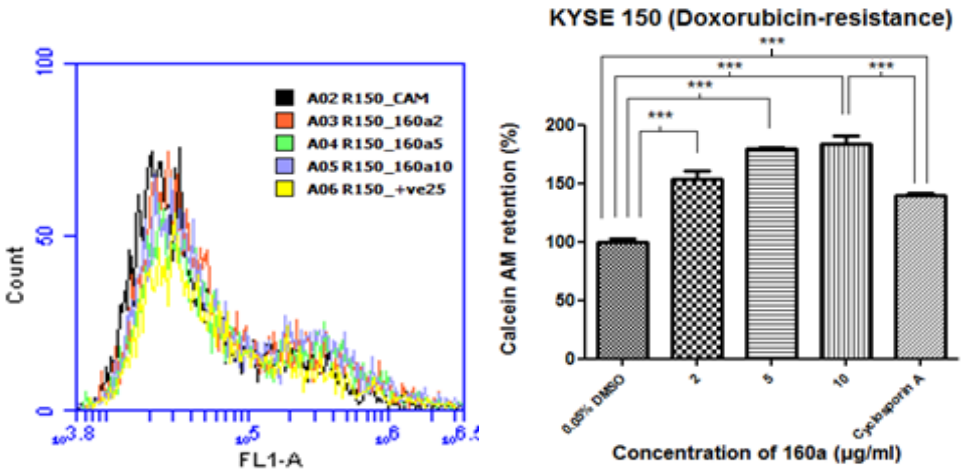
A02 R150_CAM
A03 R150_160a2
A04 R150_160a5
A05 R150_160a10
A06 R150_+ve25
Count
FL1-A
KYSE 150 (Doxorubicin-resistance)
Calcein AM retention (%)
0.05% DMSO
2
5
10
Cyclosporin A
Concentration of 160a (μg/ml)

E

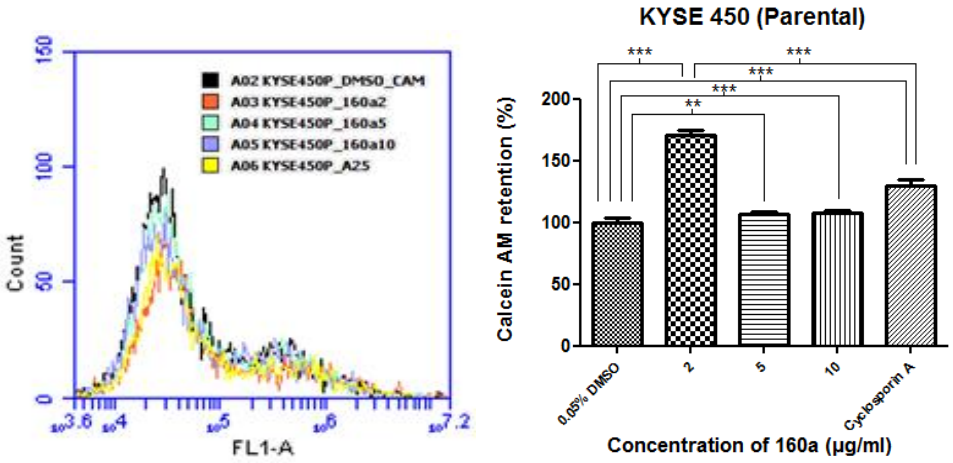

Figure 4.10. Determination of Green Fluorescent Intensity of Calcein AM in different ESCC cell lines treated with either different concentration of 160a or cyclosporin A (25 μg/ml) as the positive control by Flow cytometry. (A) KYSE70 (Parental). (B) KYSE70 (Doxorubicin-resistant). (C) KYSE150 (Parental). (D) KYSE150 (Doxorubicin-resistant). (E) KYSE450 (Parental). (F) Summary of Fluorescent Intensity in all cell lines with the treatments compared to DMSO. (* $p<0.5$, **$p<0.01$ and *** $p<0.001$).

4.5.9. *Analysis of the Synergistic Effects of 160a on Doxorubicin in ESCC treatment*

Through comparison of the MTS_{50} of either Dox with 2 μg/ml of 160a or Dox alone in KYSE450 and NE-3, the effects of combinatory use of Dox and 160a in KYSE450 and NE-3 were found and the results were shown in Figure 4.11. According to the results, the value of MTS_{50} of Dox with addition of 2μg/ml of 160a in KYSE450 was significantly decreased about 50%. However, the value of MTS_{50} of

Dox with addition of 2μg/ml of 160a in NE-3 was only decreased about 25%. It showed that the effect of 160a on enhancing the cytotoxic effect of 160a in ESCC cell line was much higher than that in non-tumor cell line.

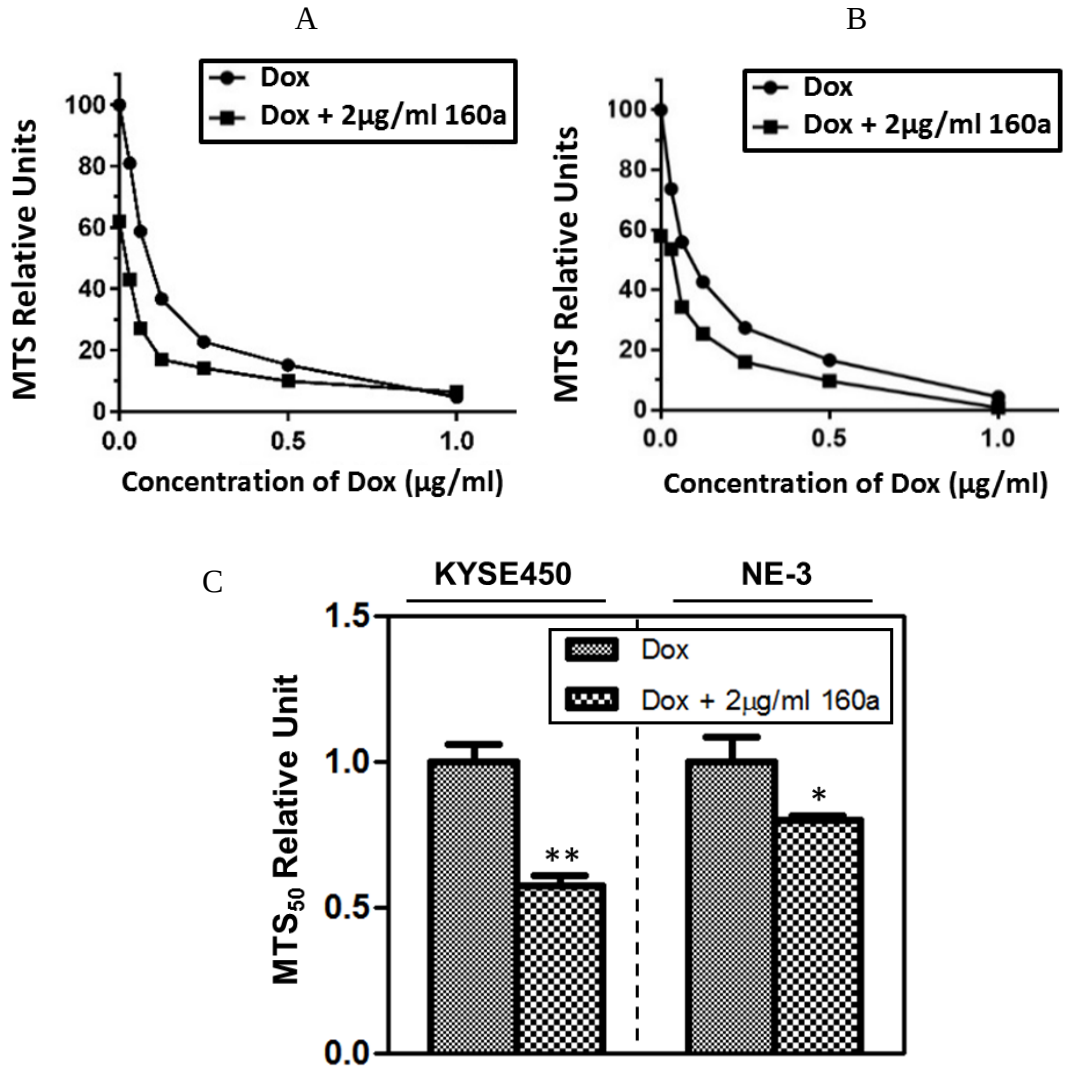

Figure 4.11. Cytotoxic effects of either Dox or Dox with 2μg/ml 160a on ESCC or non-tumor cell line. (A) KYSE450. (B) NE-3. (C) Comparison of MTS_{50} relative unit of Dox and Dox with 2μg/ml 160a in KYSE450 and NE-3.

The synergistic effect of 160a on the cytotoxicity of Dox in ESCC cell line compared to non-tumor cell line was determined though calculating the CI_{50} value by using CompuSyn program, the results were shown in table 4.5 and Figure 4.11.

From the results, the CI of combinatory use of Dox and 160a in the ratio of 1:5 or 5:1 in the treatment of KYSE450 were 0.30 and 0.63 respectively. However, the CI of combinatory use of Dox and 160a in the ratio of 1:5 or 5:1 in the treatment of NE-3 were 1.34 and 5.17 respectively. It has been reported that CI value <1 and CI value >1 indicates the synergistic effect and antagonistic effect respectively.[157]It means that 160a showed a synergistic effect on Dox in suppressing KYSE450 but an antagonistic effect on Dox in NE-3. Moreover, according to the Figure 4.11, the CI value (circle dots or square dots) of combinatory use of Dox and 160a was always lower than 1(the middle horizontal line), it indicated that 160a was highly possible to increase the effect of Dox. However, the CI value of combinatory use of Dox and 160a was always higher than 1, it indicated that 160a might reduce the effect of Dox in NE-3.

Cell lines	RatioofDox: 160a	CI	r	DRI of Dox	DRI of 160a
KYSE450	1:5	*0.30*	-0.977	3.77	25.44
	5:1	*0.63*	-0.987	1.59	267.4
NE-3	1:5	*1.34*	-0.998	0.83	7.19
	5:1	*5.17*	-0.984	0.19	41.95

Table 4.5. Analysis of synergistic effect of 160a on Dox in the treatment of KYSE450 or NE-3 by calculating the CI_{50} by using CompuSyn program.

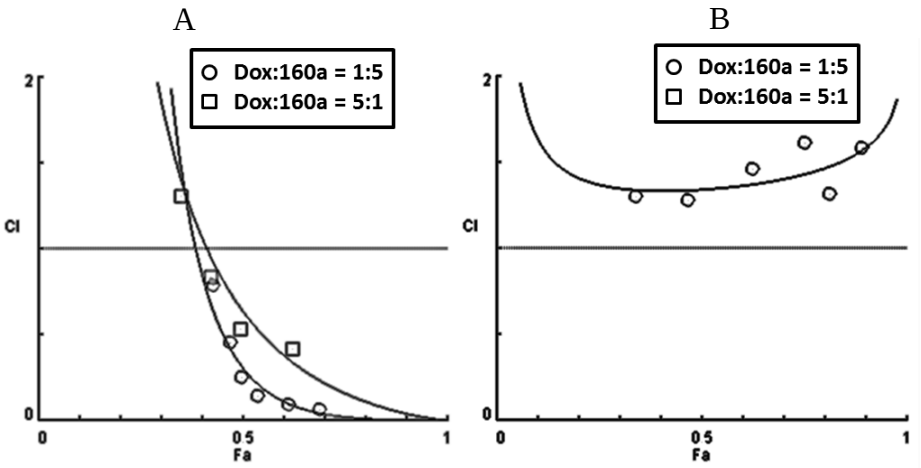

Figure 4.12. Analysis of synergistic effect of 160a on Dox in the treatment of KYSE450 or NE-3 by using CompuSyn program.(A) KYSE450 and (B) NE-3.

Dosages of Drug Combination	**C_{Dox}**	**C_{160a}**	**FICI**
Dox alone	0.102 (C'_{Dox})	0	1
160a alone	0	4.891(C'_{160a})	1
70% of MTS_{40} of Dox + 30% of MTS_{40} 160a	0.0398	0.1705	0.425056
50% of MTS_{40} of Dox + 50% of MTS_{40} 160a	0.0435	0.3486	0.497744

Table 4.6. Analysis of synergistic effect of 160a on Dox in the treatment of KYSE450 by calculating the value of FICI.

According to the Table 4.6 the FICI of different combination of Dox and 160a in the treatment of KYSE450 was obtained. The equation of FICI calculation was shown below:[154, 155]

$$FICI = FIC_{Dox} + FIC_{160a} = (C_{Dox}/C'_{Dox}) + (C_{160a}/C'_{160a})$$

C'_{Dox} and C'_{160a} indicates the MTS_{40} of Dox and 160a alone respectively, where C_{Dox} and C_{160a} were the MTS_{40} of the Dox and 160a in combinatory use in suppressing KYSE450. The value of FICI > 1 and FICI < 0.5 indicates the interaction between Dox and 160a were antagonistic and synergistic respectively.[156] From the results, the FICIs of the two combinations of Dox and 160a in treatment of KYSE450 were 0.425 and 0.498 which were lower than 0.5, it showed that 160a increased the cytotoxic effects of Dox on ESCC treatment.

4.6. DISCUSSION

Combination chemotherapy against cancers has been reported to be more effective than only a single agent used and it is also widely used as the treatments for different types of cancers in human.[158-160] Combination treatment with paclitaxel and doxorubicin, which were also approved by the U.S. Food and Drug Administration (FDA) for cancer treatment, were demonstrated to show the markedly increased anti-proliferative effects in ESCC cells.[160] However, some studied revealed that higher dosages of either paclitaxel or doxorubicin can also lead to significant toxicities in kidney and liver, this seriously limits the effectiveness of the treatment involving these strong anti-cancer drugs.[160, 161] Hence, an anti-cancer

drug with less toxicity used in combination treatment is much important to maintain the effectiveness of the existing chemotherapeutic treatments.

In this chapter, the anti-cancer effects of 160a on human ESCC cell lines were characterized.

At the beginning of the investigation, the structure of 160a was firstly validated through ^{1}H-NMR and ^{13}C-NMR followed by ESI-MS. The results showed that the structure of 160a was consistent to the expected structure.

After validation of the structure of 160a, the SEA program was performed to predict the possible targets of 160a in human. There were many possible targets were predicted, but only the first seven targets with the lower expected value were taken out for further evaluation. The relationship between P-gp and 160a was then chosen for further investigation because P-gp was the target of 160a with the second lowest expected value and the highest maximum target complementary value. P-gp, as mentioned, was a widely identified anti-therapeutic protein, therefore, it is deserved to assess the effects of 160a on P-gp. Other possible targets predicted by the SEA program will be investigated in future.

In silico binding assessment, as discussed in chapter 3, was also performed to determine the binding affinity of 160a to P-gp compared to other P-gp blockers or substrates. It showed that 160a bound to the specific site of P-gp as well as the P-gp

substrate, Dox, bound, 160a also showed the stronger binding affinity to P-gp than some widely used P-gp blockers such as Cyclosporin A and Vinblastin.

Afterwards, the expression of P-gp in some human ESCC cell lines was determined compared to the non-tumor cell lines. From the results, the mRNA and protein expressions of P-gp were higher in ESCC cell lines than that in non-tumor cells; it revealed the potential of using 160a to reverse the multi-drug resistance conferred by P-gp in ESCC cell lines with the treatment of anti-cancer drugs which were originally the substrates of P-gp.

From the results in Figure 4.8, the proliferation rates of KYSE150 and KYSE450 treated with 160a, Dox or both were determined. It showed that both of Dox and 160a could also lower the proliferation rate of the ESCC cell lines, but the proliferation rates of both cell lines treated with 160a were recovered and close to the cell lines without any treatment after 4 days. However, combination of the treatment of Dox with 160a showed the significantly suppressed effects on the proliferation of both ESCC cell lines, the viable cells treated with the both Dox and 160a were about 4-5 folds lower than the cells without treatments. It revealed the ability of 160a to increase the cytotoxicity of Dox in treating ESCCs.

Afterwards, the effect of 160a on reversion of multi-drug resistance of P-gp in ESCC was determined by using confocal microscopy and flow cytometry, Calcein

AM was used instead of P-gp substrates. From the results of these two methods, it also showed that 160a could increase the green fluorescent intensity produced by Calcein AM in different ESCC cell lines. It demonstrated the ability of 160a to reverse the resistance conferred by P-gp and the anti-cancer drugs which were originally the P-gp substrates such as Dox can be retained inside of ESCC cells to trigger their cytotoxic effects. As mentioned above, paclitaxel is one of the anti-cancer drugs which is usually used with doxorubicin for cancer therapy, it has been reported that paclitaxel kills cancer through induction of mitotic arrest and results in cell apoptosis.[161, 162]Because of its mechanisms against cancer cells, it always causes harmful side-effects in human in higher dosages during cancer treatments.[161] However, the mechanism of 160a against cancer cells seems different; it targets on P-gp and hinder the functions of P-gp. P-gp is widely known as a cancer biomarker and overexpression of P-gp was shown in the ESCC cell line compared with non-tumor cell.[163]Therefore, it is possible that 160a can be used with doxorubicin in cancer treatment with less toxicity against non-tumor cells.

Finally, the synergistic effect of 160a on Dox in the treatment of ESCCs was determined by different methods. At first, from the results shown in Figure 4.11, it demonstrated that 2μg/ml of 160a significantly ($p<0.01$) increased the inhibitory effect of Dox in ESCC cell line, KYSE-450, rather than that in non-tumor cell line,

NE-3. It is very important to reduce the side-effects from the therapeutics by combinatory use of different anti-cancer drugs and lowering the dosage of each drug. Furthermore, the synergistic effect of 160a on Dox in ESCC was also examined through determination of CI value and FICI, 160a also revealed its synergistic effect on Dox in suppressing ESCC because of the lower CI value and FICI.

4.7. CONCLUSION

In summary, the anti-cancer activities of 160a and its synergistic effect on Dox in human esophageal cancers were determined. Moreover, the ability of 160a to reverse the drug-efflux mechanisms conferred by P-gp was also demonstrated. 160ashowed its potential as an anti-cancer agent used to suppress tumor growth and also increase the cytotoxicity of other cancer drugs on ESCC by reducing the multi-drug resistance of the tumor cells.

Chapter 5 INVESTIGATION OF THE ANTI-CANCER EFFECTS OF TWO NOVEL THIOSEMI- CARBAZONES IN HUMAN PROSTATE CANCER AND COLORECTAL CANCERS

5.1. INTRODUCTION

As mentioned, prostate cancers and colorectal cancers are also the very severe diseases with high incident and mortality rate in either developing countries or undeveloped countries, the 5-year survival rate of patients suffered from these diseases was extremely low.[1, 20, 22] It indicates that the existing therapeutics are not sufficient for treating all cases of prostate and colorectal cancers, the novel approaches to treat these cancers are needed.

In this chapter, the anti-cancer effects of two novel thiosemicarbazones designed by Prof. Des Richardson's research team were investigated in prostate and colorectal cancer cell lines.

5.2. BACKGROUNDS OF TWO NOVEL THIOSEMICARBAZONES (DpC and Dp44mT)

The two novel thiosemicarbazones, DpC and Dp44mT, were the lead compounds investigated in Prof. Des Richardson's research teams for cancer treatments, they showed the excellent potentials in cancer treatments. DpC

(di-2-pyridylketone 4-cyclohexyl-4-methyl-3-thiosemicarbazone) and Dp44mT (di-2-pyridylketone-4,4-dimethyl-3-thiosemicarbazone) were developed as the iron-chelators that can chelates the intracellular irons to induce apoptosis in cancer cells through different mechanisms. For example, it has been found that these compounds can up-regulate a protein call N-myc downstream regulated 1 (NDRG1) through either hypoxia inducible factor-1α-dependent or -independent mechanisms, NDRG1 has been identified as a metastatic suppressor and it plays an important role in apoptotic signaling pathways in tumor cells. Moreover, some studies have reported that these iron chelators can bind iron and copper molecules to form cytotoxic redox complexes which are active in killing cancers or induction of cell apoptosis in cancer cells.[164]

The cytotoxic effects of Dp44mT on prostate cancer cells and colorectal cancer cells were determined. The IC_{50} of Dp44mT for prostate cancer cell lines including DU145 and PC-3 were 0.02 ± 0.00μM and 0.01 ± 0.00 μM, and for colorectal cancer cell lines, HT-29, it was 0.02 ± 0.02 μM.[165] However, the IC_{50} of Dp44mT for non-tumor prostate epithelial cells, PrEC, was 0.19 ± 0.07 μM.[165] It demonstrated the anti-cancer effects of Dp44mT on prostate and colorectal cancer cells with few side-effects. On another hand, it has been shown that the IC_{50} of DpC for HT-29 was 0.03 ± 0.10 μM.[166] The anti-cancer mechanisms are still being

investigated currently, it is convenient that both of these compounds can now be purchased in Sigma-Aldrich.

Dpc has just entered the phase I clinical trial for oral administration to patients with advanced solid tumors. They showed the powerful abilities in anti-cancer therapies, it is deserved to further investigate the anti-cancer effects of these iron chelators in cancer treatments.

5.3. MECHANISMS OF IRON-CHELATORS RELATED TO CANCERDEVELOPMENT

5.3.1. *Biological Functions of Iron in our Body*

Iron is a biologically essential element in every living organisms and it plays the important roles in many biological functions in different species.[167] In human body, Iron is usually found in the forms of complex with the proteins as the heme groups such as hemoglobin or myoglobin, heme enzymes, transferrin, ferritin, flavin-iron enzymes and so on, they are responsible for different functions to maintain the normal body health. More than half of iron in body is found in hemoglobin which is accumulated in the circulating erythrocytes, about one-fourths of body iron is found in the iron store and they are mobilizable. Besides, about 10% of iron is usually bound to myoglobin in muscle tissues and the rest are involved in enzymes. [110, 114, 167]

Iron, as mentioned, is one of the most important elements for normal body functions, they are hence recycled and conserved by different methods in the body. For example, the iron is usually obtained by dietary heme and they are metabolized into the free Fe^{2+} ion by heme oxygenase 1 (HO-1). They are delivered to different tissues through circulating transferrin which captures them in plasma from intestinal enterocytes or reticulo-endothelial macrophages. Binding of iron-containing transferrin to transferrin receptor 1 (TfR-1) on cell surface lead to endocytosis, the internalized iron is transported to mitochondria for heme synthesis. The excess iron will be stored and detoxified in cytosolic ferritin.[167-169]

As Iron participates in many body functions including formation of hemoglobin in red blood cells, myoglobin and many enzymatic function, deficiency of body iron results in the severe and fetal disease of iron-deficiency anemia and other symptoms of iron-deficiency including fatigue, hair loss, irritability and so on.[170]

However, some studies have reported that excess amount of body iron can cause the damages of cell and tissue and it would consequently contribute to some severe disease including cardiovascular diseases, liver cirrhosis, type II diabetes, septicemia, early onset neurodegenerative diseases and cancers, particularly of liver and colorectal cancers.[110, 171, 172]

5.3.2. *The roles of Iron in Tumor Development*

It has been identified that the uptake and efflux of iron would be changed in the malignant cells, it is due to the expression of some proteins responsible for iron regulation are altered. TfR-1, as mentioned, is the protein for transporting iron into the cells, some reports showed that overexpression of TfR-1 was found in many cancers including colorectal cancers, prostate cancers, liver cancers, lung cancers, breast cancers and so on. Inhibition of the TfR-1 by TfR-1 antibodies was found to suppress tumor growth and cell invasion.[114, 167, 173] It implied that iron promotes cancer developments through some pathways.

Moreover, it has been found that over-load of iron can results in higher express ion of ferritin which intimately connected to nuclear factor κB (NFκB) signaling pathways.[174, 175] NF-κB is a transcription factors participates in many cancer development processes such as proliferation and cell invasion after it is activated by tumor necrosis factor alpha (TNFα).[174] Moreover, the expression of NDRG1, which is a metastatic suppressor, has been found to be regulated by the cellular iron level. It has been reported that excess amount of cellular iron leads to down-regulation of NDRG1 and finally results in epithelial–mesenchymaltransition (EMT) which is mediated by TNFα-activated NFκB in colon and prostate cancers.[176]

Besides, there are many evidences to show the relationship and signaling pathways between iron over-load and tumor development.

5.3.3. *Mechanisms of Iron Chelators in Suppression of Cell Migration and Tumor Development*

As mentioned, over-load of cellular iron results in tumor growth, invasion and metastasis, therefore, depletion of cellular iron by using iron chelators showed the suppressive effects on cancer growth and cell invasion.[110, 173] One of the well-known mechanisms of iron-chelators to suppress cancer growth is up-regulation of NDRG1, it can trigger a series of anti-cancer signaling pathways through interacting with different targets. For example, it has been found that up-regulation of NDRG1 by iron chelators can suppress the cell invasion induced by NFκB-mediated EMT.[176] The NFκB-mediated EMT requires activation by TNFα and this process was also found to be co-activated by another protein called lysine-rich CEACAM1 co-isolated protein (LYRIC), also known as metadherin (MTDH) or astrocyte elevated gene-1 (AEG-1), which is an onco-protein and is also activated by TNFα.[177] LYRIC can co-activate the NFκB pathway through promoting the degradation of the inhibitor of NFκB (IκB) and this results in release of NFκB-p50/p65 complex which can then translocate into the nucleus to induce EMT,

cell invasion and tumor growth through promoting the gene transcription of cell invasion markers such as interleukin-8. Besides, LYRIC can also act as a cofactor that directly bind to NFκB-p65 and co-translocate into the nucleus to induce transcription of genes for EMT, cell invasion, and metastasis.[177]

Now we understand that LYRIC, under the mediation of TNFα, could promote the translocation of NFκB to proceed transcription and result in EMT and tumor development. In contrary, up-regulation of NDRG1 by iron chelators could suppress the TNFα-mediated EMT and tumor development. Therefore, it is possible that NDRG1 could suppress or down-regulate LYRIC and hence inhibit the EMT, cell invasion and tumor development through inactivation of NFκB and other onco-proteins.

In this Chapter, the relationships between NDRG1, LYRIC and NFκB with addition of TNFα were demonstrated followed by determination of the effects of the novel thiosemicarbazone (DpC and Dp44mT)on NDRG1, LYRIC and NFκB with addition of TNFα; cell invasion ability and other onco-proteins in prostate and colorectal cancers.

Names	Structures of the Iron Chelators
Desferrioxamine (DFO)	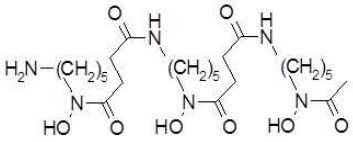
DpC	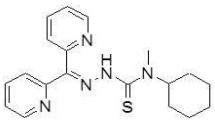
Dp44mT	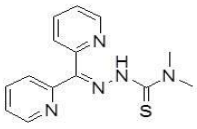
Bp2mT	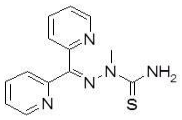

Table 5.1. Structure of the iron chelators used in this chapter, DFO was the positive control, whereas Bp2mt was the negative control.

5.4. EXPERIMENTAL DESIGNS

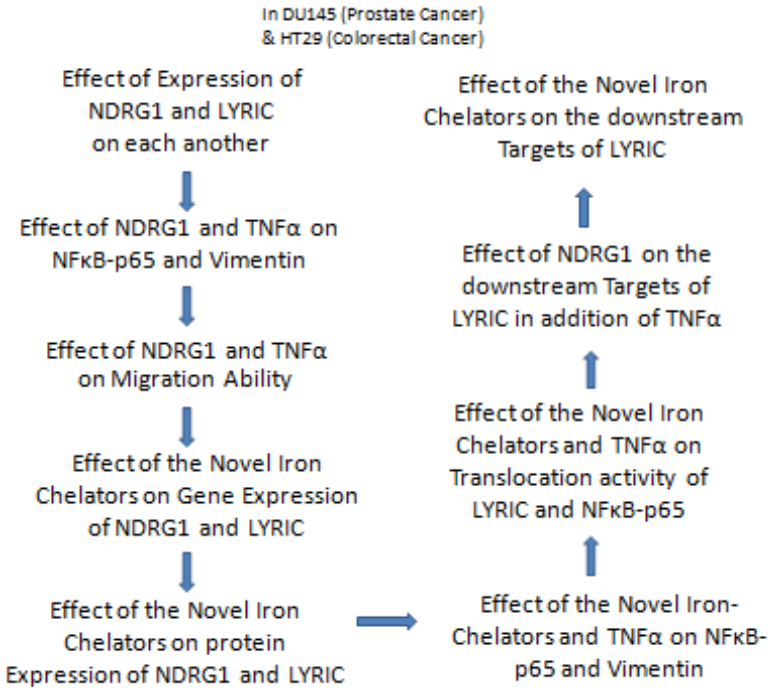

Figure5.1. Experimental plan for the studies of the effects and mechanisms ofthe two novel iron chelators, DpC and Dp44mT.

As mentioned, the main objectives in this chapter were to investigate the relationships between NDRG1, LYRIC and NFκB with addition of TNFα followed by characterizing the anti-cancer effects of DpC and Dp44mT in prostate and colorectal cancers through the pathways of NDRG1, LYRIC and NFκB. Therefore, it is necessary to understand the relationship between NDRG1 and LYRIC, the effects of novel thiosemicarbazone including DpC and Dp44mT on NDRG1 and LYRIC, and the oncogenic pathways that the iron chelators were involved to suppress the cancer developments and cancer invasion in prostate and colorectal cancers.

At first, the effects of expression of either NDRG1 or LYRIC on each another in prostate and colorectal cancer cell lines (DU145 and HT29) were determined by western blot, the relationship between NDRG1 and LYRIC was then understood. Afterwards, the effects of NDRG1 expression on LYRIC, NFκB and vimentin, and also the migration ability of the DU145 and HT29 with addition of TNFα were determined also by western blot and cell migration assay respectively, hence we can predict the effects of DpC and Dp44mT on either the expression of these proteins or

the cell migration ability of the cancer cells as it has been widely reported that iron chelators could up-regulate the expression of NDRG1.

Therefore, the effects of DpC and Dp44mT on the expression of both the gene and protein of NDRG1 and LYRIC in DU145 and HT29 were then determined by RT-PCR followed by real-time PCR and western blot respectively.

After the effects of DpC and Dp44mT on the expression of NDRG1 and LYRIC were found, the effects of DpC and Dp44mT on the expression of LYRIC, NFκB and vimentin with addition of TNFα in DU145 and HT29 were determined. As mentioned, NFκB could translocate into the nucleus through independent or LYRIC-dependent pathway to promote cell migration and tumor growth by up-regulation of the onco-genes after it is activated by TNFα. Therefore, the effects of DpC and Dp44mT on the translocation activity of NFκB and LYRIC with addition of TNFα were determined by immunofluorescent staining.

Finally, the effects of NDRG1 expression and the iron chelator including DpC and Dp44mT on the expression of the downstream targets of LYRIC were determined also by western blot to further understand the ability of DpC and Dp44mT to suppress tumor development and invasion in prostate and colorectal cancers through NDRG1 and LYRIC.

In all the experiments, DFO is a widely used iron chelator which was used as the positive control where Bp2mT was used as the negative control compound to confirm the effects of DpC and Dp44mT on iron-chelation were due to the specific functional groups.

5.5. RESULTS

5.5.1. *Effect of NDRG1 Expression on LYRIC*

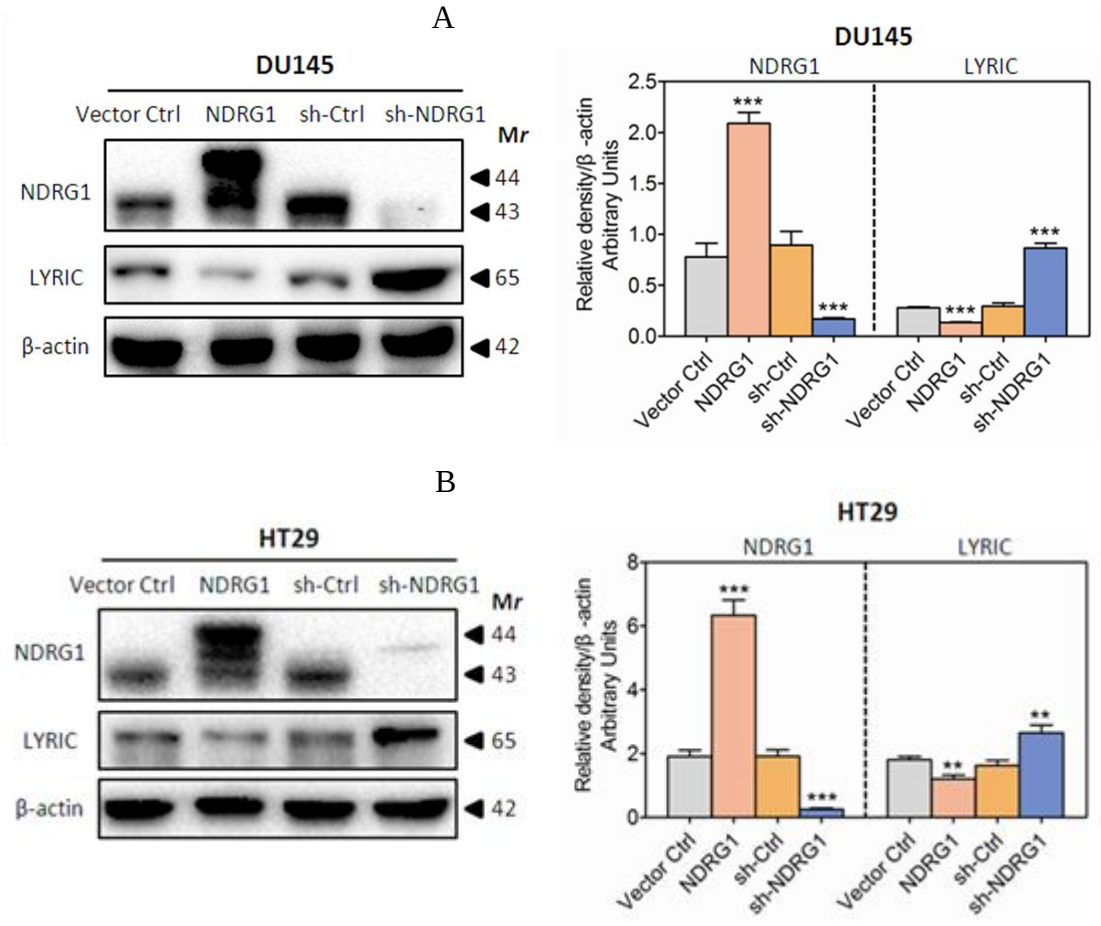

Figure 5.2. Western blot to determine the effects of NDRG1 expression on LYRIC. (A) DU145 and (B) HT29. (**p<0.01 and ***p<0.001).

The effects of NDRG1 expression on LYRIC in DU145 and HT29 were determined by western blotting, the results were shown in Figure 5.2. From the results, it firstly demonstrated that the expression of NDRG-1 was under expectation as the expression of NDRG1 in the NDRG1 over-expressing cell line (denoted NDRG1) was significantly($p<0.001$) increased compared to the vector control cell line (denoted Vector Ctrl) in both cell lines, where the expression of NDRG-1 in the NDRG1-silenced cell line (denoted sh-NDRG1) was significantly ($p<0.001$) decreased compared to the empty control vector (denoted sh-Ctrl)in both DU145and HT29.

Moreover, it showed that the expression of LYRIC was significantly down-regulated in NDRG1 over-expressing cell including DU145 ($p<0.001$) and HT29 ($p<0.01$). In contrary, the expression of LYRIC was significantly increased in NDRG1-silenced DU145 ($p<0.001$) and HT29 ($p<0.01$). It demonstrated the ability of NDRG1 expression to down-regulate the onco-protein, LYRIC.

5.5.2. *Effect of LYRIC expression on NDRG1*

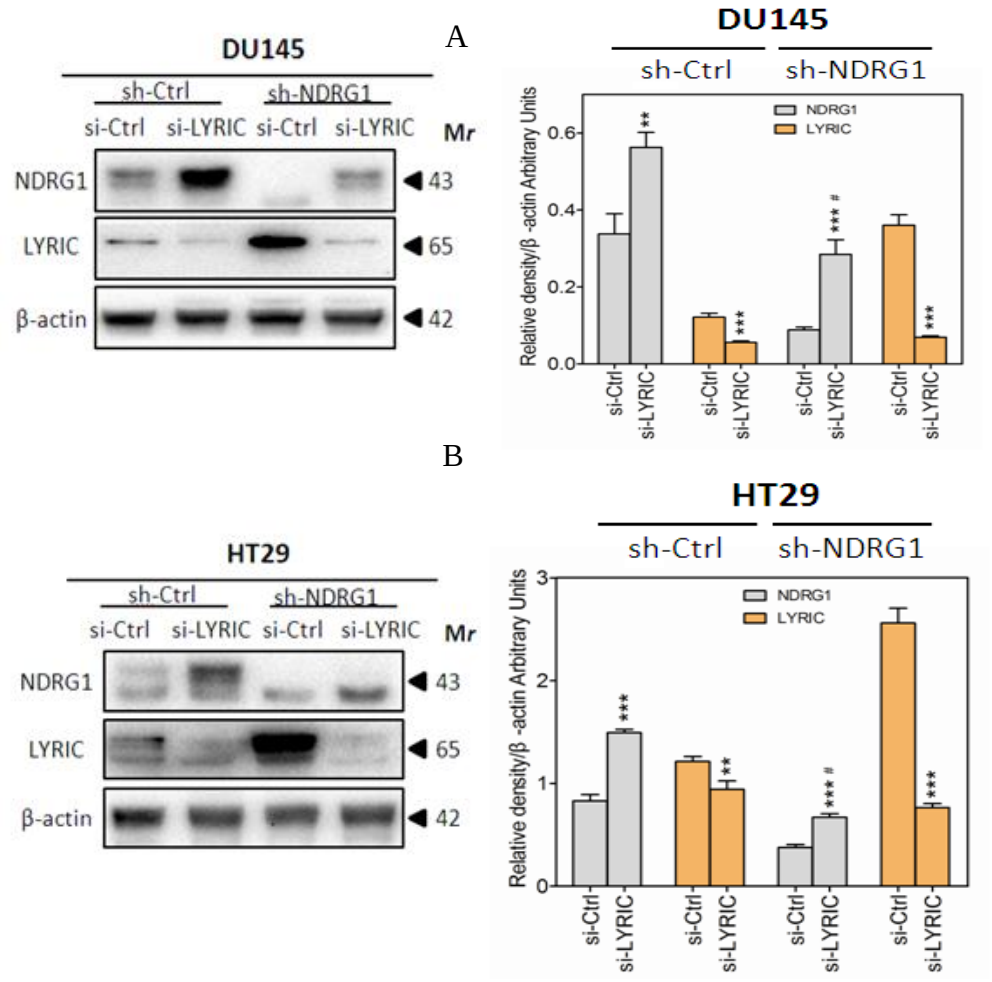

Figure 5.3. Western blot to determine the effects of NDRG1 expression on LYRIC. (A) DU145 and (B) HT29.(Relative to Vector Ctrl or sh-Ctrl without TNFa: **p<0.01 and ***p<0.001; Relative to VectorCtrl or sh-Ctrl with TNFa: #p<0.05).

The effects of LYRIC expression on NDRG1 in DU145 and HT29 were determined also by western blotting, the results were shown in Figure 5.3. It showed that the expressions of NDRG1 were significantly up-regulated in both sh-Ctrl DU145($p<0.01$) and HT29 ($p<0.001$) cell lines when the expression of LYRIC was silenced by siRNA. At the same time, the expressions of NDRG1 in both

NDRG1-silenced cell lines were also significantly($p<0.001$) increased by silencing the expression of LYRIC.

This demonstrated that NDRG1 and LYRIC were interrelated and they negatively influenced each another.

5.5.3. *Effect of NDRG1 Expression on LYRIC, NFκB-p65 and Vimentin with addition of TNFα*

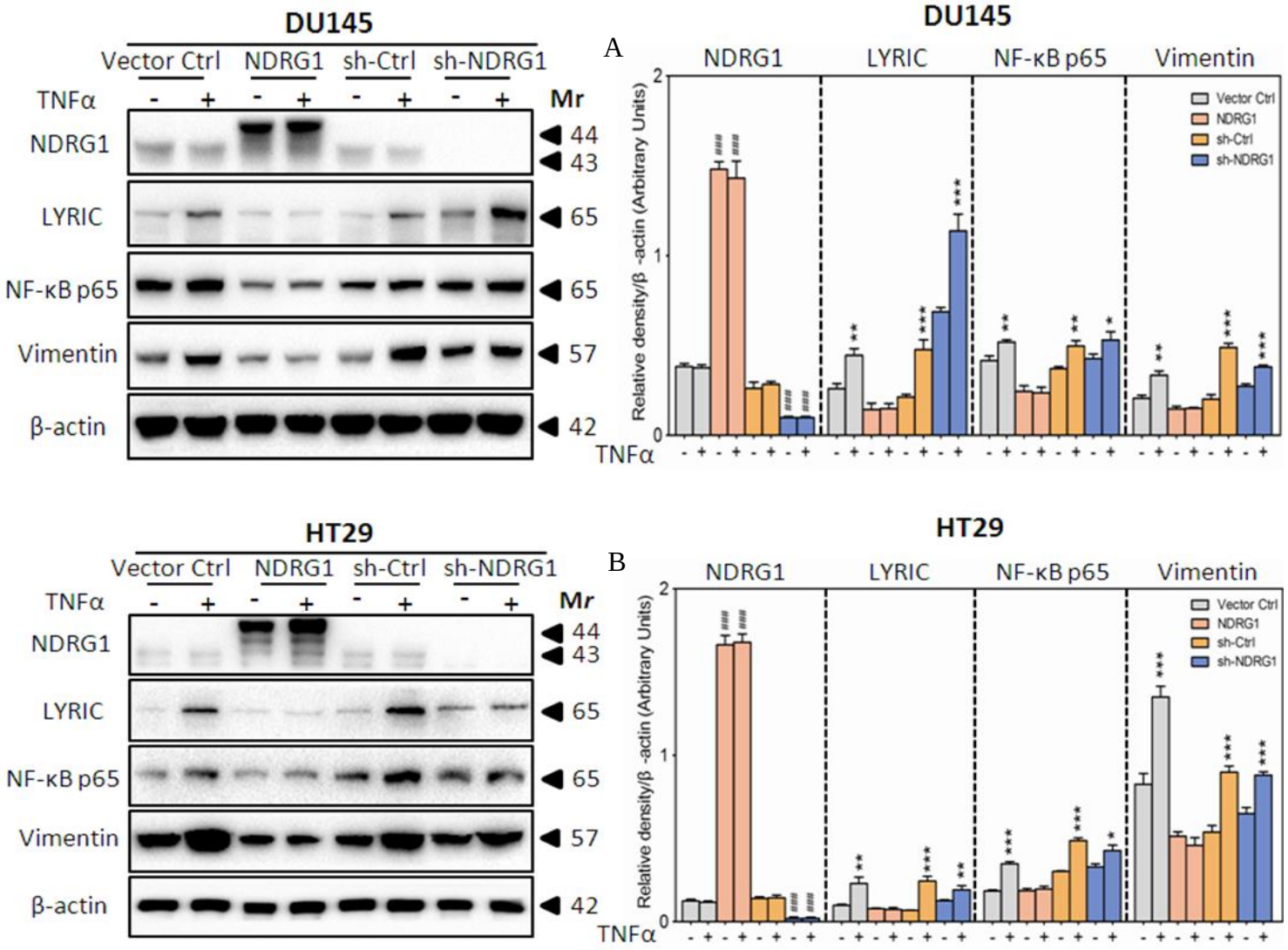

Figure 5.4. Western blot to determine the effects of NDRG1 expression on LYRIC, NFκB and Vimentin with addition of TNFα. (A) DU145 and (B) HT29. (Relative to Vector Ctrl or sh-Ctrl without TNFa: *p<0.05, **p<0.01 and ***p<0.001; Relative to VectorCtrl or sh-Ctrl with TNFa: ###p<0.001).

The effects of NDRG1 expression on LYRIC, NFκB-p65 and Vimentin with addition of TNFα in DU145 and HT29 were also determined by western blot, the results were shown in Figure 5.4.

It was found that the expression of LYRIC was significantly ($p<0.01$ and $p<0.001$) up-regulated by TNFα in all cell lines except the NDRG-1 over-expressing cell lines, and it also showed that increase in the expression of LYRIC would further up-regulate the expression of NFκB-p65 and Vimentin. Both of the NFκB-p65 and Vimentin are also the EMT and cell invasion markers, it showed that up-regulation of LYRIC by TNFα could promote EMT, cell invasion and other onco-genic pathways. However, over-expression of NDRG-1 significantly reduced the TNFα-mediated expression of LYRIC, NFκB-p65 and Vimentin.

5.5.4. *Effect of NDRG1 and TNFα on Trans-well Migration Ability*

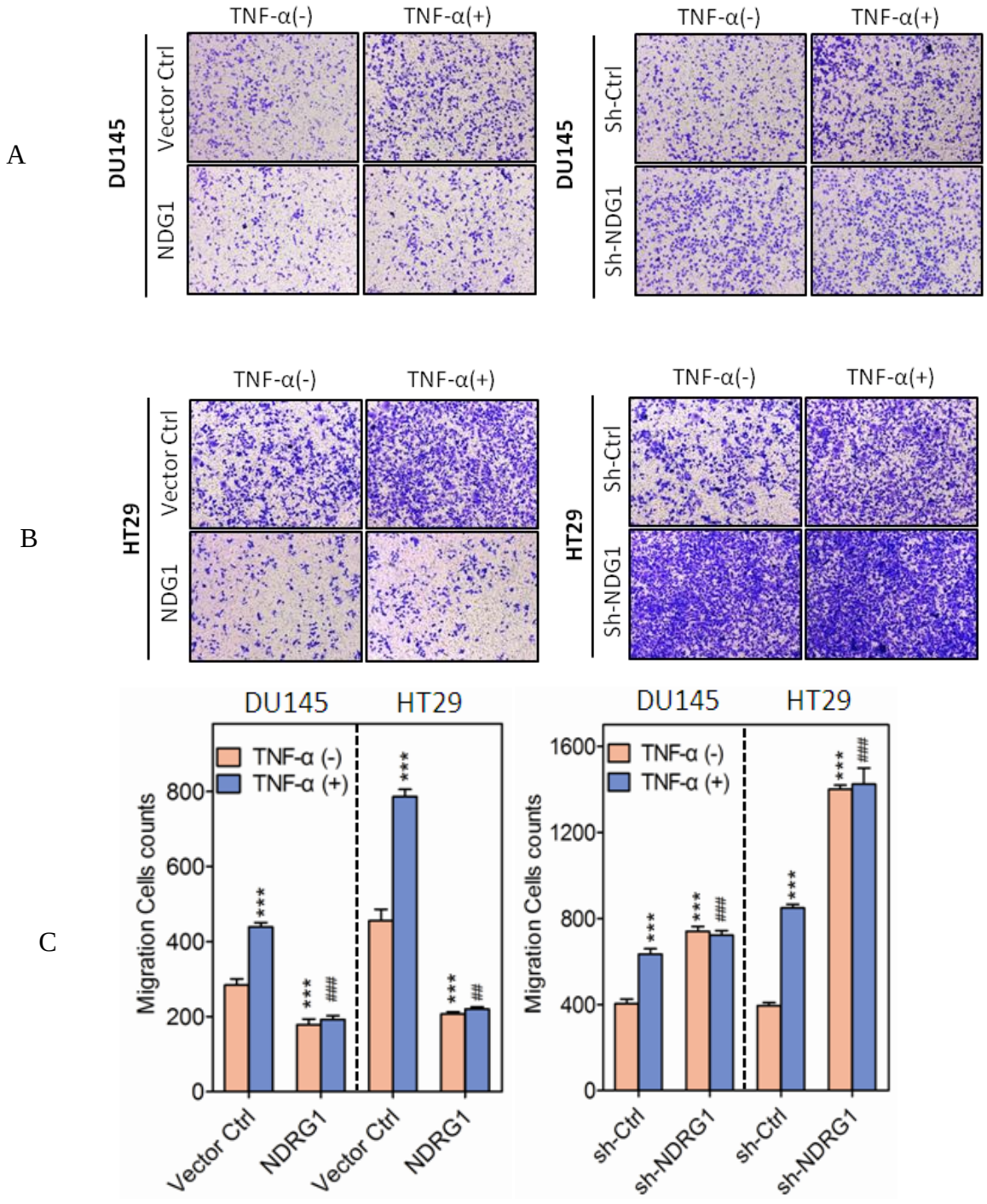

Figure 5.5. Transwell migration assay to determine the effects of NDRG1 expression on cell migration with addition of TNFα. (A) DU145, (B) HT29 and (C) Summary and comparison of each groups in two

cell lines. (Relative to Vector Ctrl or sh-Ctrl without TNFa:***p<0.001; Relative to VectorCtrl or sh-Ctrl with TNFa: ##p<0.01 and ###p<0.001).

The effects of NDRG1 expression on cell migration with addition of TNFα in DU145 and HT29 were determined by trans-well migration assay, the results were shown in Figure 5.5.

It showed that treatment of TNFα significantly increased the migration ability in DU145 and HT29, whereas overexpression of NDRG1 significantly attenuated the TNFα-mediated migration in both cell lines. Moreover, the cell migration ability of NDRG1-silenced HT29 dramatically elevated, it indicated that expression of NDRG1 was negatively related to the TNFα-mediated migration which was probably due to the down-regulation of LYRIC, NFκB-p65 and Vimentin.

5.5.5. *Effect of Iron Chelators on Gene Expression of NDRG1 and LYRIC*

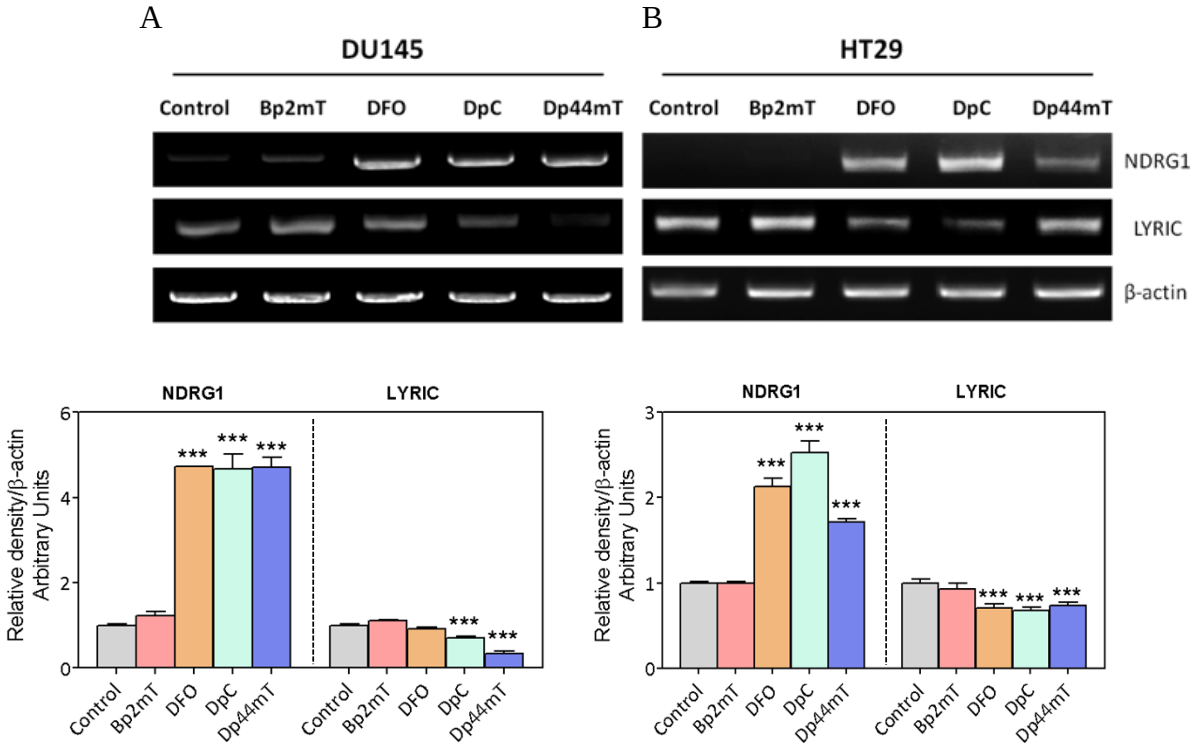

Figure 5.6. RT-PCR to assess the mRNA of NDRG1 and LYRIC in DU145 and HT29 treated with either Bp2mT (10μM), DFO (250μM), Dp44mT (5μM)or DpC (5μM)for 24 hours at 37°C. (A) DU145 and (B) HT29.(***p<0.001).

RT-PCR was performed to assess the effects of the novel thiosemicarbazone on the expression of NDRG1 and LYRIC, the results were shown on Figure 5.7

As reported in Figure 5.6, the mRNA level of NDRG1 was significantly ($p<0.001$) up-regulated by the two novel thiosemicarbazones and the positive control, DFO, in DU145 and HT29, whereas no significant effects of the negative control

compound on NDRG1 expression were found in the two cell lines. On another hand, it showed that DpC and Dp44mT significantly ($p<0.001$) down-regulated the mRNA level of LYRIC in both cell lines, however, DFO only significantly ($p<0.001$) increased the mRNA level of LYRIC in HT29 but not DU145.

These results were further confirmed by using real-time PCR, the results were shown in Figure 5.7.

It showed that the two novel thiosemicarbazones and DFO significantly up-regulated NDRG1 in both cell lines as well as the results from RT-PCR. However, the mRNA levels of LYRIC were significantly down-regulated by DpC ($p<0.001$), Dp44mT ($p<0.001$) and DFO ($p<0.01$ and $p<0.001$) in both DU145 and HT29.

A

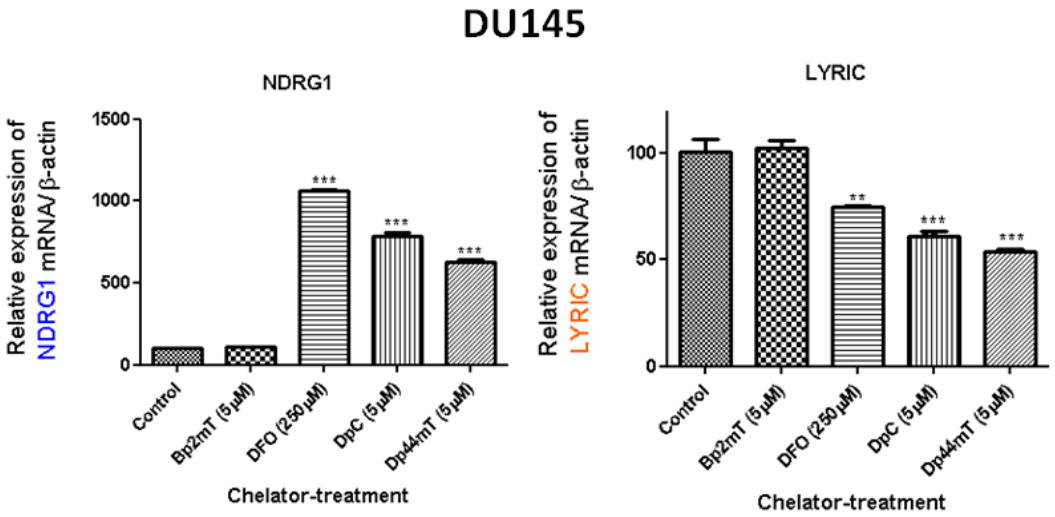

B

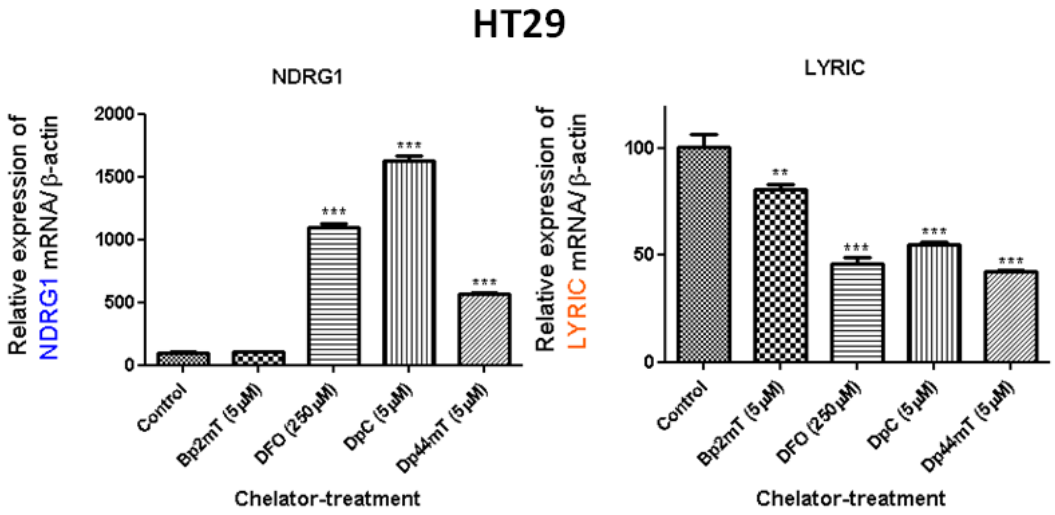

Figure 5.7. Real-time PCR to assess the mRNA of NDRG1 and LYRIC in DU145 and HT29 treated with either Bp2mT (5μM), DFO (250μM), Dp44mT (5μM)or DpC (5M)for 24 hours at 37°C. (A) DU145 and (B) HT29. (**p<0.01 and ***p<0.001).

5.5.6. *Effects of Novel thiosemicarbazones on the Protein Expression of NDRG1 and LYRIC*

A

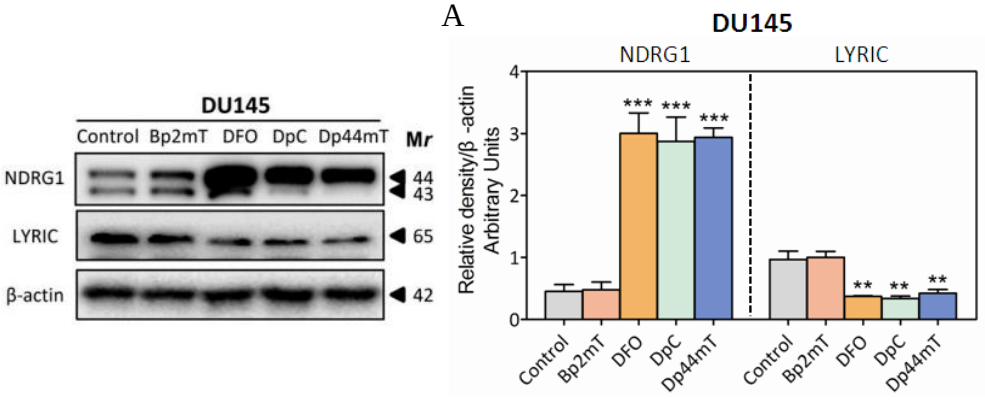

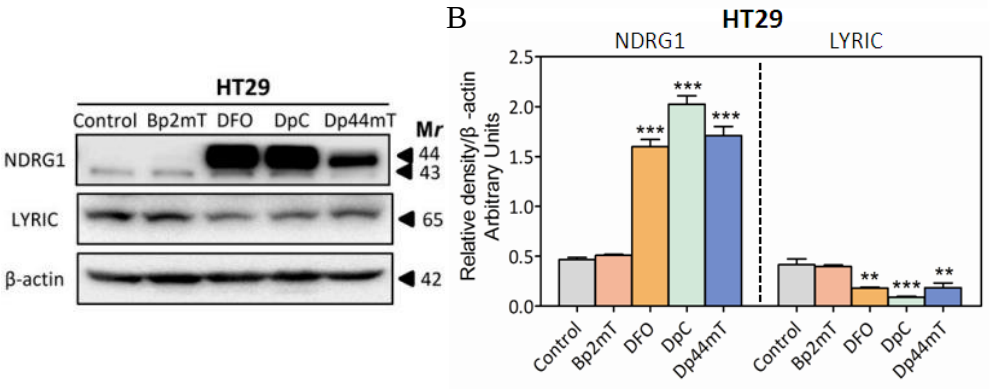

Figure 5.8. Western blot to determine the protein expression of NDRG1 and LYRIC in DU145 and HT29 treated with either Bp2mT (5μM), DFO (250μM), Dp44mT (5μM)or DpC (5μM)for 24 hours at 37°C. (A) DU145 and (B) HT29.(**p<0.01 and ***p<0.001).

Western blotting was performed to determine the effect of the novel thiosemicarbazones on the protein expression of NDRG1 and LYRIC in DU145 and HT29, the results were shown in Figure 5.8.

It showed that all Dpc, Dp44mT and DFO significantly ($p<0.001$) upregulated the expression of NDRG1, but the negative control compound Bp2mT showed no significant effects on NDRG1 expression. Besides, DpC, Dp44mT and DFO also significantly reduced the expression of LYRIC ($p<0.01$ to $p<0.001$)

Therefore, the up-regulation and downregulation effects of the novel thisemicarbazones on the expression of NDRG1 and LYRIC respectively were demonstrated.

5.5.7. *Effect of Novel thiosemicarbazones on LYRIC, NFκB-p65 and Vimentin with addition of TNFα*

The effects of the novel thiosemicarbazones DpC and Dp44mT on the protein expression of LYRIC, NFκB-p65 and Vimention with or without TNFα in DU145 and HT29 were examined by western blot, the results were shown in Figure 5.9.

It showed that the expression of NDRG1 in both cell lines were significantly ($p<0.001$) up-regulated by DpC, Dp44mT and DFO, whereas the negative compound Bp2mT showed no effects on it, and up-regulation of NDRG1 due to the iron chelators resulted in a significant down-regulation of LYRIC in both cell lines. On another hand, the expressions of LYRIC were significantly ($p<0.05$ to 0.001) increased in both cell lines without the treatment or with the treatment of either Bp2mT or DFO, however, both cell lines with the treatment of DpC and Dp44mT showed no significant ($p>0.05$) changes of LYRIC expression with the addition of TNFα. It demonstrated the effects of DpC and Dp44mT on upregulation of NDRG1 and suppression of the TNFα-mediated upregulation of LYRIC.

Moreover, TNFα-mediated upregulation of LYRIC significantly increased the expression of NFκB-p65 and Vimentin in both cell lines with the treatment of Bp2mT or without treatment. Even with the treatment of DFO, the expression of NFκB-p65 was still up-regulated by addition of TNFα. However, no significant ($p>0.05$) changes

were found in the expression of NFκB-p65 and Vimentin DpC and Dp44mT also inhibited the TNFα-mediated upregulation of NFκB-p65 and Vimentin in both cell lines, therefore, it demonstrated the effects of DpC and Dp44mT on the suppression of cell migration and invasion.

A

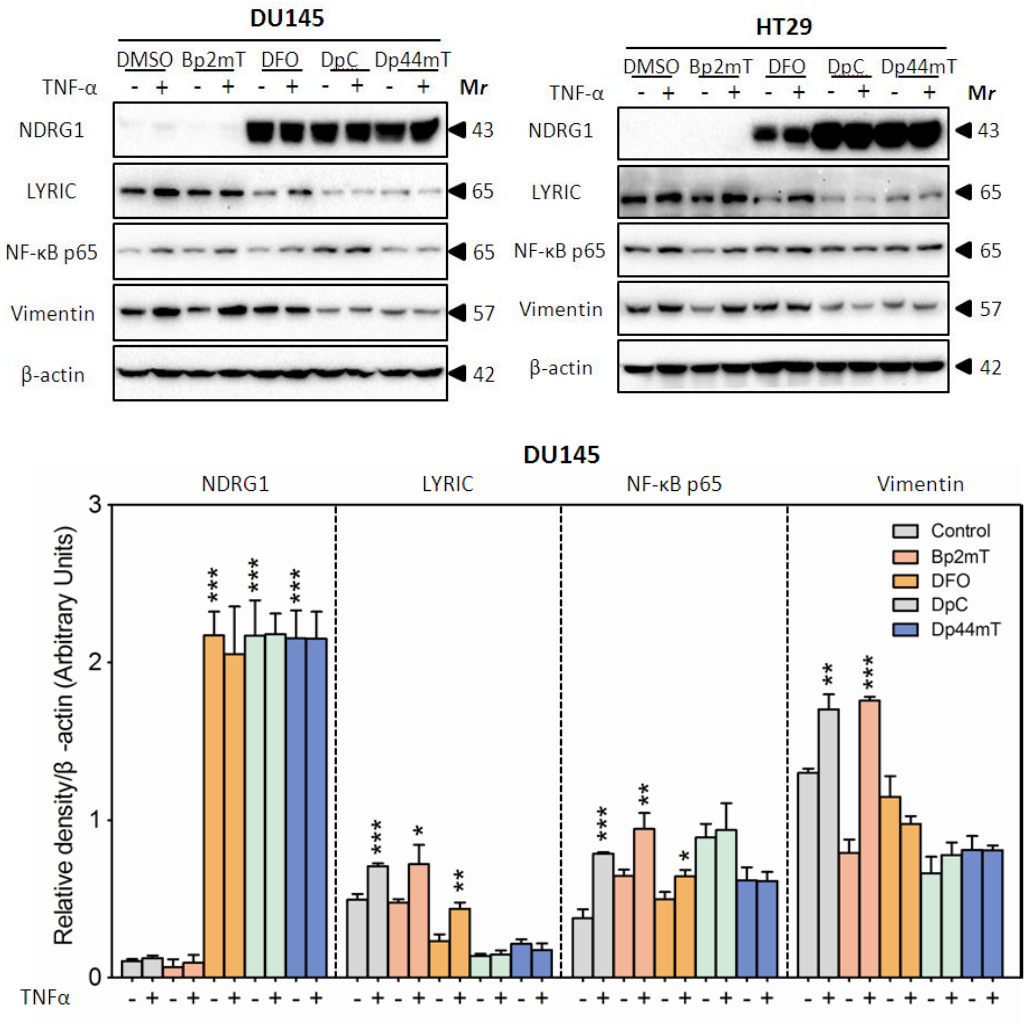

B

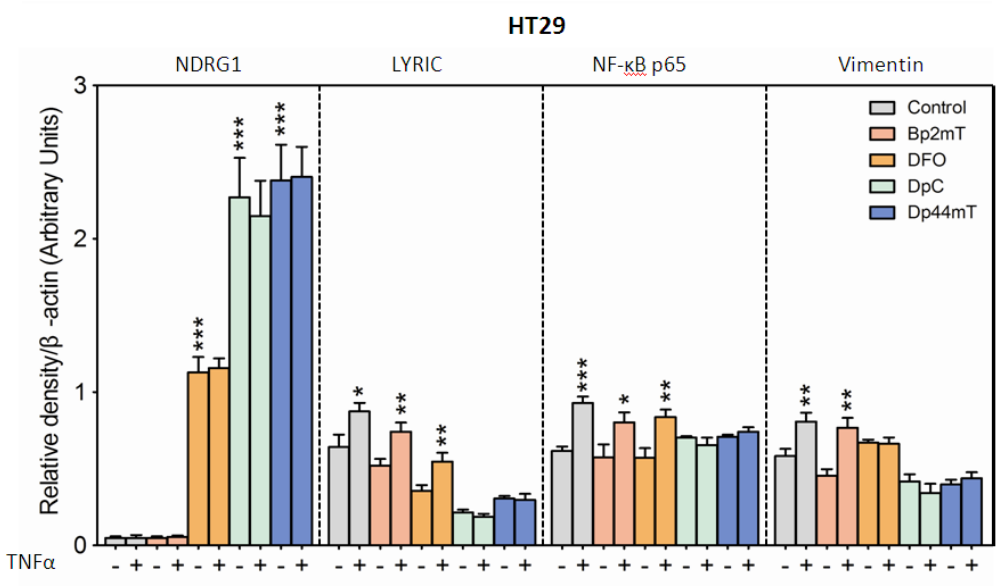

Figure 5.9. Western blot to determine the effect of Bp2mT (5μM), DFO (250μM), Dp44mT (5μM)or DpC (5μM) on the protein expression of LYRIC, NFκB-p65 and Vimentin in addition with TNFα in DU145 and HT29 treated with either (A) DU145 and (B) HT29. (*p<0.05, **p<0.01 and ***p<0.001).

5.5.8. *Effects of the Novel Thiosemicarbazones on Translocation activity of LYRIC and NFκB-p65 with addition of TNFα*

A

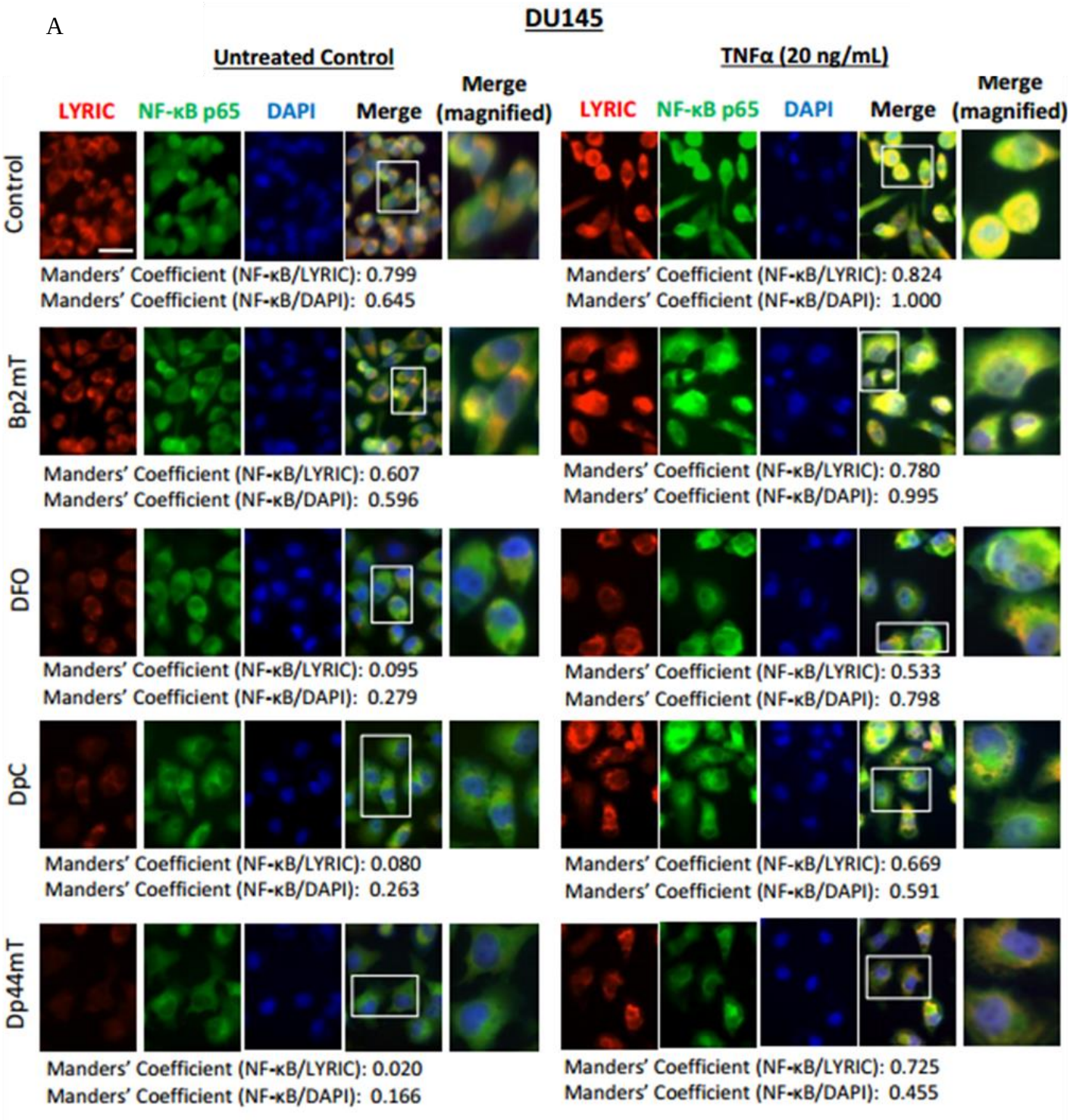

B

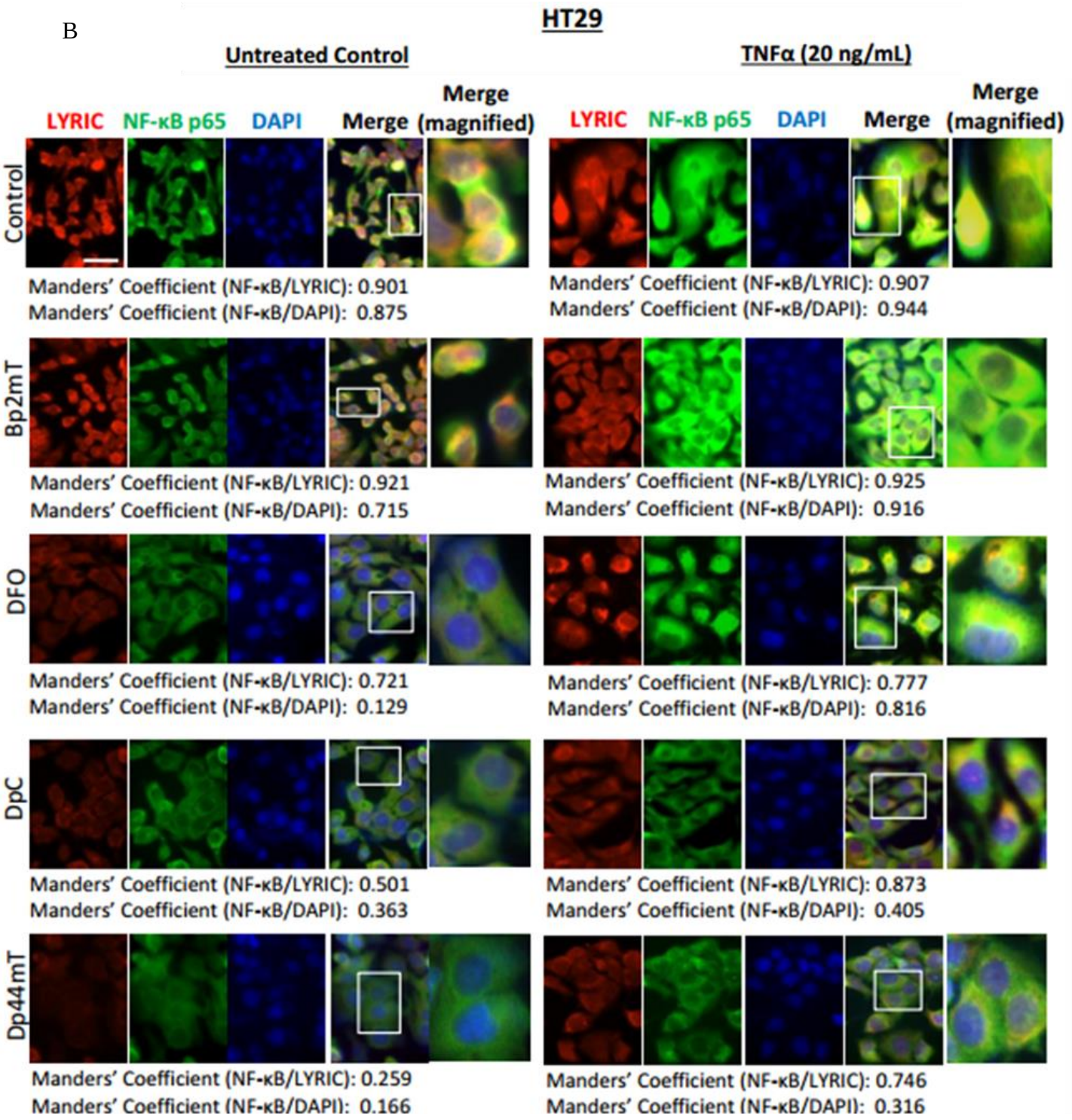
HT29
Untreated Control
TNFα (20 ng/mL)
LYRIC
NF-κB p65
DAPI
Merge
Merge (magnified)
Control
Manders' Coefficient (NF-κB/LYRIC): 0.901
Manders' Coefficient (NF-κB/DAPI): 0.875
Manders' Coefficient (NF-κB/LYRIC): 0.907
Manders' Coefficient (NF-κB/DAPI): 0.944
Bp2mT
Manders' Coefficient (NF-κB/LYRIC): 0.921
Manders' Coefficient (NF-κB/DAPI): 0.715
Manders' Coefficient (NF-κB/LYRIC): 0.925
Manders' Coefficient (NF-κB/DAPI): 0.916
DFO
Manders' Coefficient (NF-κB/LYRIC): 0.721
Manders' Coefficient (NF-κB/DAPI): 0.129
Manders' Coefficient (NF-κB/LYRIC): 0.777
Manders' Coefficient (NF-κB/DAPI): 0.816
DpC
Manders' Coefficient (NF-κB/LYRIC): 0.501
Manders' Coefficient (NF-κB/DAPI): 0.363
Manders' Coefficient (NF-κB/LYRIC): 0.873
Manders' Coefficient (NF-κB/DAPI): 0.405
Dp44mT
Manders' Coefficient (NF-κB/LYRIC): 0.259
Manders' Coefficient (NF-κB/DAPI): 0.166
Manders' Coefficient (NF-κB/LYRIC): 0.746
Manders' Coefficient (NF-κB/DAPI): 0.316

C

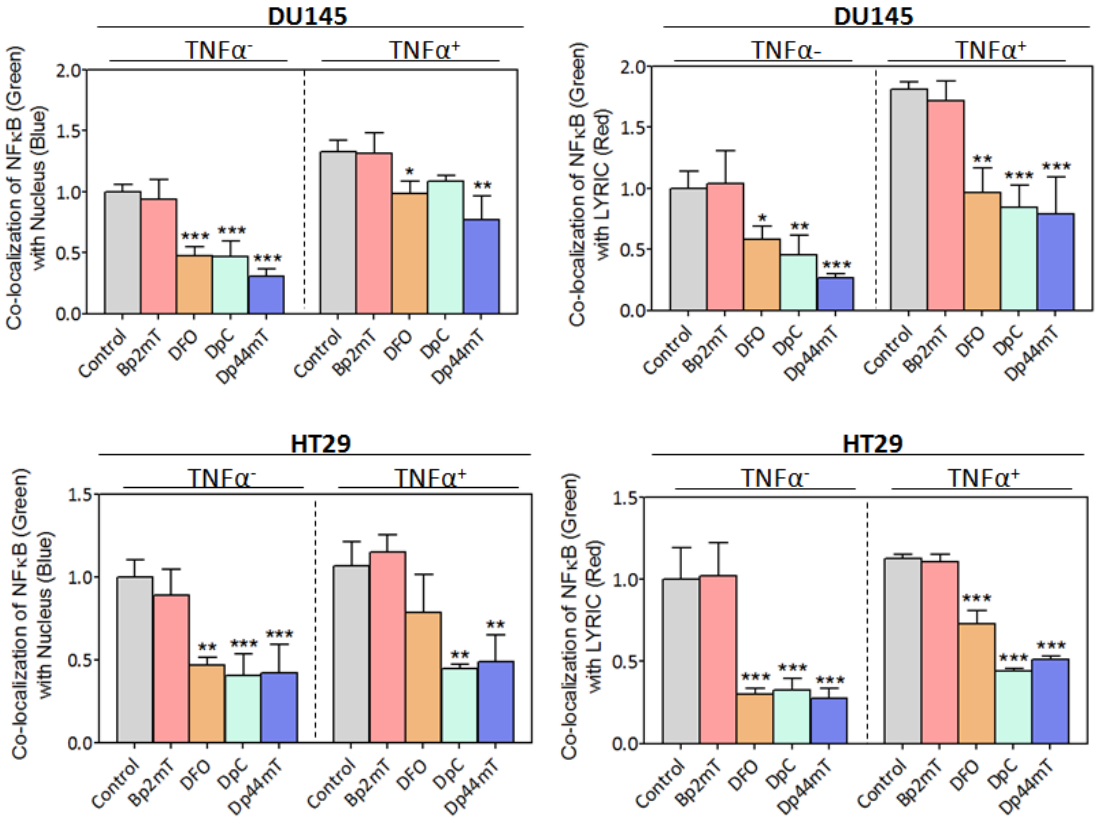

Figure 5.10. Immuno-fluorescent staining to determine the translocation activity of NFκB-p65 and LYRIC in DU145 and HT29 with Bp2mT (5μM), DFO (250μM), Dp44mT (5μM)or DpC (5μM) for 24 day with addition of TNFα. (A) DU145, (B) HT29 and (C) Summary of the co-localization intensity of NFκB-p65 against nucleus and NFκB-p65 against LYRIC.

The effects of the novel thiosemicarbazones on translocation activity of LYRIC and NFκB-p65 with addition of TNFα in DU145 and HT29 were determined by using immuno-fluorescent staining, the results were shown in Figure 5.10. For this test, green fluorescence referred to NFκB-p65, red fluorescence referred to LYRIC and blue fluorescence referred to nucleus.

As shown in Figure 5.10, the expression and translocation activity of NFκB-p65 and LYRIC in both cell lines without addition TNFα were reduced by the treatment of DFO, and the novel thiosemicarbazones DpC and Dp44mT, since it showed that the fluorescent intensity of the red and green light were decreased and the blue color referring the nucleus was much clear in the cell lines after treatments. However, it also show that addition of TNFα increased the expression and translocation of NFκB-p65 and LYRIC as it was clear that the fluorescent intensities of green and red color were increased in both cytoplasm and inside of nucleus. Whereas, the TNFα-mediated up-regulation of NFκB-p65 and LYRIC; and their translocation activity were also increased. However, in both DU145 and HT29 cell lines, over-expression of NDRG1 by DFO, DpC and Dp44mT reduced the expression of NFκB-p65 and LYRIC; and significantly ($p<0.05$ to 0.01) suppressed the translocation activity of them according to the co-localization intensity of NFκB-p65 versus DAPI in both cell lines shown in Figure 5.10C.

5.5.9. *Effect of the Novel Theiosemicarbazoneson the downstream Cancer-related protein Targets of LYRIC*

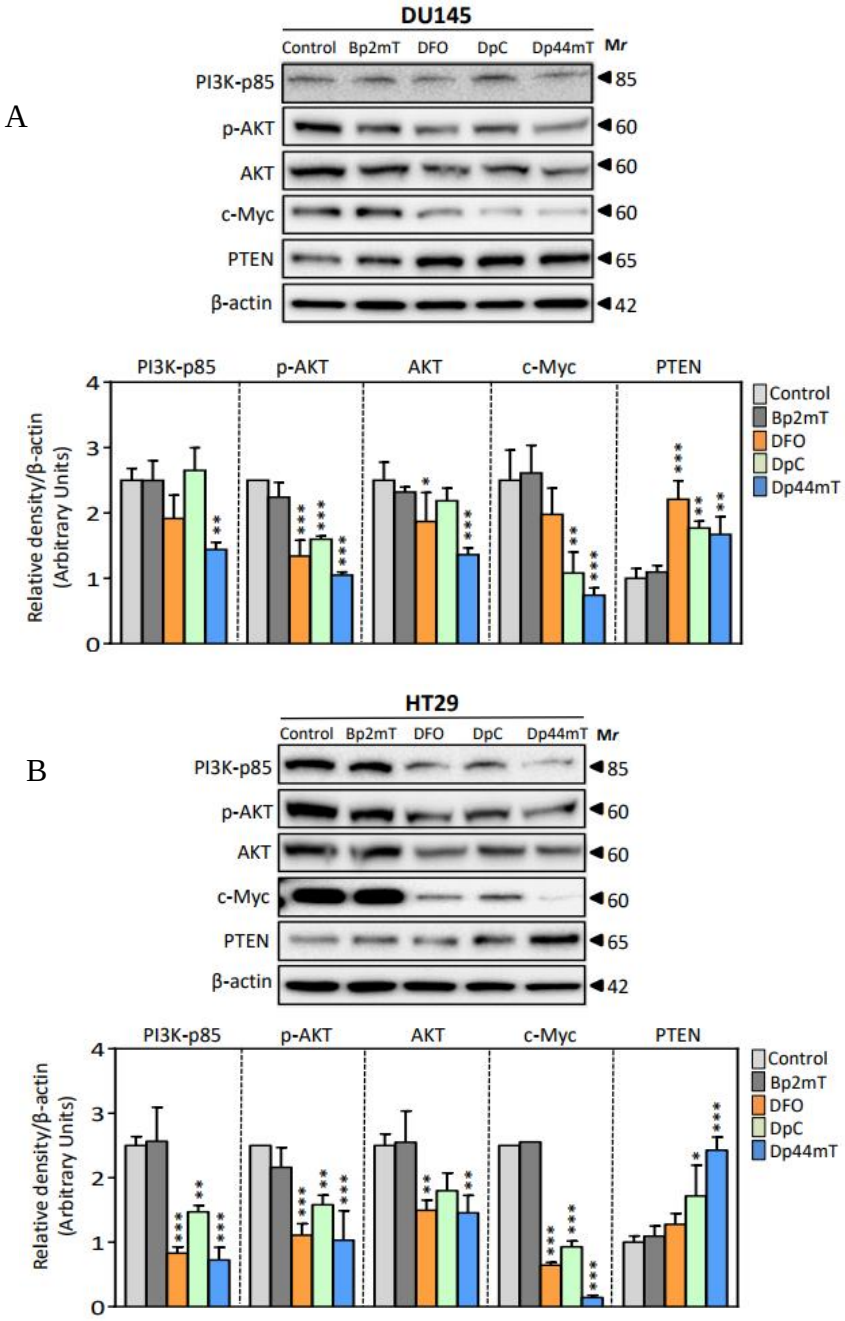

Figure 5.11. Western blot to determine the effects of DFO, DpC and Dp44mT on the downstream cancer-related proteins of LYRIC. (A) DU145 and (B) HT29.

The effects of the novel theiosemicarbazones on the downstream cancer-related protein targets of LYRIC in DU145 and HT29 were determined by western blotting, the results were shown in Figure 5.11.

From the results, it showed that the expression of AKT was significantly ($p<0.05$ to 0.001) reduced by the treatment of DFO and Dp44mT in both cell lines, where DpC showed no significant ($p>0.05$) effect on the expression of AKT though it seems there was a slight reduction. However, all DFO, DpC and Dp44mT also significantly ($p<0.01$ to 0.001) decreased the expression of p-AKT. Besides, all DFO, DpC and Dp44mT significantly ($p<0.001$) reduced the expression of c-Myc in HT29, but only DpC and Dp44mT showed the significant reduction effects on c-Myc in DU145. Although DFO also seemed to reduce the expression of c-Myc in DU145, the reduction was not significant ($p>0.05$). Moreover, the expression of the tumor suppressor PTEN was significantly ($p<0.01$ to 0.001) increased by the treatment of DFO, DpC and Dp44mT in DU145, whereas only DpC and Dp44mT showed the significant induction effects on PTEN in HT29. Furthermore, all DFO, DpC and Dp44mT also significantly ($p<0.01$ to 0.001) reduced the expression of PI3K-p85 subunit in HT29, but only Dp44mT showed a significant downregulation effect on PI3K-p85 in DU145.

5.6. DISCUSSION

As mention, the incident and mortality rate of colorectal and prostate cancers remain high globally with a subsequent low 5-year survival rate, hence there is an urgent need to provide the improved approach to kill these cancers.[178, 179]Moreover, it has been reported that the 5-year survival rate of the patients suffered from colorectal cancers is apparently decreased while the cancers was identified as metastatic state which makes the cancers to be treated more difficulty.[179, 180] It has been widely known that NDRG1 is a metastatic suppressor, the research group under Prof. Des Richardson provided and demonstrated two novel thiosemicarbazones, DpC and Dp44mT, used in up-regulation of NDRG1 in order to hinder the metastasis of colorectal and prostate cancers.[164, 166]

In this chapter, the effects of the novel thiosemicarbazones DpC and Dp44mT on LYRIC related to EMT, cell invasion and tumor developments through up-regulation of the metastatic suppressor NDRG1 in colorectal ad prostate cancers were analyzed.

At the beginning, the relationship of NDRG1 and LYRIC was found to be negatively interrelated in DU145 and HT29 by western blot, it is very important as we knew that our novel thiosemicarbazones DpC and Dp44mT can significantly up-regulate NDRG1. Then it was found that down-regulation of LYRIC could results

in significant reduction of the EMT and cell migration markers including NFκB and Vimentin, even the TNFα was added to enhance their expression and activities. Trans-well assay also showed us up-regulation of NDRG1 can suppress the TNFα-mediated cell migration, then it is possible that our novel thiosemicarbazones DpC and Dp44mT could do the same things through up-regulation of NDRG1.

Therefore, the effects of DpC and Dp44mT on the regulation of NDRG1 and LYRIC in both cancer cell lines were determined by western blotting, it showed that the DpC and Dp44mT can down-regulate LYRIC by up-regulation of NDRG1. Furthermore, the effects of DpC and Dp44mT on the EMT and cell migration markers were also determined, it showed that DpC and Dp44mT could down-regulate the level of both markers in DU145 and HT29 cell lines. They also showed the significant down-regulation effects on the translocation activity of NFκB and LYRIC into the nucleus, it demonstrated that both DpC and Dp44mT could suppress the EMT, cell invasion and tumor development through reduction of the NFκB-mediated transcription of the targets for cell migration and tumor growth.

It is important to show that the cell invasion was significantly reduced by DpC and Dp44mT through up-regulation of NDRG1 and down-regulation of LYRIC. As we mentioned, obstruction of cell invasion can help the cancer treatment and improve the survival rate of patients suffered from cancers.[166, 180]

Finally, the effects of DpC and Dp44mT on the downstream cancer-related targets of LYRIC including AKT, c-Myc, PI3K and PTEN in both DU145 and HT29 cell lines were determined. Although the regulations of these cancer-related genes by DpC and Dp44mT were not completely the same in both DU145 and HT29 cell lines, it apparently showed the anti-cancer effects in both cell lines through down-regulation of LYRIC. Since there was the trend that DpC and Dp44mT showed the up-regulation effects on tumor suppressor PTEN and down-regulation effects on onco-proteins such as AKT and c-Myc in both cell lines.

5.7. CONCLUSION

To conclude, the anti-cancer effects of both novel thiosemicarbazones DpC and Dp44mT on EMT, cell migration and tumor developments through up-regulation of NDRG1 and down-regulation of LYRIC in prostate and colorectal cancer cell lines were evaluated. It showed the excellent potentials of DpC and Dp44mT to be developed as the anti-cancer drug for being used.

Chapter 6 OVERALL DISCUSSION AND FUTURE PERSPECTIVES

In this study, the effects of the novel quinoline derivatives 83b1 and 160a, and thiosemicarbazone derivatives DpC and Dp44mT on different types of cancers were determined, they all showed the significant anti-cancer effects on certain types of cancers. The mechanisms of these novel anti-cancer compounds were determined by different assays with computational approaches.

6.1. STUDY For THE CHARACTERIZATION OF 83b1 IN HUMAN ESOPHAGEAL CANCER CARCINOMAS

As mentioned, the carcinogenesis of PPARD was still not cleared understood.[140, 141]Through the study in Chapter 3, more information about the participation of PPARD in ESCC was obtained. It showed that the participation of PPARD in tumor promotion and its over-expression in ESCC. Moreover, 83b1 has also been shown to suppress esophageal cancer development by targeting PPARD, this result in down-regulation of COX-2, reduction of COX-2 derived PGE_2 production and some downstream oncogenic targets such as AKT, JNK-1, MAPK, MEK-1 and so on. 83b1 showed its high potential in cancer treatment because of its low toxicity compared with the existing anti-cancer drugs.[122, 161, 181] However,

before being an anti-cancer drug used in the real treatment against cancers, many scientific research and studies are necessary. For example, chemical modification of the structure of 83b1 might lead to a better affinity against PPARD with higher cytotoxicity in cancer and lower toxicity in normal cells; some safety assessments and clinical studies are also needed to further characterize the effects of 83b1 in human.

6.2. STUDY OF CHARACTERIZATION OF 160a IN HUMAN ESOPHAGEAL CANCER CARCINOMAS

The study of 160a in Chapter 4 showed the potential of 160a in combination chemotherapeutic treatments against esophageal cancers. Through this study, it demonstrated the ability of 160a to reverse the drug resistance of P-gp and resulted in higher effectiveness of an anti-cancer drug, doxorubicin in cancer treatment. The currently anti-cancer compounds used in combination treatment against cancers such as paclitaxel usually showed severe adverse effects in human while higher dosage is used.[161, 162] However, 160a ,because of its mechanism which is directly targeting and blocking P-gp, showed a much lower toxicity in non-tumor cells and 160a also showed the synergistic effect with doxorubicin in combination treatment against ESCC cell lines. This suggested that anti-cancer drug used in combination treatment might be designed with high affinity against the multi-drug resistant proteins which

are overexpressed in cancer as the biomarkers, it should highly reduce the adverse effects.[163] However, more studies have to be conducted such as the safety assessment in human, binding affinity in human, studies in other cancer types, and so on.

6.3. STUDY OF CHARACTERIZATION OF DpC and Dp44mT IN HUMAN PROSTATE AND COLORECTAL CANCERS

Some anti-cancer mechanisms of the novel thiosemicarbazone derivatives DpC and Dp44mT have been demonstrated already.[165, 166, 182] In this study, the effects of these two compounds in tumor suppression related to NDRG1 and LYRIC were found. They can up-regulate NDRG1 and reduce the expression of LYRIC, it leads to down-regulation of NFκB, suppression of translocation of both NFκB and TNF α -mediated cell migration. Eventually, it inhibits tumor development.[118]

However, most of the experiments conducted for these potential compounds still stayed at in vitro level, the cytotoxicity, bioavailability, efficacy and other important parameters are largely different in animals or even in human. Therefore, more in vivo experiments for these compounds are needed in the future. Moreover, the structures of these compounds can also be further modified in order to design the anti-cancer

compound with higher selectivity and potency against cancers without serious side-effects.

Chapter 7 REFERENCES

1. Siegel, R.L., K.D. Miller, and A. Jemal, *Cancer Statistics, 2016.* Ca-a Cancer Journal for Clinicians, 2016. **66**(1): p. 7-30.
2. Cassileth, B.R., *Complementary therapies: Overview and state of the art.* Cancer Nursing, 1999. **22**(1): p. 85-90.
3. Bauer, K.H., *INTRODUCTION TO TOPIC PROBLEM OF CANCER.* Langenbecks Archiv Fur Chirurgie, 1975. **339**: p. 37-40.
4. Kennedy, B.J., *ONCOLOGY - AN INTRODUCTION TO CANCER ISSUE.* Geriatrics, 1970. **25**(10): p. 95-&.
5. Ferlay, J., et al., *Cancer incidence and mortality worldwide: Sources, methods and major patterns in GLOBOCAN 2012.* International Journal of Cancer, 2015. **136**(5): p. E359-E386.
6. Kingham, T.P. and C. Are, *Introduction to JSO global cancer edition Introduction.* Journal of Surgical Oncology, 2017. **115**(5): p. 511-512.
7. Farber, E., *APPROACHES TO CANCER PREVENTION - INTRODUCTION AND PERSPECTIVE.* Proceedings of the American Association for Cancer Research, 1988. **29**: p. 527-528.
8. Munstedt, K. and W. Kunzel, *Introduction to the topic: Oncologic supportive therapy. Part 2.* Gynakologe, 2003. **36**(8): p. 657-657.
9. Sigman, M., *Introduction: Cancer treatment and male fertility: effects of therapy and current and future management options.* Fertility and Sterility, 2013. **100**(5): p. 1179-1179.
10. Therasse, P., *Introduction to cancer clinical trials.* European Journal of Cancer, 1998. **34**: p. S128-S128.
11. Day, N.E., *SOME ASPECTS OF EPIDEMIOLOGY OF ESOPHAGEAL CANCER.* Cancer Research, 1975. **35**(11): p. 3304-3307.
12. Gallo, A. and C. Cha, *Updates on esophageal and gastric cancers.* World Journal of Gastroenterology, 2006. **12**(20): p. 3237-3242.

13. DeMeester, S.R., *Evaluation and Treatment of Superficial Esophageal Cancer.* Journal of Gastrointestinal Surgery, 2010. **14**: p. 94-100.
14. Essadi, I., I. Lalya, and H. Mansouri, *Esophageal Carcinoma.* New England Journal of Medicine, 2015. **372**(15): p. 1470-1471.
15. Faivre, J., C. Lepage, and A.M. Bouvier, *Recent data on the epidemiology of esophageal cancer.* Gastroenterologie Clinique Et Biologique, 2005. **29**(5): p. 534-539.
16. Barbetakis, N., C. Asteriou, and A. Kleontas, *Esophageal cancer surgery: Concerns.* Indian Journal of Cancer, 2014. **51**(4): p. 458-458.
17. Cummings, L.C. and G.S. Cooper, *Epidemiology of esophageal carcinoma in a statewide cancer registry.* Gastroenterology, 2006. **130**(4): p. A456-A456.
18. Berney, D.M., *Early Prostate Cancer.* Journal of Pathology, 2012. **226**: p. S3-S3.
19. Brody, H., *Prostate cancer.* Nature, 2015. **528**(7582): p. S117-S117.
20. Haas, G.P., et al., *The worldwide epidemiology of prostate cancer: perspectives from autopsy studies.* Canadian Journal of Urology, 2008. **15**(1): p. 3866-3871.
21. Thapa, R., M. Lakhey, and P.K. Yadav, *Clinico-pathological Study of Colorectal Carcinoma.* Journal of Nepal Medical Association, 2013. **52**(7): p. 449-452.
22. Siegel, R.L., et al., *Colorectal cancer statistics, 2017.* Ca-a Cancer Journal for Clinicians, 2017. **67**(3): p. 177-193.
23. Fernandez, F.G., et al., *Five-year survival after resection of hepatic metastases from colorectal cancer in patients screened by positron emission tomography with F-18 fluorodeoxyglucose (FDG-PET).* Annals of Surgery, 2004. **240**(3): p. 438-447.
24. Nuzzo, G., et al., *Resection of hepatic metastases from colorectal cancer.* Hepato-Gastroenterology, 1997. **44**(15): p. 751-759.
25. Berry, M.F., *Esophageal cancer: staging system and guidelines for staging and treatment.* Journal of Thoracic Disease, 2014. **6**: p. S289-S297.
26. Mathieu, L.N., et al., *Esophageal cancer gender disparity.* Journal of Clinical Oncology, 2012. **30**(30).
27. Lundell, L.R., *Etiology and Risk Factors for Esophageal Carcinoma.* Digestive Diseases, 2010. **28**(4-5): p. 641-644.

28. Green, J.A., R. Amaro, and J.S. Barkin, *Symptomatic gastroesophageal reflux as a risk factor for esophageal adenocarcinoma*. Digestive Diseases and Sciences, 2000. **45**(12): p. 2367-2368.
29. Anderson, L.A., et al., *Risk factors for Barrett's oesophagus and oesophageal adenocarcinoma: Results from the FINBAR study.* World Journal of Gastroenterology, 2007. **13**(10): p. 1585-1594.
30. Figueroa, J.D., et al., *Cigarette smoking, body mass index, gastro-esophageal reflux disease, and non-steroidal anti-inflammatory drug use and risk of subtypes of esophageal and gastric cancers by P53 overexpression.* Cancer Causes & Control, 2009. **20**(3): p. 361-368.
31. Pourshams, A. and E. Jafari, *Risks factors associated with esophageal cancer in Iran; a review.* Journal of Gastroenterology and Hepatology, 2013. **28**: p. 747-748.
32. Silvera, S.A.N., et al., *Dietary and lifestyle patterns and risk of subtypes of esophageal and gastric cancer: Factor analysis.* Journal of Nutrition, 2004. **134**(12): p. 3531S-3531S.
33. Lin, P. and W. Tang, *EPIDEMIOLOGY AND ETIOLOGY OF ESOPHAGEAL CANCER IN CHINA.* Journal of Cancer Research and Clinical Oncology, 1980. **96**(2): p. 121-130.
34. Chornokur, G., et al., *Risk factors of prostate cancer in African American men.* Cancer Research, 2012. **72**.
35. Rosenblatt, K.A., J.L. Stanford, and K.G. Wicklund, *Sexual factors and the risk of prostate cancer.* American Journal of Epidemiology, 2000. **151**(11): p. S78-S78.
36. Allam, M.F. and R.A. Lucena, *Aetiology of sex differences in colorectal cancer.* European Journal of Cancer Prevention, 2001. **10**(3): p. 299-300.
37. Faivre, J., A.M. Bouvier, and C. Bonithon-Kopp, *Epidemiology and screening of colorectal cancer.* Best Practice & Research in Clinical Gastroenterology, 2002. **16**(2): p. 187-199.
38. Murtaugh, M.A., et al., *Obesity, and diet in etiology of colorectal cancer.* Cancer Epidemiology Biomarkers & Prevention, 2004. **13**(11): p. 1891S-1892S.
39. Holmes, R.S. and T.L. Vaughan, *Epidemiology and pathogenesis of esophageal cancer.* Seminars in Radiation Oncology, 2007. **17**(1): p. 2-9.

40. Stubbs, R.S., *THE ETIOLOGY OF COLORECTAL-CANCER.* British Journal of Surgery, 1983. **70**(6): p. 313-316.
41. Gregory, C.D., *Apoptosis in Cancer Pathogenesis and Anti-cancer Therapy New Perspectives and Opportunities Preface,* in *Apoptosis in Cancer Pathogenesis and Anti-Cancer Therapy: New Perspectives and Opportunities*, C.D. Gregory, Editor. 2016. p. VII-X.
42. Benmoussa, A., et al., *Colorectal cancer: Comparison of clinicopathologic features between Moroccans patients less than 50 years old and older.* Pathologie Biologie, 2013. **61**(3): p. 117-119.
43. Minna, J.D., et al., *Molecular pathogenesis of lung cancer with translation to the clinic.* Journal of Thoracic Oncology, 2007. **2**(8): p. S178-S179.
44. Jaiswal, P.K., A. Goel, and R.D. Mittal, *Survivin: A molecular biomarker in cancer.* Indian Journal of Medical Research, 2015. **141**: p. 389-397.
45. Abrams, J.A., et al., *Cigarette smoking and risk of lung metastasis from esophageal cancer.* Cancer Epidemiology Biomarkers & Prevention, 2008. **17**(10): p. 2707-2713.
46. Vidovic, V., et al., *Unusual metastasis of esophageal cancer.* Vojnosanitetski Pregled, 2014. **71**(10): p. 975-977.
47. Diamandis, E.P., *Clinical applications of tumor suppressor genes and oncogenes in cancer.* Clinica Chimica Acta, 1997. **257**(2): p. 157-180.
48. Johnston, J.M.N., *P-glycoprotein and multidrug resistance.* New England Journal of Medicine, 1996. **334**(20): p. 1336-1336.
49. Cole, S.P.C., *Multidrug Resistance Protein 1 (MRP1, ABCC1), a "Multitasking" ATP-binding Cassette (ABC) Transporter.* Journal of Biological Chemistry, 2014. **289**(45): p. 30880-30888.
50. McCormick, J.W., P.D. Vogel, and J.G. Wise, *Multiple Drug Transport Pathways through Human P-Glycoprotein.* Biochemistry, 2015. **54**(28): p. 4374-4390.
51. Varma, M.V.S., et al., *P-glycoprotein inhibitors and their screening: a perspective from bioavailability enhancement.* Pharmacological Research, 2003. **48**(4): p. 347-359.
52. Breier, A., et al., *Reversal of P-glycoprotein mediated vincristine resistance by analogues of pentoxifylline.* Febs Journal, 2006. **273**: p. 230-230.

53. Wheeler, R.D., et al., *Inhibition of vincristine uptake into P-glycoprotein-containing vesicles by the resistance modifier, XR9051.* British Journal of Pharmacology, 1999. **126**.
54. Hotta, T., et al., *P-glycoprotein-expressing tumor cells are resistant to anticancer drugs in human gastrointestinal cancer.* Surgery Today-the Japanese Journal of Surgery, 1999. **29**(7): p. 591-596.
55. Xu, H.B., L. Li, and G.Q. Liu, *Reversal of P-glycoprotein-mediated multidrug resistance by guggulsterone in doxorubicin-resistant human myelogenous leukemia (K562/DOX) cells.* Pharmazie, 2009. **64**(10): p. 660-665.
56. Kim, R.B., *Drugs as P-glycoprotein substrates, inhibitors, and inducers.* Drug Metabolism Reviews, 2002. **34**(1-2): p. 47-54.
57. Furst, D.E., *Perspectives on the cyclooxygenase-2/cyclooxygenase-1 hypothesis.* Jcr-Journal of Clinical Rheumatology, 1998. **4**(5): p. S40-S48.
58. Zidar, N., et al., *Expression of cyclooxygenase-1 and cyclooxygenase-2 in the normal human heart and in myocardial infarction.* Cardiovascular Pathology, 2007. **16**(5): p. 300-304.
59. Chiblak, S., et al., *Cyclooxygenase 2-driven inflammation in pancreatic cancer.* Ejc Supplements, 2010. **8**(5): p. 76-76.
60. Jubb, A.M., et al., *Cyclooxygenase-2 expression in sporadic colorectal cancer.* Journal of Pathology, 2001. **195**: p. 4A-4A.
61. Liu, Y.S., et al., *Expression of p53, p16 and cyclooxygenase-2 in esophageal cancer with tissue microarray.* Journal of Digestive Diseases, 2007. **8**(3): p. 133-138.
62. Song, Y.S. and S.R.L. Medimond, *Cyclooxygenase-2 in ovarian cancer.* Proceedings of the XIX Asian and Oceanic Congress of Obstetrics & Gynecology, 2005: p. 171-171.
63. Saitoh, Y., Y. Yaginuma, and M. Ishikawa, *Analysis of Bcl-2, Bax and Survivin genes in uterine cancer.* International Journal of Oncology, 1999. **15**(1): p. 137-141.
64. Korsmeyer, S.J., *Bcl-2 gene family and the regulation of cell death.* Faseb Journal, 1997. **11**(9): p. A866-A866.
65. Cory, S., et al., *Regulation of cell survival by the bcl-2 gene family.* Faseb Journal, 1997. **11**(9): p. A866-A866.
66. Cory, S., et al., *Regulation of Apoptosis by the Bcl-2 Family.* European Journal of Cancer, 2012. **48**: p. S11-S12.

67. Oren, M. and V. Rotter, *Introduction: p53 - the first twenty years.* Cellular and Molecular Life Sciences, 1999. **55**(1): p. 9-11.
68. Jiang, W., H. Ananthaswamy, and M.L. Kripke, *The role of P53 mutations in UV carcinogenesis and immune suppression.* Photochemistry and Photobiology, 1999. **69**: p. 65S-66S.
69. Popp, W., et al., *p53 mutations in lung cancers of former German uranium miners.* European Journal of Cancer, 1997. **33**: p. 1067-1067.
70. Soussi, T., *Focus on the p53 gene and cancer: Advances in TP53 mutation research.* Human Mutation, 2003. **21**(3): p. 173-175.
71. Jiang, X.J., et al., *p53 overexpression and colorectal cancer.* Cancer Research, 2009. **69**.
72. Tandle, A., T. Teni, and D. Saranath, *Tumor suppressor gene p53 in human oral cancers*. 17th International Cancer Congress, Vol 1 and 2, ed. M. Moraes, R. Brentani, and R. Bevilacqua. 1998. 171-174.
73. Cheung, B., et al., *Growth inhibitory retinoid, effects after recruitment of retinoid X receptor beta to the retinoic acid receptor beta promoter.* International Journal of Cancer, 2003. **105**(6): p. 856-867.
74. De Oliveira, L.P., et al., *Rexinoid therapy for poorly differentiated thyroid cancer: A pilot clinical phase II trial and correlation to retinoid and peroxisome-proliferator activated receptor gamma receptors expression.* Journal of Clinical Oncology, 2010. **28**(15).
75. Liu, T., et al., *The retinoid anticancer signal: mechanisms of target gene regulation.* British Journal of Cancer, 2005. **93**(3): p. 310-318.
76. Barden, D., *Hope for early cancer diagnosis.* Chemistry World, 2011. **8**(6): p. 23-23.
77. Croce, C., *Introduction to the Role of MicroRNAs in Cancer Diagnosis, Prognosis, and Treatment.* Cancer Journal, 2012. **18**(3): p. 213-214.
78. Scully, C. and S. Petti, *Overview of cancer for the healthcare team: Aetiopathogenesis and early diagnosis.* Oral Oncology, 2010. **46**(6): p. 402-406.
79. Kim, Y.D., et al., *Comparison of endoscopic biopsy and histopathologic diagnosis after endoscopic submucosal dissection.* Journal of Gastroenterology and Hepatology, 2006. **21**: p. A490-A490.

80. Tytgat, G.N.J. and J.G. Ignacio, *Technicalities of endoscopic biopsy.* Endoscopy, 1995. **27**(9): p. 683-688.
81. Banno, K., et al., *Confocal Endomicroscopy for a Phenotypic Diagnosis of Gastric Cancers.* Gastrointestinal Endoscopy, 2009. **69**(5): p. AB175-AB175.
82. Casiraghi, O., et al., *Imaging by confocal endomicroscopy: New insight for in vivo tissue diagnosis of head and neck cancer.* Virchows Archiv, 2012. **461**: p. S142-S142.
83. Bisschops, R., *Confocal laser endomicroscopy: finally ready to change clinical practice?* Gastrointestinal Endoscopy, 2011. **74**(4): p. 781-783.
84. Mendy, M. and R. Walton, *Molecular pathogenesis and early detection of hepatocellular carcinoma - Perspectives from West Africa.* Cancer Letters, 2009. **286**(1): p. 44-51.
85. Mitra, A.P., et al., *Biomarker profiling for cancer diagnosis, prognosis and therapeutic management.* National Medical Journal of India, 2005. **18**(6): p. 304-312.
86. Salto-Tellez, M. and E.S.C. Koay, *Molecular diagnostic cytopathology: definitions, scope and clinical utility.* Cytopathology, 2004. **15**(5): p. 252-255.
87. Zhang, X.W., et al., *Molecular diagnosis of human cancer type by gene expression profiles and independent component analysis.* European Journal of Human Genetics, 2005. **13**(12): p. 1303-1311.
88. Clark, D. and L. Mao, *Cancer biomarker discovery: Lectin-based strategies targeting glycoproteins.* Disease Markers, 2012. **33**(1): p. 1-10.
89. Kitajima, T., et al., *Angiopoietin-like protein 2 as a novel serum biomarker for diagnosis and prognosis in patients with colorectal cancer.* Cancer Research, 2014. **74**(19).
90. Zhao, Y.C., W.N.P. Lee, and G.G. Xiao, *Quantitative proteomics and biomarker discovery in human cancer.* Expert Review of Proteomics, 2009. **6**(2): p. 115-118.
91. Rodrigo, M.A.M., et al., *MALDI-TOF MS as evolving cancer diagnostic tool: A review.* Journal of Pharmaceutical and Biomedical Analysis, 2014. **95**: p. 245-255.
92. Nakajima, M. and H. Kato, *Treatment options for esophageal squamous cell carcinoma.* Expert Opinion on Pharmacotherapy, 2013. **14**(10): p. 1345-1354.

93. Leong, T., *Chemotherapy and radiotherapy in the management of gastric cancer.* Current Opinion in Gastroenterology, 2005. **21**(6): p. 673-678.
94. Yamashita, T., et al., *Association between lymphangiogenesis-/micrometastasis- and adhesion-related molecules in resected stage I NSCLC.* Lung Cancer, 2010. **70**(3): p. 320-328.
95. Cruz, C., et al., *Recurrence and Risk Factors for Relapse in Patients with Non-Small Cell Lung Cancer Treated by Surgery with Curative Intent.* Oncology, 2017. **92**(6): p. 347-352.
96. Mariette, C. and J.P. Triboulet, *Radiotherapy and chemotherapy in the treatment of oesophageal carcinoma.* Annales De Chirurgie, 2004. **129**(9): p. 489-496.
97. Allgayer, H. and S. Fulda, *An introduction to molecular targeted therapy of cancer.* Advances in Medical Sciences, 2008. **53**(2): p. 130-138.
98. Kaur, V., et al., *Therapeutic potential of nanocarrier for overcoming to P-glycoprotein.* Journal of Drug Targeting, 2014. **22**(10): p. 859-870.
99. Ning, Y. and H.J. Lenz, *Targeting IL-8 in colorectal cancer.* Expert Opinion on Therapeutic Targets, 2012. **16**(5): p. 491-497.
100. Kumar, S., S. Bawa, and H. Gupta, *Biological Activities of Quinoline Derivatives.* Mini-Reviews in Medicinal Chemistry, 2009. **9**(14): p. 1648-1654.
101. Marella, A., et al., *Quinoline: A versatile heterocyclic.* Saudi Pharmaceutical Journal, 2013. **21**(1): p. 1-12.
102. Mroczek, T. and K. Glowniak, *TLC and HPTLC assay of quinoline and quinuclidine alkaloids in Cinchonae cortex and pharmaceutical preparations.* Jpc-Journal of Planar Chromatography-Modern Tlc, 2000. **13**(6): p. 457-462.
103. Lee, H.W., J.Y. Yang, and H.S. Lee, *Quinoline-2-carboxylic Acid Isolated from Ephedra pachyclada and Its Structural Derivatives Show Inhibitory Effects against alpha-Glucosidase and alpha-Amylase.* Journal of the Korean Society for Applied Biological Chemistry, 2014. **57**(4): p. 441-444.
104. Starratt, A.N. and S. Caveney, *Quinoline-2-carboxylic acids from Ephedra species.* Phytochemistry, 1996. **42**(5): p. 1477-1478.

105. Solomon, V.R. and H. Lee, *Quinoline as a Privileged Scaffold in Cancer Drug Discovery.* Current Medicinal Chemistry, 2011. **18**(10): p. 1488-1508.
106. Chan, S.H., et al., *Synthesis of 8-Hydroxyquinoline Derivatives as Novel Antitumor Agents.* Acs Medicinal Chemistry Letters, 2013. **4**(2): p. 170-174.
107. Keri, R.S. and S.A. Patil, *Quinoline: A promising antitubercular target.* Biomedicine & Pharmacotherapy, 2014. **68**(8): p. 1161-1175.
108. Lobana, T.S., et al., *Bonding and structure trends of thiosemicarbazone derivatives of metals-An overview.* Coordination Chemistry Reviews, 2009. **253**(7-8): p. 977-1055.
109. Hicks, J.W., et al., *Synthesis, Characterization, and Antifungal Activity of Boron-Containing Thiosemicarbazones.* Chemistry & Biodiversity, 2008. **5**(11): p. 2415-2422.
110. Chaston, T.B. and D.R. Richardson, *Iron Chelators for the treatment of iron overload disease: Relationship between structure, redox activity, and toxicity.* American Journal of Hematology, 2003. **73**(3): p. 200-210.
111. Opletalova, V., et al., *Identification and characterization of thiosemicarbazones with antifungal and antitumor effects: Cellular iron chelation mediating cytotoxic activity.* Chemical Research in Toxicology, 2008. **21**(9): p. 1878-1889.
112. Pavan, F.R., et al., *Thiosemicarbazones, semicarbazones, dithiocarbazates and hydrazide/hydrazones: Anti-Mycobacterium tuberculosis activity and cytotoxicity.* European Journal of Medicinal Chemistry, 2010. **45**(5): p. 1898-1905.
113. Kalinowski, D.S., P. Quach, and D.R. Richardson, *Thiosemicarbazones: the new wave in cancer treatment.* Future Medicinal Chemistry, 2009. **1**(6): p. 1143-1151.
114. Kalinowski, D.S. and D.R. Richardson, *The evolution of iron chelators for the treatment of iron overload disease and cancer.* Pharmacological Reviews, 2005. **57**(4): p. 547-583.
115. Keiser, M.J., et al., *Relating protein pharmacology by ligand chemistry.* Nature Biotechnology, 2007. **25**(2): p. 197-206.
116. Bikadi, Z. and E. Hazai, *Application of the PM6 semi-empirical method to modeling proteins enhances docking accuracy of AutoDock.* Journal of Cheminformatics, 2009. **1**.

117. Zhang, M.F., Q. Liu, and G.X. Jia, *Reference gene selection for gene expression studies in lily using quantitative real-time PCR.* Genetics and Molecular Research, 2016. **15**(2).
118. Xi, R.X., et al., *Novel Thiosemicarbazones Inhibit Lysine-Rich Carcinoembryonic Antigen-Related Cell Adhesion Molecule 1 (CEACAM1) Coisolated (LYRIC) and the LYRIC-Induced Epithelial-Mesenchymal Transition via Upregulation of N-Myc Downstream-Regulated Gene 1 (NDRG1).* Molecular Pharmacology, 2017. **91**(5): p. 499-517.
119. Kong, F.N., et al., *Selection of reference genes for gene expression normalization in Pyropia yezoensis using quantitative real-time PCR.* Journal of Applied Phycology, 2015. **27**(2): p. 1003-1010.
120. Livak, K.J. and T.D. Schmittgen, *Analysis of relative gene expression data using real-time quantitative PCR and the 2(T)(-Delta Delta C) method.* Methods, 2001. **25**(4): p. 402-408.
121. Eslick, G.D., *Epidemiology of Esophageal Cancer.* Gastroenterology Clinics of North America, 2009. **38**(1): p. 17-+.
122. Pun, I.H.Y., et al., *Anti-cancer Effects of a Novel Quinoline Derivative 83b1 on Human Esophageal Squamous Cell Carcinoma through Down-Regulation of COX-2 mRNA and PGE(2).* Cancer Research and Treatment, 2017. **49**(1): p. 219-229.
123. Muller, R., *PPAR beta/delta in human cancer.* Biochimie, 2017. **136**: p. 90-99.
124. Park, J.I. and J.Y. Kwak, *The Role of Peroxisome Proliferator-Activated Receptors in Colorectal Cancer.* Ppar Research, 2012.
125. Zieleniak, A., M. Wojcik, and L.A. Wozniak, *Structure and physiological functions of the human peroxisome proliferator-activated receptor gamma.* Archivum Immunologiae Et Therapiae Experimentalis, 2008. **56**(5): p. 331-345.
126. Wu, C.W., J. Yu, and J.J.Y. Sung, *Peroxisome proliferator-activated receptor delta and gastric cancer (Review).* Oncology Reports, 2009. **22**(3): p. 451-457.
127. Peters, J.M., F.J. Gonzalez, and R. Muller, *Establishing the Role of PPAR beta/delta in Carcinogenesis.* Trends in Endocrinology and Metabolism, 2015. **26**(11): p. 595-607.

128. Foreman, J.E., et al., *Functional Characterization of Peroxisome Proliferator-Activated Receptor-beta/delta Expression in Colon Cancer.* Molecular Carcinogenesis, 2011. **50**(11): p. 884-900.
129. Xu, L.H., C. Han, and T. Wu, *A novel positive feedback loop between peroxisome proliferator-activated receptor-delta and prostaglandin E-2 signaling pathways for human cholangiocarcinoma cell growth.* Journal of Biological Chemistry, 2006. **281**(45): p. 33982-33996.
130. Burdick, A.D., et al., *The role of peroxisome proliferator-activated receptor-beta/delta in epithelial cell growth and differentiation.* Cellular Signalling, 2006. **18**(1): p. 9-20.
131. Han, S.W., et al., *Activation of peroxisome proliferator-activated receptor beta/delta (PPAR beta/delta) increases the expression of prostaglandin E-2 receptor subtype EP4 - The roles of phosphatidylinositol 3-kinase and CCAAT/enhancer-binding protein beta.* Journal of Biological Chemistry, 2005. **280**(39): p. 33240-33249.
132. Park, B.H., B. Vogelstein, and K.W. Kinzler, *Genetic disruption of PPAR delta decreases the tumorigenicity of human colon cancer cells.* Proceedings of the National Academy of Sciences of the United States of America, 2001. **98**(5): p. 2598-2603.
133. You, M.L., et al., *PPAR delta Signaling Regulates Colorectal Cancer.* Current Pharmaceutical Design, 2015. **21**(21): p. 2956-2959.
134. Takayama, O., et al., *Expression of PPAR delta in multistage carcinogenesis of the colorectum: implications of malignant cancer morphology.* British Journal of Cancer, 2006. **95**(7): p. 889-895.
135. Fukumoto, K., et al., *Peroxisome proliferator-activated receptor delta as a molecular target to regulate lung cancer cell growth.* Febs Letters, 2005. **579**(17): p. 3829-3836.
136. D'Angelo, B., et al., *Signal Transduction Pathways Involved in PPAR beta/delta-Induced Neuronal Differentiation.* Journal of Cellular Physiology, 2011. **226**(8): p. 2170-2180.
137. Ham, S.A., et al., *Ligand-activated PPAR delta modulates the migration and invasion of melanoma cells by regulating Snail expression.* American Journal of Cancer Research, 2014. **4**(6): p. 674-+.

138. Han, S.W., et al., *Activation of Peroxisome Proliferator-Activated Receptor beta/delta Induces Lung Cancer Growth via Peroxisome Proliferator-Activated Receptor Coactivatior gamma-1 alpha.* American Journal of Respiratory Cell and Molecular Biology, 2009. **40**(3): p. 325-331.
139. Wagner, K.D., et al., *Peroxisome proliferator-activated receptor beta/delta (PPAR beta/delta) is highly expressed in liposarcoma and promotes migration and proliferation.* Journal of Pathology, 2011. **224**(4): p. 575-588.
140. He, T.C., et al., *PPAR delta is an APC-regulated target of nonsteroidal anti-inflammatory drugs.* Cell, 1999. **99**(3): p. 335-345.
141. Tachibana, K., et al., *The Role of PPARs in Cancer.* Ppar Research, 2008.
142. Ali, A.T., J.E. Paiker, and N.J. Crowther, *The relationship between anthropometry and serum concentrations of alkaline phosphatase isoenzymes, liver enzymes, albumin, and bilirubin.* American Journal of Clinical Pathology, 2006. **126**(3): p. 437-442.
143. Dimitrijevic-Sreckovic, V., et al., *Liver Function Test Changes in Centrally Obese Youth with Metabolic Syndrome in a Serbian Population.* Metabolic Syndrome and Related Disorders, 2013. **11**(6): p. 427-433.
144. Penndorf, V., et al., *Liver Parameters in Intensive Care Medicine.* Zentralblatt Fur Chirurgie, 2013. **138**(6): p. 636-642.
145. Wen, D.S., et al., *A rapid and sensitive UHPLC-MS/MS method for quantification of 83b1 in plasma and its application to bioavailability study in rats.* Journal of Pharmaceutical and Biomedical Analysis, 2017. **134**: p. 71-76.
146. Becker, J.P., et al., *Molecular models of human P-glycoprotein in two different catalytic states.* Bmc Structural Biology, 2009. **9**.
147. Schinkel, A.H., *The pharmacological role of P-glycoprotein.* Naunyn-Schmiedebergs Archives of Pharmacology, 1998. **358**(1): p. R25-R25.
148. Chang, G., et al., *Structure of P-glycoprotein.* Drug Metabolism Reviews, 2010. **42**: p. 6-7.
149. Lin, J.H. and M. Yamazaki, *Role of P-glycoprotein in pharmacokinetics - Clinical implications.* Clinical Pharmacokinetics, 2003. **42**(1): p. 59-98.

150. Jin, M.S., et al., *Crystal structure of the multidrug transporter P-glycoprotein from Caenorhabditis elegans.* Nature, 2012. **490**(7421): p. 566-+.
151. Orind, M., et al., *Modulation of P-glycoprotein on tumour cells*. Calcium and Cellular Metabolism: Transport and Regulation, ed. J.R. Sotelo and J.C. Benech. 1997. 117-124.
152. Clarke, G., et al., *Verapamil in treatment resistant depression: a role for the P-glycoprotein transporter?* Human Psychopharmacology-Clinical and Experimental, 2009. **24**(3): p. 217-223.
153. Legrand, O., et al., *Pgp and MRP activities using calcein-AM are prognostic factors in adult acute myeloid leukemia patients.* Blood, 1998. **91**(12): p. 4480-4488.
154. Meletiadis, J., et al., *Defining Fractional Inhibitory Concentration Index Cutoffs for Additive Interactions Based on Self-Drug Additive Combinations, Monte Carlo Simulation Analysis, and In Vitro-In Vivo Correlation Data for Antifungal Drug Combinations against Aspergillus fumigatus.* Antimicrobial Agents and Chemotherapy, 2010. **54**(2): p. 602-609.
155. Te Dorsthorst, D.T.A., et al., *Comparison of fractional inhibitory concentration index with response surface modeling for characterization of in vitro interaction of antifungals against itraconazole-susceptible and -resistant Aspergillus fumigatus isolates.* Antimicrobial Agents and Chemotherapy, 2002. **46**(3): p. 702-707.
156. Chou, T.C., *Drug Combination Studies and Their Synergy Quantification Using the Chou-Talalay Method.* Cancer Research, 2010. **70**(2): p. 440-446.
157. Yang, L., et al., *Multilayer photodynamic therapy for highly effective and safe cancer treatment.* Acta Biomaterialia, 2017. **54**: p. 271-280.
158. Benson, A.B., et al., *Colon Cancer, Version 1.2017 Clinical Practice Guidelines in Oncology.* Journal of the National Comprehensive Cancer Network, 2017. **15**(3): p. 370-398.
159. Japanese Gastric Canc, A., *Japanese gastric cancer treatment guidelines 2014 (ver. 4).* Gastric Cancer, 2017. **20**(1): p. 1-19.
160. Lee, H.H., et al., *Combination treatment with paclitaxel and doxorubicin inhibits growth of human esophageal squamous cancer*

cells by inactivation of Akt. Oncology Reports, 2014. **31**(1): p. 183-188.
161. Marupudi, N.I., et al., *Paclitaxel: a review of adverse toxicities and novel delivery strategies.* Expert Opinion on Drug Safety, 2007. **6**(5): p. 609-621.
162. Weaver, B.A., *How Taxol/paclitaxel kills cancer cells.* Molecular Biology of the Cell, 2014. **25**(18): p. 2677-2681.
163. Tan, C., et al., *Potential biomarkers for esophageal cancer.* Springerplus, 2016. **5**.
164. Bae, D.H., et al., *The role of NDRG1 in the pathology and potential treatment of human cancers.* Journal of Clinical Pathology, 2013. **66**(11): p. 911-917.
165. Dixon, K.M., et al., *Dp44mT targets the AKT, TGF-beta and ERK pathways via the metastasis suppressor NDRG1 in normal prostate epithelial cells and prostate cancer cells.* British Journal of Cancer, 2013. **108**(2): p. 409-419.
166. Kovacevic, Z., et al., *The Metastasis Suppressor, N-MYC Downstream-regulated Gene-1 (NDRG1), Down-regulates the ErbB Family of Receptors to Inhibit Downstream Oncogenic Signaling Pathways.* Journal of Biological Chemistry, 2016. **291**(3): p. 1029-1052.
167. Torti, S.V. and F.M. Torti, *Iron and cancer: more ore to be mined.* Nature Reviews Cancer, 2013. **13**(5): p. 342-355.
168. Gumienna-Kontecka, E., et al., *Iron Chelating Strategies in Systemic Metal Overload, Neurodegeneration and Cancer.* Current Medicinal Chemistry, 2014. **21**(33): p. 3741-3767.
169. Wang, H.Z., et al., *Iron Overload Coordinately Promotes Ferritin Expression and Fat Accumulation in Caenorhabditis elegans.* Genetics, 2016. **203**(1): p. 241-+.
170. Drozd, M., et al., *Iron Therapy in Patients with Heart Failure and Iron Deficiency: Review of Iron Preparations for Practitioners.* American Journal of Cardiovascular Drugs, 2017. **17**(3): p. 183-201.
171. Chin, A.P., P.V. Bernhardt, and D.R. Richardson, *Orally active Chelators for the treatment of iron overload diseases.* Journal of Inorganic Biochemistry, 2003. **96**(1): p. 118-118.
172. Richardson, D.R. and P. Ponka, *Orally effective iron chelators for the treatment of iron overload disease: The case for a further look at*

pyridoxal isonicotinoyl hydrazone and its analogs. Journal of Laboratory and Clinical Medicine, 1998. **132**(4): p. 351-352.
173. Buss, J.L., F.M. Torti, and S.V. Torti, *The role of iron chelation in cancer therapy.* Current Medicinal Chemistry, 2003. **10**(12): p. 1021-1034.
174. Andrews, M. and M. Arredondo, *Hepatic and adipocyte cells respond differentially to iron overload, hypoxic and inflammatory challenge.* Biometals, 2012. **25**(4): p. 749-759.
175. Wessling-Resnick, M., *Iron Homeostasis and the Inflammatory Response.* Annual Review of Nutrition, Vol 30, 2010. **30**: p. 105-122.
176. Ai, R.N., et al., *NDRG1 overexpression promotes the progression of esophageal squamous cell carcinoma through modulating Wnt signaling pathway.* Cancer Biology & Therapy, 2016. **17**(9): p. 943-954.
177. Emdad, L., et al., *AEG-1/MTDH/LYRIC: Signaling Pathways, Downstream Genes, Interacting Proteins, and Regulation of Tumor Angiogenesis.* Aeg-1/Mtdh/Lyric Implicated in Multiple Human Cancers, 2013. **120**: p. 75-111.
178. O'Neil, B.H. and R.M. Goldberg, *Innovations in Chemotherapy for Metastatic Colorectal Cancer: An Update of Recent Clinical Trials.* Oncologist, 2008. **13**(10): p. 1074-1083.
179. Pascale, M., et al., *The outcome of prostate cancer patients treated with curative intent strongly depends on survival after metastatic progression.* Bmc Cancer, 2017. **17**.
180. Zacharakis, M., et al., *Predictors of Survival in Stage IV Metastatic Colorectal Cancer.* Anticancer Research, 2010. **30**(2): p. 653-660.
181. Dasari, S. and P.B. Tchounwou, *Cisplatin in cancer therapy: Molecular mechanisms of action.* European Journal of Pharmacology, 2014. **740**: p. 364-378.
182. Chen, Z.Q., et al., *The Iron Chelators Dp44mT and DFO Inhibit TGF-beta-induced Epithelial-Mesenchymal Transition via Up-Regulation of N-Myc Downstream-regulated Gene 1 (NDRG1).* Journal of Biological Chemistry, 2012. **287**(21): p. 17016-17028.